

**DESIGN, SYNTHESIS, AND BIOLOGICAL EVALUATION OF POTENT
HIV-1 PROTEASE INHIBITORS WITH NOVEL BICYCLIC
OXAZOLIDINONE AND BIS SQUARAMIDE SCAFFOLDS**

by

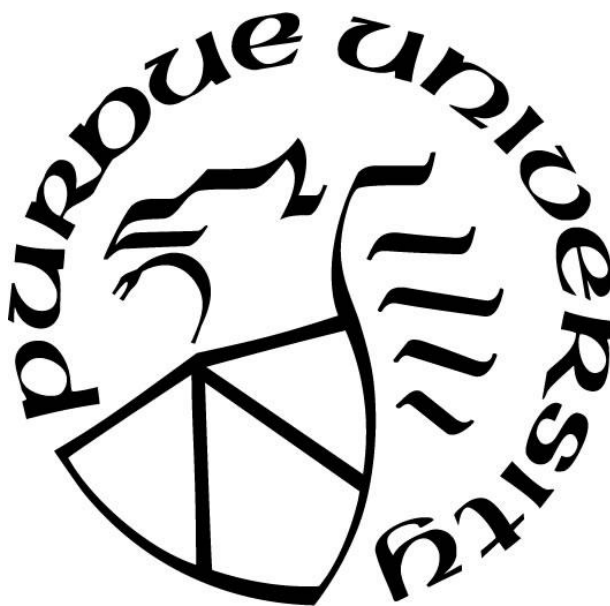
Jacqueline N. Williams

A Dissertation

Submitted to the Faculty of Purdue University

In Partial Fulfillment of the Requirements for the degree of

Doctor of Philosophy



Department of Chemistry

West Lafayette, Indiana

August 2019

THE PURDUE UNIVERSITY GRADUATE SCHOOL
STATEMENT OF COMMITTEE APPROVAL

Dr. Arun K. Ghosh, Chair

Department of Chemistry

Dr. Andrew Mesecar

Department of Biochemistry

Dr. Christopher Uyeda

Department of Chemistry

Dr. Abram Axelrod

Department of Chemistry

Approved by:

Dr. Christine Hyrcyna

Head of the Graduate Program

To my loving grandmother, for her constant support and encouragement.

ACKNOWLEDGMENTS

First and foremost, I would like to express my gratitude to Professor Arun K. Ghosh - thank you for your guidance and mentorship. It was truly an honor to learn from you throughout my graduate career. To my thesis committee members, Professor Andrew Mesecar, Professor Christopher Uyeda, and Professor Bram Axelrod - a special thanks for your support and advice. I would like to sincerely thank our collaborators Dr. Irene T. Weber and Dr. Hiroaki Mitsuya for their work on X-ray crystallography and biological studies.

To the NMR facility staff, Dr. John Harwood, Dr. Huaping Mo, Jerry Hirschinger, and Donna Bertram - thank you for your advice, words of encouragement and support during my NMR appointment. I would like to thank the department staff, Dr. Christine Hyrcyna, Betty Dexter, Lynn Ryder, and Debra Packer for their guidance throughout my graduate studies. A special thanks to Suzanne Snoeberger for your constant assistance and direction.

To the current and past Ghosh group members - thank you for your advice, and support during my time in the Ghosh group, particularly Dr. Anthony Tomaine, Dr. Anindya Sarkar, Dr. Chandu Guddeti, Dr. Garth Parham, Dr. Heather Osswald, Dr. Luke Kassekert, Dr. Margherita Brindisi, Dr. Sidhu Akasapu, Dr. Vasudeva Dodda, Dr. Vasu Garidi, Dr. Satish Kovala, Dr. Zilei Xia, Hannah Simpson, Megan Johnson, and Rachel Ho.

TABLE OF CONTENTS

| | |
|---|----|
| LIST OF TABLES | 8 |
| LIST OF FIGURES | 9 |
| LIST OF SCHEMES | 11 |
| LIST OF ABBREVIATIONS | 13 |
| ABSTRACT | 16 |
| CHAPTER 1. DESIGN, SYNTHESIS, AND BIOLOGICAL EVALUATION OF HIV-1 PROTEASE INHIBITORS WITH A P2 BICYCLIC OXAZOLIDINONE LIGAND | 17 |
| 1.1 The History of Human Immunodeficiency Virus and Acquired Immunodeficiency Syndrome | 17 |
| 1.2 Taxonomy of HIV | 18 |
| 1.3 The HIV Life Cycle | 18 |
| 1.4 Treatments of HIV/AIDS | 24 |
| 1.4.1 Entry and Fusion Inhibitors | 28 |
| 1.4.2 Reverse Transcriptase Inhibitors | 30 |
| 1.4.2.1 Nucleoside Reverse Transcriptase Inhibitors | 31 |
| 1.4.2.2 Non-Nucleoside Reverse Transcriptase Inhibitors | 32 |
| 1.4.3 Integrase Inhibitors | 34 |
| 1.4.4 Protease Inhibitors | 35 |
| 1.5 HIV-1 Protease | 35 |
| 1.5.1 First Generation HIV Protease Inhibitors | 39 |
| 1.5.2 Second Generation HIV Protease Inhibitors | 41 |

| | |
|---|-----|
| 1.5.3 The Fight Against Drug Resistance | 42 |
| 1.5.3.1 Backbone Binding Concept..... | 43 |
| 1.5.3.2 Darunavir..... | 43 |
| 1.6 Design, Synthesis, and Biological Evaluation of HIV-1 Protease Inhibitors with an Oxazolidinone P2 ligand | 44 |
| 1.6.1 Introduction | 44 |
| 1.6.2 Design of HIV Protease Inhibitors with an Oxazolidinone P2 Ligand | 45 |
| 1.6.3 Results..... | 48 |
| 1.6.3.1 Synthesis of Inhibitors | 49 |
| 1.6.3.2 Biological Evaluation..... | 65 |
| 1.6.3.3 X-ray Crystallographic Analysis | 73 |
| 1.6.4 Discussion | 73 |
| 1.7 Conclusion | 81 |
| 1.8 Experimental Section..... | 82 |
| CHAPTER 2. DESIGN, SYNTHESIS, AND BIOLOGICAL EVALUATION OF HIV-1 PROTEASE INHIBITORS WITH A NOVEL BIS SQUARAMIDE SCAFFOLD | 113 |
| 2.1 Introduction..... | 113 |
| 2.2 Design, Synthesis, and Biological Evaluation of HIV-1 Protease Inhibitors with a Novel Bis Squaramide P2 Ligand | 114 |
| 2.2.1 Design of HIV Protease Inhibitors with a Bis Squaramide P2 Ligand | 114 |
| 2.2.2 Results..... | 118 |
| 2.2.2.1 Synthesis of Inhibitors | 118 |
| 2.2.2.2 Biological Evaluation..... | 127 |

| | |
|-------------------------------|-----|
| 2.2.3 Discussion | 129 |
| 2.3 Conclusion | 129 |
| 2.4 Experimental Section..... | 130 |
| APPENDIX: NMR Spectra | 138 |
| REFERENCES | 193 |
| VITA | 206 |
| PUBLICATION..... | 207 |

LIST OF TABLES

| | |
|---|-----|
| Table 1.1: FDA Approved HIV/AIDS Drugs..... | 27 |
| Table 1.2: HIV-1 Proteases Inhibitory and Antiviral Activity of Inhibitors 1.65a and 1.65b with <i>N</i> -Hydride Group..... | 65 |
| Table 1.3: HIV-1 Proteases Inhibitory and Antiviral Activity of Inhibitors 1.65c , 1.65d , 1.65f , and 1.65h with <i>N</i> -Alkyl Group | 66 |
| Table 1.4: HIV-1 Proteases Inhibitory and Antiviral Activity of Inhibitors 1.65e and 1.65g with Saturated <i>N</i> -Alkyl Group | 67 |
| Table 1.5: HIV-1 Proteases Inhibitory and Antiviral Activity of Inhibitors 1.65i-l with <i>N</i> -Aryl Group | 68 |
| Table 1.6: HIV-1 Proteases Inhibitory and Antiviral Activity of Inhibitors 1.65m with <i>N</i> -MOM Group | 69 |
| Table 1.7: HIV-1 Proteases Inhibitory and Antiviral Activity of Inhibitor 1.65n with Varying P2' | 69 |
| Table 1.8: Antiviral Activity of 1.65g , 1.65h , and Other FDA PIs Against Multi-Resistant-HIV-1 Strains | 71 |
| Table 1.9: Cytotoxicity and Selectivity Index for Selected Inhibitors..... | 77 |
| Table 2.1: HIV-1 Proteases Inhibitory and Antiviral Activity of Inhibitors 2.22a-d | 128 |

LIST OF FIGURES

| | |
|--|----|
| Figure 1.1: The HIV-1 viral particle. | 20 |
| Figure 1.2: HIV-1 Fusion with a Host T cell. | 21 |
| Figure 1.3: HIV Life Cycle..... | 23 |
| Figure 1.4: Structures of Initial Antiretroviral Drugs for the Treatment of HIV/AIDS | 25 |
| Figure 1.5: Structure of Entry Inhibitor Enfuvirtide | 28 |
| Figure 1.6: Structures of CCR5 and CXCR4 Inhibitors..... | 29 |
| Figure 1.7: Inhibition of HIV-1 Entry..... | 30 |
| Figure 1.8: Reverse Transcriptase Active Site: Thumb, Palm, Fingers, and Connection. | 31 |
| Figure 1.9: Structures of Nucleoside Reverse Transcriptase Inhibitors..... | 32 |
| Figure 1.10: Active site of Nonnucleoside Reverse Transcriptase Inhibitors. | 33 |
| Figure 1.11: Structures of Nonnucleoside Reverse Transcriptase Inhibitors | 34 |
| Figure 1.12: Structures of Integrase Inhibitors | 35 |
| Figure 1.13: X-ray Crystal Structure of Wild-Type HIV-1 Protease (PDB: 2PCO) | 36 |
| Figure 1.14: Mechanism of Catalytic Aspartic Acids Hydrolyzing the Native Peptide Bond | 37 |
| Figure 1.15: Native Substrate Bound to HIV-PR Enzyme..... | 38 |
| Figure 1.16: Important Hydrogen Bond Interactions of HIV-1 PR with Substrate ⁷⁹ | 39 |
| Figure 1.17: X-ray Structure of SQV Complexed to HIV-PR. (PDB: 3OXC) | 40 |
| Figure 1.18: First Generation of Protease Inhibitors..... | 41 |
| Figure 1.19: Second Generation of Protease Inhibitors | 42 |
| Figure 1.20: X-ray Structure of HIV-1 PR Bound to Darunavir (PDB: 2IEN)..... | 44 |
| Figure 1.21: Structures of Darunavir and TMC-126..... | 45 |

| | |
|---|-----|
| Figure 1.22: Structures of 1.3 - 1.5 | 46 |
| Figure 1.23: Structures of Pyrrolidone 1.6 and Proline-like 1.7 | 46 |
| Figure 1.24: Structures of <i>N</i> -aryl oxazolidinone Derivatives 1.8 – 1.10 | 47 |
| Figure 1.25: Base Model of Inhibitors | 48 |
| Figure 1.26: Synthesis of Optically Active Bicyclic Oxazolidinone Ligand 1.39 | 56 |
| Figure 1.27: Structures of Ligand Alcohol Precursors..... | 62 |
| Figure 1.28: Structures of Activated Carbonates 1.64a-m | 63 |
| Figure 1.29: Structures of Final Inhibitors | 64 |
| Figure 1.30: Inhibitor 1.65a Bound with Wild Type HIV-1 Protease (PDB:6E9A) | 78 |
| Figure 1.31: Overlay of DRV (light blue) Bound to HIV-1 PR with Inhibitor 1.65a (purple) | 79 |
| Figure 1.32: Overlay of DRV (light blue) with Inhibitor 1.65a (purple)..... | 80 |
| Figure 1.33: Inhibitor 1.65i Bound with Wild Type HIV-1 Protease (PDB: 6E7J) | 81 |
| Figure 2.1: Structures and Nomenclature of Squarate Derivatives..... | 114 |
| Figure 2.2: Squaramide Potential Drug Candidates..... | 115 |
| Figure 2.3: Base Model of Inhibitors | 117 |
| Figure 2.4: Synthesis of Optically Active Amine 2.15 | 122 |

LIST OF SCHEMES

| | |
|--|-----|
| Scheme 1.1: Synthesis of Epoxide 1.14 and 1.15 | 49 |
| Scheme 1.2: Synthesis of Mesylate 1.19 | 50 |
| Scheme 1.3: Synthesis of Bicyclic Oxazolidinone 1.22 | 51 |
| Scheme 1.4: Synthesis of Isostere Amine 1.25 | 52 |
| Scheme 1.5: Synthesis of Diastereomeric Final Inhibitors 1.27 and 1.28 | 53 |
| Scheme 1.6: Outline of Explored Lipase Conditions..... | 54 |
| Scheme 1.7: Synthesis of Monoacetate 1.31 and 1.33 | 55 |
| Scheme 1.8: Synthesis of Optically Active Bicyclic Oxazolidinone Ligand 1.36 | 56 |
| Scheme 1.9: Synthesis of <i>N</i> -Me 1.42 | 57 |
| Scheme 1.10: Synthesis of <i>N</i> -Me 1.45 | 57 |
| Scheme 1.11: Synthesis of <i>N</i> -Allyl 1.47 and <i>N</i> -propyl 1.48 Ligand | 58 |
| Scheme 1.12: Synthesis of <i>N</i> -Isobutylene 1.50 and <i>N</i> -Isobutyl 1.51 Ligand..... | 58 |
| Scheme 1.13: Synthesis of <i>N</i> -Aryl 1.58-1.61 | 60 |
| Scheme 1.14: Synthesis of <i>N</i> -MOM 1.63 | 61 |
| Scheme 1.15: Synthesis of Final Inhibitors 1.65a-m | 61 |
| Scheme 1.16: Synthesis of Final Inhibitors 1.65n | 62 |
| Scheme 2.1: Synthesis of Squaramide 2.3: an Anti-Chagasic Agent | 116 |
| Scheme 2.2: Synthesis of Racemic bis-THF Alcohol 2.8 | 119 |
| Scheme 2.3: Synthesis of Optically Active bis-THF Alcohol 2.9 and 2.11 | 119 |
| Scheme 2.4: Double Mitsunobu Attempt Toward Amine 2.15 | 120 |
| Scheme 2.5: Reduction Amination of 2.16 | 121 |

| | |
|---|-----|
| Scheme 2.6: Optimized Conditions for the Synthesis of Enantiopure bis-THF Amine 2.17 | 122 |
| Scheme 2.7: Synthesis of Final Inhibitor 2.22a | 123 |
| Scheme 2.8: Synthesis of Final Inhibitor 2.22b | 124 |
| Scheme 2.9: Synthesis of bis-THF Methylamine 2.24 and 2.26 | 125 |
| Scheme 2.10: Synthesis of Final Inhibitor 2.22c and 2.22d | 126 |

LIST OF ABBREVIATIONS

| | |
|-------------------|--|
| 1D | one dimensional |
| 2D | two dimensional |
| 3D | three dimensional |
| Å | angstrom |
| AIBN | azobisisobutyronitrile |
| AIDS | acquired immunodeficiency syndrome |
| Ala | alanine |
| APV | amprenavir |
| CM | cross metathesis |
| DBU | 1,8-diazabicyclo[5.4.0]undec-7-ene |
| DIBAL-H | diisobutylaluminum hydride |
| DIPEA | <i>N,N</i> -diisopropylethylamine |
| DMAP | 4-(dimethylamino)pyridine |
| DMF | <i>N,N</i> -dimethylformamide |
| DMP | Dess-Martin periodinane |
| DMSO | dimethylsulfoxide |
| DNA | deoxyribonucleic acid |
| dr | diastereomeric ratio |
| DRV | darunavir |
| EA | ethyl acetate |
| <i>ee</i> | enantiomeric excess |
| Et ₂ O | diethyl ether |
| EtOH | ethanol |
| FDA | food and drug administration |
| HARRT | highly active antiretroviral therapy |
| HPLC | High Performance Liquid Chromatography |
| HRMS | High Resolution Mass Spectrometry |
| HIV | human immunodeficiency virus |
| Hz | hertz |

| | |
|--------------------------------|---|
| IC ₅₀ | inhibitory concentration at 50% |
| Imid. | imidazole |
| IN | integrase |
| KHMDS | potassium hexamethyldisilazide |
| K ₂ CO ₃ | potassium carbonate |
| LAH | lithium aluminum hydride |
| LCMS | liquid chromatography mass spectrometry |
| LRMS | low-resolution mass spectrometry |
| Lys | lysine |
| <i>m</i> -CPBA | 3-chloroperbenzoic acid |
| MeCN | acetonitrile |
| MeOH | methanol |
| MS | molecular sieves |
| NaH | sodium hydride |
| NaOH | sodium hydroxide |
| NIS | <i>N</i> -iodosuccinimide |
| NK | natural killer cells |
| nM | nanomolar |
| NMM | 4-methylmorpholine |
| NMP | 1-methyl-2-pyrrolidinone |
| NMR | Nuclear Magnetic Resonance |
| Pd/C | palladium on carbon |
| Ph | phenyl |
| pH | potential of hydrogen |
| PhH | benzene |
| PhMe | toluene |
| PI | protease inhibitor |
| PMB | p-methoxybenzyl |
| PR | protease |
| Pro | proline |
| Py | pyridine |

| | |
|----------------|----------------------------------|
| PMB | 4-methoxybenzyl |
| ppm | chemical shift, part per million |
| RCM | ring-closing metathesis |
| R _f | retention factor |
| RNA | ribonucleic acid |
| RT | reverse transcriptase |
| SAR | structure-activity relationship |
| SIV | simian immunodeficiency virus |
| SQV | saquinavir |
| TBAF | tetrabutylammonium fluoride |
| TBDPS | <i>tert</i> -butyldiphenylsilyl |
| TBS | <i>tert</i> -butyldimethylsilyl |
| <i>tert</i> | tertiary |
| TFA | trifluoroacetic acid |
| THF | tetrahydrofuran |
| TLC | thin layer chromatography |
| TMS | trimethylsilyl |
| TPAP | tetrapropylammonium perruthenate |
| TsOH | tosylic acid |
| UV | ultraviolet |
| α | alpha |
| β | beta |
| μ M | micromolar |

ABSTRACT

Author: Williams, Jacqueline, N. Ph.D.

Institution: Purdue University

Degree Received: August 2019

Title: Design, Synthesis and, Biological Evaluation of Potent HIV-1 Protease Inhibitors with Novel Bicyclic Oxazolidinone and Bis Squaramide Scaffolds

Committee Chair: Arun K. Ghosh

In 2018, the World Health Organization (WHO) reported approximately 37 million people are living with the Human Immunodeficiency Virus (HIV). Suppressing replication of the virus down to undetectable levels was achieved by combination antiretroviral therapy (cART) which effectively reduced the mortality and morbidity rates of HIV positive individuals. Despite the improvements towards combatting HIV/AIDS, no successful treatment exists to eradicate the virus from an infected individual. Treatment regimens are lifelong and prompt less than desirable side effects including but not limited to; drug-drug interactions, toxicity, systemic organ complications, central nervous system HIV triggered disorders and most importantly, drug resistance. Current therapies are becoming ineffective against highly resistant HIV strains making the ability to treat long-term viral suppression a growing issue. Therefore, potent and more effective HIV inhibitors provide the best chance for long-term successful cART.

HIV-1 protease (PR) enzyme plays a critical role in the life cycle and replication of HIV. Significant advancements were achieved through structure-based design and X-ray crystallographic analysis of protease-bound to HIV-1 and brought about several FDA protease inhibitors (PI). Highly mutated HIV-1 variants create a challenge for current and future treatment regimens. This thesis work focuses on the design, synthesis, and evaluation of two new classes of potent HIV-1 PIs that exhibit a novel bicyclic oxazolidinone feature as the P2 ligand and a novel bis squaramide scaffold as the P2/P3 ligand. Several inhibitors displayed good to excellent activity toward HIV-1 protease and significant antiviral activity in MT-4 cells. Inhibitors **1.65g** and **1.65h** were further evaluated against a panel of highly resistant multidrug-resistant HIV-1 variants and displayed antiviral activity similar to Darunavir. X-ray crystal structures of inhibitor **1.65a** and inhibitor **1.65i** were co-crystallized with wild type HIV-1 protease and solved at a 1.22 Å and 1.30 Å resolution and maintained strong hydrogen bond with the backbone of the PR enzyme.

CHAPTER 1. DESIGN, SYNTHESIS, AND BIOLOGICAL EVALUATION OF HIV-1 PROTEASE INHIBITORS WITH A P2 BICYCLIC OXAZOLIDINONE LIGAND

1.1 The History of Human Immunodeficiency Virus and Acquired Immunodeficiency Syndrome

In the early 1980s, *Morbidity and Mortality Weekly Report* published a public health digest on five previously healthy young homosexual men in the Los Angeles area whom suddenly contracted *Pneumocystis carinii* pneumonia (PCP), an uncommon opportunistic infection.¹ Concern increased when two of the infected individuals died from their continued declined of cellular-immune response to other opportunistic infections. Within a couple of years, hundreds of cases were reported on homosexual men with PCP and their development of similar, severe immunodeficiency symptoms. Soon after, the United States Centers for Disease Control and Prevention (CDC) named this unknown infection as acquired immune deficiency syndrome (AIDS).² In 1983, individuals who received a blood transfusion became infected with AIDS.³ It quickly became apparent that homosexual men were not the only affected individuals and additional modes of transmission exist for this deadly virus.

In 2008, Françoise Barré-Sinoussi and Luc Antoine Montagnier were awarded the Nobel Prize in Medicine for their discovery, isolation, and identification of the human immunodeficiency virus (HIV). The mysterious disease started to present itself in France in the early 1980s. Work began when Barré-Sinoussi notified Luc Montagnier of a young homosexual man who showed early signs of AIDS. Montagnier and Barré-Sinoussi teamed up at the Pasteur Institute to identify the unknown virus and attempt to identify if it was responsible for the AIDS epidemic. The retrovirus was successfully isolated from the lymph nodes of the affected individual with AIDS. Montagnier and Barré-Sinoussi named the viral isolates lymphadenopathy-associated virus (LAV).⁴ Extensive studies showed the virus was indeed a new class of lentiviruses that did exist in humans. Discovery of LAV was the first major scientific breakthrough on this unknown disease and its possible connection to immunodeficiency.⁵ In 1985, R. Gallo and coworkers produced results in favor of the association between a similar retrovirus and immunodeficiency.⁶ Initially, R. Gallo reported the virus he isolated as the human T-lymphotropic virus (HTLV). Results showed HTLV was the same virus reported earlier by Montagnier. In 1986, the International

Committee on Taxonomy of Viruses officially recognized the viral isolates as human immunodeficiency virus (HIV) instead of lymphadenopathy-associated virus or the human T-lymphotropic virus.⁷ It became apparent that HIV/AIDS was a severe fatal disease affecting all regions and further scientific advancements of prevention, awareness, and treatment were essential.

1.2 Taxonomy of HIV

Most common human infectious diseases have animal origins, and HIV is no exception. The HIV comprises of two major subtypes: HIV-1 and HIV-2. HIV-1 and HIV-2 resulted from multiple independent cross-species transmission of genetically different simian immunodeficiency viruses (SIV) from nonhuman primates to humans.⁸ Exposure to infected blood during hunting, processing of infected non-human primate for bushmeat, bites, and injuries from non-human primates kept as pets are rational theories for the initial transmission between species.⁹ Studies have shown, HIV-1 originated from cross-species transmission of chimpanzees infected with SIVcpz and gorillas infected with SIVgor.¹⁰ HIV-2 cross-species occurred from Old World monkeys, sooty mangabeys, who harbored the SIVsmm infection.¹¹ Overtime, four different groups of HIV-1 have been identified and labeled as group M, N, O and P and eight species cross-over events yielded HIV-2 groups A-H.^{12,13 14} The HIV-1 infections are frequent and more severe than the HIV-2. HIV and SIV high genetic diversity are the result of the viruses' very rapid and erroneous replication process.

1.3 The HIV Life Cycle

HIV is an RNA human lentivirus.⁵ The term “lenti” stems from the Latin meaning latent or slow. Lentiviruses are known for their long incubation phases and induction of inflammatory diseases in humans and other mammalian species. HIV transmission occurs through contact with blood products, breast milk, mucous secretions, genital secretion, and semen. The exposure routes have been narrowed down to maternal transmission of mother to child during birth, sexual intercourse, use of contaminated needles, and physical contact with infectious materials.^{15,16} HIV progresses through three significant stages known as acute, clinical latency or asymptomatic, then AIDS.

The acute HIV infection arises within a two to four-weeks upon initial infection, where the individual will start to experience flu-like symptoms. The virus triggers and attacks the host's immune response by infecting a variety of white blood cells that contain a CD4 surface receptor including blood monocytes, macrophages, T lymphocytes, natural killer (NK) cells, dendritic cells, and microglial cells.^{17,18} Replication begins and continues the spread of the virus. Without treatment, the level of HIV circulating throughout the blood is at an all-time high. The virus incorporates itself into bodily tissues to continue its replication process because T cells in peripheral blood exist in a resting state and HIV fails to replicate well in resting CD4-positive T cell's and ends up targeting differentiated tissue macrophage mimic cells.¹⁹ Once levels of the virus in peripheral blood becomes very low, it progresses to stage two, clinical latency or asymptomatic. People with clinical latency may not experience HIV-related symptoms. Without treatment, the virus suppresses the immune system further and destroys the ability to fight off opportunistic infections. Known opportunistic infections for HIV positive patients include *Pneumocystis carinii*, *cytomegalovirus*, *mycobacterial*, *herpesvirus*, and others.^{20,21,22,23,24} These opportunistic infections directly cause poor quality of life, development of life threatening malignancies, and death. Typically, the lifespan for patients who express AIDS is around three years. Extensive studies of the HIV life cycle and viral RNA genome have led to many successful antiretroviral therapies. No vaccine exists to eradicate the virus from an infected individual.

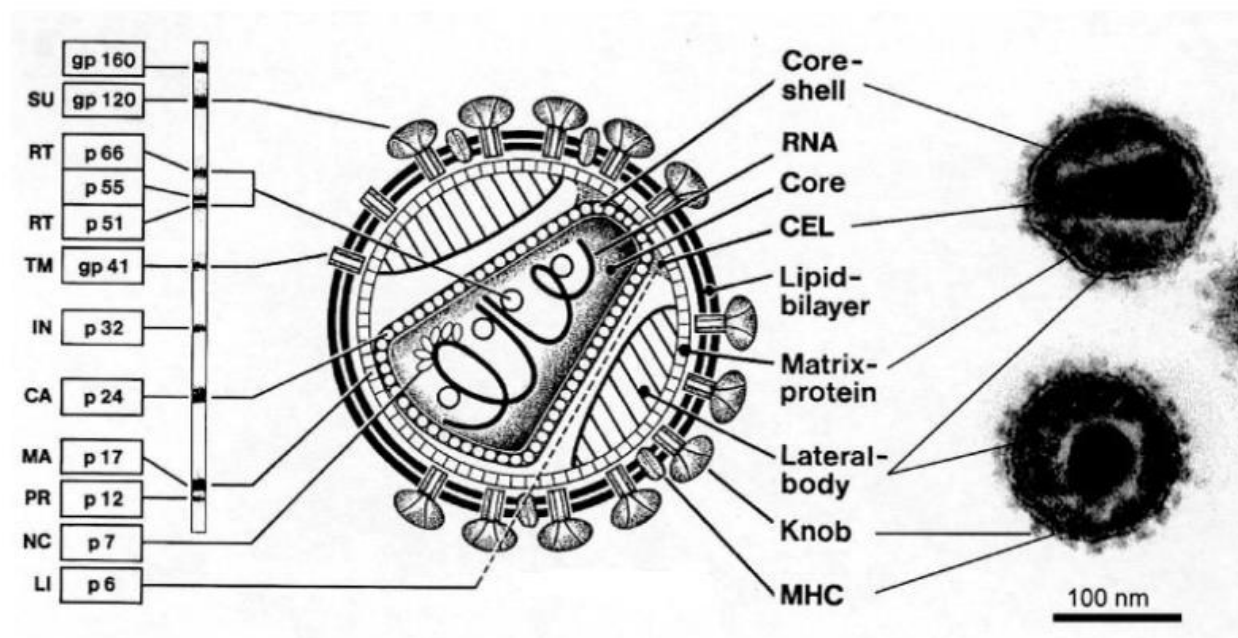


Figure 1.1: The HIV-1 viral particle.

Figure adapted from German Advisory Committee Blood et al.²⁵

The HIV-1 is the most common type and is largely responsible for the HIV/AIDS epidemic. This discussion will focus on HIV-1 going forward. A mature HIV-1 virus exists as a spherical particle with spikes of glycoproteins (gp160) on the outer lipid bilayer. Inside, it contains a distinct cone-shaped capsid with two single-stranded RNA genomes encoding for three large polypeptide precursors - Gag, Gag-Pol, Env, and several essential regulatory proteins necessary for infection and replication, shown in Figure 1.1. Once HIV-1 enters the body, seven stages of its life cycle take place: binding, fusion, reverse transcription, integration, replication, assembly, and budding.^{26,27}

The viral's genome RNA contains a total of nine genes: Gag, Gag-pol, Env, Tat, Rev, Vif, Vpr, Vpu, and Nef. Only Gag, Gag-pol and Env are equivalent to other retroviruses, and the other six genes encode only HIV-1 specific functions. The gag precursor is a group specific antigen that encodes for the capsid protein (CA, p24), the matrix protein (MA, p17), nucleocapsid protein (NC, p7), p6 protein and two spacer peptides (p1 and p2).²⁸ The viral protease will process the polypeptides into their structural proteins that will later comprise the virus capsid structure. The gag-pol encodes for the viral enzymes: protease (PR), reverse transcriptase (RT), RNase H, and integrase (IN) that are necessary for replication of the virus. Tat is a transcriptional activator

protein and it is responsible for the transcription of viral genes and triggers cellular processes from neighboring cells that ingest it.²⁹ Rev is an RNA binding protein required for HIV-1 replication. Rev binds to the viral RNAs and secures a pathway out of the nucleus without going through the host cell native pathway of RNA splicing.³⁰ The other four genes Vif, Vpr, Vpu, and Nef are important for CD4 T-cell depletion, enhance infectivity of the HIV-1, and are not required for replication.³¹

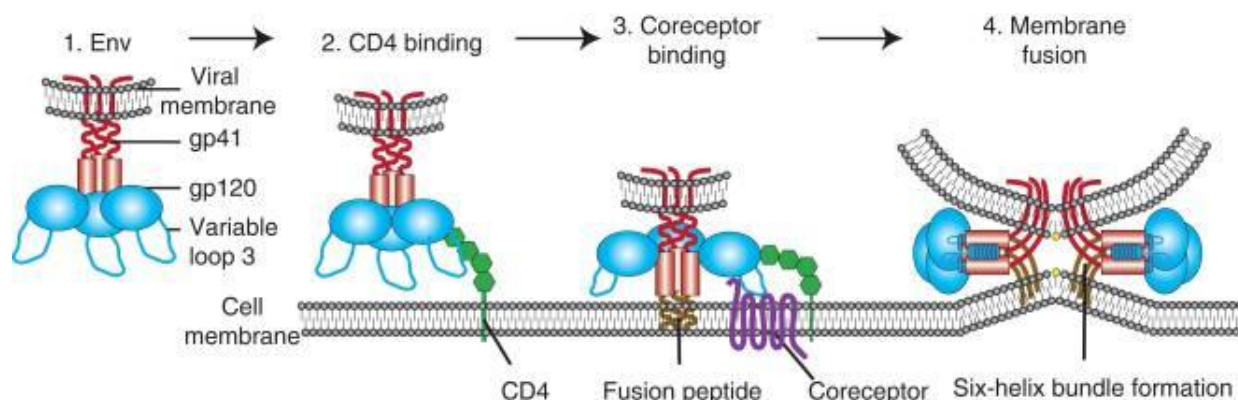


Figure 1.2: HIV-1 Fusion with a Host T cell.

Figure Adapted from Wilen et al.³²

HIV-1 engages with the host cells through an interaction between the viral surface-expressed Env protein, a glycoprotein gp160, and the host cells CD4 receptor. Gp160 is composed of gp120 and gp41. HIV-1 gp120 binds to the CD4 receptor and triggers a conformational change establishing an additional interaction with the host's chemokine receptor CCR5 or CXCR4.^{33,34,35} Previous binding events activate the gp120-CD4-chemokine receptor complex to dissociate from the Env protein and exposes the HIV's gp41 fusion peptide. HIV's gp41 is responsible for pulling the viral and cell bilayers together thereby creating an entry into the plasma membrane of the host cell, outlined in Figure 1.2.

The virus's ability to bind CCR5 versus CXCR4 is called viral tropism and depends on what co-receptor is present at the time of infection. Nearly 90% of early transmitted HIV virions use the CCR5 co-receptor to start the fusion mechanism and are termed macrophage-tropic (M-tropic).³⁶ Macrophages are found in almost every bodily tissue and are often overlooked during initial infection because past methods to cultivate these human-derived macrophages were very difficult

and unsuccessful. Macrophages serve as a primary reservoir for infection, are more resilient than T-cells to cytopathic effects, and undergo a unique budding from the cell into cellular multivesicular bodies. CCR5 co-receptor's relative expression is higher than its counterpart CXCR4 and is present not only on macrophages but also on dendritic cells, T memory cells, T-activated CD4 lymphocytes, gut-associated lymphoid tissues, and microglia. Expression of CXCR4 mainly occurs on T naïve cells, T resting CD4 lymphocytes, B cells, neutrophils, and eosinophils. Eventually, the virus in around 50-60% of infected individuals will develop the preference for cells that express the CXCR4 co-receptor and become T-lymphocyte tropic (T-tropic). Some HIV infections display a dual-tropic function for both CCR5 and CXCR4.^{37,38}

After complete fusion with the target cell, the viral capsid enters the cytoplasm of the cell. A controlled uncoating process begins at the start of the conical shell, which then dissociates to reveal the virion's genomic RNA and regulatory proteins.³⁹ Following the entry into the cell, the viral RNA is converted into proviral DNA by viral enzyme reverse transcriptase (RT). Upon completion, transportation of the viral DNA into the nucleus of the cell takes place wherein the virals' integrase (IN) enzyme binds the viral DNA and inserts itself into the host cell DNA randomly. The host cell machinery produces the viral's proteins as long polyproteins containing genetic material encoding for Gag, Gag-pol, Env polyproteins, and other accessory proteins through transcription and translation. The HIV infected cell will continue to harbor and replicate proviral DNA for the entire lifespan of the cell. The newly synthesized viral proteins and RNA start to gather around the inner membrane and begin to bud immature viral particles from the host cell. Proteases (PR) cleave the polyproteins into fully formed individual structural and functional proteins. The immature particles then become mature, infectious virions and continue to infect further cells.^{28,26} Each phase of the HIV viral life cycle is represented in Figure 1.3.

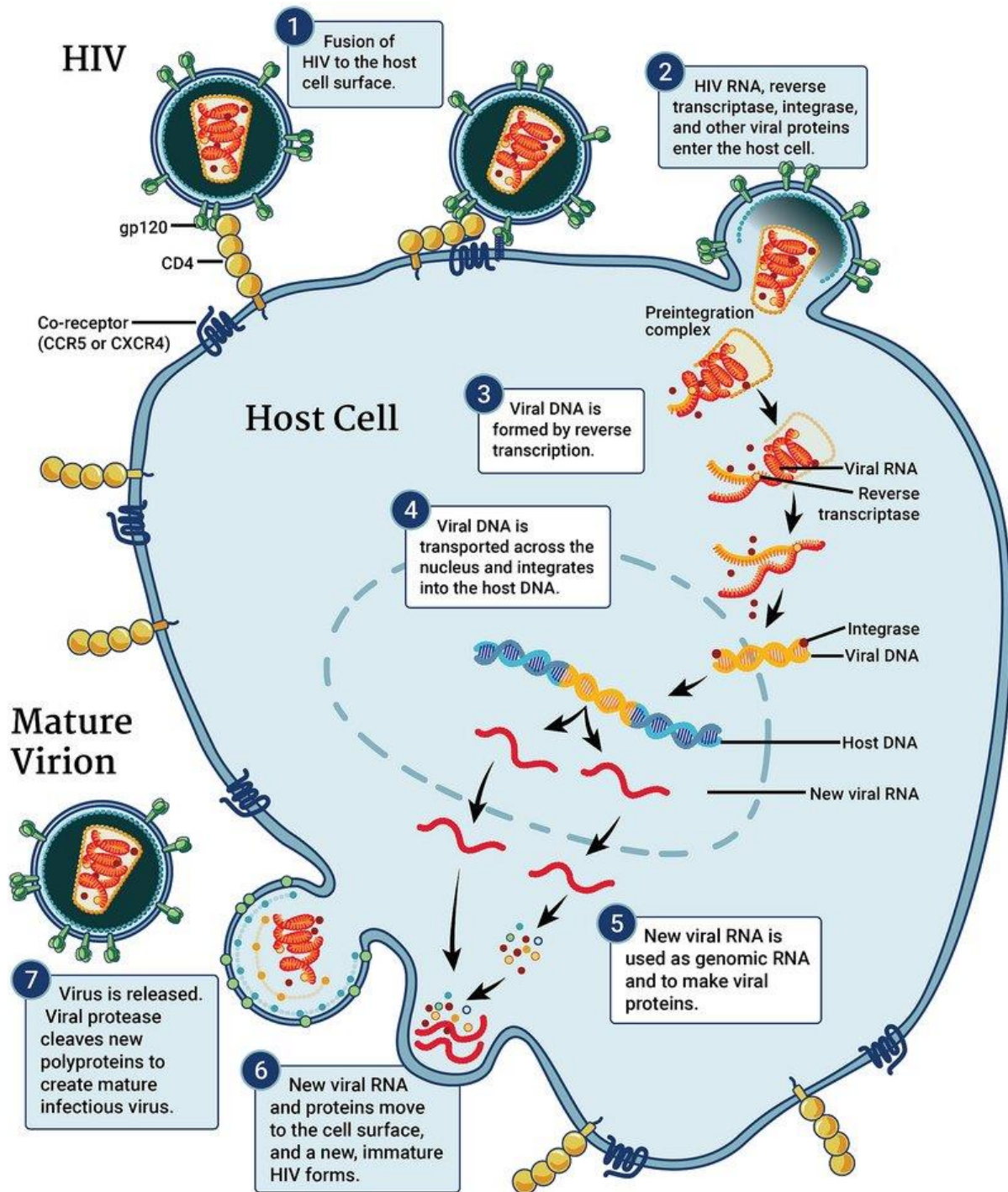


Figure 1.3: HIV Life Cycle.

Adapted from The National Institute of Allergy and Infectious Diseases⁴⁰

1.4 Treatments of HIV/AIDS

To date, two cases involving the complete resolution of HIV have been documented. Both patients are no longer taking antiretroviral drugs and months have passed with no detection of the virus. The technique was first successful in 2008 on a male patient who contracted both HIV and acute myeloid leukemia. The conventional treatment for patients with leukemia who fail to respond to any chemotherapy is an allogeneic bone-marrow transplant as their next plausible treatment option. However, no transplant has ever been successful in an HIV positive patient. HIV relies on a CD4 surface receptor and CCR5 or CXCR4 receptor to enter macrophages and helper T cells. CCR5 co-receptor has proved to be critical for HIV-1 infection and transmission. Complete knockout of CCR5 prevented the HIV-1 infection in cultured transgenic macrophages.^{41,42} Haematologist, Gero Hütter, noted these previous studies and found a donor who had a genetic deletion for the CCR5 co-receptor. The patient from Berlin, Timothy Ray Brown, was cured of both HIV-1 and acute myeloid leukemia by difficult stem-cell transplantation.⁴³ Efforts to reproduce this miracle were unsuccessful until a decade later. In March of 2019, a second patient was cleared of the HIV infection after receiving a similar stem-cell transplant.⁴⁴ A bone-marrow transplant is a very difficult procedure in general. All of the patient's blood cells are destroyed and restored with stem cells from a healthy donor. This technique leaves the patient susceptible to further infections and rejection of the planned transplant. Also, the risks that accompany such treatment are a lot higher and outweigh those of an antiretroviral drug therapy plan. Another strain of HIV-1 can bind the CXCR4 receptor, and some patients contain both HIV strains that utilize either CCR5 or CXCR4 receptors which renders this treatment not an option for those infected HIV patients. After years of scientific advancements, could this be the end of the HIV/AIDS epidemic? The two success stories are very encouraging but non-reproducible.

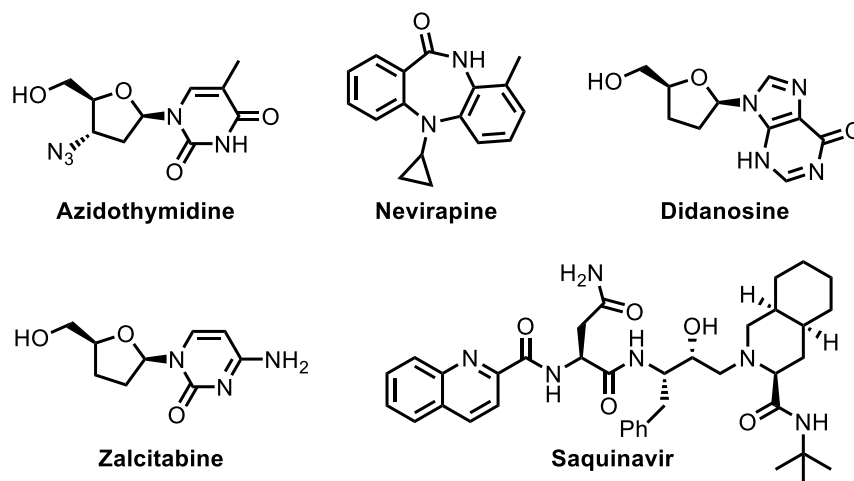


Figure 1.4: Structures of Initial Antiretroviral Drugs for the Treatment of HIV/AIDS

Combination antiretroviral therapy (cART) has been shown to reduce the HIV rate of replication, lower the risk of transmission, and help HIV infected patients to live longer and healthier lives. Azidothymidine (AZT) was the first antiretroviral drug approved for the treatment of HIV/AIDS. AZT was designed as a cancer treatment by NCI long before the AIDS epidemic but proved ineffective as an anti-cancer therapy drug. NCI underwent a screening protocol for possible drug targets for HIV/AIDS.⁴⁵ AZT tested positive as a promising treatment option and quickly was advanced to the clinical market. Studies revealed AZT to slow down the progression of the HIV infection and decrease AIDS-related deaths.⁴⁶ In 1987, the U.S. Food and Drug Administration (FDA) approved AZT. However, patients soon started to present serious side effects from taking AZT and the virus was building up a resistance to AZT within a few days rendering the treatment plan ineffective.^{47,48} Researchers focused on reducing the rate of HIV progression with combination drug therapy with AZT. Results from a clinical trial in 1996 presented that a combination drug therapy of AZT, Nevirapine, and Didanosine was more effective compared to patients who received only AZT.⁴⁹ In the more advanced stages of HIV, the double drug combination showed no significant improvement in reducing the viral infection. Initial drug regimens focused on using only nucleoside reverse transcriptase inhibitors (NRTI). Incorporation of Saquinavir (SQV) in 1995-1996, a protease inhibitor, along with the two-drug therapies reduced the virus to minimal levels and increased the effectiveness of the treatment regimen.⁵⁰ Structures

of initial antiretroviral inhibitors are shown in Figure 1.4. Combination of two different inhibitor classes created highly active antiretroviral therapy (HAART) and is a potential treatment option for the HIV/AIDS epidemic.

Extensive studies of binding, fusion, reverse transcription, integration, replication, assembly, and budding of HIV has allowed for the development of multiple antiretroviral FDA approved drugs for the treatment of the HIV-1 infection, shown in Table 1.1.⁵¹ Entry inhibitors block the binding of gp120 to CD4. The fusion peptide gp41 is needed to bind and penetrate the host cell membrane and inhibition of this pathway led to fusion inhibitors. Reverse transcriptase inhibitors contain two classes: nucleoside reverse transcriptase inhibitors and non-nucleoside reverse transcriptase inhibitors. In general, RT promotes the transcription of the viral RNA into DNA and reverse transcriptase inhibitors halt this process and slow down HIV viral replication. Integrase inhibitors overturn the enzyme integrase ability to incorporate the proviral cDNA into the host cell DNA. Lastly, protease inhibitors disrupt the development of mature virions by inhibiting the processing of immature viral polyproteins to active enzymes and structural proteins that are necessary for further infection.

Table 1.1: FDA Approved HIV/AIDS Drugs

| Drug Class | | | |
|--|-----------------------------|--------------|--------------------|
| | Generic Name | Brand Name | FDA Approval Date |
| Nucleoside Reverse Transcriptase Inhibitors (NRTIs) | | | |
| | zidovudine (azidothymidine) | Retrovir | March 19, 1987 |
| | didanosine | Videx | October 9, 1991 |
| | zalcitabine | Hivid | June 19, 1992 |
| | stavudine | Zerit | June 27, 1994 |
| | lamivudine | Epivir | November 17, 1995 |
| | abacavir | Ziagen | December 17, 1998 |
| | tenofovir | Viread | October 26, 2001 |
| | adefovir | Hepsera | September 20, 2002 |
| | emtricitabine | Emtriva | July 2, 2003 |
| Non-Nucleoside Reverse Transcriptase Inhibitors (NNRTIs) | | | |
| | nevirapine | Viramune | June 21, 1996 |
| | | Viramune XR | March 25, 2011 |
| | delavirdine | Rescriptor | June 12, 1997 |
| | efavirenz | Sustiva | September 17, 1998 |
| | etravirine | Intelence | January 18, 2008 |
| | rilpivirine | Edurant | May 20, 2011 |
| | doravirine | Pifeltro | August 30, 2018 |
| Protease Inhibitors (PIs) | | | |
| | saquinavir | Invirase | December 6, 1995 |
| | ritonavir | Norvir | March 1, 1996 |
| | indinavir | Crixivan | March 13, 1996 |
| | amprenavir | Agenerase | April 15, 1999 |
| | atazanavir | Reyataz | June 20, 2003 |
| | fosamprenavir | Lexiva | October 20, 2003 |
| | tipranavir | Aptivus | June 22, 2005 |
| | darunavir | Prezista | June 23, 2006 |
| Fusion Inhibitors/Entry Inhibitors | | | |
| | enfuvirtide | Fuzeon | March 13, 2003 |
| | maraviroc | Selzentry | August 6, 2007 |
| | ibalizumabuiyk | Trogarzo | March 6, 2018 |
| Integrase Inhibitors (INs) | | | |
| | raltegravir | Isentress | October 12, 2007 |
| | | Isentress HD | May 26, 2017 |
| | dolutegravir | Tivicay | August 13, 2013 |
| | elvitegravir | Vitekta | September 24, 2014 |
| Pharmacokinetic Enhancers | | | |
| | cobicistat | Tyboost | September 24, 2014 |

1.4.1 Entry and Fusion Inhibitors

Inhibitors that target different aspects of HIV-1 entry and fusion pathways are effective towards highly resistant HIV strains, lower the number of latent HIV reservoirs, decrease the cytopathic immune response, and increase the immune responses.^{52,53} Thus, the HIV entry and fusion mechanisms offer multiple antiviral targets and provide emerging opportunities for drug development. Entry and fusion antiviral drugs mainly target the gp120-CD4 interaction, gp120 interaction with co-receptor, gp41 pocket, and fusion. Enfuvirtide was approved by the FDA in 2003⁵¹ and is still the only fusion inhibitor to date. Enfuvirtide binds to HIVs gp41 protein preventing the HIV and host cell membranes from interfering.⁵⁴ The structure of Enfuvirtide is shown in Figure 1.5.

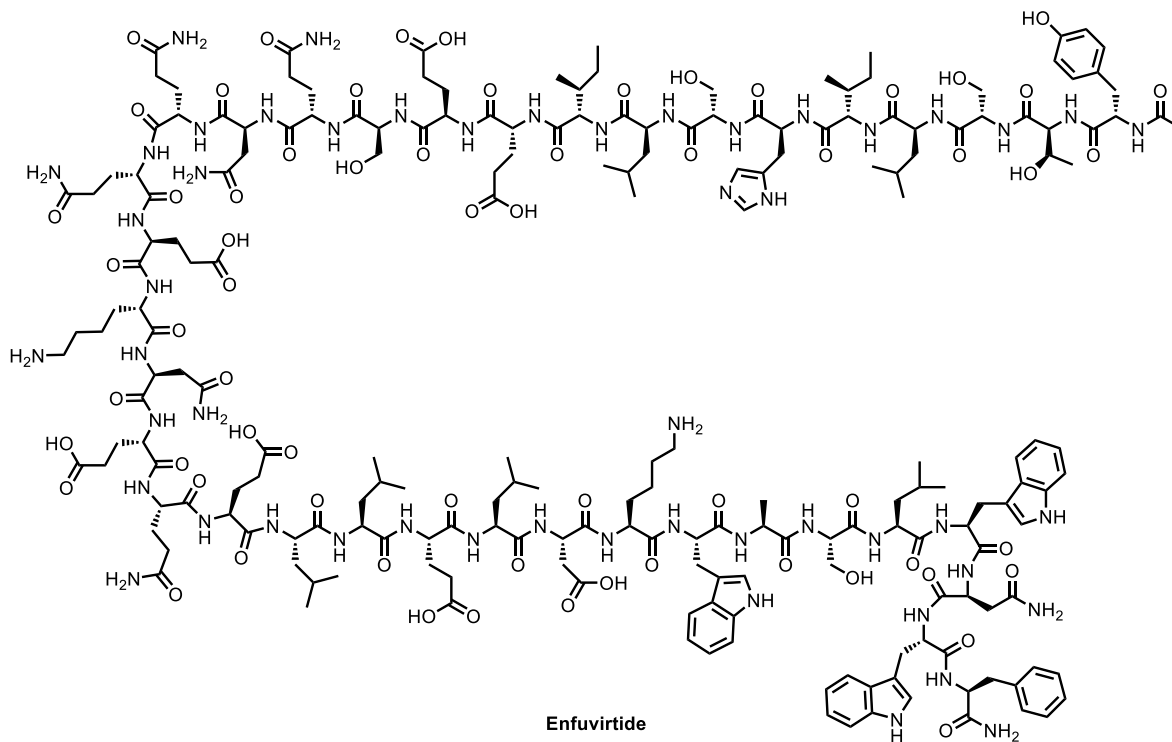


Figure 1.5: Structure of Entry Inhibitor Enfuvirtide

During the initial stages of infection, HIV-1 predominantly exists as an R5-tropic virus that enters the host cell via the CCR5 co-receptor.³³ TAK-779 was the first potent antagonist that blocked HIV-1 from binding to CCR5, but the bioavailability profile was not suitable for further development and was therefore halted.⁵⁵ However, TAK-779 did set the stage for further advancement of CCR5 inhibitors and investigations towards CXCR4 inhibitors. AMD3100 was

the first potent CXCR4 antagonist but was halted due to its low oral bioavailability.⁵⁶ CCR5 and CXCR4 inhibitors offer patients with advanced HIV-1 infection another treatment option because their mechanism of action was unique from other antiretroviral therapies. The binding of either CCR5 or CXCR4 inhibitors alter the conformation of the CCR5 or CXCR4 receptor thus preventing it from engaging with the CD4-gp120 complex and obstructs the HIV-1 infection.⁵⁵ Initial *in vitro* studies revealed the virus's ability to create different conformations of its viral gp120 protein and induce resistance towards this class of inhibitors which created a need for further advancements of the current compounds. Maraviroc (MVC) was FDA approved in 2007 and has been the only successful CCR5 inhibitor. One major limitation of MVC was the requirement of the identification of viral tropism present in the infected patient before administration of treatment. Structures of TAK-779, AMD3100 and MVC are shown in Figure 1.6. In 2018, Ibalizumab was approved by the FDA as a post-attachment inhibitor.⁵¹ Ibalizumab, a monoclonal antibody, prevents HIV-1 gp120/gp41 conformational change by binding to the CD4 extracellular domain and prevents the secondary binding to co-receptors CCR5 and CXCR4, thus, averting viral entry. This significant interaction allows Ibalizumab to be a successful treatment option for both CCR5 and CXCR4-tropic HIV strains.^{57,58} Inhibition of the HIV-1 entry sites for therapeutic opportunities are shown in Figure 1.7.

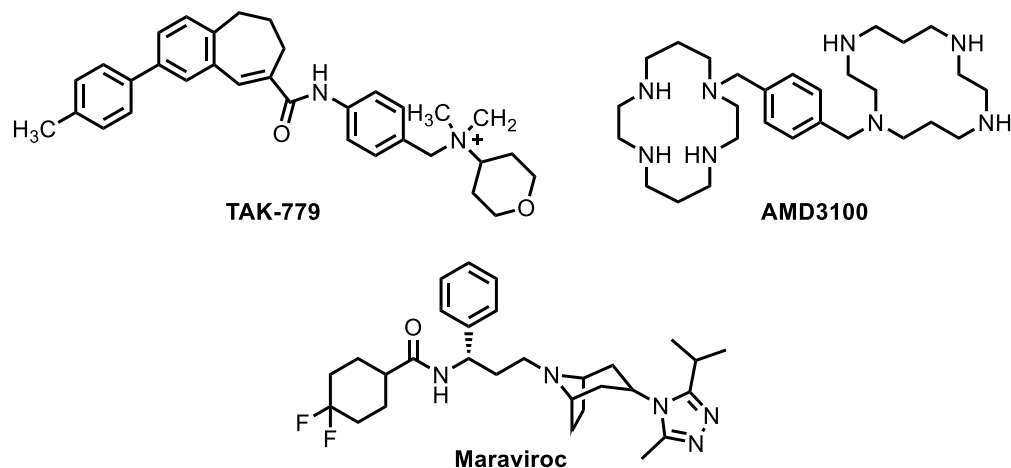


Figure 1.6: Structures of CCR5 and CXCR4 Inhibitors

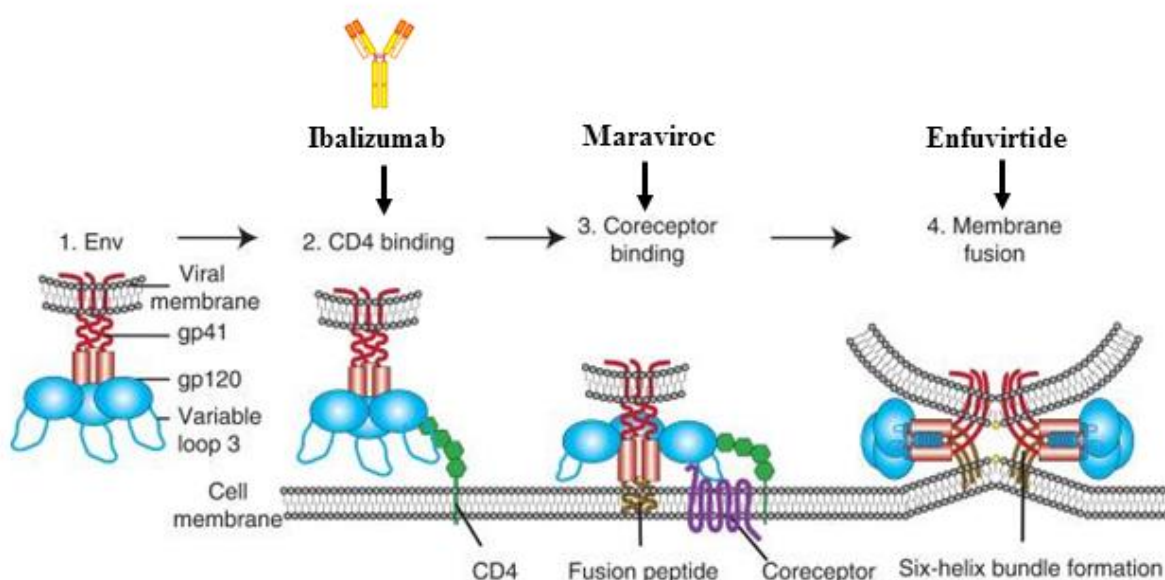


Figure 1.7: Inhibition of HIV-1 Entry.

Figure Modified from Wilen et al.³²

1.4.2 Reverse Transcriptase Inhibitors

Reverse transcriptase (RT) is an RNA-dependent DNA polymerase which reverse transcribes the virions positive single-stranded RNA into double-stranded proviral DNA. RT is a heterodimer composed of two major subunits, labeled p51 and p66. Each subunit adapts a ternary complex in the shape of a claw. The large p66 contains two major active sites: Polymerase and Ribonuclease H (RNase H). Polymerase copies DNA or RNA templates and mirrors the human right hand. RT enzymatic active sites contain the thumb, palm, fingers, and connecting regions which are shown in Figure 1.8. The active site formed in the palm region of p66 acts as a clamp to position the DNA or RNA template-primer to this catalytic site. RNase H cleaves the RNA-DNA complex and its active site centralizes between the connection region and p51 subunit.^{59,60} Deletion of RNase H resulted in non-infectious HIV. Thus, the RNase H domain is an additional drug target for antiviral therapies.⁶¹ The smaller p51 subunit contains similar domains as p66 but plays more of a structural role for the RT enzyme.

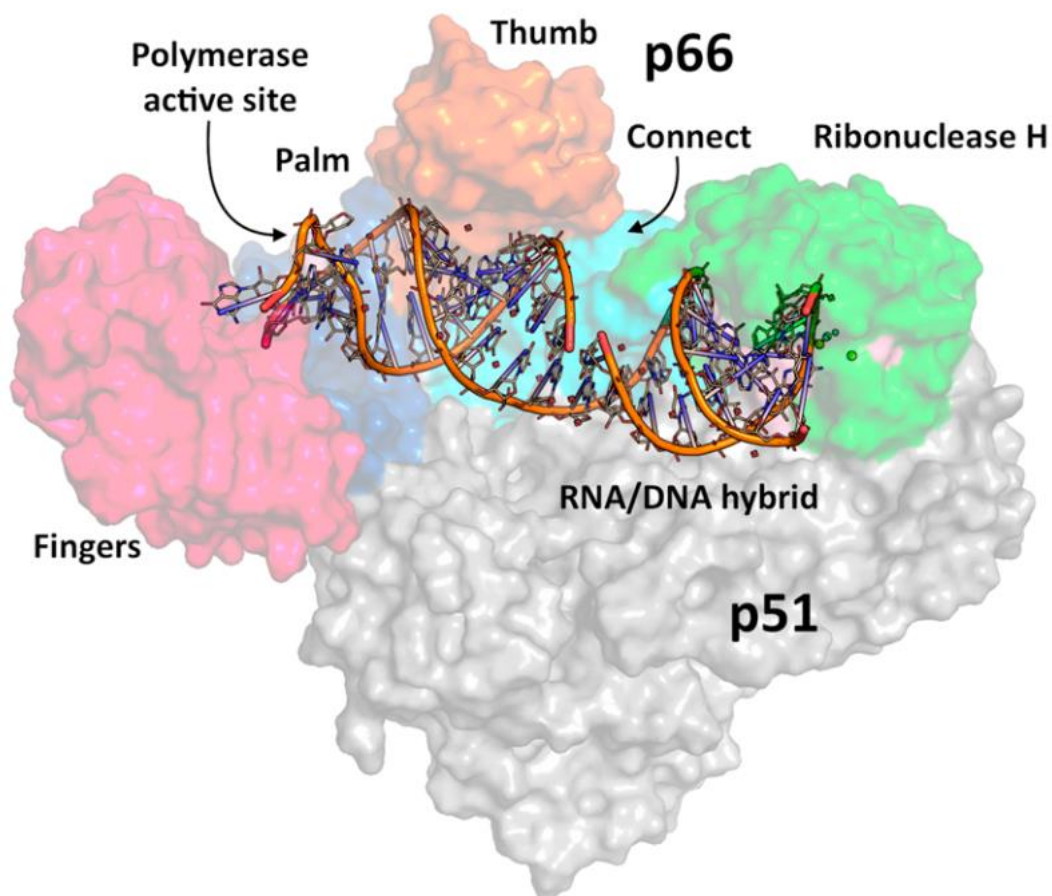


Figure 1.8: Reverse Transcriptase Active Site: Thumb, Palm, Fingers, and Connection.

Figure Adapted from Namasivayam et al⁶²

RT was the first HIV enzyme targeted for antiretroviral activity and nearly half of current FDA approved antiretroviral drugs target RT, shown in Table 1.1.⁵¹ HIV-1 reverse transcriptase inhibitors break into two main classes: nucleoside reverse transcriptase inhibitors (NRTIs) and non-nucleoside reverse transcriptase inhibitors (NNRTIs).

1.4.2.1 Nucleoside Reverse Transcriptase Inhibitors

Since the discovery of AZT in 1987, eight additional NRTIs have been created. Structures are shown in Figure 1.9. NRTIs originated from natural DNA synthesis substrates (purines and pyrimidines). AZT is a derivative of thymidine and Emtricitabine, Lamivudine a derivative of

cytidine, and Abacavir from deoxyguanosine. When initially dosed, these inhibitors are inactive. NRTIs are converted to active phosphorylated nucleoside analogs by cellular kinases in three different phosphorylation stages. The first phosphorylation occurs by deoxynucleoside kinases and often is the rate-limiting step. Nucleoside monophosphate (NMP) kinases are responsible for the second phosphorylation and a variety of cellular kinases can undergo the final phosphorylation step.⁶³ These NRTI triphosphates act as RT inhibitors by competing with the host's endogenous nucleosides for their incorporation into the viral DNA. Each inhibitor lacks a key 3'-hydroxyl group that is needed for the natural binding of the next nucleotide, thus, halting the viral DNA from elongating and terminating viral replication.^{64,65}

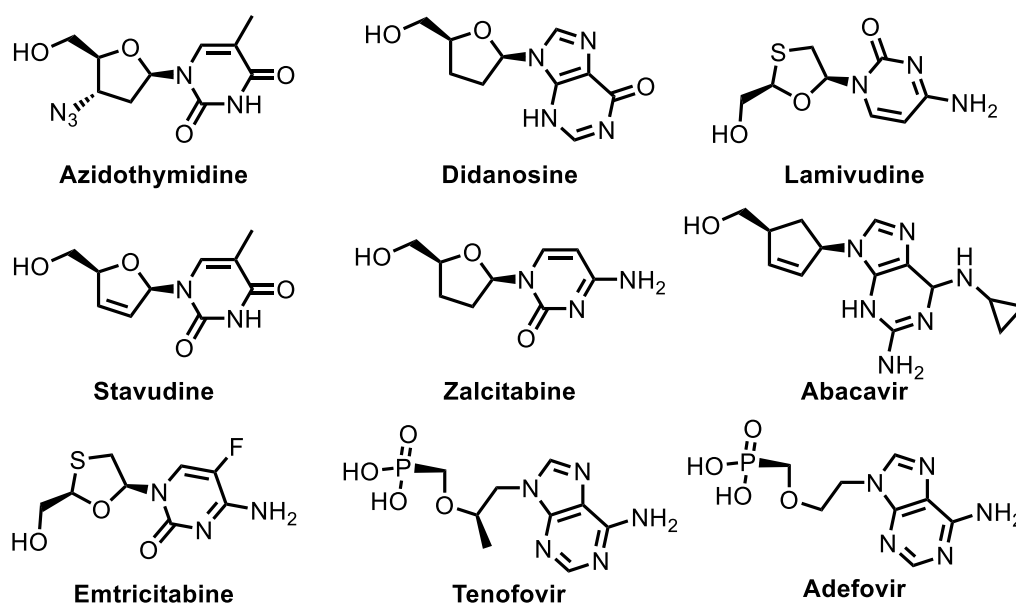


Figure 1.9: Structures of Nucleoside Reverse Transcriptase Inhibitors

1.4.2.2 Non-Nucleoside Reverse Transcriptase Inhibitors

The non-nucleoside reverse transcriptase inhibitors (NNRTIs) are allosteric inhibitors that bind directly to RT and induce the formation of a hydrophobic pocket that is around 10 Å from the polymerase active site.⁵⁹ This pocket is known as the NNRTI-binding pocket (NNIBP) and has been shown to not interfere with the RT active site directly. This unique feature has allowed both NNRTI and NRTIs to be used in combination to enhance cART. Binding of NNRTIs creates a

structural change that reduces the polymerase activity and restricts the viral DNA synthesis. The first generation of inhibitors were Nevirapine, Delavirdine, and Efavirenz. They all experience a butterfly-like binding motif, as demonstrated in Figure 1.10. A significant π - π interaction takes place between Tyr181 and Tyr188. HIV-RT is a very error-prone enzyme, and mutations that occur in or nearby the NNIBP led to major resistance towards the first generation of NNRTIs. This low-genetic barrier was observed because the initial drugs were structurally rigid and could not bind to the NNIBP successfully.⁶⁶ The second generation consists of Etravirine and Rilpivirine. They are known to accommodate mutations that occur in the NNIBP by increasing their structural flexibility and their ability to adopt a horseshoe-like confirmation, shown in Figure 1.10.⁶⁷ This allowed an additional interaction with residue W229 which is a less frequent mutated residue. The third generation of Doravirine emerged recently to incorporate a vital hydrogen bond to the backbone of the enzyme with carbonyl K101.⁶²

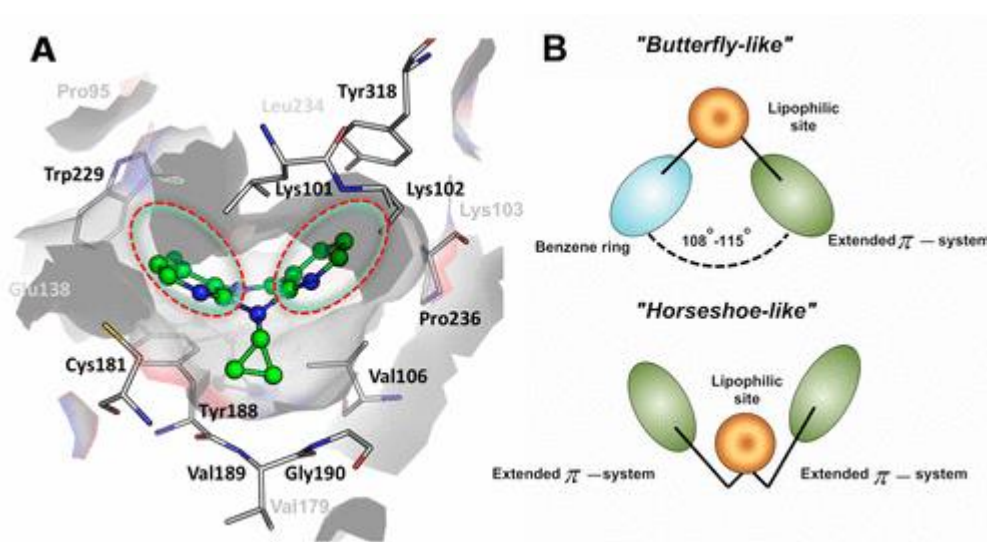


Figure 1.10: Active site of Nonnucleoside Reverse Transcriptase Inhibitors.

Figure Adapted from Namasivayam et al⁶²

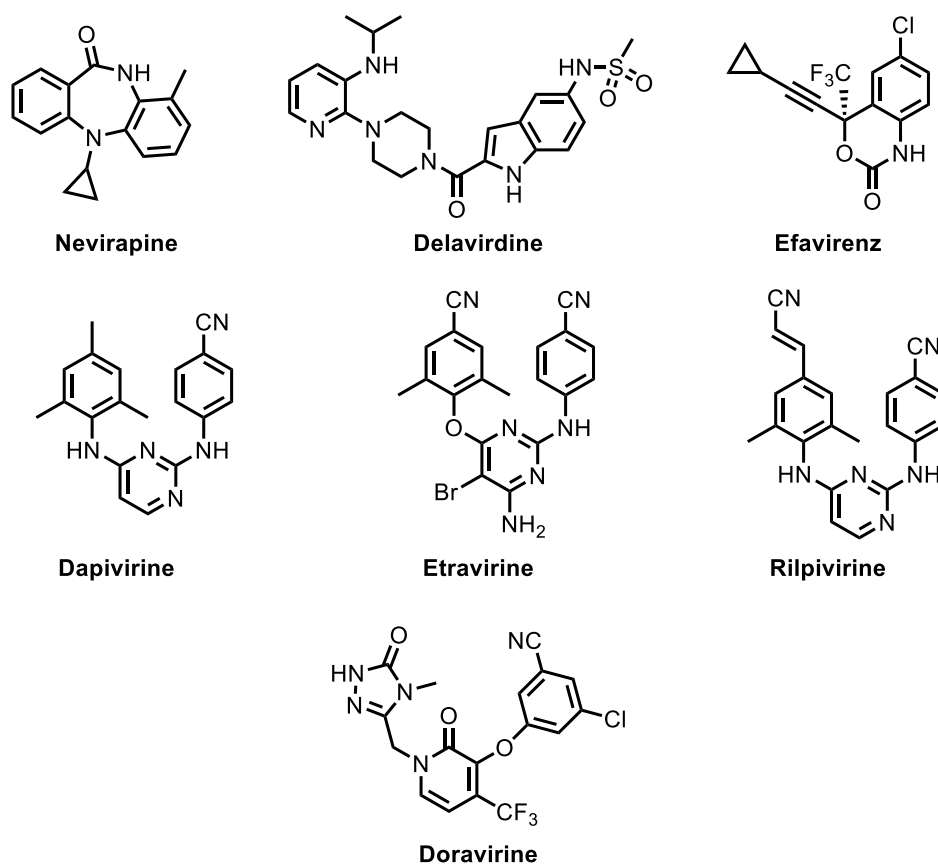


Figure 1.11: Structures of Nonnucleoside Reverse Transcriptase Inhibitors

1.4.3 Integrase Inhibitors

The HIV integrase (IN) inserts viral DNA irreversibly into the host cellular DNA via four major steps. Directly following RT, IN enzyme first interacts with a new viral DNA transcript and cellular cofactors to form the pre-integration complex (PIC). IN removes the terminal nucleotides on each viral DNA which exposes the desired 3' hydroxyl group. The PIC enters the host cell and DNA strand transfer begins. The HIV IN binds to the DNA of the host cell and slices each DNA strand in order to expose the 5' phosphate groups. PIC then covalently binds the host cell 5' phosphate groups to the viral DNA 3' hydroxyl groups. Completion of the strand transfer triggers the host cell enzymes to make repairs to any of the gaps between the viral and host cell DNA. Current IN inhibitors prevent the PIC from binding to the host cell DNA and halts integration and replication.⁶⁸ IN inhibitors Raltegravir, Elvitegravir, and Dolutegravir, shown in Figure 1.12, binds

with high affinity to the PIC only when it is complexed with the host cell DNA and stops the strand transfer.⁶⁹ Structures of IN inhibitors are shown in Figure 1.12.

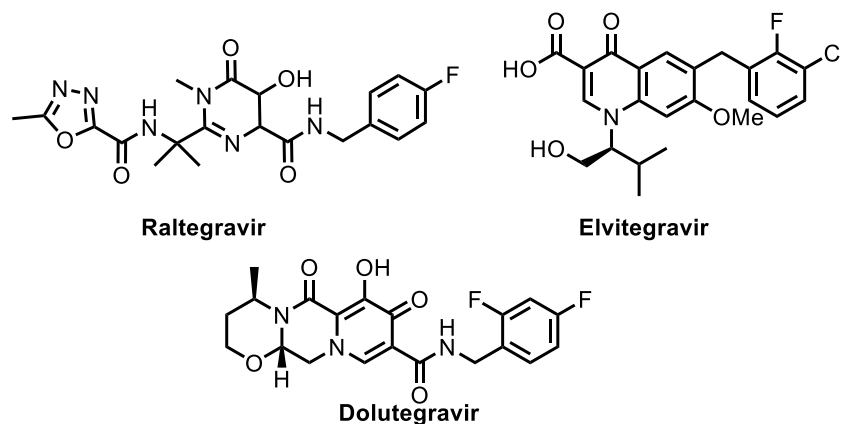


Figure 1.12: Structures of Integrase Inhibitors

1.4.4 Protease Inhibitors

During the final stages of the HIV life cycle, the viral RNA, Gag, Gag-Pol polyprotein precursors and accessory proteins all migrate to the host cell's outer membrane. The various genetic material begins to bud immature viral particles from the cell. At this point, the HIV proteases (PR) are activated and cleave themselves from the Gag-Pol polyprotein. The free PR enzyme starts to cleave specific peptide bonds on the Gag and Gag-Pol polyproteins to construct the viral's specific enzymes: reverse transcriptase (RT), integrase (IN), and other structural proteins. The completion of this process alters the outer capsid structure and yields fully mature infectious virions.⁷⁰ Inactivation or absence of retroviral PR prevents the maturation of viral particles, and as a result, infectious virions are never formed. This makes viral PR a potential antiretroviral drug target.⁷¹ In 1995, Saquinavir was the first HIV-1 PR inhibitor to become an FDA approved the protease inhibitor (PI) and led to the development of a total of ten clinically approved PIs.⁷²

1.5 HIV-1 Protease

The HIV-1 protease is classified as a retroviral aspartic acid protease and structurally very similar to human and other eukaryotic aspartic proteases: pepsin, renin, and others. Creating a

particular drug without inhibiting the host enzymes made initial drug development towards retroviral proteases a challenging task. The discovery of renin inhibitors by a substrate-based approach promoted a higher selectivity of viral proteases. Crystal structures of many aspartic proteinases have been identified and reveal that many are monomeric, bilobal, and are twice as large as HIV-1 proteases.

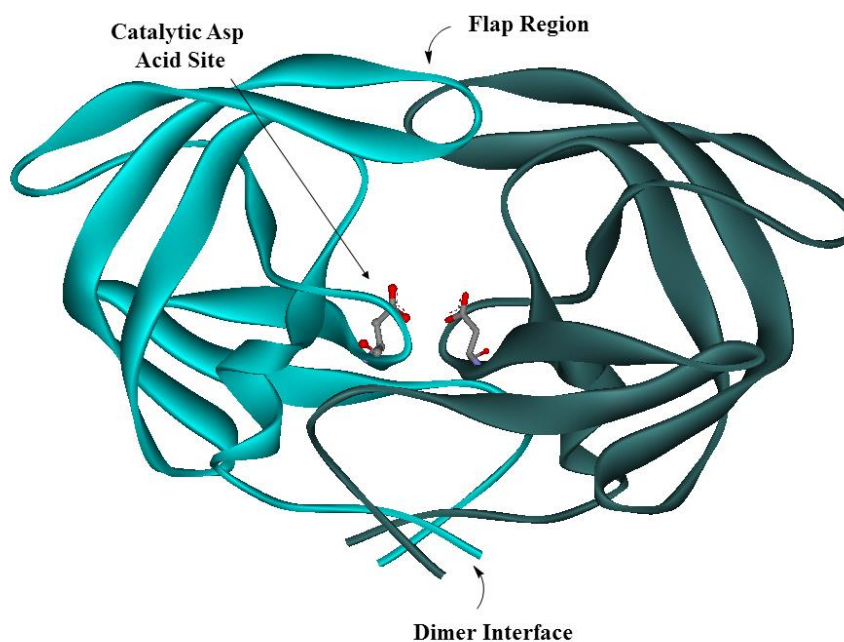


Figure 1.13: X-ray Crystal Structure of Wild-Type HIV-1 Protease (PDB: 2PCO)

X-ray crystal structures of the HIV-1 protease demonstrate that the viral PR is a dimer and each monomer contains 99 amino acids, as shown in Figure 1.13.⁷³ All aspartic proteases, including HIV-PR, share common catalytic active sites within a conserved Asp-Thr-Gly sequence - two catalytic aspartic acid groups tightly bonded to a water molecule and a flap region. Specifically, the HIV-PR active site takes place at the interfaces of where the monomers come together forming a symmetrical and open active site. Structurally, one beta strand from each monomer come together in the shape of a glycine-rich flexible loop to serve as the entrance into the active site known as the flap region. The flap exists in an open conformation in the absence of a substrate and folds down in the presence of a substrate. The base of the active site consists of the two N and C-termini coming together to form a dimer interface. The catalytic active site consists

of Asp25-Thr26-Gly27 and Asp25'-Thr26'-Gly27' residues from each subunit. This catalytic Asp-Thr-Gly triad interacts via a hydrogen bonding network in the absence of a substrate. The catalytic aspartic acid residues Asp25 and Asp25' mediate the cleavage of the peptide bond. Asp25 and Asp25' activates the conserved water to participate in a nucleophilic addition to the carbonyl on the native peptide. A stabilized geminal diol tetrahedral intermediate results and undergoes a hydrolysis step to complete the cleavage of the peptide bond to yield two new products, shown in Figure 1.14.⁷⁴

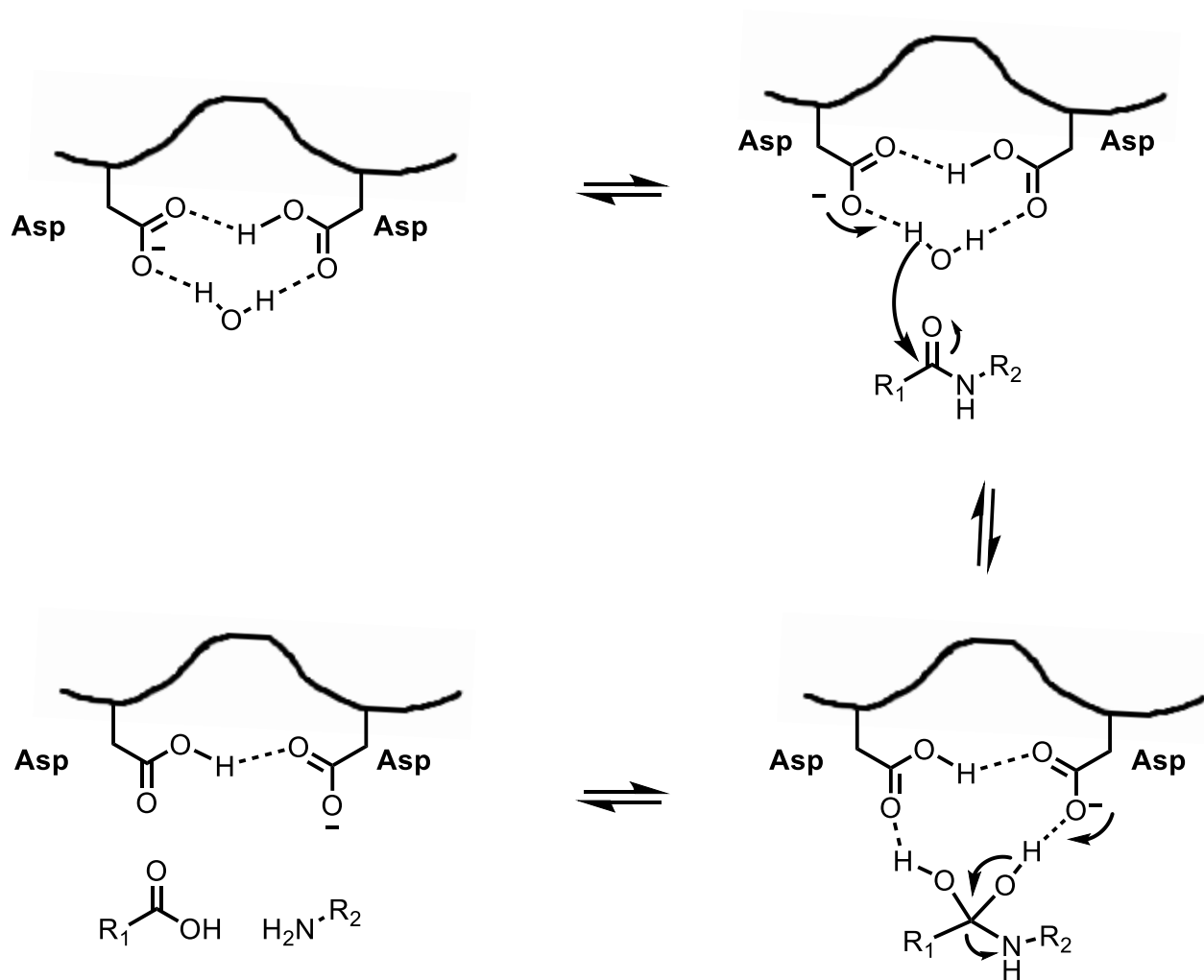


Figure 1.14: Mechanism of Catalytic Aspartic Acids Hydrolyzing the Native Peptide Bond

The major differences between HIV PR and non-retroviral aspartic proteases are the orientation, interactions of the flap region, and the more symmetrical environment in the viral protease's ligand binding site. HIV PR contains two flaps that lay parallel to the bound substrate and the non-viral aspartic proteases only have one flap that lies perpendicular to the bound substrate.⁷⁵ Also, the flap region moves approximately 7 Å where the single flap of non-aspartic proteases deviates about 2 Å.⁷⁶ These substantial conformational changes in the flap region allow the substrate to interact more closely and accounts for six hydrogen bonds between the enzyme and inhibitor whereas its counterpart only involves two to three hydrogen bond interactions. Another difference between the two is the size of the active site; HIV PR prefers a minimum of seven residues and non-aspartic proteases require only five residues for efficient catalysis.

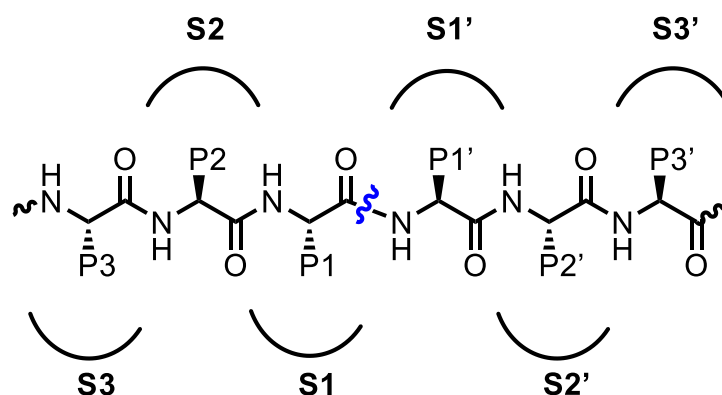


Figure 1.15: Native Substrate Bound to HIV-PR Enzyme

Studies have revealed the HIV-PR active site is a highly specific enzyme and the binding of the native substrates favor an extended conformation with a minimum of seven residues that interact strongly with the enzyme, shown in Figure 1.15. Standard nomenclature labels the ligands branching to the left of the cleavage site in chronological order: P1, P2, P3, and P4. The same is true for the other subunit with the nomenclature as P1', P2', and P3'. As shown in Figure 1.15, the scissile bond is colored blue and located in the center of the enzyme in between P1 and P1'. The subsites of the enzyme are S4 to S3' and numbering stems from its binding to its matched P ligand. Typically, the enzymes S1, S1', S3, and S3' subsites mainly prefer hydrophobic-like residues. Whereas, S2 and S2' subsites can accommodate either polar or hydrophobic residues.⁷⁷ Earlier X-ray studies revealed important hydrogen bond interactions with the enzyme and substrate are

shown in Figure 1.16. The binding patterns to various peptidomimetic inhibitors served as a basic model for drug development.⁷⁸

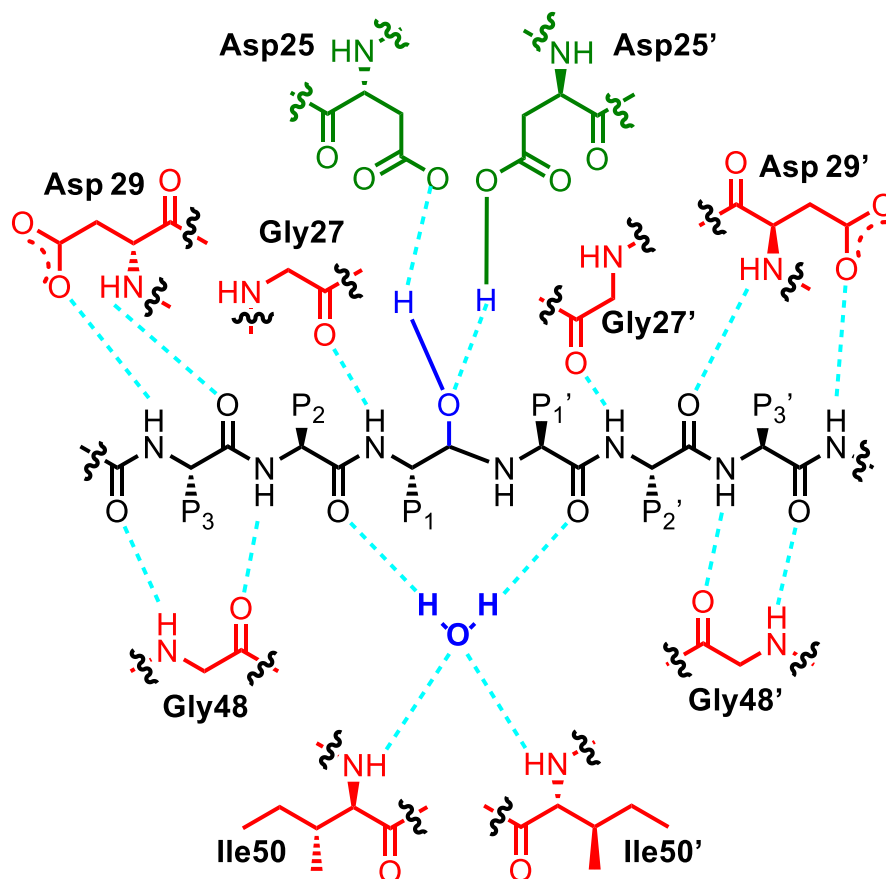


Figure 1.16: Important Hydrogen Bond Interactions of HIV-1 PR with Substrate⁷⁹

1.5.1 First Generation HIV Protease Inhibitors

Saquinavir (SQV) was the first FDA approved PI, in 1995. When adding SQV and reverse transcriptase (RT) inhibitors together for treatment, they greatly reduced HIV-1 viral loads and replication of the virus. SQV based treatment marked the beginning of HAART because patients were finally showing improvements and reducing the onset of AIDS. SQV features a hydroxyethylamine isostere that is non-cleavable and binds to the HIV-PR in an extended fashion. The central hydroxyl group hydrogen bonds to the catalytic aspartic acid residues and mimics the transition state of the hydrolysis step by the formation of the tetrahedral intermediate, shown as Figure 1.17.^{80,81} SQV acts as a competitive inhibitor with the natural substrate and displays an

enzyme inhibitory activity K_i of 0.12 nM. Soon Ritonavir, Indinavir, Nelfinavir, and Amprenavir were created and contained a similar hydroxyethylamine isostere, shown in Figure 1.18. Abbott Laboratories developed Ritonavir with an activity of K_i of 0.015 nM.⁸² Ritonavir also deactivated the enzyme, cytochrome P450 that allowed its overall pharmacokinetic properties to increase.⁸³ Today, treatment regimens continue to dose ritonavir as a pharmacokinetic booster with other PIs. The Merck group found that a larger hydroxyethylene isostere was well accommodated and led to a more potent compound, Indinavir with a K_i of 0.36 nM.⁸⁴ Nelfinavir is an enhanced version of SQV and has a K_i of 2.0 nM.⁸⁵ Nelfinavir incorporated a unique phenyl thioether that interacts in the S1 and branches into the S3 subsite for additional favorable interaction with the active site. Amprenavir features an aminobenzenesulfonamide group that interacts closely with the flap region via water-mediated hydrogen bonds.⁸⁶ This first generation's highly peptidic chemical structures caused their low half-life, poor oral bioavailability properties, and undesirable side effects. The most concerning problem was the emergence of drug-resistant strains rendering most of this generation to lose activity. New inhibitors with less peptide-like features, activity towards drug resistance strains, lower drug toxicity, and improved bioavailability were the next focus.

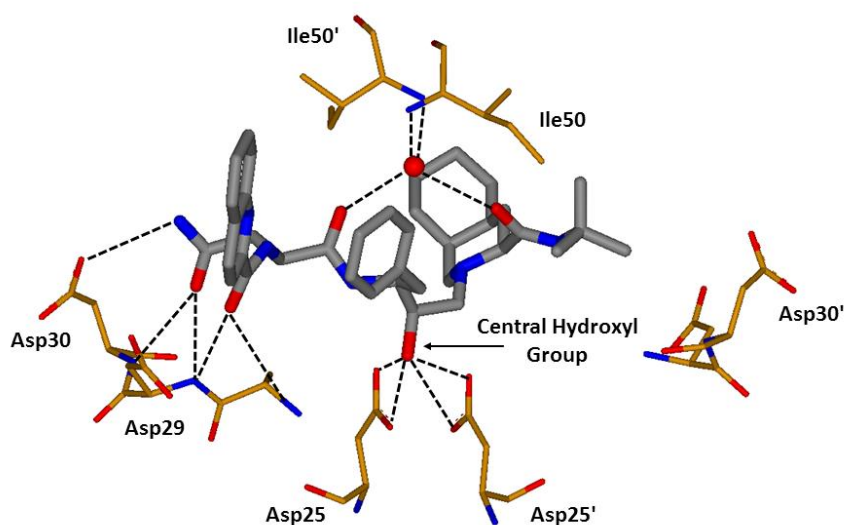


Figure 1.17: X-ray Structure of SQV Complexed to HIV-PR (PDB: 3OXC)

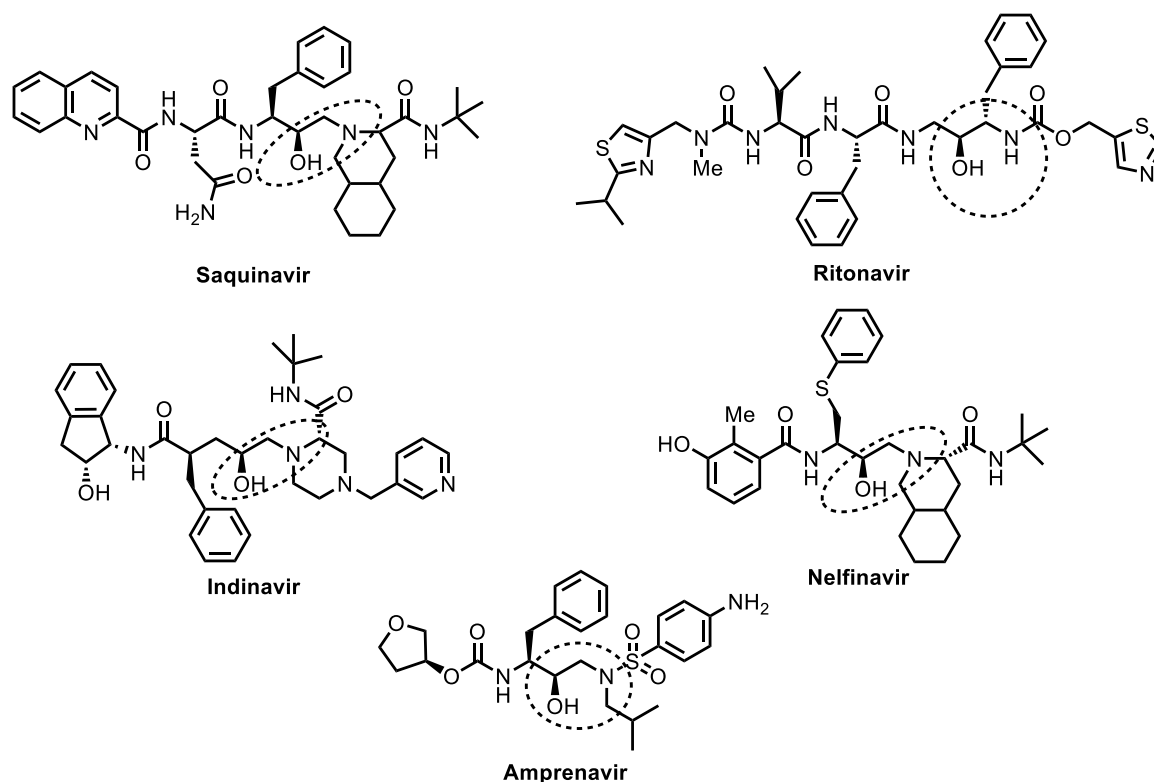


Figure 1.18: First Generation of Protease Inhibitors

1.5.2 Second Generation HIV Protease Inhibitors

Due to the limitations of the first generation of HIV PIs, the second generation of PIs was developed: Lopinavir, Atazanavir, Amprenavir, Tipranavir, and Darunavir, shown in Figure 1.19. Lopinavir was developed to overcome ritonavir resistant HIV-1 strains with a K_i of 1.3 pM.⁸⁷ Atazanavir had an impressive bioavailability and antiviral activity profile towards HIV resistant strains with a K_i of 2.66 nM.⁸⁸ Atazanavir was the first PI that allowed a single daily dose. Tipranavir is a non-peptidic PI with an impressive antiviral profile and a K_i of 8 pM. Today, Tipranavir containing regimens are mainly used as a last resort against highly resistant HIV strains because of its severe cytotoxicity toward the patient.⁸⁹ Darunavir displayed the greatest antiviral activity profile, minimal cytotoxicity and a high genetic barrier towards multidrug-resistant HIV-1 strains.⁹⁰ DRV HIV-1 resistant strains started to emerge making drug resistance a growing issue.

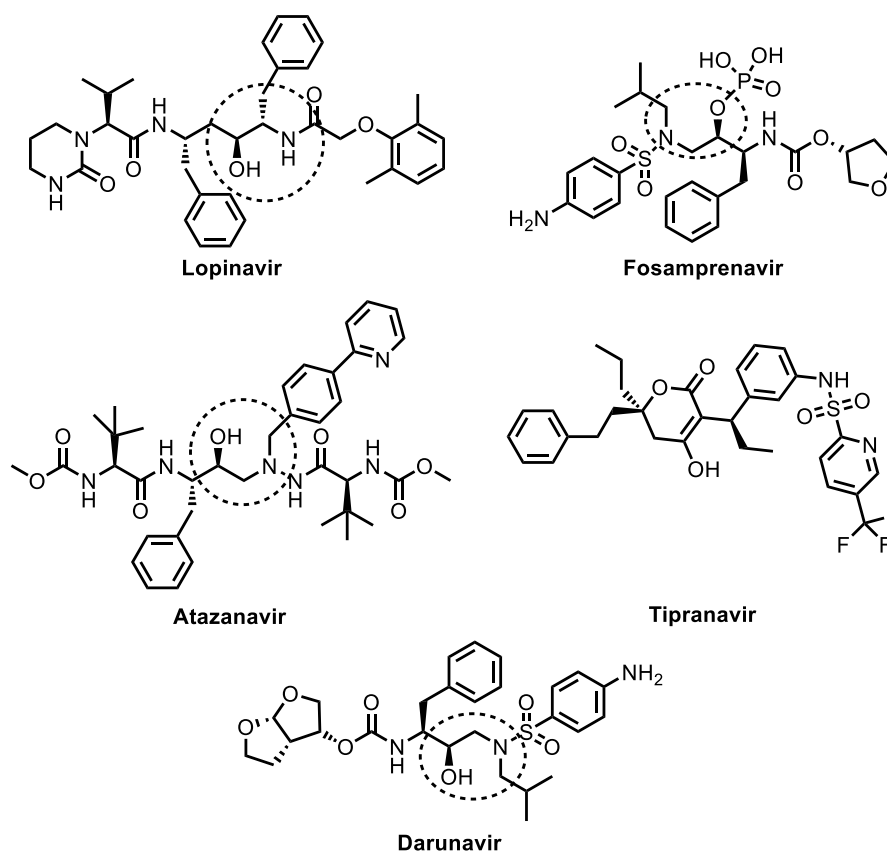


Figure 1.19: Second Generation of Protease Inhibitors

1.5.3 The Fight Against Drug Resistance

The World Health Organization (WHO) installed a global plan for minimizing the emergence of HIV drug-resistant strains because despite scientific advancements HIV drug-resistant strains are a global threat and render current treatments ineffective.⁹¹ During the replication process of HIV, reverse transcription takes the viral RNA and creates viral DNA to incorporate into the host cell. RT is very error prone because it lacks major proofreading mechanisms and replicates at a very high rate.⁹² This process is a result of the evolutionary pressure of the virus to survive and replicate under any harsh conditions. Thus, many genetic variations are produced, and the new mutant strains can then further replicate to generate even more diverse variants. These mutations affect the ability of drug or combination of drugs to inhibit replication of the virus due to their inability to bind/inhibit their specific target.

HIV-1 PR mainly takes part in two types of mutations: primary and secondary. Primary mutations are mutations of active site residues and they disrupt substrate binding. Secondary mutations occur outside of the active site and are known to accommodate a primary mutation to balance the active site into order to retain native substrate binding. It has been well documented that 45 residues of the 99 residue amino acid sequence of HIV PR are known to mutate, but maintain normal function.⁹³ Interestingly, only 11 of the residues are primary mutations, and the remaining mutations take place in the flap region, dimer interface or distal sections of the PR enzyme.⁹³

1.5.3.1 Backbone Binding Concept

All of the current PIs have a known mutation that reduces overall binding affinity. Many mutations based inhibitor designs have added ways to combat drug resistance. However, another strategy arose when X-ray structures of the inhibitor bound to wild-type HIV-1 PR were compared to various mutant proteases. The results showed that the backbone conformation of the active site essentially remained unchanged. The minimal distortion can be explained by the virus' need to maintain native substrate binding. Knowledge of this phenomenon led to the concept and application of "backbone binding" for further inhibitor design to combat drug resistance.⁹⁴ This strategy was built on the basis that a PI will interact with the backbone carbonyl oxygens and amide nitrogens of the enzyme extensively and maintain its interactions in the presence of multiple mutant variants.

1.5.3.2 Darunavir

Darunavir (DRV) revealed extensive hydrogen bonding to the backbone of the active site and is the first FDA approved PIs that is used as first-line therapy for the treatment of HIV. DRV has maintained an impressive antiviral profile against many multidrug-resistant HIV-1 strains. DRV potency can be explained by its dual mechanism of action to forms extensive interaction with the backbone of the active site and inhibition of HIV PR dimerization. DRV incorporates a privileged bis-tetrahydrofuranyl (bis-THF) ligand as the P2 ligand along with an (*R*)-(hydroxyethylamino)sulfonamide isostere amine as the P2' ligand, shown in Figure 1.20.⁹⁰ X-ray crystal structure of DRV-bound to HIV-1 PR illustrated a series of important hydrogen-bonds (HB) to occur mainly in the S2 and S2' subsite.⁹⁵ Both oxygens on the bis-THF ligand form HB to the

backbone residues, Asp30 and Asp29. The P2' portion of DRV hydrogen bonds to the backbone of the active site and interacts with a water molecule to further access an additional HB interaction. Specifically, HB interactions are with Gly27, Asp25, Asp25' and water-mediated HBs are with Ile50' and Ile50, shown in Figure 1.20. These stated unique binding properties have been used to expand upon the ligand-binding interactions of the active site of HIV-1 protease and provide significant insight towards many new generations of PIs.

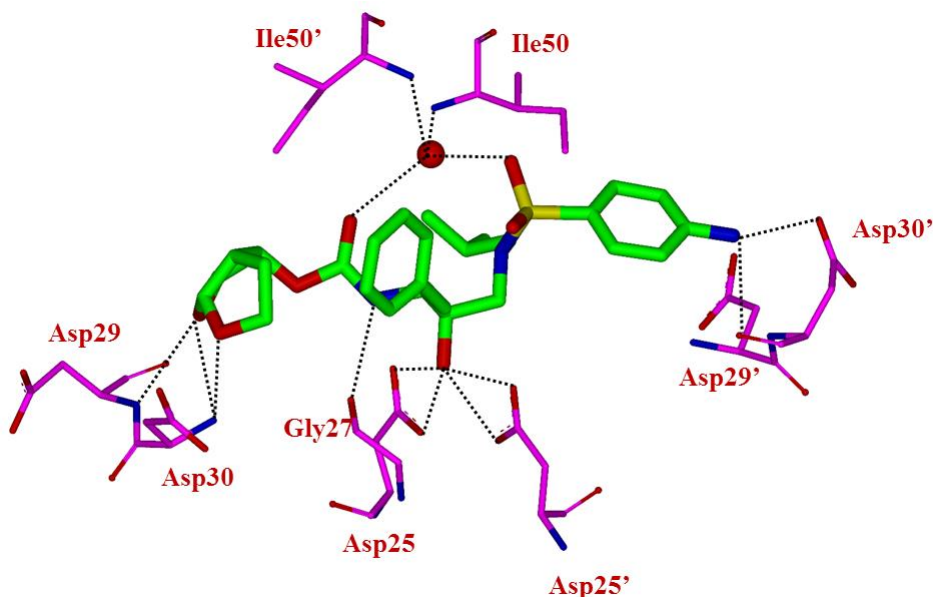


Figure 1.20: X-ray Structure of HIV-1 PR Bound to Darunavir (PDB: 2IEN)

1.6 Design, Synthesis, and Biological Evaluation of HIV-1 Protease Inhibitors with an Oxazolidinone P2 ligand

1.6.1 Introduction

Despite the advancements in combatting HIV/AIDS, no treatment exists to eradicate the virus from an infected individual. Treatment regimens are lifelong and prompt less than desirable side effects; drug-drug interactions, toxicity, systemic organ complications, central nervous system HIV-1 triggered disorders and most importantly, drug resistance.⁹⁶ Current therapies are becoming ineffective against these highly virulent strains and make treating long-term viral suppression a growing issue. Therefore, potent and more effective HIV-1 protease inhibitors (PIs) are needed for long-term successful cART.

1.6.2 Design of HIV Protease Inhibitors with an Oxazolidinone P2 Ligand

X-ray crystallographic analysis of both Darunavir (DRV) and TMC-126 exhibited significant hydrogen bonding interactions with the backbone of the active site; chemical structures are shown in Figure 1.21.⁹⁷ Thus, DRV and related TMC-126 facilitated further development of new effective PIs. The Ghosh group and others focused on maximizing hydrogen bonding interactions and polar contacts with the backbone of HIV-1 protease's active site which proved to be an effective strategy towards designing inhibitors that display potent activity against HIV-1 protease. Modifications of multiple PIs throughout the S2 to S2' subsites created very potent inhibitors and showed areas of the active site that can be further exploited.

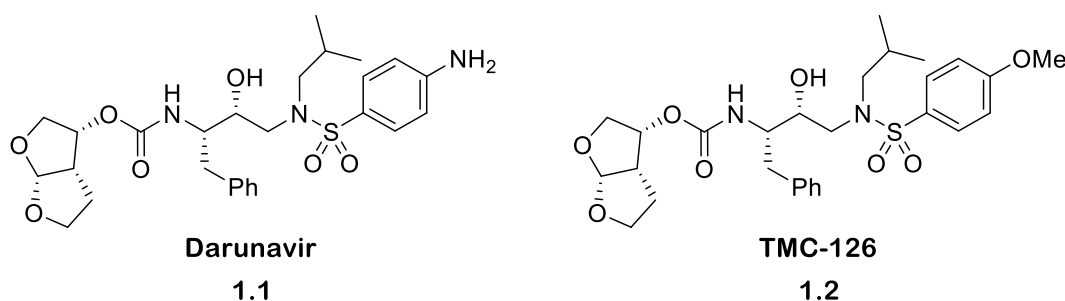


Figure 1.21: Structures of Darunavir and TMC-126

The related compounds **1.3-1.5** were created to enhance interactions in the HIV-1 protease active site and provide insight towards a new generation of potent PIs. Inhibitors **1.3**, **1.4**, and **1.5** were each designed with a similar cyclopentyltetrahydrofuran (Cp-THF) P2 ligand.^{98,99,100} The Cp-THF binds in the S2 subsite and mimics the interactions bis-THF. Inhibitor **1.3** displayed a more potent enzymatic activity than DRV with a K_i of 0.0045 nM and an IC_{50} of 1.8 nM, whereas DRV enzyme inhibition was K_i of 0.016 nM and IC_{50} of 3.2 nM.⁹⁸ Inhibitor **1.3** THF oxygen maintains an important hydrogen bond with the backbone amide NH of Asp29. Inhibitor **1.4** was then designed to incorporate a 1,3-dioxolane, and the X-ray crystal structure revealed the inhibitor to have a similar HB interaction as DRV and **1.3** to Asp29. However, the internal oxygen on the dioxolane ring adds a water-mediated hydrogen bond interaction to Gly48. **1.4** displayed a K_i of 0.11 nM, and antiviral activity IC_{50} of 3.8 nM.⁹⁹ Addition of the internal oxygen maintained the impressive potency profile of previous inhibitors and suggested a potential new binding interaction

with Gly48. Inhibitor **1.5** utilizes a similar moiety as **1.3**, but integrates a methylcarbamate substituent that functions as both a hydrogen bond donor and acceptor to gain access to Gly 48 directly. Inhibitor **1.5** displayed a K_i of 0.0018 nM, and an antiviral activity IC_{50} of 1.6 nM.¹⁰⁰ X-ray data verified that the carbamate nitrogen to form a hydrogen bond with Gly48 carbonyl. A polar contact of the carbamate carbonyl oxygen interacts with Arg8' through a water-mediated hydrogen bond.

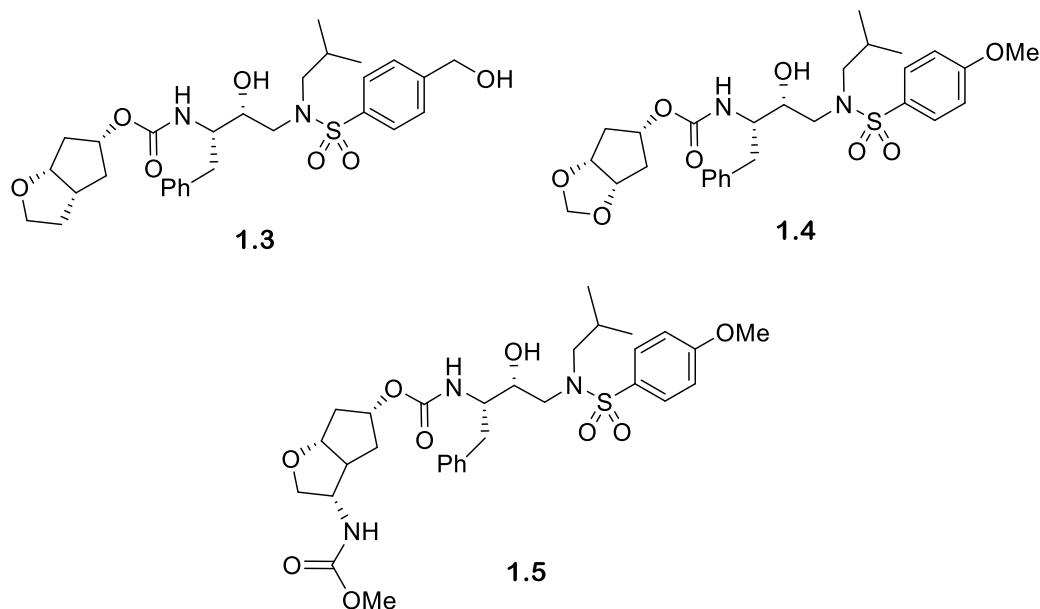


Figure 1.22: Structures of **1.3** - **1.5**

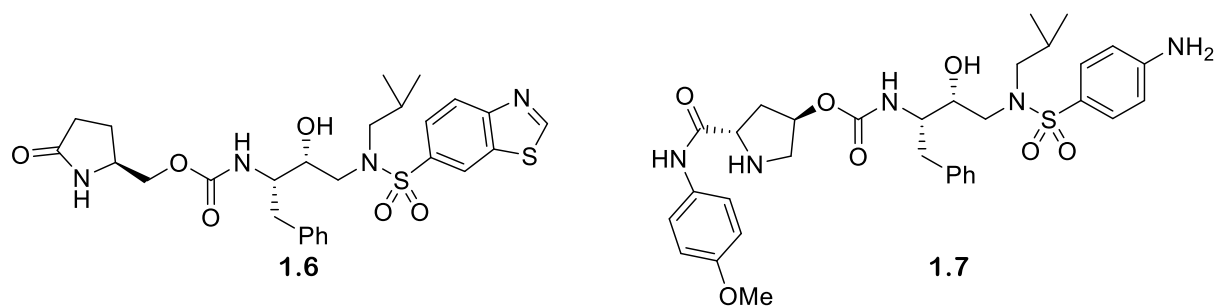


Figure 1.23: Structures of Pyrrolidone **1.6** and Proline-like **1.7**

Incorporation of pyrrolidone and proline-like derivatives in the P2 site have been explored, structures shown in Figure 1.23. Inhibitor **1.6** displayed an enzymatic inhibition of K_i of 0.003 nM

and an EC_{50} of 15.5 nM.¹⁰¹ X-ray analysis of Inhibitor **1.6** showed the carbonyl of the pyrrolidone ligand formed a hydrogen bond interaction with backbone Asp29 amide NH and took part in a water-mediated hydrogen bond with Gly27. Also, the free amine on the ligand picked up an additional water-mediated hydrogen bond with Asp30 amide NH. Furthermore, inhibitor **1.7** displayed an antiviral activity IC_{50} of 15.4 nM.¹⁰² Only a docking study was performed on inhibitor **1.7**; but results showed the ligand's methoxy oxygen making a polar contact with Arg8', the cyclic proline amine interacting in a hydrogen bonding event with Gly48 carbonyl oxygen and the carbamate amine interacting with Asp30 via a hydrogen bond.

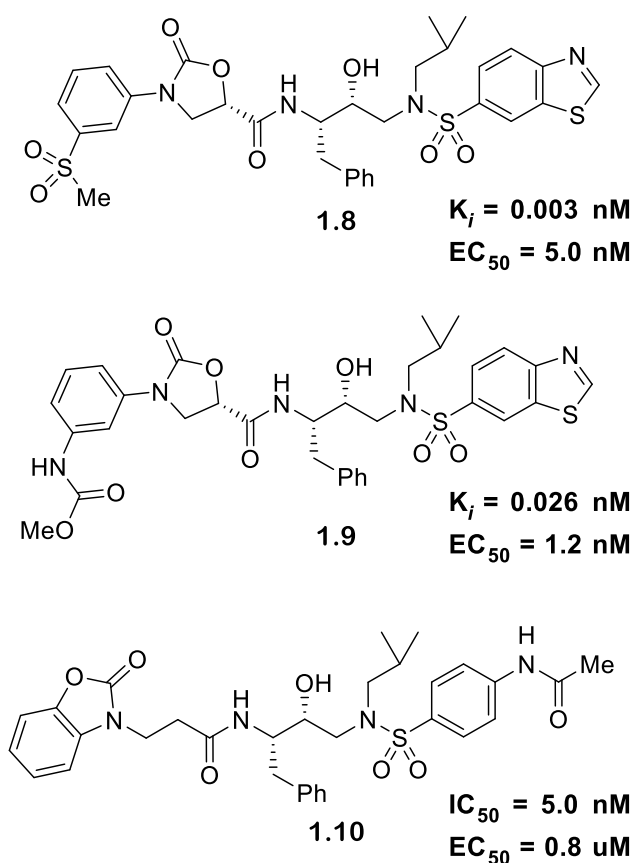


Figure 1.24: Structures of *N*-aryl oxazolidinone Derivatives **1.8** – **1.10**

Furthermore, *N*-aryl oxazolidinone derivatives in the P2 site have also been designed and examined, structures and enzymatic activities are shown in Figure 1.24. Inhibitors **1.8-1.10** all have displayed potent antiviral activity. Inhibitors **1.8** and **1.9** feature an *N*-aryl oxazolidinone and

their K_i values were 0.003 nM, and 0.026 nM and their EC_{50} values were 5.0 nM and 1.2 nM.¹⁰³ Also, **1.8** and **1.9** were tested against mutant HIV-1 variants, and their respective potency was maintained and outperformed FDA approved Lopinavir. **1.10** incorporated a benzoxazolidinone fused ring and displayed the highest potency with an IC_{50} value of 5.0 nM and an EC_{50} value of 0.8 nM.¹⁰⁴

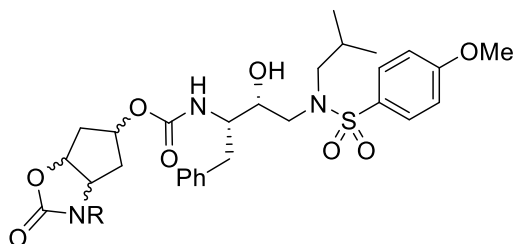


Figure 1.25: Base Model of Inhibitors

Thus, there have been many efforts to discover the preferred occupancy of the S2 subsite by a protease inhibitor that also maintains potency against highly mutated variants. Darunavir bis-THF ligand is well accommodated in the S2 subsite. However, DRV resistant HIV-1 viruses are arising and contribute to the challenge of solving the drug resistance problem. Therefore, it is reasonable to believe that incorporating a different P2 ligand that can expand further on the ligand-binding interactions in the HIV-1 protease active site would be optimal for addressing the fight against highly DRV resistant strains. A new scaffold was envisioned to expand upon previous P2 ligands to function as a hydrogen bond donor and acceptor in a conformationally constrained fused ring system, as seen with DRV and other related structures. This work focuses on transforming the P2 ligand to a novel bicyclic oxazolidinone in order to access new interactions in the active site that have not yet been explored, the structure of the base design of inhibitors is shown in Figure 1.25.

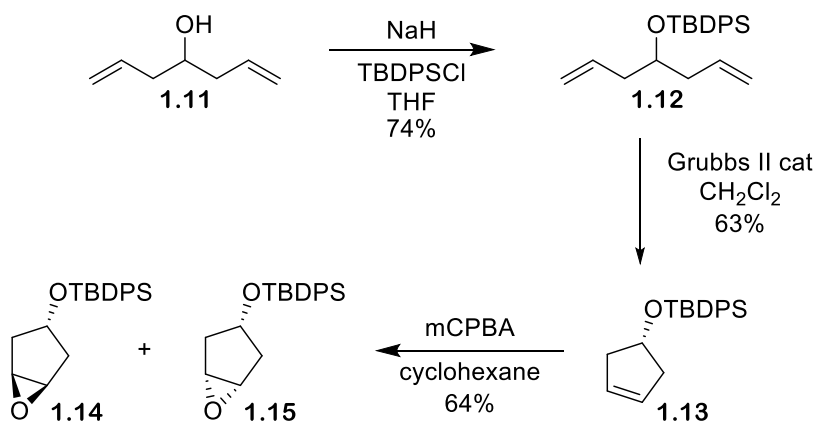
1.6.3 Results

Numerous known protease inhibitors incorporate a diverse range of P2 ligands and maintain potency but fail against highly resistant HIV-1 variants. Previous examinations of the X-ray structure of DRV and other inhibitor-bound HIV-1 proteases suggested that a stereochemically defined bicyclic oxazolidinone P2 ligand would be well accommodated by the HIV-1 active site and afford potential new binding interactions that have not yet been explored. It was planned to

investigate the potential ligand-binding interactions of the P2 subsite further by synthesizing an array of bicyclic oxazolidinone ligands. Also, the oxazolidinone heterocycles are rather small in size and stable to peptidases, which could render favorable pharmacokinetic properties. Thus, an efficient enantiomeric synthesis of various bicyclic oxazolidinone was devised. These inhibitors were evaluated against HIV-1 protease for their enzymatic and antiviral activities. X-ray co-crystal structures of two selected inhibitors bound to HIV-1 protease provided important structural binding interactions in the active site.

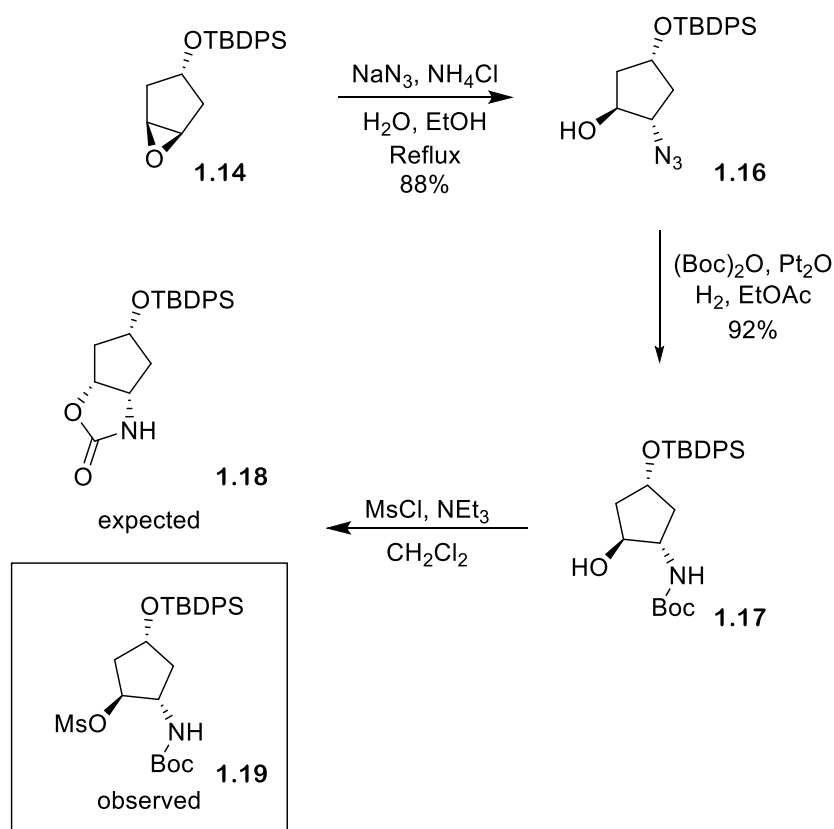
1.6.3.1 Synthesis of Inhibitors

A stereochemically defined inhibitor class was essential for understanding the inhibitors potential binding interactions with the HIV-1 protease active site. Thus, an efficient stereoselective synthesis was devised to incorporate a key optically active P2 ligand with a bicyclic oxazolidinone scaffold and an (*R*)-(hydroxyethylamino)sulfonamide isostere. The synthesis started from commercially available 1,6-hetpadien-4-ol **1.11**; the free alcohol was easily protected with tert-Butyldiphenylsilane **1.12** in 74% yield. Grubbs second generation catalyst was then used to construct silyl protected 3-cyclopentene-1-ol **1.13**.¹⁰⁵ The internal alkene was reacted with *m*-chloroperbenzoic acid (*m*CPBA) to afford a mixture of stereoisomers, trans-epoxide **1.14** and *cis*-epoxide **1.15**.¹⁰⁶ The trans-epoxide was predominantly favored by utilizing cyclohexane as the reaction solvent in a 3 to 1 ratio. Separation of the two diastereomers was performed by column chromatography, and isolation provided the desired trans-epoxide in an overall 64% yield, shown in Scheme 1.1.



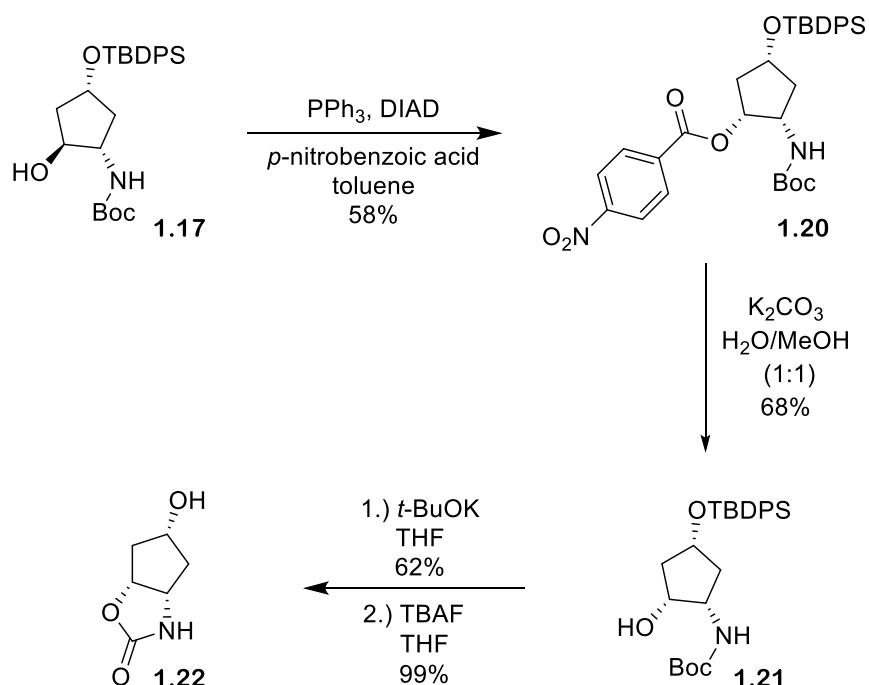
Scheme 1.1: Synthesis of Epoxide **1.14** and **1.15**

Treating the trans-epoxide **1.14** with sodium azide, ammonium chloride in water and ethanol at refluxing temperatures provided the ring opened 1,2-azido alcohol **1.16** in 88% yield.¹⁰⁶ It should be noted that the nucleophilic azide can attack the symmetrical epoxide from either side, thus, producing a racemic mixture. A standard one-pot conversion of azide to Boc-protected amine **1.17** was achieved with Adam's catalyst, di-*tert*-butyl dicarbonate in ethyl acetate under 50 psi of hydrogen in 92% yield.¹⁰⁷ The formation of oxazolidinone **1.18** from Boc protected 1,2-aminoalcohol **1.17** was thought to occur through a base mediated cyclization. However, treatment of **1.17** with methanesulfonyl chloride, triethylamine in dichloromethane was unsuccessful in forming the expected bicyclic oxazolidinone **1.18**, and the observed product was the mesylate intermediate **1.19**, shown in Scheme 1.2. Further attempts to displace the mesylate group and form the desired cyclic product **1.18** were unsuccessful.



Scheme 1.2: Synthesis of Mesylate **1.19**

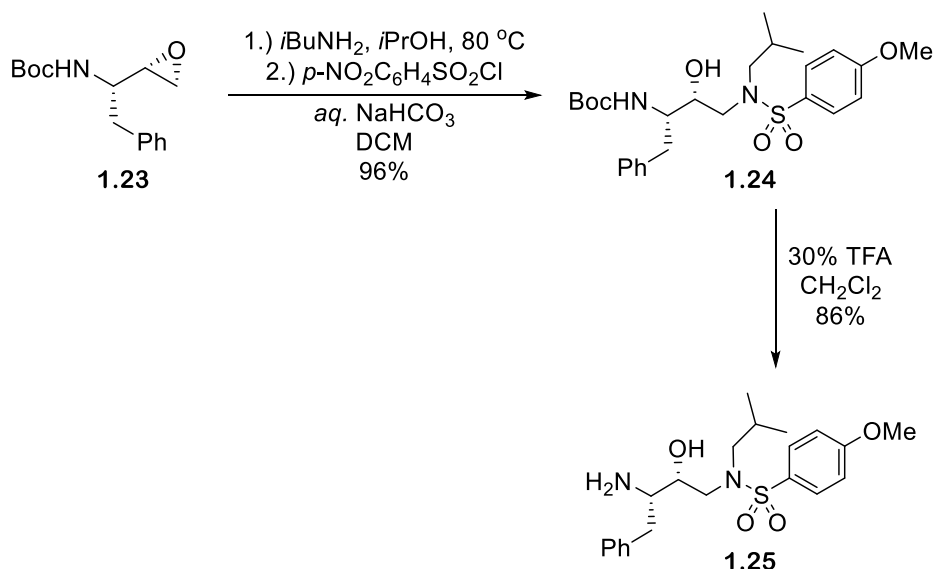
1.17 was then exposed to Mitsunobu conditions of triphenylphosphine, diisopropyl azodicarboxylate (DIAD), and *para*-nitrobenzoic acid in toluene, in 58%.¹⁰⁸ The reaction system gave the corresponding ester **1.20** with inversion of the configuration of the secondary alcohol, shown in Scheme 1.3. Subsequent hydrolysis with potassium carbonate in 1:1 ratio of water/methanol gave alcohol **1.21** in 68%. Potassium *tert*-butoxide in tetrahydrofuran (THF) promoted the base-mediated cyclization in 62%. Finally, the alcohol was deprotected with tetra-*n*-butylammonium fluoride (TBAF) in THF to give the asymmetric bicyclic oxazolidinone scaffold **1.22** quantitatively.



Scheme 1.3: Synthesis of Bicyclic Oxazolidinone **1.22**

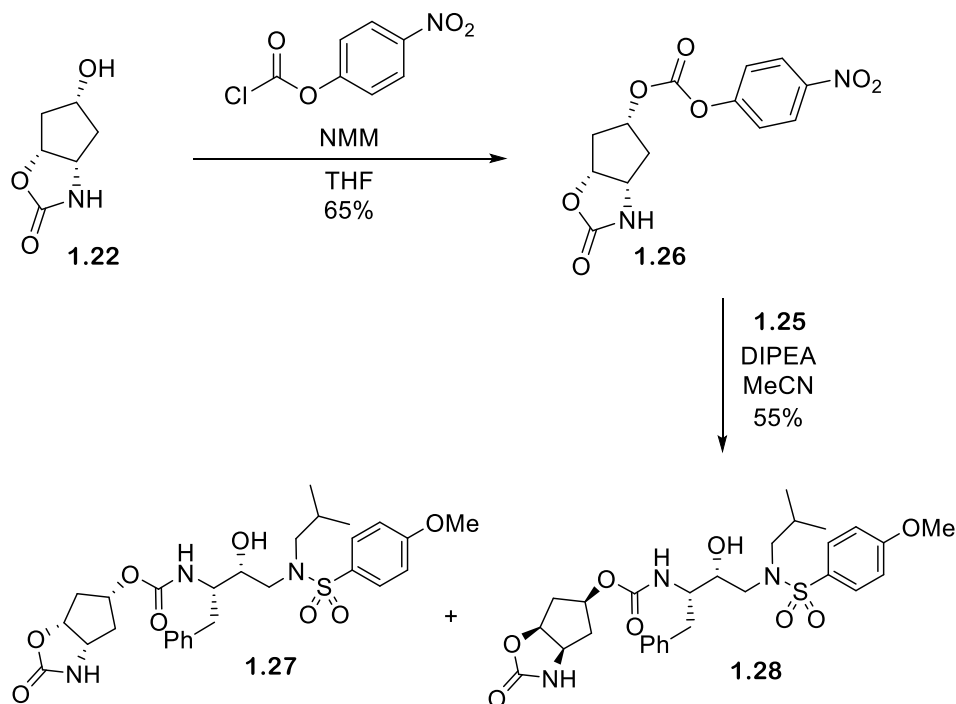
The final HIV-1 inhibitors were synthesized by coupling activated carbonate **1.26** and amine isostere **1.24**, shown in Scheme 1.5.¹⁰⁰ The required isostere was achieved by treating commercially available (2*S*,3*S*)-1,2-epoxy-3-(Boc-amino)-4-phenyl butane **1.23** with isobutylamine in isopropanol at refluxing temperature to give hydroxyethylamine which was then subjected to *p*-methoxybenzenesulfonyl chloride in DCM and aqueous sodium bicarbonate (NaHCO_3) to furnish the desired boc protected-sulfonamide isostere **1.24** in 96% yield, over two

steps. The *tert*-butoxycarbonyl protecting group was easily cleaved with 30% trifluoroacetic acid in DCM to give isostere amine **1.25** in nearly quantitative yield, shown in Scheme 1.4.¹⁰⁹



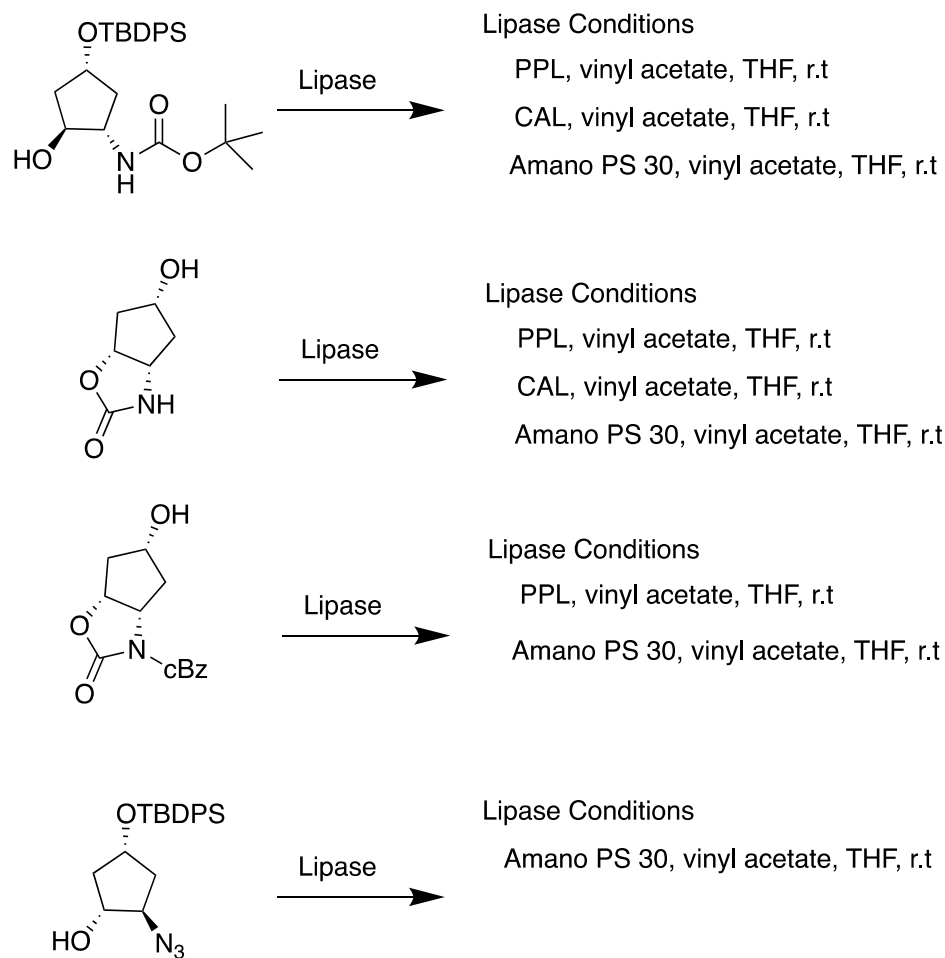
Scheme 1.4: Synthesis of Isostere Amine **1.25**

The activated alcohol **1.26** was achieved by subjecting oxazolidinone **1.22** to *p*-nitrophenyl chloroformate, *N*-methylmorpholine in THF provided nitrophenyl carbonate **1.26** in 65% yield. Finally, isostere **1.25** was coupled with the activated nitrophenyl carbonate **1.26** in the presence of *N,N*, diisopropylethylamine (DIPEA) in acetonitrile (MeCN), furnished a 1 : 1 mixture of diastereomeric isomers **1.27** and **1.28** in 55% yield.¹⁰⁰ The final inhibitors were separated on HPLC with an ODSA pack column in MeCN to water gradient, and each inhibitor was purified further by HPLC to ensure >95% purity, which was essential for biological testing.



Scheme 1.5: Synthesis of Diastereomeric Final Inhibitors **1.27** and **1.28**

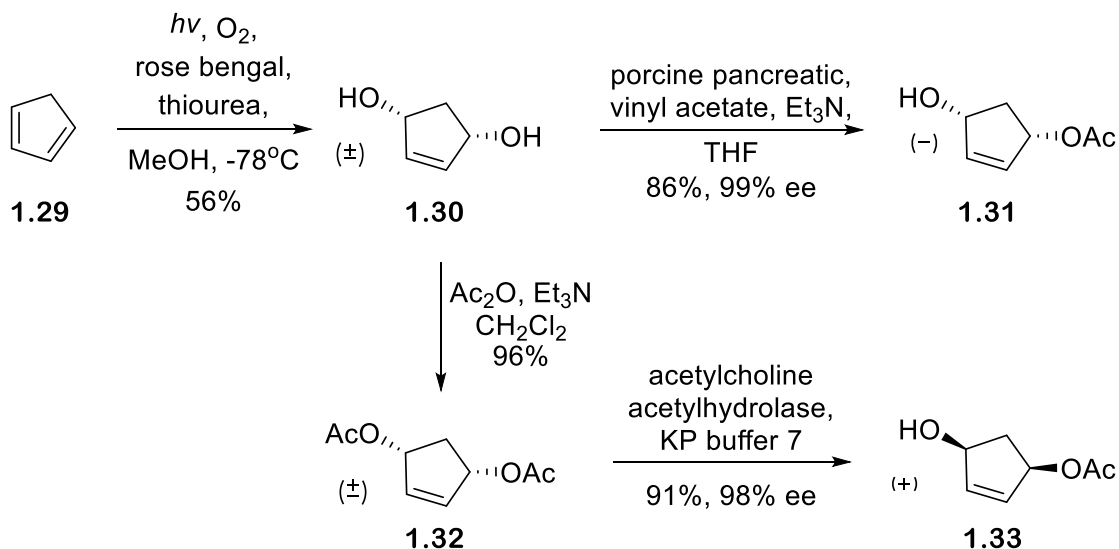
Initial enzymatic inhibitory data on inhibitor **1.27** and **1.28** revealed incorporating the bicyclic oxazolidinone as the P2 ligand to be a promising new class of HIV-1 inhibitors and worth further investigations. At first, inhibitor **1.27** and **1.28** were examined as a racemic mixture with a K_i of 36 nM and separation of the racemic mixture proved to be difficult but was achieved by via reverse phase HPLC. The two diastereoisomers **1.27** and **1.28** demonstrated potent K_i values 0.0012 nM and 1.33 nM respectively, which further enhanced the demand of a more efficient route. Multiple compounds were exposed to numerous enzymatic resolution conditions and produced less than desired results and full recovery of starting material, shown in Scheme 1.6.



Scheme 1.6: Outline of Explored Lipase Conditions

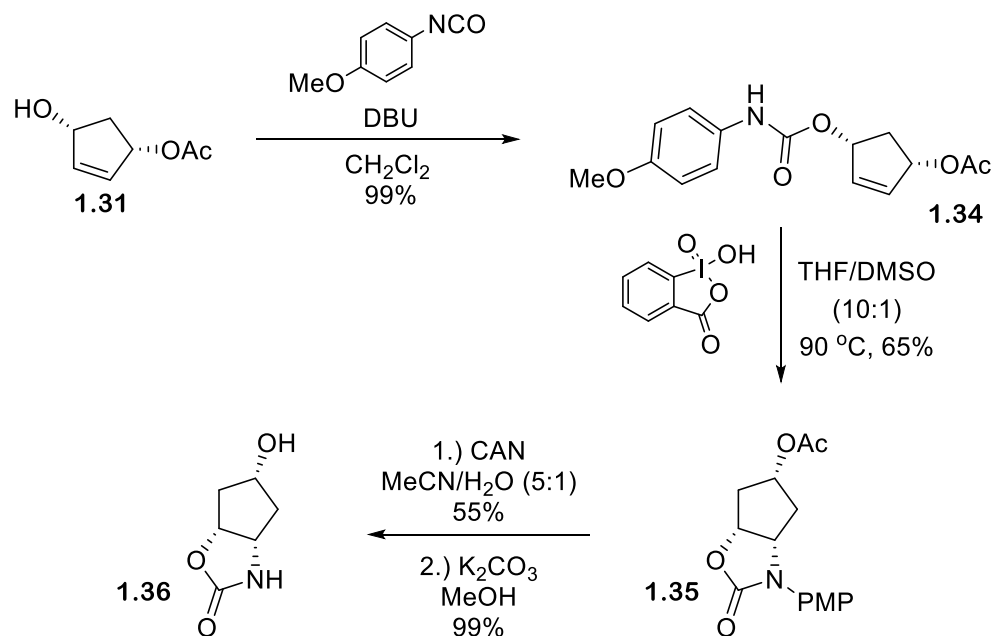
It was soon recognized that the above route would not be an efficient means of generating multiple inhibitors. The low yields associated with this process, failure to generate optically active material and HPLC separation justified the need for a different approach. Using **1.31** and **1.33** as a chiral source led to the development of a new enantioselective synthesis. Cracking of dicyclopentadiene gave pure cyclopentadiene **1.29** was then further subjected to molecular oxygen, rose Bengal, thiourea in methanol at $-78\text{ }^{\circ}\text{C}$ and irradiated with a mercury lamp to produce diol **1.30** in 56% yield.¹¹⁰ The enzymatic resolution of *cis*-2-cyclopentene-1,4-diol **1.30** was achieved with porcine pancreatic (PPL) to afford (-) monoacetate **1.31** in 86% yield and 99% enantiomeric excess (ee). Racemic *cis*-2-cyclopentene-1,4-diol **1.30** was protected as the diacetate **1.32** and subjected

to acetylcholine acetylhydrolase, KP buffer pH 7.0 to afford the other desired enantiomer (+) monoacetate **1.33** in 91% yield and 98% *ee*, shown in Scheme 1.7.^{111,112}



Scheme 1.7: Synthesis of Monoacetate **1.31** and **1.33**

Optically active (1*R*,4*S*)-*cis*-4-acetoxy-2-cyclopenten-1-ol **1.31** was used to establish two of three desired stereocenters in >99% *ee*. Monoacetate **1.31** was treated with 4-methoxyphenyl isocyanate and 1,8-diazabicyclo[5.4.0] (10 mol%) to provide aryl carbamate **1.34** in 99% yield, Scheme 1.8.¹¹³ Utilization of Nicolaou and Baran's *o*-iodoxybenzoic acid (IBX) mediated cyclization conditions proved to be successful for the generation of the key bicyclic core **1.35**.¹¹⁴ Aryl carbamate **1.34** was reacted with freshly prepared IBX¹¹⁵ in tetrahydrofuran and dimethyl sulfoxide (10:1) at 90 °C to give **1.35** as a single diastereomer in 65% yield. Furthermore, the *p*-methoxyphenyl group was successfully cleaved with ceric ammonium nitrate (CAN) in MeCN and water (5:1) in 71% yield to give protected oxazolidinone.¹¹⁶ The acetate group was easily removed with potassium carbonate (K_2CO_3) in methanol (MeOH) to provide the optically active bicyclic oxazolidinone ligand **1.36** in 99% yield.



Scheme 1.8: Synthesis of Optically Active Bicyclic Oxazolidinone Ligand **1.36**

In order to determine the significance of the ligand's absolute stereochemistry, the corresponding enantiomer **1.39** was easily synthesized by swapping out **1.31** with its enantiomer and exposing the monoacetate **1.33** to the same conditions outlined in Scheme 1.8. Structures are shown in Figure 1.26.

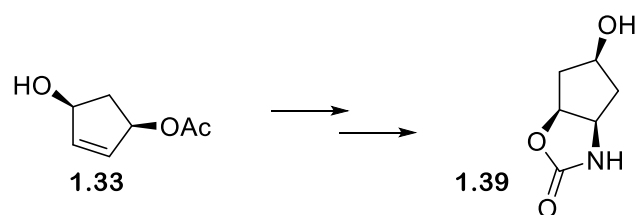
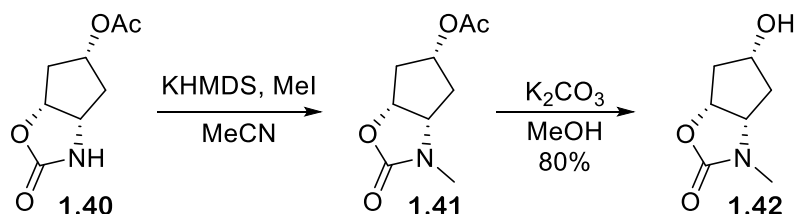
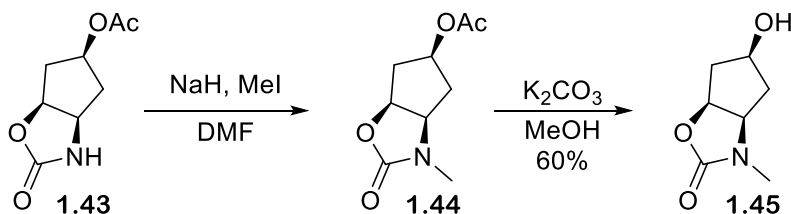


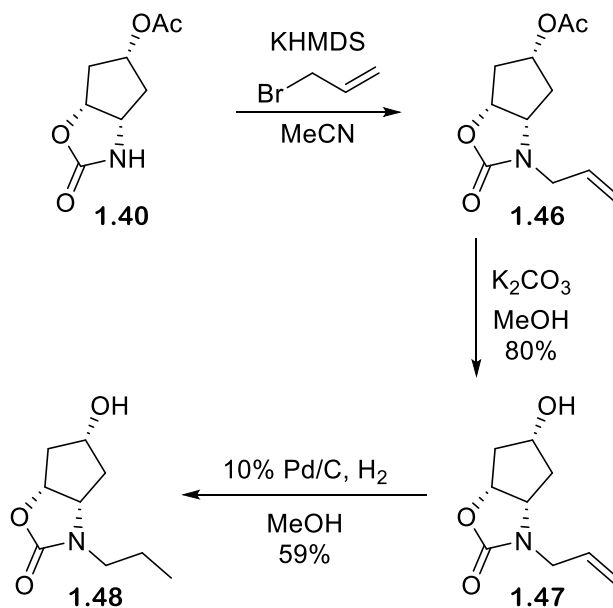
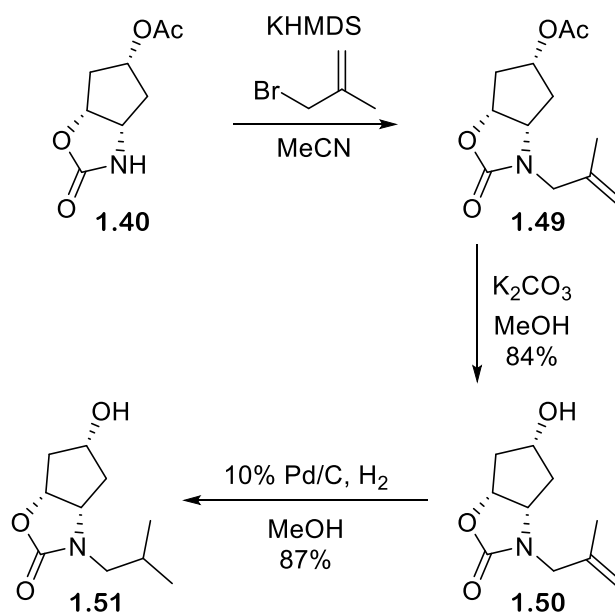
Figure 1.26: Synthesis of Optically Active Bicyclic Oxazolidinone Ligand **1.39**

Scheme 1.9: Synthesis of *N*-Me **1.42**

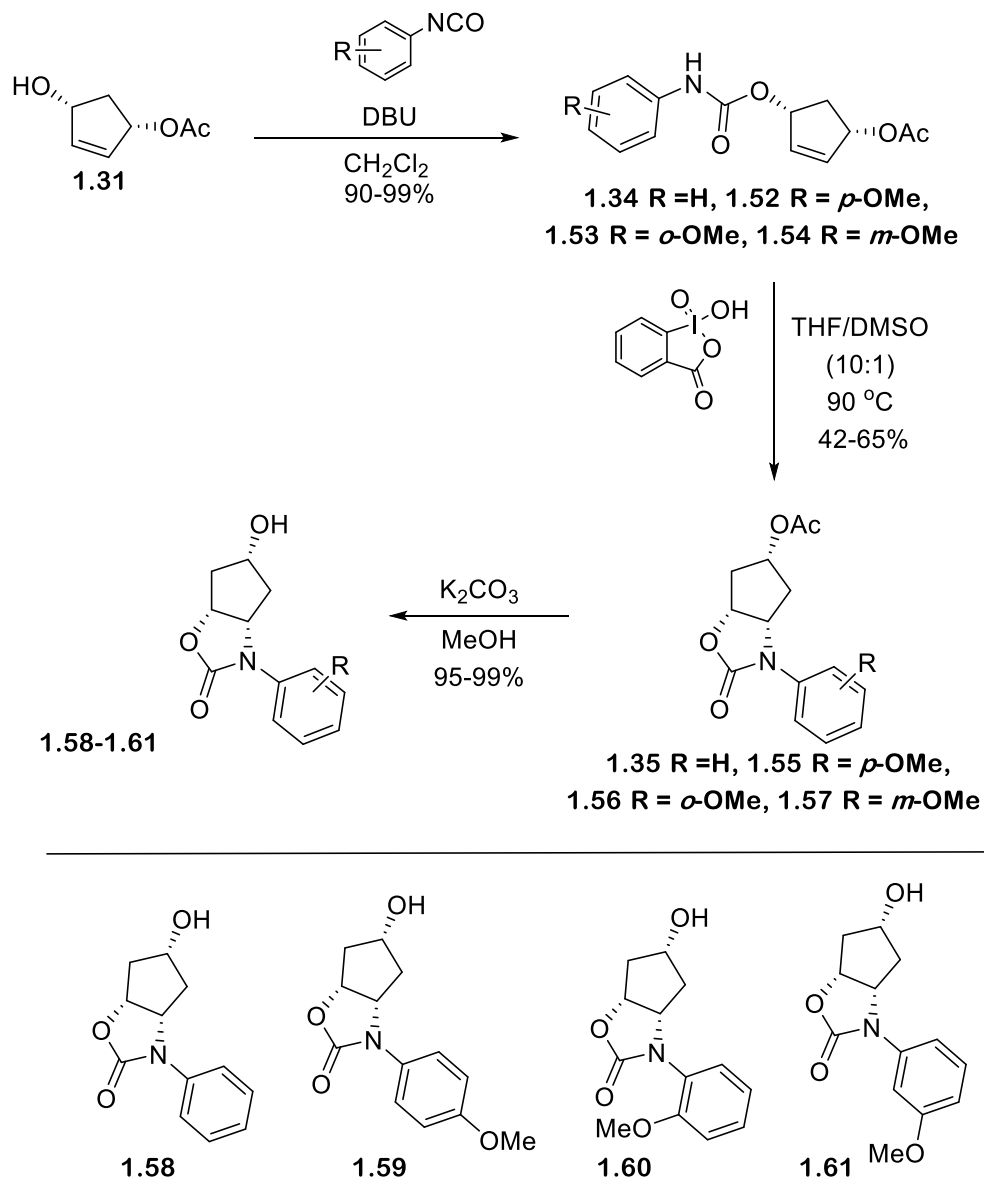
To afford varying P2 ligands, the acetate-oxazolidinone's **1.40** cyclic amine was deprotonated with potassium bis(trimethylsilyl)amide (KHMDs) and then reacted with iodomethane in MeCN to yield the methylated species **1.41** which was further subjected to K_2CO_3 in MeOH to give **1.42** in 80%. The respective enantiomer was synthesized similarly, but sodium hydride (NaH) was used as the base. **1.43** was deprotonated with NaH and then reacted with iodomethane in dimethylformamide (DMF) to yield the methylated species **1.44** which was further subjected to K_2CO_3 in MeOH to give **1.45** in 60%, shown in Scheme 1.10. It should be noted that further alkylations utilized KHMDs in MeCN for the sole purpose of producing a higher yield.

Scheme 1.10: Synthesis of *N*-Me **1.45**

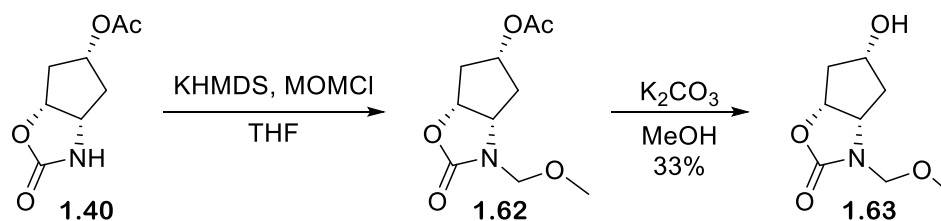
In order to further access *N*-propyl **1.48** and *N*-isobutyl **1.51** derivative, acetate-oxazolidinone **1.40** was first exposed to KHMDS and then reacted with either allyl bromide and 3-Bromo-2-methylpropan-1-ol to produce **1.46** and **1.49** respectively, which was then subjected to the same hydrolysis stated above to yield allyl **1.47** and isobutyl **1.50**. **1.47** and **1.50** were further exposed to 10% of Pd/C under hydrogenation conditions in methanol to give the reduced *N*-propyl ligand **1.48** in 87% yield and the *N*-isobutyl **1.51** in 80% yield, shown in Scheme 1.11 and Scheme 1.12.

Scheme 1.11: Synthesis of *N*-Allyl **1.47** and *N*-Propyl **1.48** LigandScheme 1.12: Synthesis of *N*-Isobutylene **1.50** and *N*-Isobutyl **1.51** Ligand

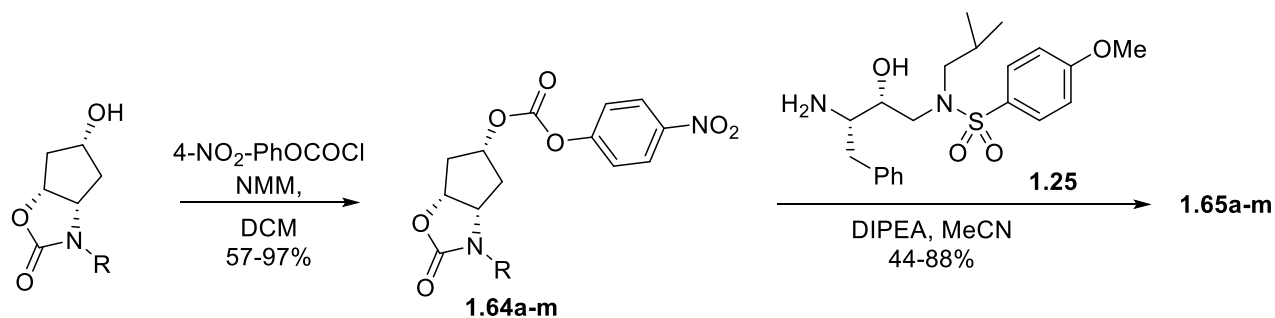
The structure-activity relationship was expanded to include aryl bicyclic oxazolidinones **1.58-1.61**, shown in Scheme 1.13. Monoacetate **1.31** was reacted with a diverse set of isocyanates: aryl isocyanate, *p*-methoxy, *o*-methoxy, and *m*-methoxy isocyanate. **1.31** was treated with its respective isocyanate and 1,8-diazabicyclo[5.4.0] (10 mol%) to provide aryl carbamate **1.34**, **1.52-1.54** in quantitative yield. Aryl carbamate **1.34**, **1.52-1.54** then underwent the same IBX cyclization described earlier and provided the *para*, *ortho*, *meta*- methoxyphenyl *N*-aryl derivatives **1.35**, **1.55-1.57** in 42-65% yield. All *N*-aryl containing compounds were exposed to potassium carbonate in methanol to produce the free alcohol ligands **1.58 – 1.61** in quantitative yield.

Scheme 1.13: Synthesis of *N*-Aryl **1.58-1.61**

Acetate-oxazolidinone **1.40** was again exposed to KHDMS and then reacted with methoxymethyl chloride in THF to give *N*-MOM **1.62** which was then subjected to the same hydrolysis stated above to yield free alcohol **1.63** in 33%, shown in Scheme 1.14.

Scheme 1.14: Synthesis of *N*-MOM **1.63**

All alcohols were first converted to their activated carbonate **1.64a-m** by treatment with 4-nitrophenyl chloroformate and 4-methylmorpholine in tetrahydrofuran at 0° C in 57-97% yield.¹⁰⁰ 4-nitrophenyl carbonates **1.64a-m** underwent selective alkoxyacylation when exposed to previously synthesized free aminosulfonamide isostere **1.25**, diisopropylethylamine (DIPEA) in MeCN to provide final protease inhibitors **1.65 a-n** in 44-88% yield, a general outline of completion of final inhibitors are shown in Scheme 1.15.

Scheme 1.15: Synthesis of Final Inhibitors **1.65a-m**

Activated carbonate **1.65c** was further coupled to a different known isostere **1.25a**. Thus, **1.65c** was subjected to isostere **1.25a** with DIPEA in MeCN to provide final inhibitor **1.65n** in 69% yield, shown in Scheme 1.16.¹¹⁷ Final structures of the entire library of ligand alcohols, activated carbonates **1.64a-m** and final inhibitors are shown in Figure 1.27,

Figure 1.28, and Figure 1.29.

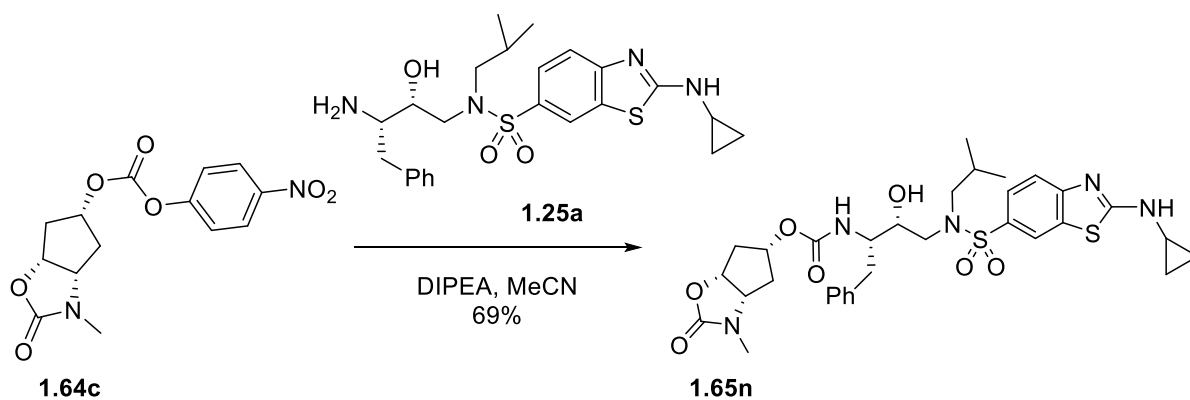
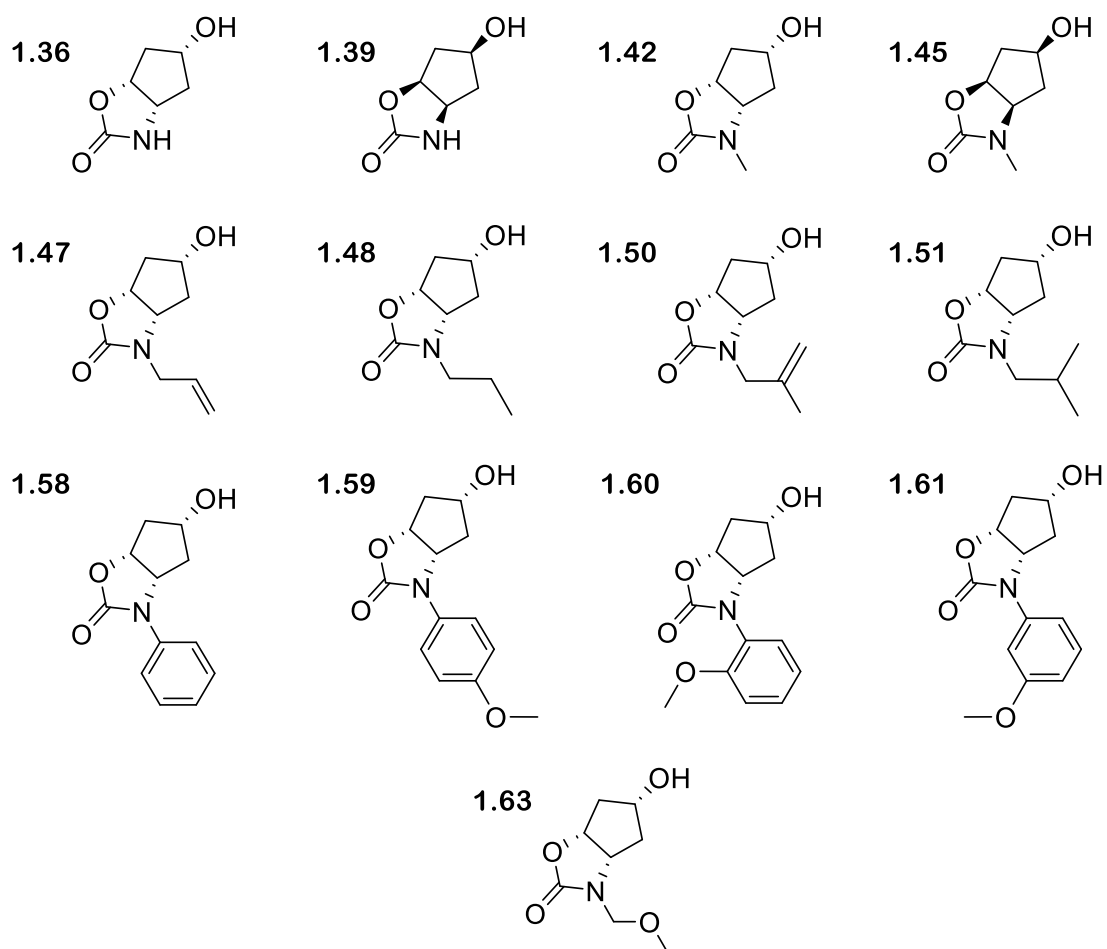
Scheme 1.16: Synthesis of Final Inhibitor **1.65n**

Figure 1.27: Structures of Ligand Alcohol Precursors

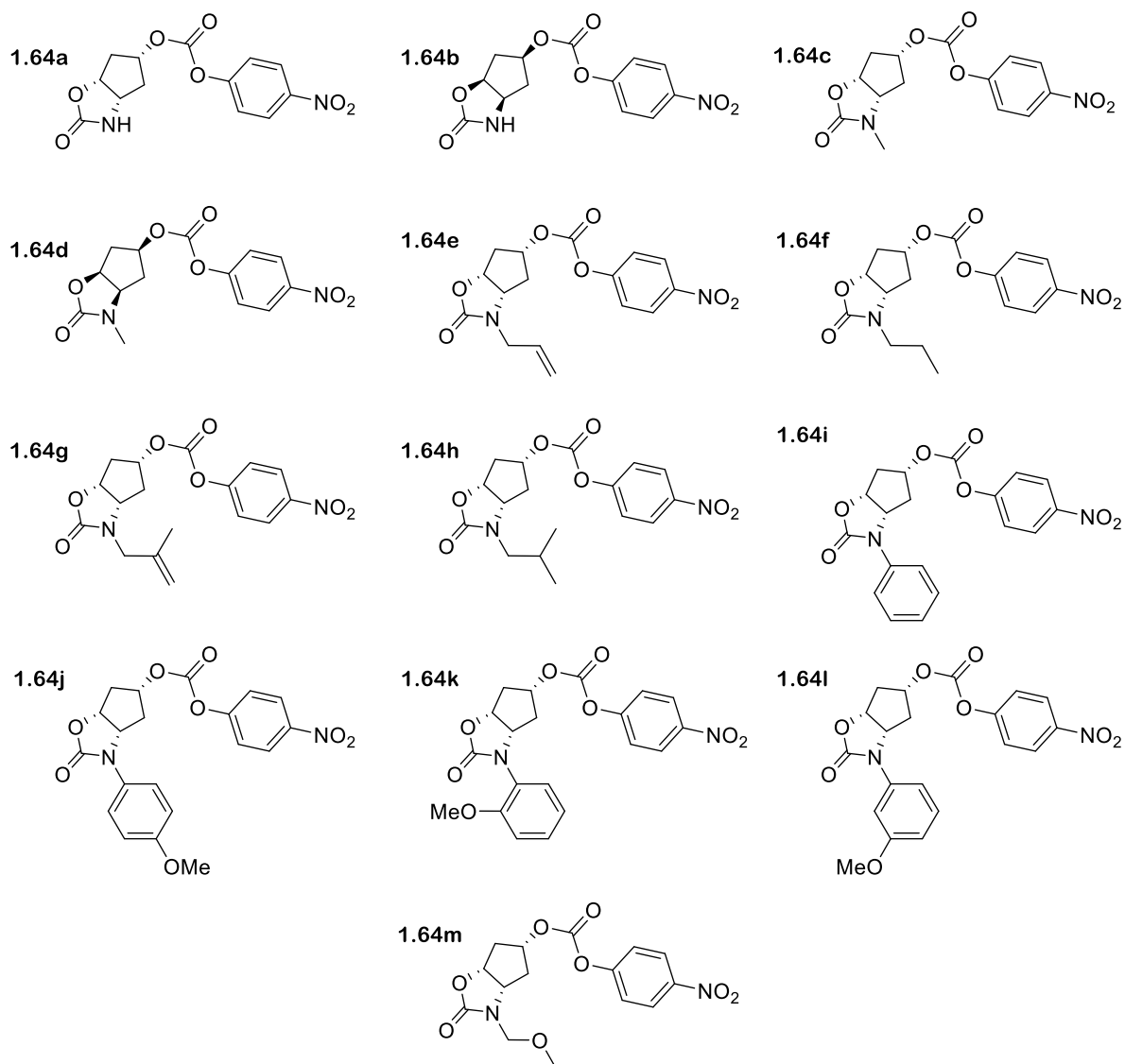


Figure 1.28: Structures of Activated Carbonates **1.64a-m**

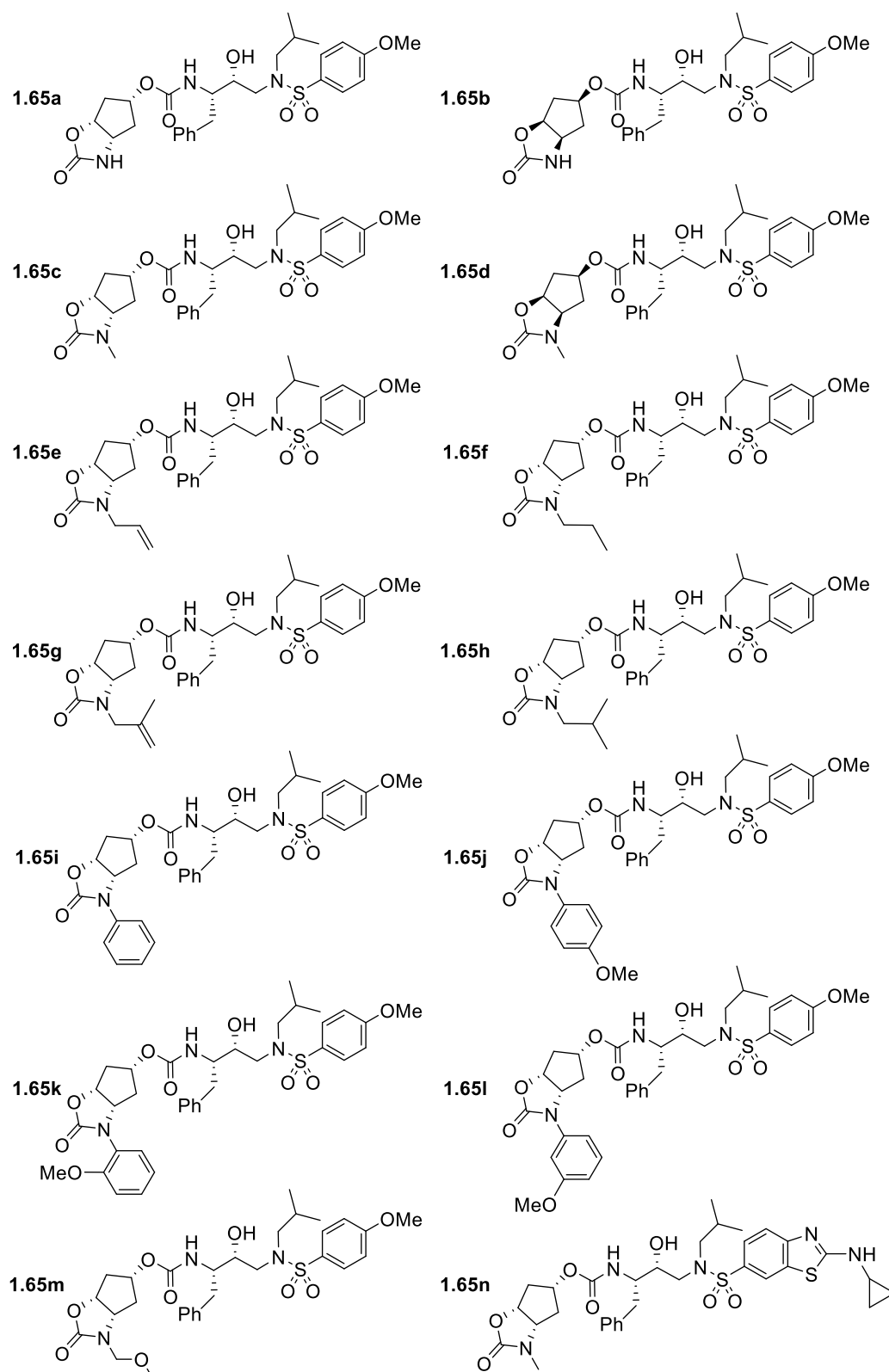
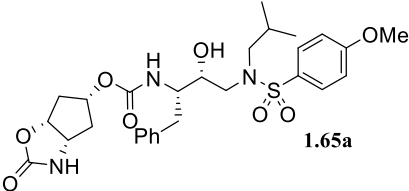
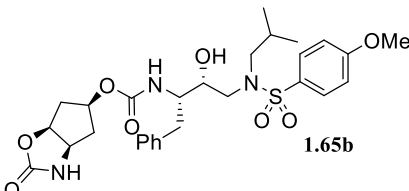


Figure 1.29: Structures of Final Inhibitors

1.6.3.2 Biological Evaluation

All new inhibitors were evaluated first in an HIV-1 protease inhibitory assay based on the known protocol described by Toth and Marshall.¹¹⁸ The enzyme inhibition K_i values can be seen in Table 1.2 -1.7. The antiviral activity of each PIs was then determined by a known MTT assay that calculates IC_{50} values. Thus, the inhibitors were exposed to HIV_{NL4-3} infected MT-4 cell lines, and the minimum concentration that was required to reduce the viral replication by 50% is the reported IC_{50} value. Viral replication was measured by the measurement inhibition of the p24 Gag protein production.¹¹⁹ The results are shown in Table 1.2 - 1.7.

Table 1.2: HIV-1 Proteases Inhibitory and Antiviral Activity of Inhibitors **1.65a** and **1.65b** with Unalkylated Oxazolidinone

| Entry | Inhibitor | K_i (nM) ^a | IC_{50} (nM) ^b |
|-------|---|-------------------------|-----------------------------|
| 1. |  1.65a | 0.0012 | 48.3 |
| 2. |  1.65b | 1.33 | >1000 |

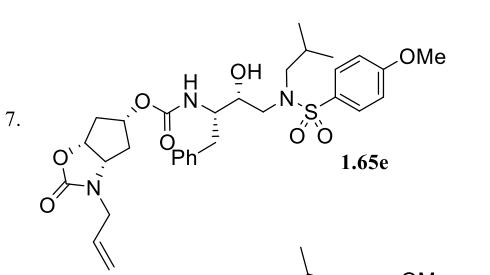
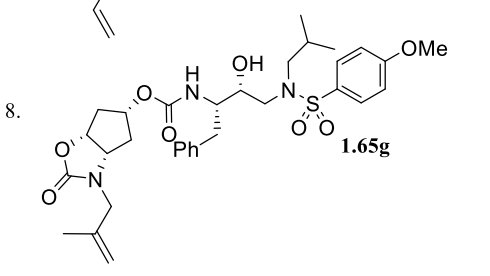
^aThe K_i values are mean values of at least four experiments. Standard error in all cases were less than 7%. Darunavir exhibited $K_i = 16$ pM. ^bHuman T-lymphocytes (MT-4) cells (10^5 /mL) were exposed to 100 TCID₅₀ of HIV-1 and were cultured in the presence of each PI. The IC_{50} values are means of at least three experiments. The IC_{50} of DRV and SQV were 3.2 nM and 21 nM. Standard error in all cases was less than 5%.

Table 1.3: HIV-1 Proteases Inhibitory and Antiviral Activity of Inhibitors **1.65c**, **1.65d**, **1.65f**, and **1.65h** with *N*-Alkyl Group

| Entry | Inhibitor | K_i (nM) ^a | IC ₅₀ (nM) ^b |
|-------|------------------|-------------------------|------------------------------------|
| 3. | 1.65c | 0.03 | 36 |
| 4. | 1.65d | 0.16 | 436 |
| 5. | 1.65f | 0.14 | 447 |
| 6. | 1.65h | 0.16 | 41 |

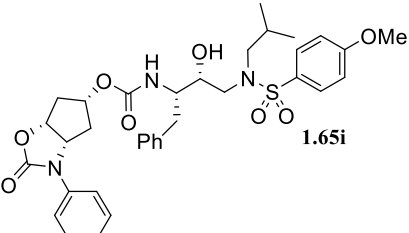
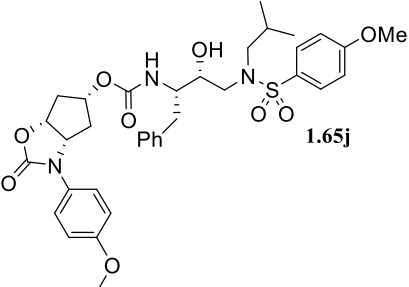
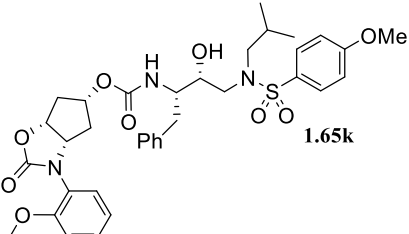
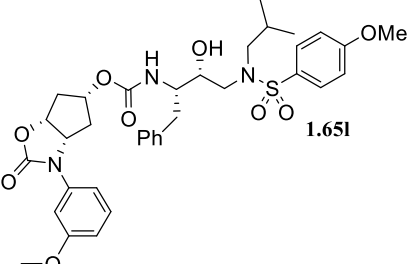
^aThe K_i values are mean values of at least four experiments. Standard error in all cases were less than 7%. Darunavir exhibited $K_i = 16$ pM. ^bHuman T-lymphocytes (MT-4) cells (10^5 /mL) were exposed to 100 TCID₅₀ of HIV-1 and were cultured in the presence of each PI. The IC₅₀ values are means of at least three experiments. The IC₅₀ of DRV and SQV were 3.2 nM and 21 nM. Standard error in all cases was less than 5%.

Table 1.4: HIV-1 Proteases Inhibitory and Antiviral Activity of Inhibitors **1.65e** and **1.65g** with Saturated *N*-Alkyl Group

| Entry | Inhibitor | K_i (nM) ^a | IC_{50} (nM) ^b |
|-------|---|-------------------------|-----------------------------|
| 7. |  <chem>COc1ccc(cc1)NS(=O)(=O)C[C@H](O)[C@@H](c2ccccc2)C(=O)O[C@H]3CC[C@H](C=C)N3C(=O)O</chem> 1.65e | 0.016 | 369 |
| 8. |  <chem>CC(=C)C[C@H]1CC[C@@H](C(=O)O[C@H]2CC[C@@H](C(=O)N[C@@H](C2)C(=O)O[C@H]3C[C@H](O)[C@@H](C3)C(=O)N4C(=O)c5ccc(OC)cc5S4(=O)=O)C1</chem> 1.65g | 0.04 | 31 |

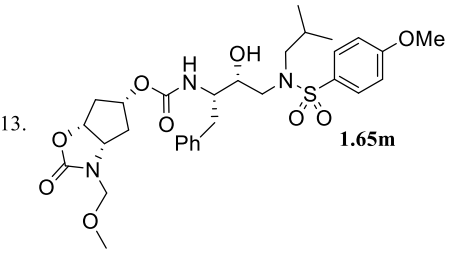
^aThe K_i values are mean values of at least four experiments. Standard error in all cases were less than 7%. Darunavir exhibited $K_i = 16$ pM. ^bHuman T-lymphocytes (MT-4) cells (10^5 /mL) were exposed to 100 TCID₅₀ of HIV-1 and were cultured in the presence of each PI. The IC_{50} values are means of at least three experiments. The IC_{50} of DRV and SQV were 3.2 nM and 21 nM. Standard error in all cases was less than 5%.

Table 1.5: HIV-1 Proteases Inhibitory and Antiviral Activity of Inhibitors **1.65i-l** with *N*-Aryl Group

| Entry | Inhibitor | K_i (nM) ^a | IC ₅₀ (nM) ^b |
|-------|--|-------------------------|------------------------------------|
| 9. |  <chem>COc1ccc(cc1)NS(=O)(=O)C[C@H](O)C(=O)N[C@@H](C1CCCC1)C(=O)Oc2ccccc2</chem> 1.65i | 0.33 | >1000 |
| 10. |  <chem>COc1ccc(cc1)NS(=O)(=O)C[C@H](O)C(=O)N[C@@H](C1CCCC1)C(=O)Oc2ccc(OC)cc2</chem> 1.65j | 0.63 | >1000 |
| 11. |  <chem>COc1ccc(cc1)NS(=O)(=O)C[C@H](O)C(=O)N[C@@H](C1CCCC1)C(=O)Oc2cccc(OC)c2</chem> 1.65k | 0.08 | 251 |
| 12. |  <chem>COc1ccc(cc1)NS(=O)(=O)C[C@H](O)C(=O)N[C@@H](C1CCCC1)C(=O)Oc2ccc(OC)cc2</chem> 1.65l | 92.8 | >1000 |

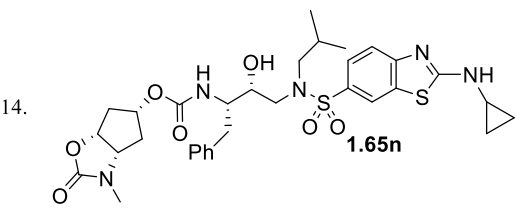
^aThe K_i values are mean values of at least four experiments. Standard error in all cases were less than 7%. Darunavir exhibited $K_i = 16$ pM. ^bHuman T-lymphocytes (MT-4) cells (10^5 /mL) were exposed to 100 TCID₅₀ of HIV-1 and were cultured in the presence of each PI. The IC₅₀ values are means of at least three experiments. The IC₅₀ of DRV and SQV were 3.2 nM and 21 nM. Standard error in all cases was less than 5%.

Table 1.6: HIV-1 Proteases Inhibitory and Antiviral Activity of Inhibitors **1.65m** with *N*-MOM Group

| Entry | Inhibitor | K_i (nM) ^a | IC_{50} (nM) ^b |
|-------|---|-------------------------|-----------------------------|
| 13. |  <chem>COc1ccc(cc1)S(=O)(=O)N[C@H](C(=O)N[C@@H](O)Cc2ccccc2)C3CCCC3C(=O)N(C)COC(=O)C3CCCC3</chem> 1.65m | 0.0016 | 84 |

^aThe K_i values are mean values of at least four experiments. Standard error in all cases were less than 7%. Darunavir exhibited $K_i = 16$ pM. ^bHuman T-lymphocytes (MT-4) cells (10^5 /mL) were exposed to 100 TCID₅₀ of HIV-1 and were cultured in the presence of each PI. The IC_{50} values are means of at least three experiments. The IC_{50} of DRV and SQV were 3.2 nM and 21 nM. Standard error in all cases was less than 5%.

Table 1.7: HIV-1 Proteases Inhibitory and Antiviral Activity of Inhibitor **1.65n** with Varying P2'

| Entry | Inhibitor | K_i (nM) ^a | IC_{50} (nM) ^b |
|-------|--|-------------------------|-----------------------------|
| 14. |  <chem>C1CCN1c2nc3cc(ccc3s2)S(=O)(=O)N[C@H](C(=O)N[C@@H](O)Cc4ccccc4)C5CCCC5C(=O)N(C)COC(=O)C5CCCC5</chem> 1.65n | 0.19 | 28 |

^aThe K_i values are mean values of at least four experiments. Standard error in all cases were less than 7%. Darunavir exhibited $K_i = 16$ pM. ^bHuman T-lymphocytes (MT-4) cells (10^5 /mL) were exposed to 100 TCID₅₀ of HIV-1 and were cultured in the presence of each PI. The IC_{50} values are means of at least three experiments. The IC_{50} of DRV and SQV were 3.2 nM and 21 nM. Standard error in all cases was less than 5%.

Developing new PIs that retain potency against a wide range of multidrug-resistant HIV-1 strains is one of the main objectives of this study. Inhibitors **1.65g** and **1.65h** were further evaluated against a panel of existing PI-resistant HIV-1 strains. The antiviral activity of **1.65g** and **1.65h** were compared to four widely used FDA-approved PIs, Lopinavir (LPV), Amprenavir (APV), Atazanavir (ATV), and Darunavir (DRV). MT-4 human T-lymphocytes were used as target cells and exposed to HIV-1_{NL4-3}, HIV-1_{ATV}^R_{5μM}, HIV-1_{LPV}^R_{5μM}, HIV-1_{APV}^R_{5μM}, HIV-1_{DRV}^R_{P20}, HIV-1_{DRV}^R_{P30}, or HIV-1_{DRV}^R_{P51}.⁹⁷ The cells were cultured in the presence of an increasing concentration of each PI. IC₅₀ values were calculated by the inhibition of the p24 Gag protein assay.¹²⁰ The results are reported in Table 1.8.

Table 1.8: Antiviral Activity of **1.65g**, **1.65h**, and Other FDA PIs Against Multi-Resistant-HIV-1 Strains

| Inhibitor | mean IC ₅₀ (nM) ± SD ^{a,b} | | | | | | |
|-------------------------|--|--|--|--|--|--|--|
| | HIV-1 _{NL4-3} | HIV-1 _{ATV^R_{5μM}} | HIV-1 _{LPV^R_{5μM}} | HIV-1 _{APV^R_{5μM}} | HIV-1 _{DRV^R_{P20}} | HIV-1 _{DRV^R_{P30}} | HIV-1 _{DRV^R_{P51}} |
| <p>Lopinavir (LPV)</p> | 6.0 ± 0.09 | 311 ± 6 | >1000 | 218 ± 6 | >1000 | >1000 | >1000 |
| <p>Amprenavir (APV)</p> | 431 ± 3 | >1000 | >1000 | >1000 | >1000 | >1000 | >1000 |
| <p>Atazanavir (ATV)</p> | 0.89 ± 0.02 | >1000 | 293 ± 4 | 2.0 ± 0.08 | >1000 | >1000 | >1000 |

Table 1.8: continued

| | | | | | | | |
|---|------------|---------------|-------------------|------------------|----------|----------|-------|
| <p>Darunavir (DRV)</p> | 3.5 ± 0.09 | 19 ± 2 (5) | 301 ± 0.2 (86) | 129 ± 3 (37) | 169 ± 15 | 426 ± 26 | >1000 |
| | 23 ± 0.1 | 36 ± 2 (1) | >1000 | 261 ± 15 (11) | >1000 | >1000 | >1000 |
| | 40 ± 1 | 33 ± 2 (1) | 615 ± 8 (15) | 309 ± 4 (7) | >1000 | >1000 | >1000 |
| <p>^aThe amino acid substitutions in the protease-encoding region compared to the wild-type HIV-1_{NL4-3} were L23I, E34Q, K43I, M46I, I50L, G51A, L63P, A71V, V82A, T91A in HIV-1_{ATV}^R_{5μM}; L10F, M46I, I54V, V82A in HIV-1_{LPV}^R_{5μM}; or L10F, M46I, I50V, I85V in HIV-1_{APV}^R_{5μM}. ^bHuman T-lymphocytes (MT-4) cells (105/mL) were exposed to 100 TCID₅₀ of HIV-1 and were cultured in the presence of each PI where the inhibition of p24 Gag protein production was used as an endpoint. All assays were conducted in duplicate, and the data shown represent mean values (± standard deviation) derived from the results of two independent experiments.¹²¹</p> | | | | | | | |

1.6.3.3 X-ray Crystallographic Analysis

Molecular insight into the binding interactions of inhibitors complex to HIV protease was revealed by X-ray crystallography. Inhibitors **1.65a** (GRL-034-17A) was co-crystallized with wild type HIV-1 protease and solved at a 1.22 Å resolution. R/R_{free} values were 15.5% and 18.8%. The X-ray crystal structure revealed inhibitor **1.65a** bound to the active site in two orientations with a 0.7/0.3 ratio. The overall backbone of this PR/**1.65a** complex was comparable to PR/DRV bound to wild type HIV-1 with a root-mean-square-deviation (RMSD) of 0.20 Å for 198 equivalent C α atoms. Inhibitor **1.65i** (GRL-042-17A) was also co-crystallized with wild type HIV-1 protease and solved at a 1.30 Å resolution in a single conformation. R/R_{free} values were 15.0% and 18.2%. The PR/**1.65i** complex defined backbone was comparable to PR/DRV bound to wild type HIV-1 with an RMSD of 0.24 Å for 198 equivalent C α atoms.^{122,123}

1.6.4 Discussion

These inhibitors were designed as reversible competitive inhibitors that bind to the enzyme's active site with multiple non-covalent interactions and compete against the native substrates. This allows the enzymes inhibition by the inhibitor to be easily measured *in vitro* and characterized by its inhibition constant, K_i value. K_i is measured by taking the change of the enzyme's activity at varying concentrations of inhibitor in the presence of the natural substrate. This is one great tool to screen many potential inhibitors and establish whether the inhibitor would be a good candidate for HIV-1 protease inhibition and can be further examined. Therefore, all new inhibitors were evaluated first in an HIV-1 protease inhibitory assay based on the known protocol described by Toth and Marshall.¹¹⁸ The antiviral activity of each PIs was then determined by a known MTT assay that calculates IC_{50} values. Thus, the inhibitors were exposed to HIV_{NL4-3} infected MT-4 cell lines, and the minimum concentration that was required to reduce the viral replication by 50% is the reported IC_{50} value. Viral replication was measured by the measurement inhibition of the p24 Gag protein production. The inhibitor structures, enzyme inhibition K_i values and antiviral activity of each PIs are shown in Table 1.2 – 1.7.

First, the stereochemical requirement was examined, and the results are shown in Table 1.2. Inhibitors **1.65a** and **1.65b** contain three stereocenters and are enantiomers of each other. Inhibitor **1.65a** with the (3a*S*, 5*R*, 6a*R*) stereochemistry exhibited very potent enzyme inhibitory K_i of 0.0012 nM and antiviral activity IC_{50} of 48.3 nM. The enantiomeric inhibitor **1.65b** displayed

a reduction of enzyme inhibitory with K_i of 1.33 nM and absolutely no antiviral activity. The 1000-fold difference of K_i between **1.65a** and **1.65b** shows that the PR enzyme prefers the stereochemistry of **1.65a** (3aS, 5R, 6aR) and these values agree with previous inhibitors. In order to explore the oxazolidinone P2 ligand further, various *N*-alkyl groups on the oxazolidinone were examined, and the results are shown in

Table 1.3. Inhibitor **1.65c** and **1.65d** are enantiomers, and both contain an *N*-Methyl group. Analysis of the biological data of inhibitor **1.65c** with the (3aS, 5R, 6aR) stereochemistry showed a potent enzyme inhibitory K_i of 0.03 nM and antiviral activity IC_{50} of 36 nM. The enantiomeric inhibitor **1.65d** maintained a good enzyme inhibitory with K_i of 0.16 nM. However, the antiviral activity was significantly reduced to IC_{50} of 436 nM. Methylating the free amine on the cyclic carbamate confirmed the desirable stereochemical requirement of this new P2 ligand to be the (3aS, 5R, 6aR)-oxazolidinone by the obvious reduction of potency of **1.65b** and **1.65d**. Thus, the (3aS, 5R, 6aR)-oxazolidinone stereochemistry will be utilized for further SAR analysis. When comparing **1.65a** and **1.65c**, there was an improvement in the antiviral activity from 48.3 nM to 36 nM.

This result encouraged the addition of more sterically demanding alkyl groups. In inhibitor **1.65f** and **1.65h**, an *N*-propyl group and an *N*-isobutyl group was incorporated respectively. In comparison, inhibitor **1.65f** showed an enzyme inhibitory K_i of 0.14 nM and antiviral activity IC_{50} of 447 nM. Inhibitor **1.65h** showed the enzyme inhibition value in close range at K_i of 0.16 nM and showed a massive improvement in antiviral activity IC_{50} of 41 nM when compared to its competitor **1.65f**. *N*-methyl derivative **1.65c** (entry 3) and *N*-isobutyl **1.65h** (entry 6) display similar biological activities, where **1.65f** shows a 5-fold reduction in antiviral activity and a 10-fold reduction of HIV-1 protease inhibitory activity. It can be determined that the incorporation of a sterically demanding alkyl side chain such as an isobutyl group does not interfere with the overall P2 ligand binding affinity and can be well accommodated by the active site. This interesting result fueled the expansion of the SAR to include saturation on the side chain.

Furthermore, *N*-allyl and *N*-isobutylene functionalities were incorporated and results are shown in Table 1.4. **1.65e** inhibitor with the *N*-allyl addition showed a similarly favorable enzyme inhibition with K_i of 0.016 nM which was comparable to *N*-methyl derivative **1.65c**. However, antiviral activity was diminished and measured at IC_{50} of 369 nM. **1.65e**'s antiviral activity was similar to the *N*-propyl derivative (entry 5) activity but exhibited a 10-fold loss when compared to

the *N*-Methyl inhibitor **1.65c**. The loss of antiviral activity of *N*-allyl and *N*-propyl is possibly due to the disproportionate lipophilicity of the overall molecules that resulted in a lower cellular permeability. On the other hand, inhibitor **1.65g** showed a slight loss of enzyme inhibition with K_i of 0.04 nM and a 5-fold increase of antiviral activity of IC_{50} of 31 nM when compared to *N*-Methyl. When compared to its unsaturated counterpart **1.65h**, inhibitor **1.65g** displayed about a 10-fold improvement of both enzymatic inhibition and antiviral activity.

A series of *N*-aryl inhibitors were generated to understand the role of larger steric bulk and effects exhibited from the S2 subsite active site; results are shown in Table 1.5. *N*-phenyl inhibitor **1.65i** displayed a significant reduction of enzyme activity with K_i of 0.33, and no significant antiviral activity was demonstrated. A methoxy functional group was introduced on to the *N*-aryl group to promote hydrogen bonding in the S2 subsite and balance out the, lipophilicity of the inhibitor. Thus, *para*, *ortho*, and *meta*-methoxy groups were explored. Of the three, the *N*-*ortho*-methoxy inhibitor **1.65l** showed the greatest enzymatic inhibition of K_i of 0.08 nM and antiviral activity of 251 nM. The *para*-methoxy inhibitor **1.65j** and *meta*-methoxy inhibitor **1.65k** showed a larger decrease of enzymatic activity with K_i of 0.63 nM and K_i of 92.8 nM, and demonstrated no antiviral activity. Overall, the incorporation of aryl groups at the *N*-oxazolidinone proved to be a disadvantage and a certain amount of steric bulk at this position was critical for antiviral activity.

Introducing a smaller side chain on *N*-oxazolidinone that also contained potential hydrogen bonding capabilities brought about the generation of inhibitor **1.65m** with an *N*-methoxymethyl side chain, results are shown in Table 1.6. **1.65m** showed a very potent enzyme inhibitory K_i of 0.016 nM and a decent antiviral activity IC_{50} of 84 nM.

It was previously shown that the addition of a cyclopropylaminobenzothiazole isostere at the P2' position enhanced potency and formed additional favorable hydrogen bonds and van der Waal interactions in the active sites S2' subsite.¹¹⁷ To further explore the effect of this new class of oxazolidinone inhibitors beyond the S2 subsite, it seemed plausible to create inhibitor **1.65n** with the *N*-methyl oxazolidinone as the P2 ligand and the advanced isostere, results are shown in

Table 1.7. Inhibitor **1.65n** displayed a 10-fold reduction of enzyme inhibition, K_i of 0.19 nM and an 8-fold enhancement of antiviral activity, IC_{50} of 28 nM, when compared to *N*-methyl **1.65c**.

This entire class of bicyclic oxazolidinone PIs was used to reveal critical ligand requirements for high antiviral HIV-1 protease activity. Developing new PIs that retain high

potency against a wide range of multidrug-resistant HIV-1 strains was one of the main objectives of this study. Inhibitors **1.65g** and **1.65h** were chosen for further evaluation against a panel of existing PI-resistant HIV-1 strains. The antiviral activity of **1.65g** and **1.65h** was then compared to four widely used FDA-approved PIs, Lopinavir (LPV), Amprenavir (APV), Atazanavir (ATV), and Darunavir (DRV). MT-4 human T-lymphocytes were used as target cells and exposed to HIV-1_{NL4-3}, HIV-1_{ATV}^R_{5μM}, HIV-1_{LPV}^R_{5μM}, HIV-1_{APV}^R_{5μM}, HIV-1_{DRV}^R_{P20}, HIV-1_{DRV}^R_{P30}, or HIV-1_{DRV}^R_{P51}. The cells were cultured in the presence of an increasing concentration of each PI. IC₅₀ values were calculated by the inhibition of the p24 Gag protein assay. The results are reported in Table 1.8. All tested inhibitors maintained good potency against wild-type HIV_{NL4-3}, except APV which also lost all significant activity towards every multidrug-resistant HIV-1 variants. Except for DRV, none of the examined PIs blocked replication of HIV-1_{DRV}^R_{P20}, HIV-1_{DRV}^R_{P30}, or HIV-1_{DRV}^R_{P51}. The effectiveness of DRV towards the three variants was not observed and showed that DRV too failed to block replication. Both **1.65g** and **1.65h** are less potent than DRV, but they still maintained good activity against all three HIV-1_{ATV}^R_{5μM}, HIV-1_{LPV}^R_{5μM}, and HIV-1_{APV}^R_{5μM} variants compared to wild-type HIV_{NL4-3}. Inhibitor **1.65h** showed antiviral activity against HIV-1_{ATV}^R_{5μM}, HIV-1_{LPV}^R_{5μM}, and HIV-1_{APV}^R_{5μM} of IC₅₀ values of 33 nM, 615 nM, and 309 nM respectively. These changes are far superior to any other PIs measured.⁷⁹ Whereas **1.65g** lost activity towards HIV-1_{LPV}^R_{5μM} but exhibited significant activity towards HIV-1_{ATV}^R_{5μM} with an IC₅₀ value of 36 nM and decent activity towards HIV-1_{APV}^R_{5μM} with an IC₅₀ value of 261nM. Again, both oxazolidinone-derived inhibitors were unsuccessful in blocking viral replication of highly DRV-resistant HIV-1 variants, and DRV continues to be superior. Overall, the impressive drug-resistance profile of **1.65g** and **1.65h** is thought to be caused by new binding interactions of the P2 oxazolidinone with the S2-site residues and possibly with the S1 site as well.

Cytotoxicity (CC_{50}) values were measured in MT-4 cells, and mostly all oxazolidinone inhibitors demonstrated low CC_{50} , results are shown in Table 1.9.¹²⁰

Table 1.9: Cytotoxicity and Selectivity Index for Selected Inhibitors

| Inhibitor | CC_{50} (μ M) | Selectivity index ^a |
|--|----------------------|--------------------------------|
| 1.65a | >100 | >2070 |
| 1.65c | >100 | >2778 |
| 1.65d | >100 | >229 |
| 1.65g | >100 | >3226 |
| 1.65h | >100 | >2439 |
| 1.65n | 43 | 1536 |
| ^a The ratio of CC_{50} to IC_{50} denotes for the selectivity index | | |

Molecular insights of the binding interactions of inhibitors **1.65a** and **1.65i** between HIV-1 protease was revealed by X-ray crystallography, shown in Figure 1.30 and Figure 1.33. Inhibitors **1.65a** (GRL-034-17A) was co-crystallized with wild type HIV-1 protease and solved at a 1.22 Å resolution. Inhibitor **1.65a** was bound to the active site in two orientations with a 0.7/0.3 ratio. Inhibitor **1.65i** (GRL-042-17A) was also co-crystallized with wild type HIV-1 protease and solved at a 1.30 Å resolution in a single conformation. Inhibitors **1.65a** and **1.65i** maintained many essential interactions with the HIV-1 PR as seen with DRV and other potent inhibitors in the S1, S1', and S2' subsites.

X-ray analysis of inhibitor **1.65a** showed the cyclic carbamate oxygen of the oxazolidinone P2 ligand to form good hydrogen bonds with the amide NH of Asp29 at a distance of 3.1-3.2 Å and the carbonyl oxygen of the ligand forms another strong hydrogen bond with Asp29 with a shorter interatomic distance of 2.8-2.9 Å, Figure 1.30. The alternative conformation formed the same hydrogen bond but at a longer 3.5 Å distance. The transition state mimic hydroxyl group interacts strongly with the carboxylate groups of catalytic Asp25 and Asp25'. A water molecule forms a tetra-coordinated hydrogen bonding interaction with the carbonyl oxygen on the carbamate portion of the inhibitor, one of the oxygens on the sulfonamide functional group, and the amide nitrogens' of the flap region, Ile 50 and Ile50'. The P2' ligand methoxy group hydrogen bonds to NH of the main chain residue Asp30'. These favorable interactions have been observed with other potent HIV-1 PR inhibitors.⁷⁹ However, the ring urethane NH forms an additional hydrogen bond to the main chain carbonyl oxygen of Gly48 with a distance of 3.0 Å and Gly 27 with a distance of 3.4Å.

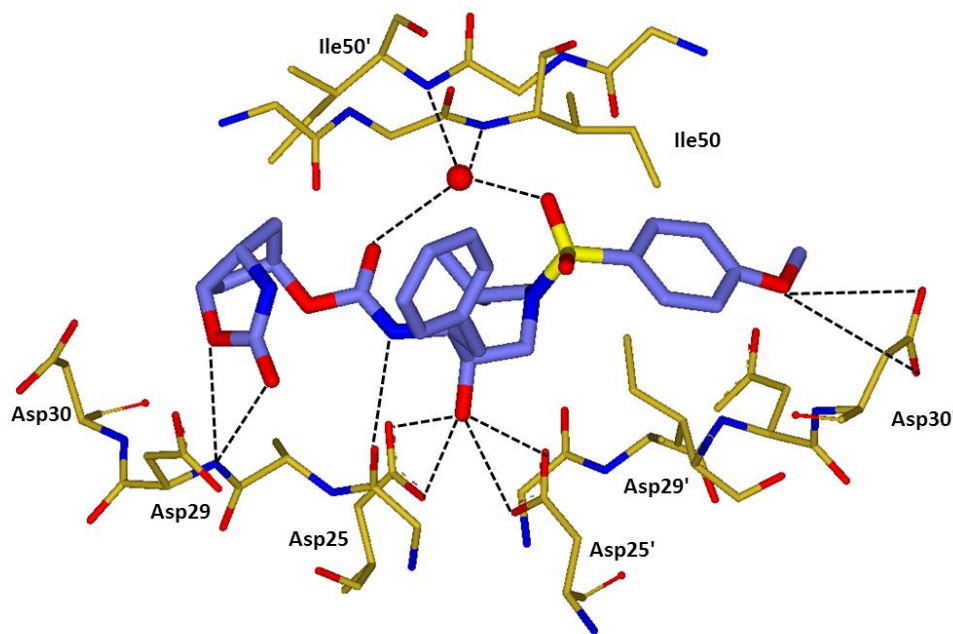


Figure 1.30: Inhibitor **1.65a** Bound with Wild Type HIV-1 Protease (PDB:6E9A)

An overlay of DRV bound to HIV-1 PR with inhibitor **1.65a** sheds even more light on the binding interactions and subtle changes of the active site. DRV is known to make an important hydrogen bond to the main chain amide NH Asp30, whereas inhibitor **1.65a** does not display this interaction at all. The oxazolidinone P2 ligand does occupy a greater volume and slightly moves the P2 ligand closer to the flap region when compared to the bis-THF ligand of DRV, shown in Figure 1.31. The active site's ability to accommodate the new interaction of the oxazolidinone ligand resulted in the flap residue Phe53 to shift 1.0 Å. The adjacent beta-strand forms the new hydrogen bond between the inhibitor urethane nitrogen and the carbonyl oxygen of Gly48 and could be the reason for the observed shift of the other flap. This feature could be advantageous for the treatment of multidrug-resistant strains, but further studies are needed to maximize and understand this new feature further. Figure 1.32 shows the protein surface interactions of DRV and **1.65a**. The oxazolidinone ligand displays van der Waals interactions with Val32, Ile47, Ile50', and Ile84 and occupies the S2 subsite slightly better than DRV bis-THF P2 ligand. The major van der Waals interactions are consistent with DRV bis-THF PR ligand.^{122,124}

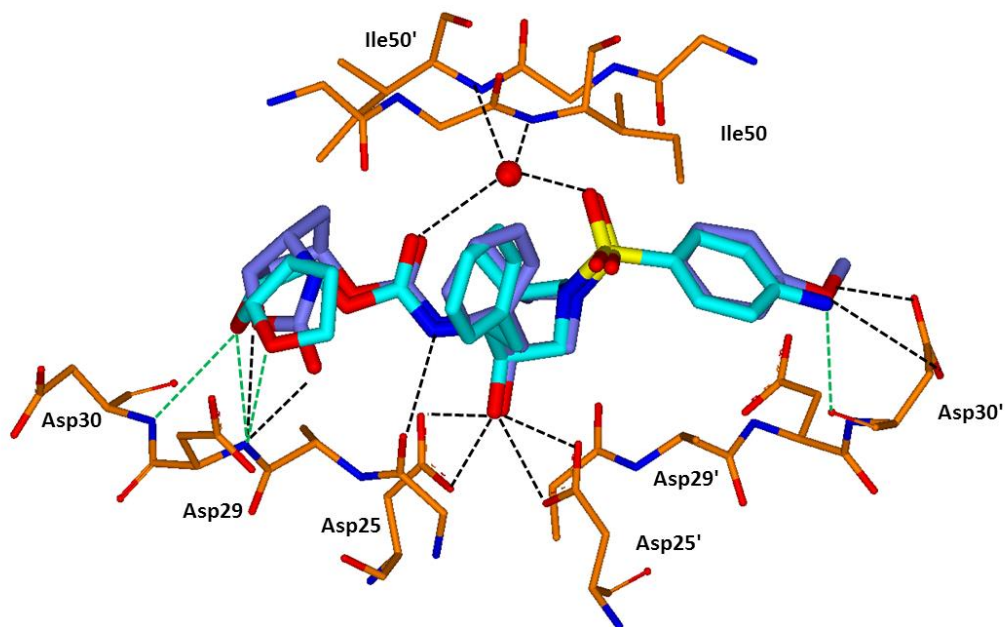


Figure 1.31: Overlay of DRV (light blue) Bound to HIV-1 PR with Inhibitor **1.65a** (purple)

X-ray analysis of inhibitor **1.65i** showed the cyclic carbamate oxygen of the oxazolidinone P2 ligand retained good hydrogen bonds with the amide NH Asp29 at a distance of 3.1 Å and the carbonyl oxygen of the ligand forms a stronger hydrogen bond with Asp29 with a distance of 2.8 Å, Figure 1.33. The transition state hydroxyl group interacts strongly with the carboxylates group of the catalytic Asp25 and Asp25' residues. A water-mediated tetra-coordinated hydrogen bond is formed with the carbonyl oxygen on the carbamate portion of the inhibitor, one of the oxygens on the sulfonamide functional group, and the amide nitrogens of the flap region, Ile 50 and Ile50'. The P2' ligand methoxy group hydrogen bonds to the main chain Asp30' NH. These favorable interactions have been observed with **1.65a** and other potent HIV-1 PR inhibitors.^{122,124}

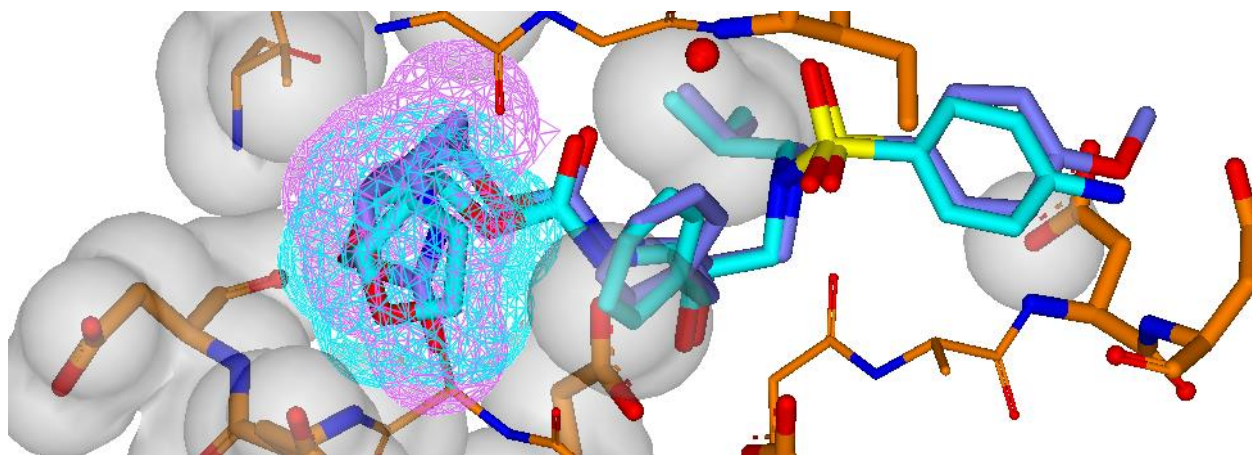


Figure 1.32: Overlay of DRV (light blue) with Inhibitor **1.65a** (purple)

The oxazolidinone ligand displays van der Waals interactions with Val32, Ile47, Ile50', and Ile84. These van der Waals interactions are consistent with DRV bis-THF PR ligand. However, **1.65i** contains a larger P2 hydrophobic phenyl group which occupies the space between guanidinium Arg8' and Gly48 carbonyl oxygen, Figure 1.33. The flap residue, Gly48 results in a shift of approximately 0.8 Å and the phenyl ring displayed several C-H \cdots π and hydrogen bond interactions at a distance of 2.8 Å with Gly48 and 3.5 Å with Arg8'. The steric hindrance of the phenyl group and the shifting of Gly48 explains the larger K_i value that was observed for **1.65i** and its decreased binding affinity when compared to similar large P2 groups as **1.65a**. As stated before, this feature is advantageous towards the treatment of highly resistant strains but further studies are needed to maximize this new shift because incorporating a phenyl group onto the

inhibitor showed that too large of group decreased enzyme inhibition and antiviral activity whereas an *N*-alkyl or NH groups were more accommodating by their increase of enzyme inhibition and antiviral activity.

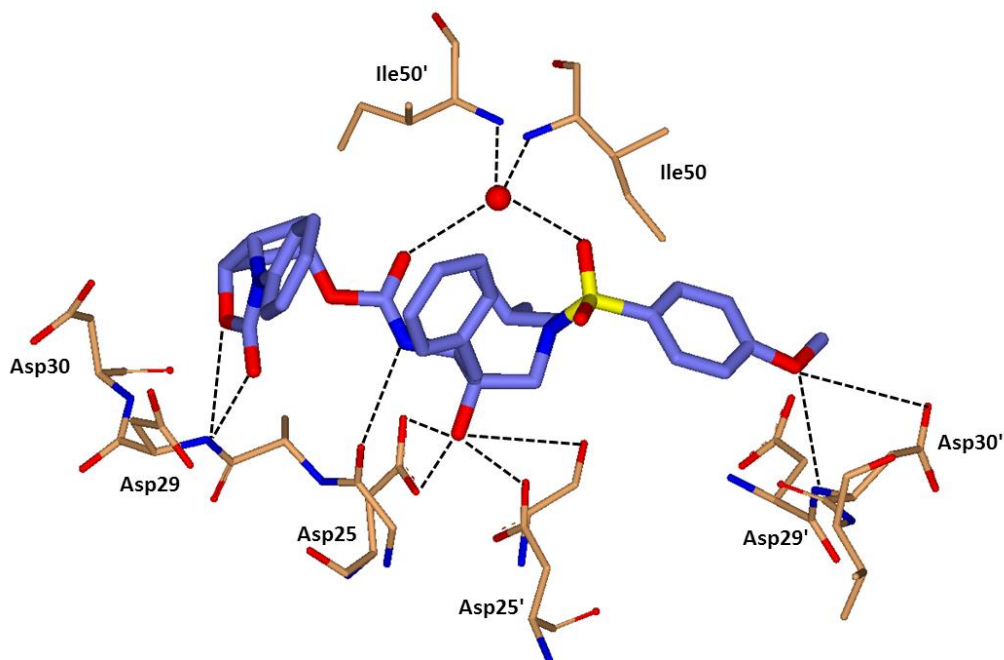


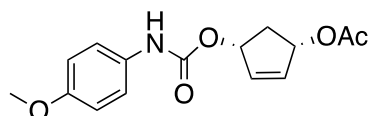
Figure 1.33: Inhibitor **1.65i** Bound with Wild Type HIV-1 Protease (PDB: 6E7J)

1.7 Conclusion

A new class of HIV-1 protease inhibitors was designed and synthesized. The newly designed bicyclic oxazolidinone ligands were synthesized in an optically active form. Nicolaou and Baran's IBX cyclization conditions were utilized to provide the key oxazolidinone intermediate in high enantiomeric purity. Several inhibitors displayed good to excellent activity towards HIV-1 protease and significant antiviral activity in MT-4 cells. Compound **1.65g** displayed the highest activity towards HIV-1 protease with a K_i of 40 pM and antiviral IC_{50} of 31 nM. Inhibitors **1.65g** and **1.65h** were further evaluated against a panel of highly resistant multidrug-resistant HIV-1 variants, and their changes in antiviral activity were similar to those observed with Darunavir. Additionally, inhibitor **1.65a** (GRL-034-17A) and inhibitor **1.65i** (GRL-042-17A) were co-crystallized with wild type HIV-1 protease and solved at a 1.22 Å and 1.30 Å resolution. X-ray data revealed important interactions in the active site that have not yet been explored.

1.8 Experimental Section

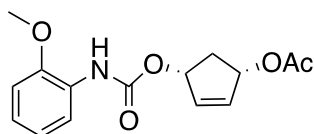
All moisture-sensitive reactions were carried out in oven-dried glassware under an argon atmosphere. All chemicals and reagents were obtained from commercial suppliers and were used without further purification. Anhydrous solvents were obtained as follows: Dichloromethane was distilled from calcium hydride under argon. Tetrahydrofuran was distilled from sodium metal/benzophenone under argon. All other solvents were reagent grade. Flash column chromatography was performed with 230-400 mesh silica gel. Thin layer chromatography was carried out using TLC silica gel 60 F254 plates. ^1H NMR and ^{13}C NMR spectra were recorded on a Bruker AV-III-400, Bruker DRX500, or Bruker AV-III-800 with chemical shifts reported in ppm (δ). Characteristic splitting patterns are as follows: s = singlet, d = doublet, t = triplet, q = quartet, m = multiplet, dd = doublet of doublets, ddd = doublet of doublet of doublets, td = triplet of doublets, dq = doublet of quartets, brs = broad singlet, app = apparent. Optical rotations were measured with a Perkin Elmer Series 341 Polarimeter, with a sodium source lamp. Low-resolution mass spectra were collected on a Waters 600 LCMS. High-resolution mass spectra were collected by the Purdue University Campus-Wide Mass Spectrometry Center.



(1S,4R)-4-(((4-methoxyphenyl)carbamoyl)oxy)cyclopent-2-en-1-yl acetate (**1.34**)

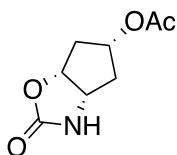
To a stirring solution of (1R,4S)-*cis*-4-acetoxy-2-cyclopenten-1-ol **1.31** (0.103 mg, 0.915 mmol) in dry dichloromethane was added 4-methoxyphenyl isocyanate (0.150 mg, 1.01 mmol) and 1,8-Diazabicyclo[5.4.0]undec-7-ene (14.0 mg, 0.091 mmol) all under an argon atmosphere. Reaction was stirred at room temperature for 1 hour. Upon completion, the residue was taken up in saturated solution of NaHCO_3 and the aqueous phase was extracted with EtOAc. The organic extracts were dried with Na_2SO_4 and the solvent was removed under reduced pressure. The crude product was purified by silica gel column chromatography (20 % EtOAc in hexane) to afford **1.34** (0.209 g, 99%). ^1H NMR (400 MHz, Chloroform-*d*) δ 7.33 – 7.22 (m, 2H), 6.84 (d, J = 9.0 Hz, 2H), 6.57 (s, 1H), 6.12 (dddd, J = 20.7, 5.6, 2.1, 1.1 Hz, 2H), 5.58 (qd, J = 6.1, 3.5, 2.1 Hz, 2H), 3.77 (s, 3H), 2.90 (qt, J = 15.1, 7.5 Hz, 1H), 2.06 (s, 3H), 1.80 (dt, J = 15.0, 3.7 Hz, 1H). ^{13}C NMR (101 MHz,

CDCl_3) δ 170.59, 155.95, 153.25, 134.85, 134.46, 130.65, 120.58, 114.17, 77.26, 76.94, 76.62, 55.40, 37.18, 21.04. LRMS-ESI (m/z) : 314.0 $[\text{M}+\text{Na}]$



(1*S*,4*R*)-4-(((2-methoxyphenyl)carbamoyl)oxy)cyclopent-2-en-1-yl acetate (1.53)

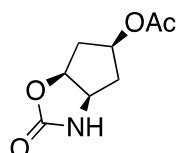
To a stirring solution of (1*R*,4*S*)-*cis*-4-acetoxy-2-cyclopenten-1-ol **1.31** (34.0 mg, 0.239 mmol) in dry dichloromethane was added 2-methoxyphenyl isocyanate (39.2 mg, 0.263 mmol) and 1,8-Diazabicyclo[5.4.0]undec-7-ene (3.60 mg, 0.024 mmol) all under an argon atmosphere. Reaction was stirred at room temperature for 12 hours. Upon completion, the residue was taken up in saturated solution of NaHCO_3 and the aqueous phase was extracted with EtOAc. The organic extracts were dried with Na_2SO_4 and the solvent was removed under reduced pressure. The crude product was purified by silica gel column chromatography (20 % EtOAc in hexane) to afford **1.53** (38.0 mg, 55%). ^1H NMR (800 MHz, $\text{Chloroform-}d$) δ 8.11 (s, 1H), 7.02 (td, $J = 7.8, 1.7$ Hz, 1H), 6.98 (t, $J = 7.6$ Hz, 1H), 6.88 (d, $J = 8.0$ Hz, 1H), 6.17 (dd, $J = 43.5, 5.4$ Hz, 2H), 5.63 (dt, $J = 46.3, 4.0, 3.4$ Hz, 2H), 3.88 (s, 3H), 2.95 (dt, $J = 15.1, 7.6$ Hz, 1H), 2.10 (s, 3H), 1.87 (dt, $J = 15.0, 3.6$ Hz, 1H). ^{13}C NMR (201 MHz, CDCl_3) δ 170.68, 152.89, 147.61, 134.94, 134.61, 127.49, 122.87, 121.15, 118.14, 110.01, 77.19, 77.03, 76.87, 55.65, 37.30, 21.15. LRMS-ESI (m/z) : 314.0 $[\text{M}+\text{Na}]$



(3a*S*,5*R*,6a*R*)-2-oxohexahydro-2*H*-cyclopenta[*d*]oxazol-5-yl acetate (1.40)

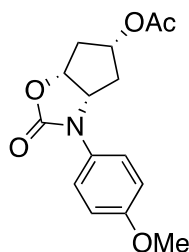
To a stirring solution of cyclic *p*-methoxyphenyl carbamate **1.35** (0.138 g, 0.474 mmol) in acetonitrile (4.76 mL) and water (0.95 mL) was added cerium ammonium nitrate (1.30 g, 2.37 mmol) at 0 °C. Reaction was stirred for 30 min. Upon completion, the residue was taken up in 5% saturated solution of NaHCO_3 and the aqueous phase was extracted with EtOAc. The organic extracts were dried with Na_2SO_4 and the solvent was removed under reduced pressure. The crude product was purified by silica gel column chromatography (80 % EtOAc in hexane) to afford **1.40**

(62.0 mg, 71%). ^1H NMR (400 MHz, Chloroform-*d*) δ 5.53 (s, 1H), 5.28 (t, J = 4.5 Hz, 1H), 5.17 (t, J = 7.0 Hz, 1H), 4.39 (t, J = 7.0 Hz, 1H), 2.44 (dd, J = 15.9, 2.9 Hz, 1H), 2.12 (dd, J = 15.4, 2.9 Hz, 1H), 2.03 (s, 3H), 1.95 (tdd, J = 15.8, 6.5, 4.6 Hz, 2H). ^{13}C NMR (101 MHz, CDCl_3) δ 170.64, 158.68, 81.26, 77.24, 77.12, 76.92, 76.60, 75.28, 55.92, 40.12, 39.33, 21.14. LRMS-ESI (m/z) : 186.1 [$\text{M}+\text{H}$]



(3aR,5S,6aS)-2-oxohexahydro-2H-cyclopenta[d]oxazol-5-yl acetate (1.43)

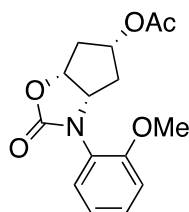
To a stirring solution of cyclic *p*-methoxyphenyl carbamate **1.38** (20.0 mg, 0.069 mmol) in acetonitrile (0.69 mL) and water (0.14 mL) was added cerium ammonium nitrate (0.188 g, 0.344 mmol) at 0 °C. Reaction was stirred for 30 min. Upon completion, the residue was taken up in 5% saturated solution of NaHCO_3 and the aqueous phase was extracted with EtOAc. The organic extracts were dried with Na_2SO_4 and the solvent was removed under reduced pressure. The crude product was purified by silica gel column chromatography (80 % EtOAc in hexane) to afford **1.43** (7.70 mg, 61%). ^1H NMR (800 MHz, Chloroform-*d*) δ 5.36 (s, 1H), 5.31 (t, J = 4.2 Hz, 1H), 5.20 (t, J = 6.8 Hz, 1H), 4.41 (t, J = 6.9 Hz, 1H), 2.47 (dd, J = 15.9, 2.2 Hz, 1H), 2.15 (dd, J = 15.3, 2.9 Hz, 1H), 2.07 (s, 3H), 1.99 (dddd, J = 30.4, 15.3, 6.6, 4.5 Hz, 2H). ^{13}C NMR (201 MHz, CDCl_3) δ 170.77, 158.66, 81.37, 77.18, 77.03, 76.87, 75.38, 55.99, 40.25, 39.44, 21.24. LRMS-ESI (m/z) : 185.9 [$\text{M}+\text{H}$]



(3aS,5R,6aR)-3-(4-methoxyphenyl)-2-oxohexahydro-2H-cyclopenta[d]oxazol-5-yl acetate (1.35)

In a sealed tube, *p*-methoxyphenyl carbamate **1.34** (0.735g, 2.53 mmol) was dissolved in dry tetrahydrofuran (46.0 mL) followed by the addition of freshly distilled dimethyl sulfoxide (4.60

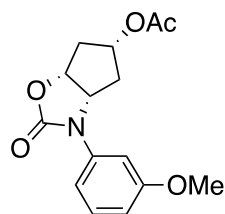
mL). Freshly made 2-iodoxybenzoic acid (1.40 g, 5.05 mmol) was added all at once. The reaction vessel was heated for 8 hours at 90 °C. Another portion of 2-iodoxybenzoic acid (1.40 g, 5.05 mmol) was added and the reaction was heated for an additional 8 hours. Upon completion, the residue was taken up in 5% saturated solution of NaHCO₃ and the aqueous phase was extracted with EtOAc. The organic extracts were dried with Na₂SO₄ and the solvent was removed under reduced pressure. The crude product was purified by silica gel column chromatography (60 % EtOAc in hexane) to afford **1.35** (0.478 g, 65%). ¹H NMR (400 MHz, Chloroform-*d*) δ 7.40 – 7.34 (m, 2H), 6.94 – 6.88 (m, 2H), 5.27 (t, *J* = 4.5 Hz, 1H), 5.14 (t, *J* = 7.2, 6.7 Hz, 1H), 4.84 (t, *J* = 7.0 Hz, 1H), 3.80 (s, 3H), 2.49 (dd, *J* = 15.9, 2.5 Hz, 1H), 2.24 (dd, *J* = 15.4, 3.0 Hz, 1H), 2.08 (ddd, *J* = 15.9, 6.4, 4.6 Hz, 1H), 2.03 (s, 3H), 1.88 (ddd, *J* = 15.4, 6.6, 4.6 Hz, 1H). ¹³C NMR (101 MHz, CDCl₃) δ 170.43, 156.84, 154.84, 130.00, 122.81, 114.45, 77.24, 76.93, 76.61, 74.94, 61.25, 55.41, 39.88, 36.66, 21.11. LRMS-ESI (*m/z*) : 292.0 [M+H]



(3a*S*,5*R*,6a*R*)-3-(2-methoxyphenyl)-2-oxohexahydro-2*H*-cyclopenta[*d*]oxazol-5-yl acetate (1.56)

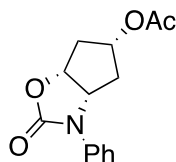
In a sealed tube, *o*-methoxyphenyl carbamate **1.53** (17.3 mg, 0.059 mmol) was dissolved in dry tetrahydrofuran (2.15 mL) followed by the addition of freshly distilled dimethyl sulfoxide (0.210 mL). Freshly made 2-iodoxybenzoic acid (33.3 mg, 0.119 mmol) was added all at once. The reaction vessel was heated for 8 hours at 90 °C. Another portion of 2-iodoxybenzoic acid (33.3 mg, 0.119 mmol) was added and the reaction was heated for an additional 8 hours. Upon completion, the residue was taken up in 5% saturated solution of NaHCO₃ and the aqueous phase was extracted with EtOAc. The organic extracts were dried with Na₂SO₄ and the solvent was removed under reduced pressure. The crude product was purified by silica gel column chromatography (60 % EtOAc in hexane) to afford **1.56** (11.0 mg, 65%). ¹H NMR (400 MHz, Chloroform-*d*) δ 7.34 – 7.26 (m, 2H), 7.03 – 6.93 (m, 2H), 5.28 (t, *J* = 4.5 Hz, 1H), 5.19 (t, *J* = 7.4, 5.7 Hz, 1H), 4.96 (t, *J* = 7.2 Hz, 1H), 3.86 (s, 3H), 2.49 (dd, *J* = 16.0, 2.6 Hz, 1H), 2.13 (s, 3H), 2.11 – 2.01 (m, 2H), 1.78 – 1.63 (m, 1H). ¹³C NMR (101 MHz, CDCl₃) δ 170.52, 156.23,

154.84, 129.58, 128.76, 124.71, 120.93, 111.88, 78.16, 77.24, 76.92, 76.60, 75.31, 60.98, 55.51, 42.57, 39.94, 36.58, 21.27. LRMS-ESI (m/z) : 292.0 [M+H]



(3a*S*,5*R*,6a*R*)-3-(3-methoxyphenyl)-2-oxohexahydro-2*H*-cyclopenta[*d*]oxazol-5-yl acetate (1.57)

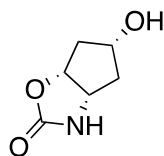
In a sealed tube, *m*-methoxyphenyl carbamate **1.54** (57.0 mg, 0.196 mmol) was dissolved in dry tetrahydrofuran (7.10 mL) followed by the addition of freshly distilled dimethyl sulfoxide (0.710 mL). Freshly made 2-iodoxybenzoic acid (0.110 g, 0.391 mmol) was added all at once. The reaction vessel was heated for 8 hours at 90 °C. Another portion of 2-iodoxybenzoic acid (0.110 g, 0.391 mmol) was added and the reaction was heated for an additional 8 hours. Upon completion, the residue was taken up in 5% saturated solution of NaHCO₃ and the aqueous phase was extracted with EtOAc. The organic extracts were dried with Na₂SO₄ and the solvent was removed under reduced pressure. The crude product was purified by silica gel column chromatography (60 % EtOAc in hexane) to afford **1.57** (24 mg, 42%). ¹H NMR (400 MHz, Chloroform-*d*) δ 7.30 – 7.23 (m, 1H), 7.21 (t, *J* = 2.3 Hz, 1H), 7.03 (ddd, *J* = 8.2, 2.1, 0.9 Hz, 1H), 6.70 (ddd, *J* = 8.3, 2.5, 0.8 Hz, 1H), 5.27 (t, *J* = 4.5 Hz, 1H), 5.14 (t, *J* = 7.1, 6.6 Hz, 1H), 4.88 (t, *J* = 7.1 Hz, 1H), 3.81 (s, 3H), 2.50 (dd, *J* = 15.9, 2.6 Hz, 1H), 2.31 (dd, *J* = 15.4, 3.0 Hz, 1H), 2.09 (ddd, *J* = 15.9, 6.2, 4.6 Hz, 1H), 2.00 (s, 3H), 1.99 – 1.90 (m, 1H). ¹³C NMR (101 MHz, CDCl₃) δ 170.44, 160.22, 154.29, 138.41, 129.83, 111.98, 109.57, 106.30, 77.25, 77.18, 76.93, 76.61, 74.82, 60.60, 55.26, 39.74, 36.99, 21.07. LRMS-ESI (m/z) : 292.0 [M+H]



(3a*S*,5*R*,6a*R*)-2-oxo-3-phenylhexahydro-2*H*-cyclopenta[*d*]oxazol-5-yl acetate (1.55)

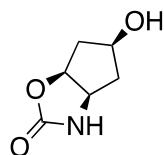
In a sealed tube, phenyl carbamate **1.52** (60.1 mg, 0.230 mmol) was dissolved in dry tetrahydrofuran (8.36 mL) followed by the addition of freshly distilled dimethyl sulfoxide (0.840

mL). Freshly made 2-iodoxybenzoic acid (0.129 g, 0.460 mmol) was added all at once. The reaction vessel was heated for 8 hours at 90 °C. Another portion of 2-iodoxybenzoic acid (0.129g, 0.460 mmol) was added and the reaction was heated for an additional 8 hours. Upon completion, the residue was taken up in 5% saturated solution of NaHCO₃ and the aqueous phase was extracted with EtOAc. The organic extracts were dried with Na₂SO₄ and the solvent was removed under reduced pressure. The crude product was purified by silica gel column chromatography (60 % EtOAc in hexane) to afford **1.55** (22.5 mg, 37%). ¹H NMR (800 MHz, Chloroform-*d*) δ 7.54 (d, *J* = 7.7 Hz, 2H), 7.42 – 7.38 (m, 2H), 7.18 (t, *J* = 7.4 Hz, 1H), 5.30 (t, *J* = 4.5 Hz, 1H), 5.18 (t, *J* = 7.0 Hz, 1H), 4.95 (t, *J* = 7.2 Hz, 1H), 2.53 (dd, *J* = 16.0, 3.1 Hz, 1H), 2.30 (dd, *J* = 15.5, 3.0 Hz, 1H), 2.12 (ddd, *J* = 16.0, 6.5, 4.5 Hz, 1H), 2.03 (s, 3H), 1.98 (ddd, *J* = 15.4, 6.8, 4.5 Hz, 1H). ¹³C NMR (201 MHz, CDCl₃) δ 170.55, 154.55, 137.25, 129.27, 124.56, 120.16, 77.36, 77.22, 77.06, 76.90, 74.97, 60.68, 42.68, 39.89, 36.99, 21.17. LRMS-ESI (*m/z*) : 262.1 [M+H]



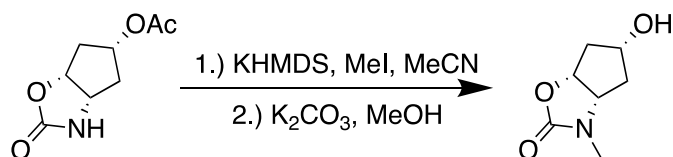
(3a*S*,5*R*,6a*R*)-5-hydroxyhexahydro-2*H*-cyclopenta[*d*]oxazol-2-one (1.36)

To a stirring solution of protected oxazolidinone **1.40** (6.00 mg, 0.032 mmol) in methanol (1.00 mL) was added potassium carbonate (5.53 mg, 0.039 mmol). Reaction was stirred at room temperature for 4 hours. Upon completion, the residue solvent was removed under reduced pressure. The crude product was purified by silica gel column chromatography (80 % EtOAc in hexane) to afford **1.36** (4.59 mg, 99%). ¹H NMR (800 MHz, Methanol-*d*₄) δ 5.14 (t, *J* = 7.0 Hz, 1H), 4.41 (t, *J* = 4.4 Hz, 1H), 4.33 (t, *J* = 7.3 Hz, 1H), 2.18 (d, *J* = 15.2 Hz, 1H), 1.99 – 1.94 (m, 2H), 1.88 (ddd, *J* = 14.5, 6.9, 4.4 Hz, 1H). ¹³C NMR (201 MHz, MeOD) δ 160.50, 82.41, 72.08, 56.63, 47.91, 47.81, 47.70, 47.59, 47.49, 47.38, 47.28, 41.55, 41.15. LRMS-ESI (*m/z*) : 144.1 [M+H]. α_D²³ = +20.0 (*c* = 1.0, MeOH)



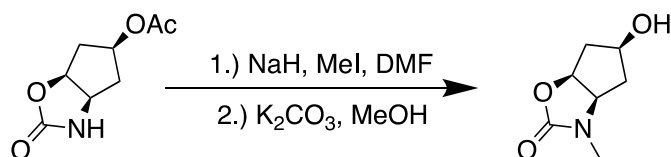
(3a*R*,5*S*,6a*S*)-5-hydroxyhexahydro-2*H*-cyclopenta[*d*]oxazol-2-one (1.39)

To a stirring solution of protected oxazolidinone **1.43** (7.70 mg, 0.041 mmol) in methanol (1.10 mL) was added potassium carbonate (6.90 mg, 0.050 mmol). Reaction was stirred at room temperature for 4 hours. Upon completion, the residue solvent was removed under reduced pressure. The crude product was purified by silica gel column chromatography (80 % EtOAc in hexane) to afford **1.39** (5.90 mg, 99%). ¹H NMR (800 MHz, Methanol-*d*₄) δ 5.14 (t, *J* = 7.0 Hz, 1H), 4.41 (t, *J* = 4.3 Hz, 1H), 4.33 (t, *J* = 7.2 Hz, 1H), 2.18 (d, *J* = 15.2 Hz, 1H), 1.99 – 1.94 (m, 2H), 1.88 (ddd, *J* = 14.5, 6.9, 4.5 Hz, 1H). ¹³C NMR (201 MHz, MeOD) δ 160.50, 82.40, 72.08, 56.63, 47.91, 47.81, 47.70, 47.59, 47.49, 47.38, 47.27, 41.56, 41.15. LRMS-ESI (*m/z*) : 144.1 [M+H]. $\alpha_D^{23} = -7.65$ (*c* = 1.35, MeOH)



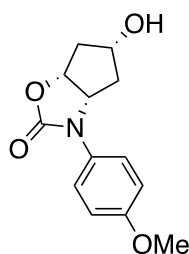
(3a*S*,5*R*,6a*R*)-5-hydroxy-3-methylhexahydro-2*H*-cyclopenta[*d*]oxazol-2-one (1.42)

Protected oxazolidinone **1.40** (21.0 mg, 0.113 mmol) was dissolved with dry acetonitrile (1.40 mL) and was placed under an argon atmosphere. Reaction mixture was cooled to 0 °C and potassium bis(trimethylsilyl)amide (0.5 M solution) (0.250 mL, 0.125 mmol) was added drop wise. The reaction stirred for 30 min. Iodomethane (17.7 mg, 0.125 mmol) was then added drop wise and the reaction mixture was allowed to warm up to room temperature for 1 hour. Upon completion, the residue was taken up in DI water and the aqueous phase was extracted with EtOAc. The organic extracts were dried with Na₂SO₄ and the solvent was removed under reduced pressure. The crude product was taken up in methanol (3.00 mL) and followed the addition of potassium carbonate (18.7 mg, 0.136 mmol). Reaction was stirred at room temperature for 12 hours. Upon completion, the residue solvent was removed under reduced pressure. The crude product was purified by silica gel column chromatography (60 % EtOAc in hexane) to afford **1.42** (14.3 mg, 80%). ¹H NMR (400 MHz, Chloroform-*d*) δ 4.98 (t, *J* = 7.0 Hz, 1H), 4.48 (t, *J* = 4.2 Hz, 1H), 4.17 (t, *J* = 7.2 Hz, 1H), 2.85 (s, 3H), 2.38 (s, 1H), 2.23 (ddd, *J* = 34.7, 15.9, 1.9 Hz, 2H), 1.94 (dddd, *J* = 15.4, 6.6, 4.3, 0.6 Hz, 1H), 1.66 (dddd, *J* = 14.8, 6.8, 4.3, 0.6 Hz, 1H). ¹³C NMR (101 MHz, CDCl₃) δ 157.60, 78.36, 77.25, 76.93, 76.62, 72.35, 61.86, 42.37, 37.59, 29.18. LRMS-ESI (*m/z*) : 158.0 [M+H]. $\alpha_D^{23} = +31.2$ (*c* = 2.20, MeOH)



(3a*R*,5*S*,6a*S*)-5-hydroxy-3-methylhexahydro-2*H*-cyclopenta[*d*]oxazol-2-one (1.45)

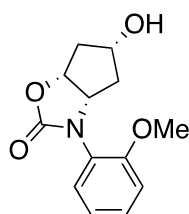
Protected oxazolidinone **1.43** (19.6 mg, 0.106 mmol) was dissolved with freshly distilled dimethylformamide (2.12 mL) and was placed under an argon atmosphere. The reaction mixture was cooled to 0 °C and sodium hydride (0.110 mmol) was added all at once. The reaction stirred for 20 min and then iodomethane (21.0 mg, 0.148 mmol) was added dropwise. The reaction was allowed to warm up to room temperature for 1 hour. Upon completion, the residue was taken up in DI water and the aqueous phase was extracted with EtOAc. The organic extracts were dried with Na₂SO₄ and the solvent was removed under reduced pressure. The crude product was taken up in methanol (2.12 mL) and followed the addition of potassium carbonate (16.7 mg, 0.136 mmol). The reaction was stirred at room temperature for 12 hours. Upon completion, the residue solvent was removed under reduced pressure. The crude product was purified by silica gel column chromatography (60 % EtOAc in hexane) to afford **1.45** (10.0 mg, 60%). ¹H NMR (800 MHz, Methanol-*d*₄) δ 5.04 (t, *J* = 8.0, 7.0 Hz, 1H), 4.40 (t, *J* = 4.3 Hz, 1H), 4.27 (t, *J* = 7.2 Hz, 1H), 2.85 (s, 3H), 2.20 – 2.13 (m, 2H), 2.03 – 1.96 (m, 2H), 1.77 – 1.71 (m, 2H). ¹³C NMR (201 MHz, MeOD) δ 158.62, 79.21, 71.81, 62.10, 47.91, 47.88, 47.81, 47.70, 47.59, 47.49, 47.38, 47.27, 41.34, 36.92, 27.89. LRMS-ESI (*m/z*) : 158.0 [M+H]. α_D²³ = −16.0 (*c* = 1.00, MeOH)



(3a*S*,5*R*,6a*R*)-5-hydroxy-3-(4-methoxyphenyl)hexahydro-2*H*-cyclopenta[*d*]oxazol-2-one (1.59)

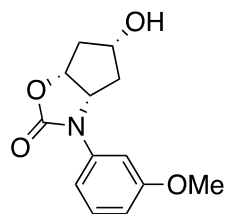
To a stirring solution of protected oxazolidinone **1.35** (6.00 mg, 0.021 mmol) in methanol (0.70 mL) was added potassium carbonate (3.40 mg, 0.025 mmol). Reaction was stirred at room temperature for 12 hours. Upon completion, the residue solvent was removed under reduced pressure. The crude product was purified by silica gel column chromatography (60 % EtOAc in

hexane) to afford **1.59** (5.08 mg, 99%). ¹H NMR (400 MHz, Chloroform-*d*) δ 7.45 – 7.36 (m, 2H), 6.95 – 6.87 (m, 2H), 5.13 (dd, *J* = 7.8, 5.2 Hz, 1H), 4.78 (t, *J* = 7.2 Hz, 1H), 4.54 – 4.46 (m, 1H), 3.80 (s, 3H), 2.41 – 2.31 (m, 1H), 2.14 (ddt, *J* = 14.9, 2.8, 1.2 Hz, 1H), 2.03 (ddd, *J* = 15.4, 6.4, 4.2 Hz, 1H), 1.78 (ddd, *J* = 14.9, 6.9, 4.3 Hz, 1H), 1.71 (d, *J* = 2.4 Hz, 1H). ¹³C NMR (101 MHz, CDCl₃) δ 156.82, 155.19, 130.32, 123.33, 114.35, 77.94, 77.24, 76.92, 76.60, 72.55, 61.70, 55.41, 42.70, 39.03. LRMS-ESI (*m/z*) : 250.0 [M+H]. α_D²³ = +75.5 (*c* = 2.00, MeOH)



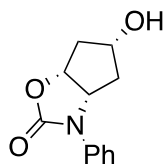
(3a*S*,5*R*,6a*R*)-5-hydroxy-3-(2-methoxyphenyl)hexahydro-2*H*-cyclopenta[*d*]oxazol-2-one
(1.60)

To a stirring solution of protected oxazolidinone **1.56** (11.0 mg, 0.038 mmol) in methanol (1.30 mL) was added potassium carbonate (6.26 mg, 0.045 mmol). Reaction was stirred at room temperature for 12 hours. Upon completion, the residue solvent was removed under reduced pressure. The crude product was purified by silica gel column chromatography (60 % EtOAc in hexane) to afford **1.60** (8.00 mg, 85%). ¹H NMR (400 MHz, Chloroform-*d*) δ 7.38 (dd, *J* = 7.7, 1.7 Hz, 1H), 7.30 (ddd, *J* = 8.3, 7.5, 1.7 Hz, 1H), 7.05 – 6.96 (m, 2H), 5.19 (t, *J* = 7.2 Hz, 1H), 4.82 (t, *J* = 7.3 Hz, 1H), 4.47 (t, *J* = 4.4 Hz, 1H), 3.87 (s, 3H), 2.39 (ddd, *J* = 15.5, 3.1, 0.9 Hz, 2H), 2.10 – 1.87 (m, 3H), 1.63 (dddd, *J* = 15.1, 6.7, 4.5, 0.6 Hz, 2H). ¹³C NMR (101 MHz, CDCl₃) δ 156.13, 155.11, 129.78, 128.98, 124.97, 121.32, 112.07, 78.99, 77.23, 77.11, 76.91, 76.60, 72.68, 62.13, 55.73, 42.98, 38.83, 29.59. LRMS-ESI (*m/z*) : 250.0 [M+H]. α_D²³ = +71.2 (*c* = 2.67, MeOH)



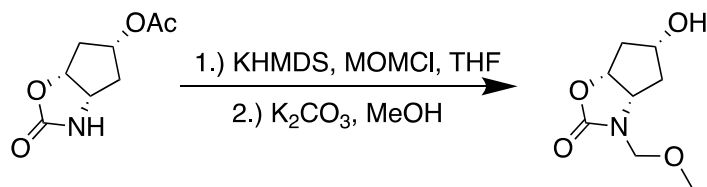
(3a*S*,5*R*,6a*R*)-5-hydroxy-3-(3-methoxyphenyl)hexahydro-2*H*-cyclopenta[*d*]oxazol-2-one (1.61)

To a stirring solution of protected oxazolidinone **1.57** (11.0 mg, 0.038 mmol) in methanol (1.30 mL) was added potassium carbonate (6.26 mg, 0.045 mmol). Reaction was stirred at room temperature for 12 hours. Upon completion, the residue solvent was removed under reduced pressure. The crude product was purified by silica gel column chromatography (60 % EtOAc in hexane) to afford **1.61** (7.60 mg, 81%). ¹H NMR (800 MHz, Chloroform-*d*) δ 7.32 – 7.26 (m, 2H), 7.07 (ddd, *J* = 8.2, 2.1, 0.9 Hz, 1H), 6.71 (ddd, *J* = 8.3, 2.5, 0.8 Hz, 1H), 5.14 (t, *J* = 7.0 Hz, 1H), 4.85 (t, *J* = 7.3 Hz, 1H), 4.54 (t, *J* = 4.3 Hz, 1H), 3.84 (s, 3H), 2.40 (dd, *J* = 15.5, 2.2 Hz, 1H), 2.23 (dd, *J* = 14.9, 2.9 Hz, 1H), 2.10 – 2.02 (m, 1H), 1.92 (dddd, *J* = 15.0, 7.1, 4.4, 0.6 Hz, 1H), 1.71 (s, 1H). ¹³C NMR (201 MHz, CDCl₃) δ 160.27, 154.66, 138.84, 129.79, 112.16, 109.80, 106.26, 77.94, 77.19, 77.04, 76.88, 72.55, 61.06, 55.38, 42.52, 39.66. LRMS-ESI (*m/z*) : 250.1 [M+H]. $\alpha_D^{23} = +98.2$ (*c* = 2.00, MeOH)



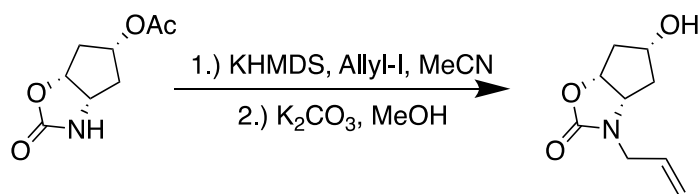
(3a*S*,5*R*,6a*R*)-5-hydroxy-3-phenylhexahydro-2*H*-cyclopenta[*d*]oxazol-2-one (1.58)

To a stirring solution of protected oxazolidinone **1.55** (22.0 mg, 0.084 mmol) in methanol (2.80 mL) was added potassium carbonate (13.9 mg, 0.101 mmol). Reaction was stirred at room temperature for 12 hours. Upon completion, the residue solvent was removed under reduced pressure. The crude product was purified by silica gel column chromatography (60 % EtOAc in hexane) to afford **1.58** (13.5 mg, 73%). ¹H NMR (800 MHz, Chloroform-*d*) δ 7.56 (dt, *J* = 8.6, 1.2 Hz, 2H), 7.39 (ddt, *J* = 8.7, 7.3, 1.7 Hz, 2H), 7.16 (td, *J* = 7.3, 1.3 Hz, 1H), 5.15 (t, *J* = 7.0 Hz, 1H), 4.88 (t, *J* = 7.3 Hz, 1H), 4.53 (t, *J* = 4.4 Hz, 1H), 2.41 (dd, *J* = 15.6, 3.0 Hz, 1H), 2.20 (ddd, *J* = 14.9, 3.0, 1.5 Hz, 1H), 2.06 (ddd, *J* = 15.5, 6.3, 4.3 Hz, 1H), 1.90 (ddd, *J* = 15.0, 7.0, 4.4 Hz, 1H), 1.84 (s, 1H). ¹³C NMR (201 MHz, CDCl₃) δ 154.86, 137.55, 129.15, 124.36, 120.39, 78.03, 77.20, 77.04, 76.88, 72.55, 61.07, 42.57, 39.48. LRMS-ESI (*m/z*) : 220.1 [M+H]. $\alpha_D^{23} = +87.6$ (*c* = 1.90, MeOH)



(3a*S*,5*R*,6a*R*)-5-hydroxy-3-(methoxymethyl)hexahydro-2*H*-cyclopenta[*d*]oxazol-2-one (1.63)

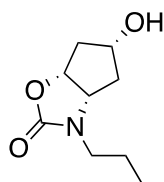
Protected oxazolidinone **1.40** (8.0 mg, 0.043 mmol) was dissolved with dry tetrahydrofuran (2.70 mL) and was placed under an argon atmosphere. Reaction mixture was cooled to 0 °C and potassium bis(trimethylsilyl)amide (0.5 M solution) (0.128 mL, 0.065 mmol) was added drop wise. The reaction stirred for 30 min. Chloromethyl methyl ether (5.7 mg, 0.069 mmol) was then added drop wise and the reaction mixture was allowed to warm up to room temperature for 1 hour. Upon completion, the residue was taken up in DI water and the aqueous phase was extracted with EtOAc. The organic extracts were dried with Na₂SO₄ and the solvent was removed under reduced pressure. The crude product was taken up in methanol (1.00 mL) and followed the addition of potassium carbonate (8.0 mg, 0.060 mmol). Reaction was stirred at room temperature for 12 hours. Upon completion, the residue solvent was removed under reduced pressure. The crude product was purified by silica gel column chromatography (60 % EtOAc in hexane) to afford **1.63** (2.70 mg, 33%). ¹H NMR (800 MHz, Methanol-*d*₄) δ 5.09 (t, *J* = 7.1 Hz, 1H), 4.77 (d, *J* = 11.0 Hz, 1H), 4.68 (d, *J* = 11.1 Hz, 1H), 4.45 – 4.40 (m, 2H), 3.35 (s, 3H), 2.20 (dd, *J* = 14.9, 1.4 Hz, 2H), 2.04 – 1.98 (m, 1H), 1.83 – 1.76 (m, 1H). ¹³C NMR (201 MHz, MeOD) δ 158.73, 79.88, 74.83, 71.92, 59.39, 54.83, 47.91, 47.88, 47.81, 47.70, 47.59, 47.49, 47.38, 47.27, 41.08, 38.34. LRMS-ESI (*m/z*) : 209.9 [M+Na]. α_D²³ = +9.87 (*c* = 2.60, MeOH)



(3a*S*,5*R*,6a*R*)-3-allyl-5-hydroxyhexahydro-2*H*-cyclopenta[*d*]oxazol-2-one (1.47)

Protected oxazolidinone **1.40** (5.50 mg, 0.030 mmol) was dissolved with dry acetonitrile (1.50 mL) and was placed under an argon atmosphere. Reaction mixture was cooled to 0 °C and potassium bis(trimethylsilyl)amide (0.5 M solution) (0.660 mL, 0.033 mmol) was added drop wise. The reaction stirred for 30 min. Allyl iodide (5.54 mg, 0.033 mmol) was then added drop wise and

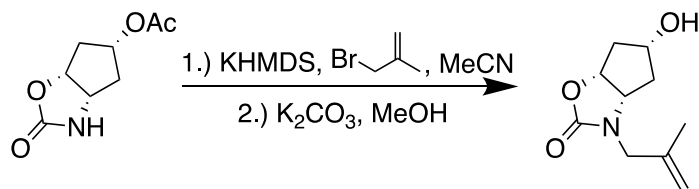
the reaction mixture was allowed to warm up to room temperature for 1 hour. Upon completion, the residue was taken up in DI water and the aqueous phase was extracted with EtOAc. The organic extracts were dried with Na₂SO₄ and the solvent was removed under reduced pressure. The crude product was taken up in methanol (1.00 mL) and followed the addition of potassium carbonate (4.93 mg, 0.036 mmol). Reaction was stirred at room temperature for 12 hours. Upon completion, the residue solvent was removed under reduced pressure. The crude product was purified by silica gel column chromatography (80 % EtOAc in hexane) to afford **1.47** (2.5 mg, 46%). ¹H NMR (800 MHz, Methanol- *d*₄) δ 5.76 (dddd, *J* = 17.2, 10.2, 7.1, 4.9 Hz, 1H), 5.22 (dq, *J* = 17.1, 1.5 Hz, 1H), 5.16 (dq, *J* = 10.2, 1.4 Hz, 1H), 4.96 (t, *J* = 7.1 Hz, 1H), 4.31 (dq, *J* = 4.3, 2.1, 1.6 Hz, 1H), 4.24 (t, *J* = 7.3 Hz, 1H), 4.04 (ddt, *J* = 15.8, 5.0, 1.7 Hz, 1H), 3.58 (ddt, *J* = 15.8, 7.1, 1.3 Hz, 1H), 2.07 (dd, *J* = 28.0, 15.3 Hz, 2H), 1.92 (ddd, *J* = 15.1, 6.5, 4.3 Hz, 1H), 1.63 (ddd, *J* = 14.7, 6.9, 4.3 Hz, 1H). ¹³C NMR (201 MHz, MeOD) δ 159.70, 133.71, 118.52, 80.87, 73.22, 61.08, 49.10, 48.99, 48.88, 46.06, 42.71, 38.70. LRMS-ESI (*m/z*) : 183.9 [M+H]. α_D²³ = +19.0 (*c* = 2.00, MeOH)



(3a*S*,5*R*,6a*R*)-5-hydroxy-3-propylhexahydro-2*H*-cyclopenta[*d*]oxazol-2-one (1.48)

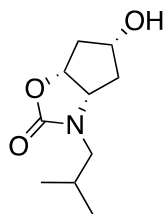
To a stirred reaction of alcohol **1.47** (2.50 mg, 0.014 mmol) in dry methanol (1.00 mL) under an argon atmosphere was added Pd/C (10% wt, 0.25 mg) and a hydrogen balloon. Reaction mixture was stirred at room temperature for 12 hours. Upon completion, the residue was filtered over celite and rinsed with dichloromethane and methanol. The solvent collected was removed under reduced pressure. The crude product was purified by silica gel column chromatography (60 % EtOAc in hexane) to afford **1.48** (1.5 mg, 59%). ¹H NMR (800 MHz, Chloroform-*d*) δ 5.02 (t, *J* = 7.0 Hz, 1H), 4.51 (t, *J* = 4.4 Hz, 1H), 4.28 (t, *J* = 7.2 Hz, 1H), 3.51 (ddd, *J* = 14.1, 8.7, 7.3 Hz, 1H), 3.04 (ddd, *J* = 13.9, 8.6, 5.2 Hz, 1H), 2.30 – 2.26 (m, 1H), 2.20 – 2.16 (m, 1H), 2.03 (ddd, *J* = 15.5, 6.5, 4.4 Hz, 1H), 1.75 (ddd, *J* = 14.9, 6.9, 4.5 Hz, 1H), 1.69 – 1.64 (m, 1H), 1.61 (ddd, *J* = 13.5, 8.0, 6.6 Hz, 1H), 0.97 (t, *J* = 7.4 Hz, 3H). ¹³C NMR (201 MHz, CDCl₃) δ 157.32, 78.32, 77.18, 77.02,

76.86, 72.77, 59.53, 44.18, 42.69, 38.34, 29.72, 20.54, 11.21. LRMS-ESI (m/z) : 186.0 [M+H].
 $\alpha_D^{23} = +14.3$ (c = 0.77, MeOH)



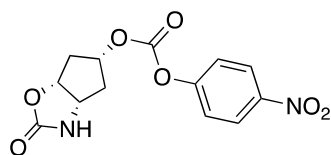
(3a*S*,5*R*,6a*R*)-5-hydroxy-3-(2-methylallyl)hexahydro-2*H*-cyclopenta[*d*]oxazol-2-one (1.50)

Protected oxazolidinone **1.40** (10.2 mg, 0.055 mmol) was dissolved with dry acetonitrile (1.00 mL) and was placed under an argon atmosphere. Reaction mixture was cooled to 0 °C and potassium bis(trimethylsilyl)amide (0.5 M solution) (0.132 mL, 0.066 mmol) was added drop wise. The reaction stirred for 30 min. 3-Bromo-2-methylpro-1-ene (8.78 mg, 0.060 mmol) was then added drop wise and the reaction mixture was allowed to warm up to room temperature for 1 hour. Upon completion, the residue was taken up in DI water and the aqueous phase was extracted with EtOAc. The organic extracts were dried with Na₂SO₄ and the solvent was removed under reduced pressure. The crude product was taken up in methanol (0.60 mL) and followed the addition of potassium carbonate (4.60 mg, 0.019 mmol). Reaction was stirred at room temperature for 12 hours. Upon completion, the residue solvent was removed under reduced pressure. The crude product was purified by silica gel column chromatography (80 % EtOAc in hexane) to afford **1.50** (3.2 mg, 84%). ¹H NMR (800 MHz, Chloroform-*d*) δ 5.03 (t, *J* = 7.0 Hz, 1H), 4.95 (d, *J* = 20.5 Hz, 2H), 4.51 (s, 1H), 4.19 (t, *J* = 7.3 Hz, 1H), 4.15 (d, *J* = 15.2 Hz, 1H), 3.58 (d, *J* = 15.3 Hz, 1H), 2.30 (dd, *J* = 15.5, 2.9 Hz, 1H), 2.19 (dt, *J* = 14.8, 1.8 Hz, 1H), 2.01 (ddd, *J* = 15.4, 6.4, 4.3 Hz, 1H), 1.77 (s, 2H), 1.69 (ddt, *J* = 19.2, 7.0, 3.7 Hz, 2H). ¹³C NMR (201 MHz, CDCl₃) δ 157.47, 140.06, 113.78, 78.54, 77.18, 77.02, 76.86, 72.68, 59.34, 48.92, 42.65, 37.95, 19.93. LRMS-ESI (m/z) : 198.0 [M+H]. $\alpha_D^{23} = +22.9$ (c = 0.67, MeOH)



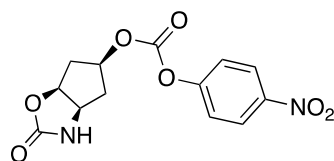
(3a*S*,5*R*,6a*R*)-5-hydroxy-3-isobutylhexahydro-2*H*-cyclopenta[*d*]oxazol-2-one (1.51)

To a stirred reaction of alcohol **1.50** (3.20 mg, 0.016 mmol) in dry methanol (1.00 mL) under an argon atmosphere was added of Pd/C (10% wt, 0.3 mg) and a hydrogen balloon. Reaction mixture was stirred at room temperature for 12 hours. Upon completion, the residue was filtered over celite and rinsed with dichloromethane and methanol. The solvent collected was removed under reduced pressure. The crude product was purified by silica gel column chromatography (60 % EtOAc in hexane) to afford **1.51** (2.8 mg, 87%). ¹H NMR (800 MHz, Chloroform-*d*) δ 5.02 (t, *J* = 6.9 Hz, 1H), 4.51 (s, 1H), 4.26 (t, *J* = 7.4 Hz, 1H), 3.33 (t, *J* = 12.5, 11.0 Hz, 1H), 2.89 (ddd, *J* = 14.1, 6.2, 2.3 Hz, 1H), 2.29 (d, *J* = 15.4 Hz, 1H), 2.19 (d, *J* = 14.7 Hz, 1H), 2.05 – 1.91 (m, 2H), 1.78 – 1.67 (m, 2H), 0.99 (d, *J* = 6.5 Hz, 3H), 0.94 (d, *J* = 6.5 Hz, 3H). ¹³C NMR (201 MHz, CDCl₃) δ 157.71, 78.38, 77.18, 77.02, 76.87, 72.65, 59.89, 49.97, 42.68, 38.03, 26.39, 20.23, 19.79. LRMS-ESI (*m/z*) : 200.1 [M+H]⁺ $\alpha_D^{23} = +65.2$ (*c* = 2.00, MeOH)



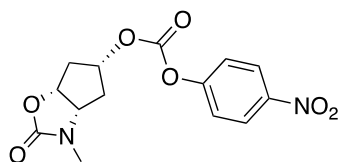
4-nitrophenyl ((3a*S*,5*R*,6a*R*)-2-oxohexahydro-2*H*-cyclopenta[*d*]oxazol-5-yl) carbonate (1.64a)

To a stirred solution of alcohol **1.36** (10.0 mg, 0.070 mmol) in dry dichloromethane (2.0 mL) was added 4-methylmorpholine (23.0 μ L, 0.210 mmol) and 4-nitrophenyl chloroformate (42.0 mg, 0.210 mmol) at 0 °C under an argon atmosphere. The reaction mixture was warmed to 23 °C and stirred for 12 h. Upon completion, solvent was removed under reduced pressure. The crude product was purified by silica gel column chromatography (80 % EtOAc in hexane) to afford **1.64a** (17.8 mg, 83%). ¹H NMR (800 MHz, Chloroform-*d*) δ 8.29 (d, *J* = 9.1 Hz, 2H), 7.40 (d, *J* = 9.1 Hz, 2H), 5.36 (t, *J* = 4.6 Hz, 1H), 5.29 (s, 1H), 5.26 (t, *J* = 6.9 Hz, 1H), 4.49 (t, *J* = 7.2 Hz, 1H), 2.67 (dd, *J* = 16.3, 3.0 Hz, 1H), 2.34 (dd, *J* = 15.6, 3.0 Hz, 1H), 2.16 (ddd, *J* = 16.2, 6.4, 4.6 Hz, 1H), 2.10 (ddd, *J* = 15.6, 6.8, 4.7 Hz, 1H). ¹³C NMR (201 MHz, CDCl₃) δ 158.14, 155.36, 151.94, 145.46, 125.30, 121.87, 81.00, 80.72, 77.18, 77.02, 76.87, 55.89, 40.20, 39.45, 29.71. LRMS-ESI (*m/z*) : 309.0 [M+H]⁺



4-nitrophenyl ((3aR,5S,6aS)-2-oxohexahydro-2H-cyclopenta[d]oxazol-5-yl) carbonate (1.64b)

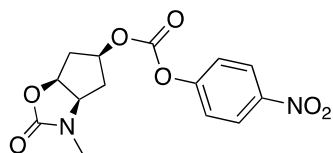
To a stirred solution of alcohol **1.39** (2.7 mg, 0.019 mmol) in dry dichloromethane (0.50 mL) was added 4-methylmorpholine (6.30 μ L, 0.057 mmol) and 4-nitrophenyl chloroformate (11.4 mg, 0.057 mmol) at 0 °C under an argon atmosphere. The reaction mixture was warmed to 23 °C and stirred for 12 h. Upon completion, solvent was removed under reduced pressure. The crude product was purified by silica gel column chromatography (80 % EtOAc in hexane) to afford **1.64b** (4.0 mg, 69%). ^1H NMR (800 MHz, Chloroform-*d*) δ 8.29 (d, J = 8.5 Hz, 2H), 7.40 (d, J = 8.7 Hz, 2H), 5.36 (t, J = 4.8 Hz, 1H), 5.26 (t, J = 7.0 Hz, 1H), 5.19 (s, 1H), 4.49 (t, J = 7.2 Hz, 1H), 2.67 (d, J = 15.9 Hz, 1H), 2.34 (d, J = 15.5 Hz, 1H), 2.15 (dt, J = 16.3, 5.5 Hz, 1H), 2.10 (dt, J = 15.6, 5.8 Hz, 1H). ^{13}C NMR (201 MHz, CDCl_3) δ 158.05, 155.35, 151.94, 145.46, 125.30, 121.87, 80.99, 80.71, 77.18, 77.02, 76.86, 55.87, 40.21, 39.45. LRMS-ESI (m/z) : 309.0 [$\text{M}+\text{H}$]



(3aS,5R,6aR)-3-methyl-2-oxohexahydro-2H-cyclopenta[d]oxazol-5-yl (4-nitrophenyl) carbonate (1.64c)

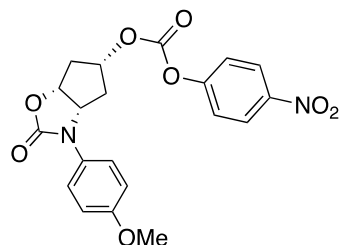
To a stirred solution of alcohol **1.42** (7.70 mg, 0.049 mmol) in dry dichloromethane (1.40 mL) was added 4-methylmorpholine (16.0 μ L, 0.147 mmol) and 4-nitrophenyl chloroformate (29.6 mg, 0.147 mmol) at 0 °C under an argon atmosphere. The reaction mixture was warmed to 23 °C and stirred for 12 h. Upon completion, solvent was removed under reduced pressure. The crude product was purified by silica gel column chromatography (60 % EtOAc in hexane) to afford **1.64c** (12.5 mg, 79%). ^1H NMR (500 MHz, Chloroform-*d*) δ 8.26 (d, J = 9.2 Hz, 2H), 7.35 (d, J = 9.2 Hz, 2H), 5.32 – 5.28 (m, 1H), 5.07 (t, J = 7.1 Hz, 1H), 4.28 (t, J = 7.1 Hz, 1H), 2.89 (s, 3H), 2.59 (dd, J = 16.3, 2.7 Hz, 1H), 2.44 (dd, J = 15.7, 3.1 Hz, 1H), 2.21 – 2.13 (m, 1H), 1.98 – 1.88 (m, 1H). ^{13}C

NMR (126 MHz, CDCl₃) δ 156.92, 155.34, 151.91, 145.45, 125.30, 121.91, 80.51, 77.30, 77.04, 76.79, 61.50, 39.70, 35.57, 29.32. LRMS-ESI (m/z) : 323.0 [M+H]



4-nitrophenyl ((3aR,5S,6aS)-2-oxohexahydro-2H-cyclopenta[d]oxazol-5-yl) carbonate (1.64d)

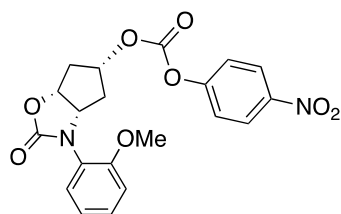
To a stirred solution of alcohol **1.45** (5.70 mg, 0.036 mmol) in dry dichloromethane (1.00 mL) was added 4-methylmorpholine (12.0 μ L, 0.109 mmol) and 4-nitrophenyl chloroformate (22.0 mg, 0.109 mmol) at 0 °C under an argon atmosphere. The reaction mixture was warmed to 23 °C and stirred for 12 h. Upon completion, solvent was removed under reduced pressure. The crude product was purified by silica gel column chromatography (60 % EtOAc in hexane) to afford **1.64d** (11.0 mg, 94%). ¹H NMR (500 MHz, Chloroform-*d*) δ 8.27 (d, *J* = 9.2 Hz, 2H), 7.36 (d, *J* = 9.2 Hz, 2H), 5.30 (t, *J* = 4.6 Hz, 1H), 5.07 (t, *J* = 7.0 Hz, 1H), 4.28 (t, *J* = 7.1 Hz, 1H), 2.89 (s, 3H), 2.45 (dd, *J* = 15.6, 3.0 Hz, 1H), 2.20 – 2.13 (m, 1H), 1.96 – 1.89 (m, 1H). ¹³C NMR (126 MHz, CDCl₃) δ 156.90, 155.33, 151.92, 145.47, 125.31, 121.91, 80.47, 77.28, 77.24, 77.03, 76.77, 61.50, 39.72, 35.59, 29.33. LRMS-ESI (m/z) : 323.0 [M+H]



(3aS,5R,6aR)-3-(4-methoxyphenyl)-2-oxohexahydro-2H-cyclopenta[d]oxazol-5-yl(4-nitrophenyl) carbonate (1.64j)

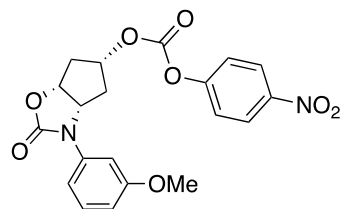
To a stirred solution of alcohol **1.59** (6.80 mg, 0.027 mmol) in dry dichloromethane (1.00 mL) was added 4-methylmorpholine (9.00 μ L, 0.082 mmol) and 4-nitrophenyl chloroformate (16.5 mg, 0.082 mmol) at 0 °C under an argon atmosphere. The reaction mixture was warmed to 23 °C and stirred for 12 h. Upon completion, solvent was removed under reduced pressure. The crude product was purified by silica gel column chromatography (40 % EtOAc in hexane) to afford **1.64j** (11.0

mg, 97%). ^1H NMR (500 MHz, Chloroform-*d*) δ 8.27 (d, J = 9.2 Hz, 2H), 7.38 (d, J = 9.1 Hz, 2H), 7.32 (d, J = 9.2 Hz, 2H), 6.92 (d, J = 9.1 Hz, 2H), 5.31 (t, J = 4.5 Hz, 1H), 5.22 (t, J = 7.1 Hz, 1H), 4.92 (t, J = 7.0 Hz, 1H), 3.81 (s, 3H), 2.69 (dd, J = 16.3, 2.8 Hz, 1H), 2.43 (dd, J = 15.7, 3.1 Hz, 1H), 2.27 – 2.19 (m, 1H), 2.03 – 1.95 (m, 1H). ^{13}C NMR (126 MHz, CDCl_3) δ 157.24, 155.31, 154.71, 151.86, 145.50, 129.77, 125.32, 123.48, 121.92, 114.61, 80.48, 77.28, 77.03, 76.77, 61.27, 55.55, 40.01, 36.70. LRMS-ESI (m/z) : 415.0 [$\text{M}+\text{H}$]



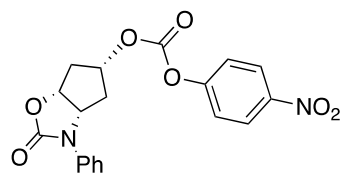
(3a*S*,5*R*,6a*R*)-3-(2-methoxyphenyl)-2-oxohexahydro-2*H*-cyclopenta[*d*]oxazol-5-yl(4-nitrophenyl) carbonate (1.64k)

To a stirred solution of alcohol **1.60** (8.00 mg, 0.027 mmol) in dry dichloromethane (1.00 mL) was added 4-methylmorpholine (10.5 μL , 0.096 mmol) and 4-nitrophenyl chloroformate (19.4 mg, 0.096 mmol) at 0 $^\circ\text{C}$ under an argon atmosphere. The reaction mixture was warmed to 23 $^\circ\text{C}$ and stirred for 12 h. Upon completion, solvent was removed under reduced pressure. The crude product was purified by silica gel column chromatography (40 % EtOAc in hexane) to afford **1.64k** (12.5 mg, 94%). ^1H NMR (800 MHz, Chloroform-*d*) δ 8.32 (d, J = 9.0 Hz, 2H), 7.42 (t, J = 8.0 Hz, 3H), 7.33 (t, J = 7.8 Hz, 2H), 7.00 (d, J = 8.0 Hz, 2H), 5.33 (t, J = 4.3 Hz, 1H), 5.28 (t, J = 7.2 Hz, 1H), 5.09 (t, J = 7.2 Hz, 1H), 3.90 (s, 3H), 2.71 (dd, J = 16.2, 3.1 Hz, 2H), 2.28 – 2.21 (m, 3H), 1.85 (ddd, J = 15.8, 6.8, 4.6 Hz, 2H). ^{13}C NMR (201 MHz, CDCl_3) δ 156.00, 155.38, 154.90, 151.97, 145.50, 129.76, 128.96, 125.36, 124.58, 121.94, 121.11, 112.03, 80.83, 77.93, 77.18, 77.02, 76.86, 60.83, 55.68, 40.06, 36.66. LRMS-ESI (m/z) : 415.1 [$\text{M}+\text{H}$]



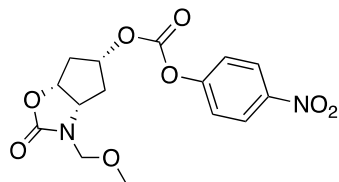
(3a*S*,5*R*,6a*R*)-3-(3-methoxyphenyl)-2-oxohexahydro-2*H*-cyclopenta[*d*]oxazol-5-yl (4-nitrophenyl) carbonate (1.64l)

To a stirred solution of alcohol **1.61** (7.60 mg, 0.030 mmol) in dry dichloromethane (0.86 mL) was added 4-methylmorpholine (10.0 μ L, 0.091 mmol) and 4-nitrophenyl chloroformate (18.4 mg, 0.091 mmol) at 0 °C under an argon atmosphere. The reaction mixture was warmed to 23 °C and stirred for 12 h. Upon completion, solvent was removed under reduced pressure. The crude product was purified by silica gel column chromatography (40 % EtOAc in hexane) to afford **1.64i** (12.1 mg, 96%). ^1H NMR (800 MHz, Chloroform-*d*) δ 8.27 (d, J = 9.2 Hz, 2H), 7.32 – 7.29 (m, 3H), 7.22 (t, J = 2.3 Hz, 1H), 7.05 (dd, J = 8.0, 1.7 Hz, 1H), 6.75 (dd, J = 8.3, 2.3 Hz, 1H), 5.32 (t, J = 4.5 Hz, 1H), 5.24 (t, J = 7.0 Hz, 1H), 4.98 (t, J = 7.1 Hz, 1H), 3.81 (s, 3H), 2.71 (dd, J = 16.2, 3.1 Hz, 1H), 2.52 (dd, J = 15.8, 3.1 Hz, 1H), 2.26 (ddd, J = 16.2, 6.6, 4.6 Hz, 1H), 2.09 (ddd, J = 15.8, 6.8, 4.5 Hz, 1H). ^{13}C NMR (201 MHz, CDCl_3) δ 160.35, 155.28, 154.14, 151.83, 145.49, 138.21, 130.02, 125.28, 121.93, 112.61, 109.89, 107.30, 80.38, 77.19, 77.03, 76.88, 60.64, 55.37, 39.86, 36.95. LRMS-ESI (m/z) : 415.0 [$\text{M}+\text{H}$]



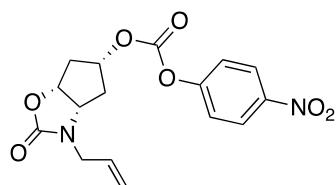
4-nitrophenyl ((3aR,5S,6aS)-2-oxohexahydro-2H-cyclopenta[d]oxazol-5-yl) carbonate (1.64i)

To a stirred solution of alcohol **1.58** (13.50 mg, 0.062 mmol) in dry dichloromethane (2.00 mL) was added 4-methylmorpholine (20.3 μ L, 0.185 mmol) and 4-nitrophenyl chloroformate (37.3 mg, 0.185 mmol) at 0 °C under an argon atmosphere. The reaction mixture was warmed to 23 °C and stirred for 12 h. Upon completion, solvent was removed under reduced pressure. The crude product was purified by silica gel column chromatography (40 % EtOAc in hexane) to afford **1.64i** (18.6 mg, 78%). ^1H NMR (800 MHz, Chloroform-*d*) δ 8.27 (dd, J = 9.0, 1.8 Hz, 2H), 7.54 (d, J = 7.9 Hz, 2H), 7.44 – 7.38 (m, 2H), 7.33 – 7.26 (m, 3H), 7.21 (t, J = 7.4 Hz, 1H), 5.33 (t, J = 4.6 Hz, 1H), 5.25 (t, J = 7.0 Hz, 1H), 5.02 (t, J = 7.1 Hz, 1H), 2.72 (dd, J = 16.3, 3.2 Hz, 1H), 2.49 (dd, J = 15.7, 3.2 Hz, 1H), 2.27 (dddd, J = 16.2, 6.4, 4.5, 1.6 Hz, 1H), 2.09 (dddd, J = 15.8, 6.5, 4.4, 1.5 Hz, 1H). ^{13}C NMR (201 MHz, CDCl_3) δ 155.28, 154.26, 151.83, 145.48, 137.00, 129.33, 125.30, 124.92, 121.90, 120.68, 80.40, 77.20, 77.04, 76.88, 60.57, 39.89, 36.90. LRMS-ESI (m/z) : 385.0 [$\text{M}+\text{H}$]



(3a*S*,5*R*,6a*R*)-3-(methoxymethyl)-2-oxohexahydro-2*H*-cyclopenta[*d*]oxazol-5-yl(4-nitrophenyl) carbonate (1.64m)

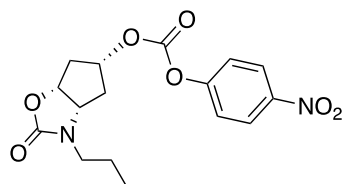
To a stirred solution of alcohol **1.63** (5.00 mg, 0.027 mmol) in dry dichloromethane (0.77 mL) was added 4-methylmorpholine (9.00 μ L, 0.081 mmol) and 4-nitrophenyl chloroformate (16.3 mg, 0.081 mmol) at 0 °C under an argon atmosphere. The reaction mixture was warmed to 23 °C and stirred for 12 h. Upon completion, solvent was removed under reduced pressure. The crude product was purified by silica gel column chromatography (60 % EtOAc in hexane) to afford **1.64m** (7.0 mg, 74%). ¹H NMR (800 MHz, Chloroform-*d*) δ 8.29 (d, *J* = 9.2 Hz, 2H), 7.38 (d, *J* = 9.2 Hz, 2H), 5.35 (t, *J* = 4.6 Hz, 1H), 5.14 (t, *J* = 7.1 Hz, 1H), 4.79 (d, *J* = 0.6 Hz, 2H), 4.48 (t, *J* = 7.1 Hz, 1H), 3.41 (s, 3H), 2.70 – 2.59 (m, 2H), 2.18 (dddd, *J* = 16.2, 6.6, 4.6, 0.7 Hz, 1H), 2.02 (dddd, *J* = 15.7, 6.9, 4.7, 0.7 Hz, 1H). ¹³C NMR (201 MHz, CDCl₃) δ 157.14, 155.33, 151.88, 145.46, 125.31, 121.83, 80.61, 78.02, 77.23, 77.18, 77.02, 76.86, 75.75, 59.37, 56.21, 39.46, 37.40. LRMS-ESI (*m/z*) : 375.0 [M+Na]



(3a*S*,5*R*,6a*R*)-3-allyl-2-oxohexahydro-2*H*-cyclopenta[*d*]oxazol-5-yl(4-nitrophenyl) carbonate (1.64e)

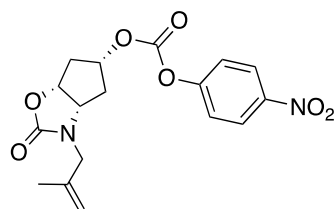
To a stirred solution of alcohol **1.47** (2.60 mg, 0.014 mmol) in dry dichloromethane (0.40 mL) was added 4-methylmorpholine (5.00 μ L, 0.043 mmol) and 4-nitrophenyl chloroformate (4.30 mg, 0.043 mmol) at 0 °C under an argon atmosphere. The reaction mixture was warmed to 23 °C and stirred for 12 h. Upon completion, solvent was removed under reduced pressure. The crude product was purified by silica gel column chromatography (60 % EtOAc in hexane) to afford **1.64e** (2.8 mg, 57%). ¹H NMR (800 MHz, Chloroform-*d*) δ 8.30 (d, *J* = 9.2 Hz, 2H), 7.39 (d, *J* = 9.2 Hz, 2H), 5.83 (dddd, *J* = 17.2, 10.1, 7.1, 5.4 Hz, 1H), 5.34 – 5.27 (m, 3H), 5.10 (t, *J* = 7.1 Hz, 1H), 4.37 (t, *J* = 7.2 Hz, 1H), 4.20 (ddt, *J* = 15.5, 5.4, 1.6 Hz, 1H), 3.69 (ddt, *J* = 15.5, 7.1, 1.2 Hz, 1H), 2.63

(dd, $J = 16.2, 2.5$ Hz, 1H), 2.48 (dd, $J = 15.7, 3.0$ Hz, 1H), 2.18 (dddd, $J = 16.2, 6.6, 4.6, 0.7$ Hz, 1H), 1.92 (dddd, $J = 15.6, 6.8, 4.7, 0.7$ Hz, 1H). ^{13}C NMR (201 MHz, CDCl_3) δ 156.64, 155.34, 151.90, 145.47, 132.28, 125.31, 121.87, 118.89, 80.51, 77.61, 77.23, 77.18, 77.02, 76.86, 59.28, 45.64, 39.66, 36.03. LRMS-ESI (m/z) : 349.0 $[\text{M}+\text{H}]$



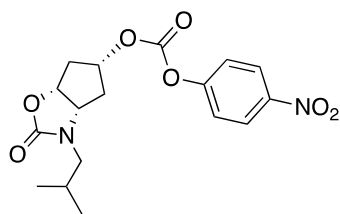
4-nitrophenyl((3a*S*,5*R*,6a*R*)-2-oxo-3-propylhexahydro-2*H*-cyclopenta[*d*]oxazol-5-yl) carbonate (1.64f)

To a stirred solution of alcohol **1.48** (1.00 mg, 0.014 mmol) in dry dichloromethane (0.50 mL) was added 4-methylmorpholine (2.00 μL , 0.016 mmol) and 4-nitrophenyl chloroformate (3.30 mg, 0.016 mmol) at 0 $^{\circ}\text{C}$ under an argon atmosphere. The reaction mixture was warmed to 23 $^{\circ}\text{C}$ and stirred for 12 h. Upon completion, solvent was removed under reduced pressure. The crude product was purified by silica gel column chromatography (60 % EtOAc in hexane) to afford **1.64f** (1.2 mg, 63%). ^1H NMR (500 MHz, Chloroform-*d*) δ 8.27 (d, $J = 9.2$ Hz, 2H), 7.36 (d, $J = 9.2$ Hz, 2H), 5.29 (t, $J = 4.6$ Hz, 1H), 5.07 (t, $J = 7.0$ Hz, 1H), 4.35 (t, $J = 7.2$ Hz, 1H), 3.47 (ddd, $J = 14.0, 8.8, 7.1$ Hz, 1H), 3.02 (ddd, $J = 14.0, 8.6, 5.2$ Hz, 1H), 2.60 (ddd, $J = 16.3, 3.0, 1.0$ Hz, 1H), 2.43 (dd, $J = 15.7, 3.0$ Hz, 1H), 2.16 (dddd, $J = 16.1, 6.5, 4.7, 0.7$ Hz, 1H), 1.94 (dddd, $J = 15.6, 6.8, 4.7, 0.7$ Hz, 1H), 1.73 – 1.57 (m, 2H), 0.95 (t, $J = 7.4$ Hz, 3H). ^{13}C NMR (126 MHz, CDCl_3) δ 156.94, 155.34, 151.94, 145.46, 125.31, 121.89, 80.50, 77.28, 77.02, 76.77, 59.38, 44.33, 39.68, 36.17, 29.71, 20.65, 11.18. LRMS-ESI (m/z) : 351.0 $[\text{M}+\text{H}]$



(3a*S*,5*R*,6a*R*)-3-(2-methylallyl)-2-oxohexahydro-2*H*-cyclopenta[*d*]oxazol-5-yl (4-nitrophenyl) carbonate (1.64g)

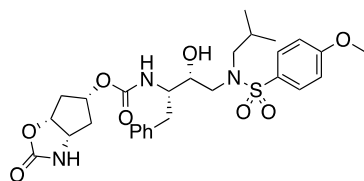
To a stirred solution of alcohol **1.50** (3.20 mg, 0.016 mmol) in dry dichloromethane (0.50 mL) was added 4-methylmorpholine (5.50 μ L, 0.049 mmol) and 4-nitrophenyl chloroformate (9.80 mg, 0.049 mmol) at 0 °C under an argon atmosphere. The reaction mixture was warmed to 23 °C and stirred for 12 h. Upon completion, solvent was removed under reduced pressure. The crude product was purified by silica gel column chromatography (60 % EtOAc in hexane) to afford **1.64g** (5.0 mg, 85%). ¹H NMR (500 MHz, Chloroform-*d*) δ 8.27 (d, *J* = 9.3 Hz, 2H), 7.36 (d, *J* = 9.2 Hz, 2H), 5.30 (t, *J* = 4.6 Hz, 1H), 5.08 (t, *J* = 7.0 Hz, 1H), 4.95 (d, *J* = 17.9 Hz, 2H), 4.26 (t, *J* = 7.2 Hz, 1H), 4.09 (d, *J* = 15.2 Hz, 1H), 3.59 (d, *J* = 15.2 Hz, 1H), 2.61 (dd, *J* = 16.4, 2.7 Hz, 1H), 2.43 (dd, *J* = 15.7, 3.0 Hz, 1H), 2.15 (dddd, *J* = 16.2, 6.5, 4.6, 0.7 Hz, 1H), 1.89 (dddd, *J* = 15.8, 7.0, 4.8, 0.7 Hz, 1H), 1.76 (t, *J* = 0.8 Hz, 3H). ¹³C NMR (126 MHz, CDCl₃) δ 157.04, 155.34, 151.94, 145.46, 139.85, 125.31, 121.88, 114.24, 80.52, 77.64, 77.29, 77.03, 76.78, 59.28, 49.21, 39.65, 35.92, 19.87. LRMS-ESI (*m/z*) : 363.0 [M+H]



(3a*S*,5*R*,6a*R*)-3-isobutyl-2-oxohexahydro-2*H*-cyclopenta[*d*]oxazol-5-yl (4-nitrophenyl) carbonate (1.64h**)**

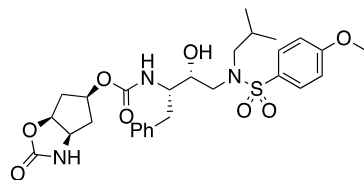
To a stirred solution of alcohol **1.51** (10.70 mg, 0.054 mmol) in dry dichloromethane (1.50 mL) was added 4-methylmorpholine (17.7 μ L, 0.161 mmol) and 4-nitrophenyl chloroformate (32.5 mg, 0.161 mmol) at 0 °C under an argon atmosphere. The reaction mixture was warmed to 23 °C and stirred for 12 h. Upon completion, solvent was removed under reduced pressure. The crude product was purified by silica gel column chromatography (60 % EtOAc in hexane) to afford **1.64h** (15.0 mg, 77%). ¹H NMR (800 MHz, Chloroform-*d*) δ 8.29 (d, *J* = 9.2 Hz, 2H), 7.38 (d, *J* = 9.2 Hz, 2H), 5.32 (t, *J* = 4.7 Hz, 1H), 5.10 (t, *J* = 7.0 Hz, 1H), 4.36 (t, *J* = 7.2 Hz, 1H), 3.33 (dd, *J* = 14.0, 8.9 Hz, 1H), 2.88 (dd, *J* = 14.0, 6.3 Hz, 1H), 2.63 (dd, *J* = 16.2, 2.6 Hz, 1H), 2.45 (dd, *J* = 15.7, 3.0 Hz, 1H), 2.20 – 2.15 (m, 1H), 2.01 – 1.93 (m, 2H), 1.00 (d, *J* = 6.7 Hz, 3H), 0.96 (d, *J* = 6.7 Hz, 3H). ¹³C NMR (201 MHz, CDCl₃) δ 157.21, 155.34, 151.93, 145.45, 125.30, 121.88, 80.47, 77.42,

77.18, 77.02, 76.86, 59.74, 50.19, 39.71, 35.97, 26.54, 20.16, 19.80. LRMS-ESI (m/z) : 365.0 [M+H]



(3a*S*,5*R*,6a*R*)-2-oxohexahydro-2*H*-cyclopenta[d]oxazol-5-yl ((2*S*,3*R*)-3-hydroxy-4-((*N*-isobutyl-4-methoxyphenyl)sulfonamido)-1-phenylbutan-2-yl)carbamate (1.65a)

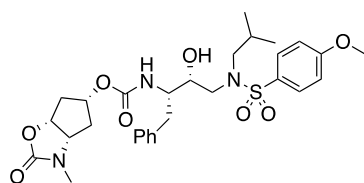
To a stirred solution of activated carbonate **1.64a** (16.0 mg, 0.052 mmol) in dry acetonitrile (1.5 mL) was added *N,N*-diisopropylethylamine (56.0 μ L, 0.331 mmol) and isostere amine **1.25** (23.0 mg, 0.057 mmol) at room temperature under argon atmosphere. The reaction mixture was stirred for 48 h. Upon completion, solvent was removed under reduced pressure. The crude product was purified by silica gel column chromatography (80 % EtOAc in hexane) to afford **1.65a** (13.0 mg, 44%). ^1H NMR (500 MHz, Methanol- d_4) δ 7.77 (d, J = 8.8 Hz, 2H), 7.30 – 7.20 (m, 4H), 7.17 (t, J = 7.3 Hz, 1H), 7.12 – 7.06 (m, 2H), 5.15 – 5.09 (m, 1H), 5.00 (t, J = 3.7 Hz, 1H), 4.34 – 4.26 (m, 1H), 3.87 (s, 3H), 3.77 – 3.68 (m, 2H), 3.34 (d, J = 2.2 Hz, 1H), 3.13 – 2.91 (m, 4H), 2.87 (ddd, J = 12.8, 7.0, 5.4 Hz, 1H), 2.61 – 2.50 (m, 1H), 2.08 – 1.92 (m, 3H), 1.85 (dt, J = 5.7, 3.3 Hz, 2H), 1.29 (s, 2H), 0.95 – 0.84 (m, 6H). ^{13}C NMR (201 MHz, CDCl_3) δ 162.94, 158.75, 155.45, 138.42, 137.53, 129.60, 128.39, 126.29, 114.34, 81.36, 81.23, 72.79, 58.61, 57.92, 55.62, 54.82, 52.19, 39.99, 39.24, 36.36, 35.95, 29.71, 27.24, 27.09, 20.15, 19.88. LRMS-ESI (m/z) : 576.2 [M+H], HRMS-ESI: 598.2185 (M+Na).



(3a*R*,5*S*,6a*S*)-2-oxohexahydro-2*H*-cyclopenta[d]oxazol-5-yl ((2*S*,3*R*)-3-hydroxy-4-((*N*-isobutyl-4-methoxyphenyl)sulfonamido)-1-phenylbutan-2-yl)carbamate (1.65b)

Compound **1.64b** (4.80 mg, 0.016 mmol) was treated with isostere **1.25** (6.90 mg, 0.017 mmol) by following the same procedure outlined for inhibitor **1.65a** to give inhibitor **1.65b**. (5.3 mg, 60%)

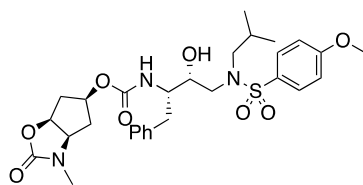
^1H NMR (800 MHz, Methanol- d_4) δ 7.77 (d, J = 8.9 Hz, 2H), 7.29 – 7.21 (m, 4H), 7.16 (tt, J = 7.0, 1.7 Hz, 1H), 7.08 (d, J = 8.9 Hz, 2H), 5.16 – 5.11 (m, 1H), 4.99 (t, J = 4.5 Hz, 1H), 4.35 (t, J = 7.1 Hz, 1H), 3.87 (s, 3H), 3.80 – 3.72 (m, 1H), 3.65 (ddd, J = 10.5, 6.8, 3.6 Hz, 1H), 3.44 (dd, J = 15.0, 3.0 Hz, 1H), 3.34 (d, J = 10.8 Hz, 1H), 3.10 – 3.02 (m, 2H), 2.93 (dd, J = 15.0, 8.6 Hz, 1H), 2.87 (dd, J = 13.6, 7.1 Hz, 1H), 2.55 (dd, J = 13.7, 10.6 Hz, 1H), 2.09 – 1.96 (m, 3H), 1.96 – 1.88 (m, 2H), 1.29 (s, 2H), 0.91 (d, J = 6.5 Hz, 3H), 0.87 (d, J = 6.6 Hz, 3H). ^{13}C NMR (201 MHz, MeOD) δ 163.13, 160.72, 156.31, 138.67, 130.78, 129.40, 129.25, 129.21, 127.95, 125.63, 113.95, 82.10, 76.35, 72.60, 57.29, 56.57, 56.24, 54.78, 52.27, 39.26, 39.12, 35.78, 26.59, 19.08, 19.00. LRMS-ESI (m/z) : 576.2 [$M+H$], HRMS-ESI: 598.2189 ($M+Na$).



(3a*S*,5*R*,6a*R*)-3-methyl-2-oxohexahydro-2*H*-cyclopenta[*d*]oxazol-5-yl ((2*S*,3*R*)-3-hydroxy-4-((*N*-isobutyl-4-methoxyphenyl)sulfonamido)-1-phenylbutan-2-yl)carbamate (1.65c)

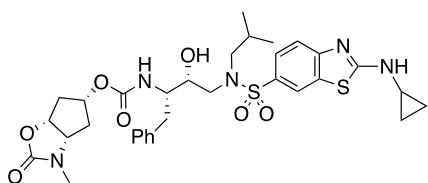
Compound **1.64c** (7.50 mg, 0.023 mmol) was treated with isostere **1.25** (10.4 mg, 0.026 mmol) by following the same procedure outlined for inhibitor **1.65a** to give inhibitor **1.65c** (3.5 mg, 88%).

^1H NMR (800 MHz, Chloroform- d) δ 7.80 – 7.74 (m, 2H), 7.35 – 7.24 (m, 4H), 7.23 – 7.16 (m, 1H), 7.04 – 6.95 (m, 2H), 5.04 (t, J = 4.3 Hz, 1H), 4.95 (q, J = 9.3, 6.9 Hz, 1H), 4.20 – 4.12 (m, 1H), 3.96 (dq, J = 9.8, 4.4 Hz, 1H), 3.89 (s, 3H), 3.79 (q, J = 17.3, 10.2 Hz, 1H), 3.22 (dd, J = 14.4, 4.2 Hz, 1H), 3.14 (dd, J = 14.9, 8.3 Hz, 2H), 3.00 (dd, J = 13.5, 8.0 Hz, 1H), 2.94 (dd, J = 13.5, 7.1 Hz, 1H), 2.75 (dd, J = 14.2, 10.1 Hz, 2H), 2.57 (s, 3H), 2.39 – 2.32 (m, 1H), 2.18 (dd, J = 15.1, 3.0 Hz, 1H), 1.97 (p, J = 6.7 Hz, 1H), 1.90 (dt, J = 15.7, 5.5 Hz, 1H), 1.63 (ddd, J = 15.5, 6.6, 4.0 Hz, 1H), 0.92 (t, J = 6.9 Hz, 6H). ^{13}C NMR (201 MHz, CDCl_3) δ 162.84, 157.57, 155.26, 138.04, 130.49, 129.50, 129.39, 128.44, 126.24, 114.27, 77.69, 75.67, 71.89, 61.26, 58.27, 55.59, 54.70, 54.60, 53.07, 39.44, 35.38, 34.89, 29.69, 28.84, 27.16, 20.20, 19.93. LRMS-ESI (m/z) : 590.3 [$M+H$], HRMS-ESI: 590.2525 ($M+H$).



(3aR,5S,6aS)-3-methyl-2-oxohexahydro-2H-cyclopenta[d]oxazol-5-yl ((2S,3R)-3-hydroxy-4-((N-isobutyl-4-methoxyphenyl)sulfonamido)-1-phenylbutan-2-yl)carbamate (1.65d)

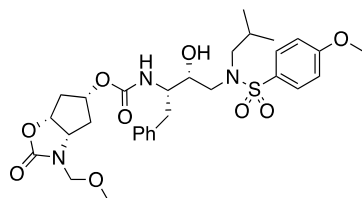
Compound **1.64d** (4.90 mg, 0.015 mmol) was treated with isostere **1.25** (6.80 mg, 0.017 mmol) by following the same procedure outlined for inhibitor **1.65a** to give inhibitor **1.65d** (6.1 mg, 68%). ¹H NMR (800 MHz, Chloroform-d) δ 7.76 (d, J = 8.4 Hz, 2H), 7.35 – 7.19 (m, 5H), 7.01 (d, J = 8.8 Hz, 2H), 5.08 (s, 1H), 4.99 (t, J = 6.7 Hz, 1H), 4.89 (d, J = 8.8 Hz, 1H), 4.23 – 4.18 (m, 1H), 3.90 (s, 3H), 3.82 (d, J = 19.1 Hz, 1H), 3.64 (s, 1H), 3.38 (s, 1H), 3.16 (dd, J = 15.0, 9.1 Hz, 1H), 3.05 – 2.96 (m, 2H), 2.82 (dd, J = 13.6, 7.6 Hz, 1H), 2.79 (s, 3H), 2.30 (d, J = 15.4 Hz, 1H), 2.19 (d, J = 15.9 Hz, 1H), 1.91 (dd, J = 15.5, 5.4 Hz, 1H), 1.88 – 1.82 (m, 1H), 1.74 – 1.69 (m, 1H), 1.67 (s, 2H), 0.92 (dd, J = 35.7, 6.6 Hz, 6H). ¹³C NMR (201 MHz, CDCl₃) δ 162.98, 157.44, 155.43, 137.65, 130.14, 129.58, 129.54, 128.57, 128.27, 126.41, 114.34, 77.64, 75.78, 72.11, 61.40, 58.59, 56.00, 55.63, 55.59, 53.37, 39.84, 35.83, 35.28, 29.71, 29.16, 28.99, 27.25, 27.04, 20.16, 19.87. LRMS-ESI (m/z) :590.6 [M+H], HRMS-ESI: 612.2358 (M+Na).



(3aS,5R,6aR)-3-methyl-2-oxohexahydro-2H-cyclopenta[d]oxazol-5-yl ((2S,3R)-4-((2-(cyclopropylamino)-N-isobutylbenzo[d]thiazole)-6-sulfonamido)-3-hydroxy-1-phenylbutan-2-yl)carbamate (1.65n)

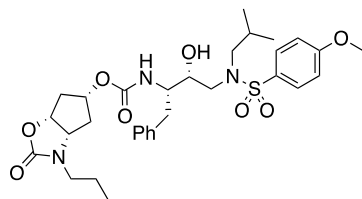
Compound **1.64c** (7.10 mg, 0.022 mmol) was treated with isostere **X** (11.8 mg, 0.024 mmol) by following the same procedure outlined for inhibitor **1.65a** to give inhibitor **1.65n** (10.2 mg, 69%) ¹H NMR (400 MHz, Chloroform-d) δ 8.17 – 8.07 (m, 1H), 7.72 (dd, J = 8.5, 1.9 Hz, 1H), 7.53 (d, J = 8.6 Hz, 1H), 7.26 (d, J = 2.8 Hz, 5H), 7.19 (dd, J = 6.7, 2.3 Hz, 1H), 5.10 (d, J = 10.3 Hz, 1H), 5.02 (s, 1H), 4.91 (t, J = 6.9 Hz, 1H), 3.89 (dd, J = 34.2, 5.3 Hz, 3H), 3.34 (s, 1H), 3.28 – 3.07 (m,

3H), 3.07 – 2.88 (m, 2H), 2.74 (td, $J = 9.7, 6.4$ Hz, 3H), 2.57 (s, 3H), 2.30 (d, $J = 15.8$ Hz, 1H), 2.15 (dd, $J = 15.2, 2.9$ Hz, 1H), 2.00 – 1.80 (m, 2H), 1.60 (ddd, $J = 15.3, 6.5, 4.1$ Hz, 1H), 0.91 (dd, $J = 13.9, 5.7$ Hz, 9H), 0.78 (t, $J = 1.8$ Hz, 2H). ^{13}C NMR (201 MHz, MeOD) δ 158.63, 156.25, 155.44, 138.81, 131.41, 130.77, 129.57, 128.95, 127.89, 127.73, 125.71, 125.28, 121.05, 120.70, 117.50, 78.85, 76.04, 72.53, 61.72, 57.40, 55.55, 52.45, 39.16, 35.30, 34.88, 27.88, 26.69, 25.94, 19.12, 19.08, 19.05, 6.45. LRMS-ESI (m/z) : 672.3 [M+H], HRMS-ESI: 672.2512 (M+H).



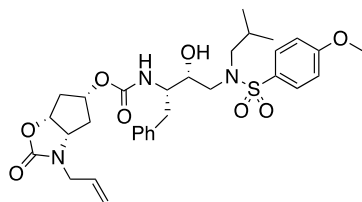
(3a*S*,5*R*,6a*R*)-3-(methoxymethyl)-2-oxohexahydro-2*H*-cyclopenta[d]oxazol-5-yl ((2*S*,3*R*)-3-hydroxy-4-((*N*-isobutyl-4-methoxyphenyl)sulfonamido)-1-phenylbutan-2-yl)carbamate (1.65m)

Compound **1.64m** (3.20 mg, 0.009 mmol) was treated with isostere **1.25** (4.06 mg, 0.010 mmol) by following the same procedure outlined for inhibitor **1.65a** to give inhibitor **1.65m** (3.4 mg, 60%). ^1H NMR (800 MHz, Methanol- d_4) δ 7.76 (d, $J = 8.8$ Hz, 2H), 7.28 – 7.19 (m, 4H), 7.19 – 7.15 (m, 1H), 7.10 – 7.05 (m, 2H), 5.12 (s, 1H), 5.06 (t, $J = 6.9$ Hz, 1H), 5.02 (t, $J = 4.6$ Hz, 1H), 4.58 (d, $J = 11.0$ Hz, 1H), 4.40 – 4.33 (m, 2H), 3.88 (s, 3H), 3.75 (ddd, $J = 14.9, 10.4, 5.1$ Hz, 1H), 3.40 – 3.32 (m, 4H), 3.22 (s, 2H), 3.18 (s, 1H), 3.09 (dd, $J = 14.2, 3.5$ Hz, 1H), 3.05 (dd, $J = 13.6, 7.9$ Hz, 1H), 2.99 (dd, $J = 14.9, 8.1$ Hz, 1H), 2.89 (dd, $J = 13.6, 7.0$ Hz, 1H), 2.57 (dd, $J = 14.2, 10.2$ Hz, 1H), 2.26 – 2.17 (m, 1H), 2.10 (dd, $J = 15.2, 2.8$ Hz, 1H), 2.08 – 2.02 (m, 1H), 1.82 (ddd, $J = 15.4, 6.9, 4.7$ Hz, 1H), 0.97 – 0.82 (m, 6H). ^{13}C NMR (201 MHz, MeOD) δ 163.14, 158.59, 156.21, 138.74, 130.80, 129.25, 128.91, 127.88, 125.78, 113.98, 79.54, 76.86, 76.18, 74.71, 72.48, 59.02, 57.32, 55.50, 54.79, 52.37, 38.92, 36.30, 35.22, 31.61, 29.30, 28.99, 26.63, 19.04. LRMS-ESI (m/z) : 620.2 [M+H], HRMS-ESI: 642.2454 (M+Na).



(3a*S*,5*R*,6a*R*)-2-oxo-3-propylhexahydro-2*H*-cyclopenta[*d*]oxazol-5-yl ((2*S*,3*R*)-3-hydroxy-4-((*N*-isobutyl-4-methoxyphenyl)sulfonamido)-1-phenylbutan-2-yl)carbamate (1.65f)

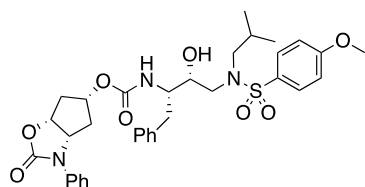
Compound **1.64f** (3.70 mg, 0.011 mmol) was treated with isostere **1.25** (4.74 mg, 0.012 mmol) by following the same procedure outlined for inhibitor **1.65a** to give inhibitor **1.65f** (4.0 mg, 62%). ¹H NMR (800 MHz, Chloroform-*d*) δ 7.78 – 7.70 (m, 2H), 7.33 – 7.22 (m, 4H), 7.20 (s, 1H), 7.02 – 6.93 (m, 2H), 5.08 – 5.02 (m, 1H), 4.98 (s, 1H), 4.94 (s, 1H), 4.22 (d, *J* = 7.7 Hz, 1H), 3.87 (d, *J* = 2.7 Hz, 3H), 3.79 (s, 1H), 3.74 (s, 1H), 3.33 – 3.25 (m, 1H), 3.14 (ddd, *J* = 17.8, 8.9, 4.7 Hz, 2H), 3.07 (d, *J* = 14.3 Hz, 1H), 2.97 (dd, *J* = 13.6, 8.2 Hz, 1H), 2.93 – 2.86 (m, 1H), 2.75 (t, *J* = 12.2 Hz, 1H), 2.67 (d, *J* = 8.7 Hz, 1H), 2.33 (d, *J* = 16.0 Hz, 1H), 2.13 (d, *J* = 15.2 Hz, 1H), 1.89 (dt, *J* = 13.2, 6.2 Hz, 2H), 1.60 – 1.50 (m, 3H), 1.48 (d, *J* = 7.2 Hz, 1H), 1.02 – 0.76 (m, 9H). ¹³C NMR (201 MHz, CDCl₃) δ 162.86, 157.46, 155.41, 137.82, 130.36, 129.51, 129.36, 128.45, 126.35, 114.28, 77.74, 75.74, 72.14, 59.01, 58.37, 55.59, 54.87, 53.18, 43.67, 39.58, 35.75, 35.36, 29.69, 27.18, 20.33, 20.17, 19.90, 11.17. LRMS-ESI (*m/z*) : 618.2 [*M*+*H*], HRMS-ESI: 640.2669 (*M*+*Na*).



(3a*S*,5*R*,6a*R*)-3-allyl-2-oxohexahydro-2*H*-cyclopenta[*d*]oxazol-5-yl ((2*S*,3*R*)-3-hydroxy-4-((*N*-isobutyl-4-methoxyphenyl)sulfonamido)-1-phenylbutan-2-yl)carbamate (1.65e)

Compound **1.64e** (17.4 mg, 0.050 mmol) was treated with isostere **1.25** (22.3 mg, 0.055 mmol) by following the same procedure outlined for inhibitor **1.65a** to give inhibitor **1.65e** (23.3 mg, 76%). ¹H NMR (400 MHz, Chloroform-*d*) δ 7.75 (d, *J* = 8.9 Hz, 2H), 7.39 – 7.22 (m, 4H), 7.22 – 7.11 (m, 1H), 7.04 – 6.86 (m, 2H), 5.68 – 5.52 (m, 1H), 5.46 (d, *J* = 8.8 Hz, 1H), 5.20 – 5.09 (m, 2H), 4.97 (d, *J* = 4.1 Hz, 1H), 4.92 (t, *J* = 6.8 Hz, 1H), 4.16 (t, *J* = 7.0 Hz, 1H), 4.02 – 3.89 (m, 2H), 3.86 (s, 3H), 3.83 – 3.70 (m, 2H), 3.29 (dd, *J* = 14.8, 5.1 Hz, 1H), 3.22 – 2.87 (m, 5H), 2.71 (dd, *J* = 14.2, 10.1 Hz, 1H), 2.32 (d, *J* = 15.9 Hz, 1H), 2.15 (d, *J* = 15.3 Hz, 1H), 2.02 – 1.93 (m, 1H), 1.85 (dd, *J* = 15.0, 9.7 Hz, 1H), 1.54 (ddd, *J* = 15.4, 6.7, 4.1 Hz, 1H), 0.88 (dd, *J* = 16.0, 6.6 Hz,

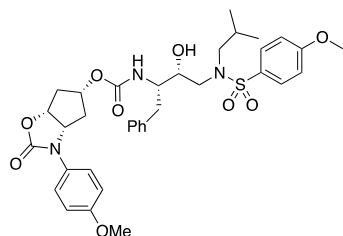
6H). ^{13}C NMR (201 MHz, CDCl_3) δ 162.82, 157.35, 155.24, 138.24, 131.94, 130.61, 129.49, 129.41, 128.44, 126.22, 118.59, 114.26, 78.11, 75.61, 71.64, 58.77, 58.16, 55.60, 54.55, 54.45, 52.93, 44.68, 39.41, 35.56, 34.47, 29.69, 27.12, 20.24, 19.99. LRMS-ESI (m/z) : 616.2 $[\text{M}+\text{H}]$, HRMS-ESI: 638.2498 ($\text{M}+\text{Na}$).



(3*aS*,5*R*,6*aR*)-2-oxo-3-phenylhexahydro-2*H*-cyclopenta[*d*]oxazol-5-yl ((2*S*,3*R*)-3-hydroxy-4-((*N*-isobutyl-4-methoxyphenyl)sulfonamido)-1-phenylbutan-2-yl)carbamate (1.65i)

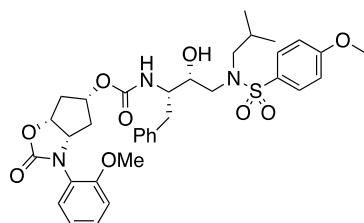
Compound **1.64i** (8.00 mg, 0.021 mmol) was treated with isostere **1.25** (9.30 mg, 0.023 mmol) by following the same procedure outlined for inhibitor **1.65a** to give inhibitor **1.65i** (6.1 mg, 45%).

^1H NMR (800 MHz, Chloroform- d) δ 7.74 (d, J = 8.4 Hz, 2H), 7.54 – 7.46 (m, 2H), 7.44 – 7.35 (m, 2H), 7.15 (dt, J = 16.1, 5.6 Hz, 6H), 6.99 (d, J = 8.4 Hz, 2H), 5.12 (q, J = 3.5 Hz, 1H), 5.09 (t, J = 6.7 Hz, 1H), 4.91 – 4.82 (m, 2H), 3.87 (s, 3H), 3.78 (s, 2H), 3.70 (s, 1H), 3.14 (dd, J = 14.9, 8.1 Hz, 1H), 3.06 – 3.00 (m, 1H), 2.97 (dd, J = 14.4, 6.8 Hz, 2H), 2.82 (dd, J = 13.4, 6.8 Hz, 1H), 2.77 (dd, J = 13.9, 8.2 Hz, 1H), 2.48 – 2.41 (m, 1H), 2.21 – 2.14 (m, 1H), 1.99 (d, J = 15.8 Hz, 1H), 1.63 (s, 2H), 0.89 (dd, J = 29.2, 6.4 Hz, 6H). ^{13}C NMR (201 MHz, CDCl_3) δ 162.91, 155.28, 154.62, 137.48, 137.32, 130.26, 129.52, 129.40, 129.28, 128.44, 126.42, 124.50, 120.28, 119.80, 114.30, 75.63, 71.97, 60.65, 58.48, 55.60, 55.27, 53.34, 39.69, 37.47, 35.80, 29.69, 27.19, 20.15, 19.85. LRMS-ESI (m/z) : 674.2 $[\text{M}+\text{Na}]$, HRMS-ESI: 674.2497 ($\text{M}+\text{Na}$).



(3a*S*,5*R*,6a*R*)-3-(4-methoxyphenyl)-2-oxohexahydro-2*H*-cyclopenta[*d*]oxazol-5-yl ((2*S*,3*R*)-3-hydroxy-4-((*N*-isobutyl-4-methoxyphenyl)sulfonamido)-1-phenylbutan-2-yl)carbamate (1.65j)

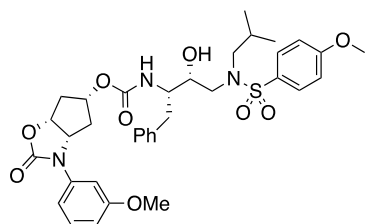
Compound **1.64j** (3.90 mg, 0.009 mmol) was treated with isostere **1.25** (4.21 mg, 0.010 mmol) by following the same procedure outlined for inhibitor **1.65a** to give inhibitor **1.65j** (2.7 mg, 47%)
¹H NMR (800 MHz, Chloroform-*d*) δ 7.72 (dd, *J* = 33.8, 8.5 Hz, 2H), 7.34 (d, *J* = 9.2 Hz, 2H), 7.20 (dd, *J* = 24.4, 7.4 Hz, 4H), 6.97 (dd, *J* = 22.4, 8.5 Hz, 3H), 6.90 (t, *J* = 7.9 Hz, 2H), 5.12 (s, 1H), 5.11 – 5.06 (m, 2H), 4.97 (d, *J* = 9.2 Hz, 1H), 4.76 (t, *J* = 7.5 Hz, 1H), 3.87 (s, 3H), 3.81 (s, 3H), 3.15 (dd, *J* = 15.0, 8.7 Hz, 1H), 3.06 (d, *J* = 15.0 Hz, 1H), 3.02 – 2.88 (m, 2H), 2.82 (ddd, *J* = 34.6, 16.1, 8.6 Hz, 2H), 2.43 (d, *J* = 15.9 Hz, 1H), 2.22 (s, 1H), 2.16 (d, *J* = 15.3 Hz, 1H), 1.96 (tt, *J* = 15.8, 4.6 Hz, 2H), 1.91 – 1.78 (m, 2H), 0.95 – 0.85 (m, 6H). ¹³C NMR (201 MHz, CDCl₃) δ 162.92, 157.05, 155.18, 137.58, 130.31, 130.13, 129.54, 129.44, 128.50, 126.48, 122.95, 114.60, 114.32, 77.39, 77.18, 77.02, 76.87, 75.80, 72.03, 61.49, 58.46, 55.62, 55.54, 55.24, 53.31, 39.83, 37.19, 35.75, 27.21, 20.17, 19.89. LRMS-ESI (*m/z*) : 682.2 [M+H], HRMS-ESI: 674.2497 (M+Na).



(3a*S*,5*R*,6a*R*)-3-(2-methoxyphenyl)-2-oxohexahydro-2*H*-cyclopenta[*d*]oxazol-5-yl ((2*S*,3*R*)-3-hydroxy-4-((*N*-isobutyl-4-methoxyphenyl)sulfonamido)-1-phenylbutan-2-yl)carbamate (1.65k)

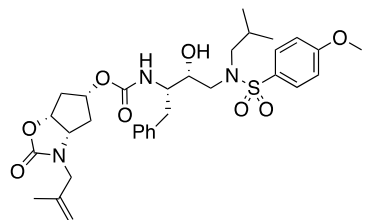
Compound **1.64k** (14.5 mg, 0.035 mmol) was treated with isostere **1.25** (15.6 mg, 0.038 mmol) by following the same procedure outlined for inhibitor **1.65a** to give inhibitor **1.65k** (12.2 mg, 51%)
¹H NMR (400 MHz, Chloroform-*d*) δ 7.72 (d, *J* = 8.5 Hz, 2H), 7.37 – 7.08 (m, 7H), 7.08 – 6.92 (m, 3H), 6.70 (d, *J* = 8.2 Hz, 1H), 5.18 – 5.02 (m, 2H), 4.83 (dd, *J* = 15.7, 5.4 Hz, 2H), 3.86 (s, 3H), 3.78 (dt, *J* = 13.8, 3.5 Hz, 5H), 3.68 (s, 1H), 3.14 (dd, *J* = 15.1, 8.7 Hz, 1H), 3.06 – 2.90 (m, 3H), 2.78 (ddd, *J* = 22.2, 13.4, 7.2 Hz, 2H), 2.43 (d, *J* = 15.9 Hz, 1H), 2.19 (d, *J* = 15.5 Hz, 1H), 2.02 – 1.79 (m, 3H), 0.88 (d, *J* = 6.8 Hz, 6H). ¹³C NMR (201 MHz, MeOD) δ 163.14, 160.49,

156.07, 155.78, 138.55, 130.77, 129.62, 129.26, 128.94, 127.78, 125.64, 114.00, 112.24, 109.54, 106.60, 78.67, 75.85, 72.15, 61.19, 57.36, 56.12, 54.81, 54.47, 52.40, 39.08, 37.22, 35.68, 26.65, 19.08, 19.03. . LRMS-ESI (m/z) : 682.2 [M+H], HRMS-ESI: 704.2602 (M+Na).



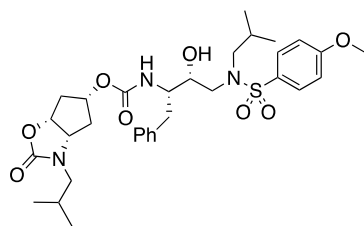
(3a*S*,5*R*,6a*R*)-3-(3-methoxyphenyl)-2-oxohexahydro-2*H*-cyclopenta[d]oxazol-5-yl ((2*S*,3*R*)-3-hydroxy-4-((*N*-isobutyl-4-methoxyphenyl)sulfonamido)-1-phenylbutan-2-yl)carbamate (1.65I)

Compound **1.64I** (13.6 mg, 0.033 mmol) was treated with isostere **1.25** (14.7 mg, 0.036 mmol) by following the same procedure outlined for inhibitor **1.65a** to give inhibitor **1.65I** (13.1 mg, 58%), HRMS-ESI: 682.2787 (M+H). ¹H NMR (800 MHz, Methanol-d₄) δ 7.77 (d, J = 7.9 Hz, 2H), 7.35 (t, J = 7.7 Hz, 1H), 7.26 (dd, J = 14.5, 7.2 Hz, 4H), 7.16 (dd, J = 22.0, 7.2 Hz, 2H), 7.09 (t, J = 7.2 Hz, 3H), 6.91 (s, 1H), 5.23 – 5.17 (m, 1H), 5.10 (s, 1H), 4.85 – 4.80 (m, 1H), 3.89 – 3.85 (m, 6H), 3.84 (s, 1H), 3.82 – 3.75 (m, 2H), 3.38 (d, J = 15.2 Hz, 1H), 3.12 (d, J = 14.3 Hz, 1H), 3.04 (dt, J = 13.1, 7.2 Hz, 2H), 2.91 (dd, J = 13.4, 7.0 Hz, 1H), 2.72 – 2.65 (m, 1H), 2.26 (d, J = 15.8 Hz, 1H), 2.10 (d, J = 15.9 Hz, 1H), 2.05 – 1.96 (m, 1H), 1.89 (d, J = 15.3 Hz, 1H), 1.74 (dd, J = 13.9, 7.0 Hz, 1H), 0.89 (dd, J = 21.6, 6.2 Hz, 6H). ¹³C NMR (201 MHz, MeOD) δ 163.12, 157.83, 156.32, 155.43, 138.72, 130.83, 129.99, 129.26, 129.00, 127.96, 125.86, 124.32, 120.54, 114.01, 111.88, 79.52, 76.16, 72.17, 61.79, 57.29, 55.94, 54.84, 54.79, 52.34, 39.51, 36.24, 35.39, 26.61, 19.10, 19.05. LRMS-ESI (m/z) : 682.2 [M+H]



(3a*S*,5*R*,6a*R*)-3-(2-methylallyl)-2-oxohexahydro-2*H*-cyclopenta[*d*]oxazol-5-yl ((2*S*,3*R*)-3-hydroxy-4-((*N*-isobutyl-4-methoxyphenyl)sulfonamido)-1-phenylbutan-2-yl)carbamate (1.65g)

Compound **1.64g** (6.10 mg, 0.017 mmol) was treated with isostere **1.25** (7.53 mg, 0.019 mmol) by following the same procedure outlined for inhibitor **1.65a** to give inhibitor **1.65g** (8.0 mg, 75%). ¹H NMR (800 MHz, Chloroform-*d*) δ 7.77 (d, *J* = 8.8 Hz, 2H), 7.36 – 7.25 (m, 4H), 7.24 – 7.15 (m, 1H), 7.00 (d, *J* = 8.9 Hz, 2H), 5.19 (s, 1H), 5.03 (s, 1H), 4.96 (t, *J* = 6.9 Hz, 1H), 4.92 (s, 1H), 4.82 (s, 1H), 4.12 (t, *J* = 7.1 Hz, 1H), 4.01 – 3.95 (m, 1H), 3.93 – 3.87 (m, 4H), 3.85 – 3.76 (m, 2H), 3.24 (dd, *J* = 15.1, 4.5 Hz, 1H), 3.14 (dd, *J* = 14.8, 8.4 Hz, 2H), 3.06 (d, *J* = 15.4 Hz, 1H), 3.01 (dd, *J* = 13.6, 8.0 Hz, 1H), 2.96 (dd, *J* = 13.6, 7.2 Hz, 1H), 2.76 (dd, *J* = 14.3, 10.1 Hz, 1H), 2.36 (d, *J* = 15.6 Hz, 1H), 2.16 (d, *J* = 15.1 Hz, 1H), 1.98 (dt, *J* = 13.1, 6.5 Hz, 1H), 1.90 (dt, *J* = 15.4, 4.8 Hz, 1H), 1.68 (s, 3H), 1.59 (ddd, *J* = 15.3, 6.7, 4.2 Hz, 1H), 0.92 (dd, *J* = 13.5, 6.6 Hz, 6H). ¹³C NMR (201 MHz, CDCl₃) δ 162.86, 157.60, 155.31, 139.36, 138.10, 130.55, 129.52, 129.41, 128.48, 126.30, 114.29, 113.97, 78.00, 75.69, 71.81, 58.58, 58.29, 55.61, 54.66, 53.06, 48.12, 39.50, 35.45, 34.78, 29.71, 27.18, 20.26, 19.99, 19.87. LRMS-ESI (*m/z*) : 630.6 [*M*+*H*], HRMS-ESI: 652.2666 (*M*+*Na*).



(3a*S*,5*R*,6a*R*)-3-isobutyl-2-oxohexahydro-2*H*-cyclopenta[*d*]oxazol-5-yl ((2*S*,3*R*)-3-hydroxy-4-((*N*-isobutyl-4-methoxyphenyl)sulfonamido)-1-phenylbutan-2-yl)carbamate (1.65h)

Compound **1.64h** (8.90 mg, 0.024 mmol) was treated with isostere **1.25** (10.9 mg, 0.027 mmol) by following the same procedure outlined for inhibitor **1.65a** to give inhibitor **1.65h** (10.0 mg, 65%). ¹H NMR (800 MHz, Chloroform-*d*) δ 7.80 – 7.75 (m, 2H), 7.30 (d, *J* = 23.2 Hz, 4H), 7.21 (t, *J* = 7.3 Hz, 1H), 7.00 (d, *J* = 8.8 Hz, 2H), 5.17 – 5.11 (m, 1H), 5.04 (t, *J* = 4.2 Hz, 1H), 4.97 (t, *J* = 6.8 Hz, 1H), 4.23 (t, *J* = 6.9 Hz, 1H), 3.98 – 3.92 (m, 1H), 3.89 (s, 4H), 3.82 (s, 1H), 3.23 (d, *J* = 12.5 Hz, 1H), 3.19 – 3.04 (m, 3H), 3.04 – 2.91 (m, 2H), 2.81 – 2.73 (m, 1H), 2.52 (d, *J* = 13.9 Hz, 1H), 2.37 (d, *J* = 15.6 Hz, 1H), 2.18 (d, *J* = 15.0 Hz, 1H), 2.01 – 1.94 (m, 1H), 1.94 – 1.82 (m, 2H), 1.71

(s, 1H), 1.64 (d, $J = 14.7$ Hz, 1H), 0.92 (dq, $J = 19.3, 6.4$ Hz, 12H). ^{13}C NMR (201 MHz, CDCl_3) δ 162.85, 157.83, 155.33, 138.04, 130.57, 129.52, 129.43, 128.47, 126.34, 114.29, 77.81, 75.70, 71.83, 59.33, 58.29, 55.61, 54.82, 53.05, 49.38, 39.54, 35.57, 34.90, 29.71, 27.18, 26.24, 20.25, 19.98, 19.75. LRMS-ESI (m/z) : 630.6 $[\text{M}+\text{H}]$, HRMS-ESI: 654.2815 ($\text{M}+\text{Na}$).

CHAPTER 2. DESIGN, SYNTHESIS, AND BIOLOGICAL EVALUATION OF HIV-1 PROTEASE INHIBITORS WITH A NOVEL BIS SQUARAMIDE SCAFFOLD

2.1 Introduction

Human immunodeficiency virus (HIV) is a prolonged infection that can lead to acquired immunodeficiency disease (AIDS). Inhibition of the proteolytic enzyme HIV protease continues to be a chemotherapy target for AIDS. However, rapid drug resistance to these protease inhibitors makes newly created peptide-based drugs ineffective. Nonpeptidyl HIV protease inhibitors with high affinity have been the focus here in the Ghosh lab. The major scaffold incorporates a bis-tetrahydrofuranyl ligand as the P2 ligand along with an (R)-(hydroxyethylamino)sulfonamide isosteres. These structural features have shown to be very potent nonpeptidyl HIV protease inhibitors and P2-bis-THF ligand has shown major drug resistance. TMC-126 and Darunavir have shown to be very potent nonpeptidyl HIV protease inhibitors. Darunavir ended up being FDA approved for the treatment of HIV/AIDS patients infected with drug-resistant strains of HIV. However, since mutations of HIV to drug-resistant strains render even the most rigorous treatments ineffective in some patients and raise concerns for effective long-term treatment options for all HIV/AIDS patients.

The current research has shown that protease inhibitors that display a broad range of activity against multidrug-resistant HIV-1 variants are essential for further drug development and new treatment options. Many diverse ligands and structural functionalities of potent HIV-1 protease inhibitors have been developed with some showing potential at the clinical stage. Thus, the HIV-1 protease enzyme remains an important therapeutic drug target. Moreover, targeting the HIV-1 PR's unique transition state binding mode with structurally defined inhibitor(s) has shown impressive results and continues to be a solid biochemical target. New potent inhibitors against highly drug-resistant HIV-1 variants started too emerged from to use of designing the inhibitor to make strong contacts with the backbone residuals of the HIV PR and proved to be an effective strategy towards designing inhibitors that display potent activity against HIV-1 protease enzyme. Efforts to modify the P3 and P2 ligand in order to access binding interactions that have not yet been explored is of great interest. Thus, the work here reports the synthesis of a new class of P2 bis squaramide containing HIV-1 protease inhibitors.

2.2 Design, Synthesis, and Biological Evaluation of HIV-1 Protease Inhibitors with a Novel Bis Squaramide P2 Ligand

2.2.1 Design of HIV Protease Inhibitors with a Bis Squaramide P2 Ligand

Isosteres and bioisosteres have been used in medicinal chemistry to improve selectivity, decrease side effects and toxicity, improve pharmacokinetic profiles, increase stability and even simplify the overall synthesis of the desired compound. However, many factors are considered when bioisosteres are used such as size, overall conformation, induction, polarizability, hydrogen bond accepting and donating capacity, pK_a , solubility, hydrophobicity, reactivity, and general stability.

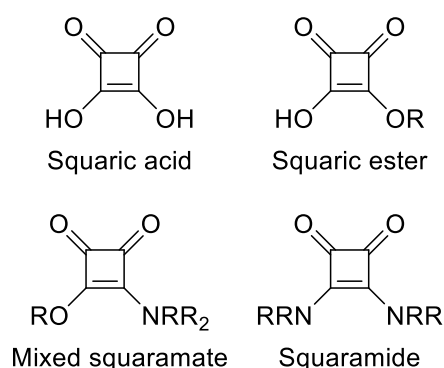


Figure 2.1: Structures and Nomenclature of Squarate Derivatives

Squaric acid, squaric esters, mixed squamates, and squaramides have shown significant bioisostere properties, structures are shown in Figure 2.1. These synthons have been used to replace carboxylic acids, ureas, peptide bonds, phosphate connection, and alpha amino acids.¹²⁵ Overall squaramides retain a very rigid structure and are mainly planar. It has been reported that the squaramide functionality is resilient to nucleophilic attack and maintains its stability even under harsh conditions. Attention to squaramides arose in the last decade because they display unique hydrogen bond donating and accepting properties that have been applied to a diverse range of research. Thus, squaramides and derivatives have been applied to medicine, supramolecular chemistry and catalysis.¹²⁶

Most recently, drug designs have started to incorporate squaric acids and esters, mixed squamates and squaramides because of their promising biological properties, such as low cytotoxicity, stability, and strong hydrogen bonding abilities. Advanced drug squaramide

containing compounds Pibutidine hydrochloride, BMY-25368, Perzinfotel, and SCH-527123 are shown in Figure 2.2. Pibutidine hydrochloride and BMY025368 are both primary squaramide containing compounds and were used as effective treatment options for ulcers.^{127,128} They both displayed affinity towards the histamine H2 receptor and acted as H2 antagonist. It should be noted that the squarate feature did not play a role in pibutidine discontinuation. Perzinfotel, a cyclic squaramide was designed as a potent NMDA antagonist.¹²⁹ Clinically, Perzinfotel's safety profile was superior to comparable drugs but oral bioavailability was not ideal and the drug was discontinued. Another bis squaramide, SCH-527123 (Navarixin) contained a potent profile against the CXC chemokine receptor 2 (CXCR2) and showed antitumor suppressor activity.¹³⁰ This drug is still currently being evaluated. However, during the optimization process, SCH-527123 revealed to be more potent than its urea counterpart and the binding mode showed stronger hydrogen bonding interactions between the squaramide and active site of CXCR2 versus the urea bound CXCR2 mode. This explains SCH-527123 impressive potent profile and increased binding time with the cell assay.¹³¹

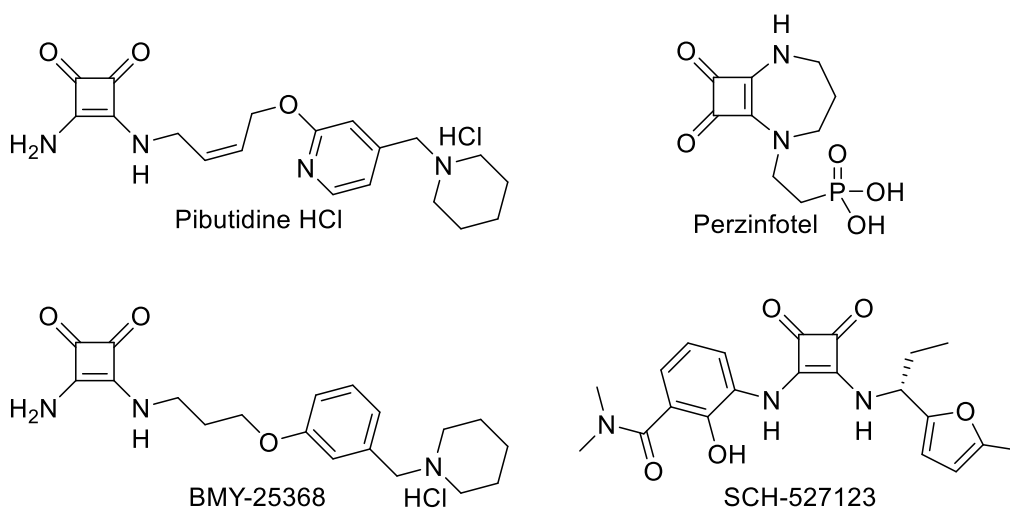
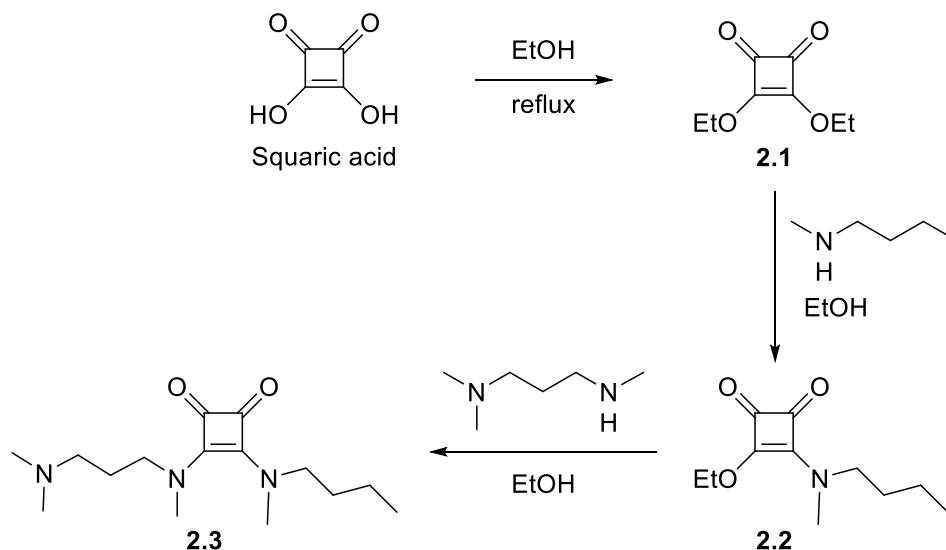


Figure 2.2: Squaramide Potential Drug Candidates

Also, incorporating the squaramide unit into a synthetic scheme has proven to be relatively easy, cheap and an attractive bioisostere for further drug development. Compound **2.1** was synthesized by Costa and co-workers in three simple steps, shown in Scheme 2.1.¹³² Squaric acid is a relatively cheap starting material and condensation occurred easily with solely ethanol under reflux conditions to give **2.1**. Subjecting **2.1** to *N*-methylbutylamine in ethanol provide the mixed

squarate **2.2** followed by addition of the second amine *N, N, N'*-Trimethyl-1,3-propanediamine in ethanol gave the desired Anti-Chagasic Agent **2.3** in a 60-90% yield over three steps.



Scheme 2.1: Synthesis of Squaramide **2.3**: an Anti-Chagasic Agent

Therefore, it can be concluded that incorporating a squaramide backbone into the HIV-1 protease inhibitor drug design would render a positive outcome from cost, to increase of stability, hydrogen bonding strength, and possibly establish a binding mode interaction in the active site that has not been explored. While squaramide has not been utilized in protease inhibitors, it has been incorporated into several clinically advanced drug candidates including Pibutidine hydrochloride, BMY-25368, Perzinfotel, and SCH-527123.

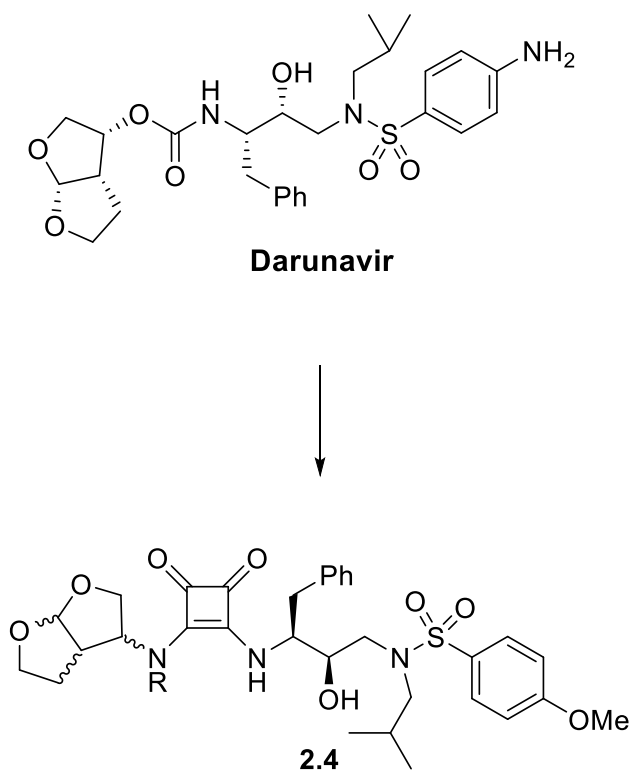


Figure 2.3: Base Model of Inhibitors

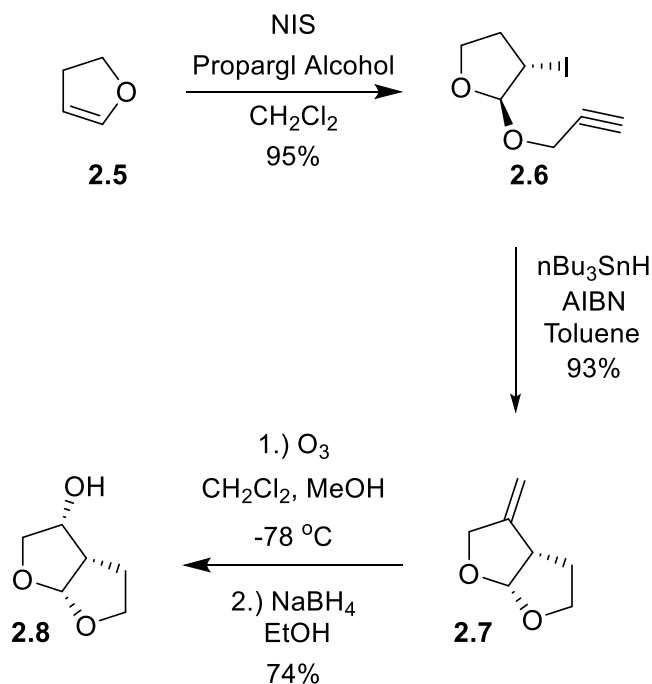
Thus, there have been many efforts to discover the preferred occupancy of the S2 subsite by a protease inhibitor that also maintains potency against highly mutated variants. Darunavir bis-THF ligand is well accommodated in the S2 subsite, however, DRV resistant HIV-1 viruses are arising and present to be a real problem. Therefore, it is reasonable to believe that incorporating a different P2 ligand that can expand further on the ligand-binding interactions in the active site of HIV-1 protease would be optimal for addressing the fight against highly resistance DRV-strains. A new scaffold was envisioned that functions as a strong hydrogen bond donor and acceptor in a conformational constrained fused cyclobutene ring system. This work focuses on transforming the P2 ligand to a novel bis squaramide in order to access new interactions in the active site that have not yet been explored, the structure of the base design of inhibitors are shown in Figure 2.3.

2.2.2 Results

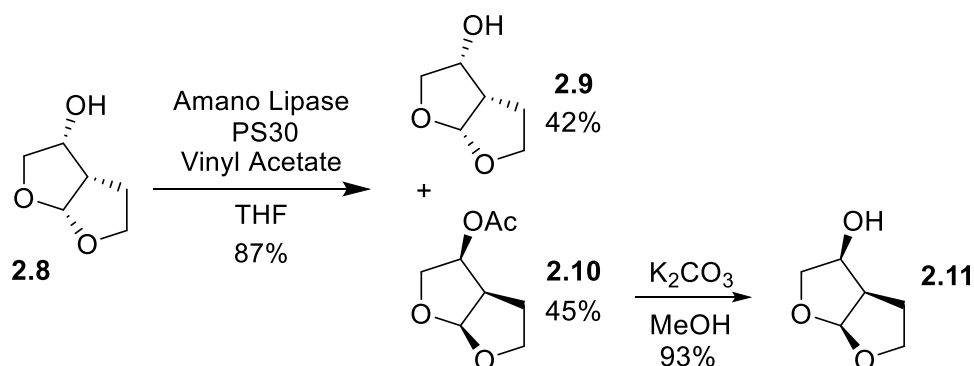
Numerous known protease inhibitors incorporate a diverse range of P2 ligands and maintain potency but fail against highly resistant HIV-1 variants. Previous examinations of the X-ray structure of DRV and other inhibitor-bound HIV-1 proteases suggested that a stereochemical bis-THF squaramide P2 ligand would be well accommodated. It was planned to investigate the potential ligand-binding interactions of the P2 subsite further by synthesizing an array bis-THF squaramide derivatives. Also, the oxazolidinone heterocycles are unique in size, shape and chemical properties, which could render favorable pharmacokinetic properties. Thus, an efficient enantiomeric synthesis of various bis-THF squaramide derivatives was devised. These inhibitors were evaluated against HIV-1 protease for their enzymatic and antiviral activities

2.2.2.1 Synthesis of Inhibitors

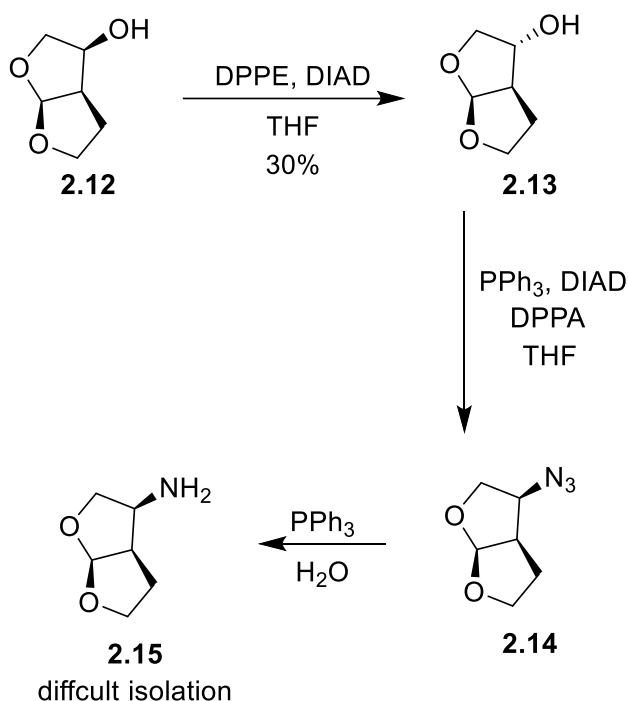
Optically active bis-tetrahydrofuranyl (bis-THF) **2.9** and **2.11** was prepared according to methods previously developed.¹³³ Commercially available 2,3-dihydrofuran **2.5** was converted to the corresponding iodo ether **2.6**, which then was cyclized under tributyltin hydride-mediated radical conditions to form a bicyclic acetal **2.7**, shown in Scheme 2.2. Ozonolytic cleavage followed by reduction of the resulting ketone with sodium borohydride provided the racemic bis-THF alcohol **2.8**.

Scheme 2.2: Synthesis of Racemic bis-THF Alcohol **2.8**

Enzymatic resolution of racemic bis-THF alcohol **2.8** was performed with Amano lipase PS-30. Amano lipase PS-30 and vinyl acetate produced alcohol **2.9** in 42% yield and the acylated alcohol **2.10** in 45% yield, shown in Scheme 2.3. The acylated alcohol **2.10** was hydrolyzed by treatment with potassium carbonate to provide the enantiomeric alcohol **2.11** in 93%.

Scheme 2.3: Synthesis of Optically Active bis-THF Alcohol **2.9** and **2.11**

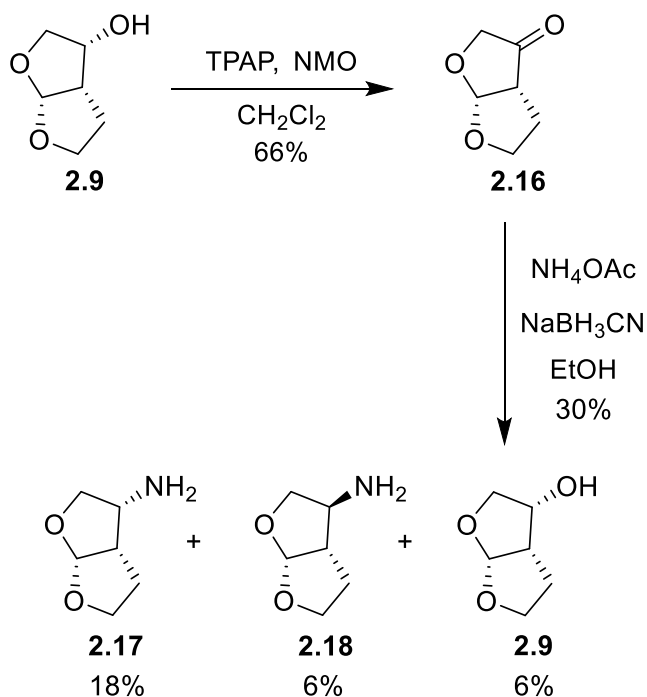
The next step in the synthesis was to convert both enantiomers of bis-THF alcohols to an amine functionality. The first attempt used a double Mitsunobu for the conversion of alcohol **2.12** to amine but the desired amine could not be isolated, Scheme 2.4. Inversion of (+) Bis-THF alcohol **2.12** under normal Mitsunobu conditions was successful and yielded **2.13** in 30%. The inverted alcohol was then subjected to similar conditions as before but diphenyl phosphoryl azide was used as the nucleophile to form the azide **2.14**. Staudinger reaction is a mild azide reduction reaction however when performed on **2.14** the desired amine **2.15** proved to be very difficult to isolate.



Scheme 2.4: Double Mitsunobu Attempt Toward Amine **2.15**

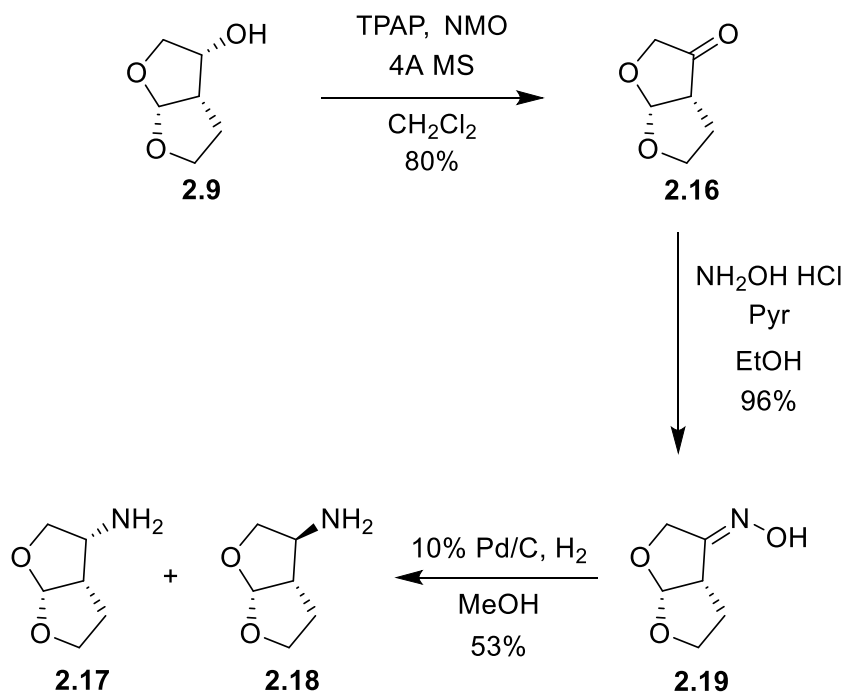
Without spending more time on the optimization of the double Mitsunobu route, reductive amination has been reported to provide amines in one step but when implemented the yield was low, non-reproducible, and generated undesirable side products, shown in, Alcohol **2.9**, first was oxidized to the corresponding ketone from previously reported literature from our lab by tetrapropylammonium perruthenate oxidation (TPAP)¹³⁴. Ketone **2.16** was then exposed to reductive amination conditions and did not yield a single isomer. Both diastereomers **2.17** and **2.18** were formed along with an over-reduction of ketone gives back alcohol **2.9**, showed in Scheme

2.5. Thus, the insufficient results and low yielding of the reductive amination step inspired another route.



Scheme 2.5: Reduction Amination of **2.16**

Alternatively, enantiomerically pure bis-THF amine **2.17** synthesized from converting alcohol **2.9** to ketone **2.16** by improved TPAP oxidation. Yields increased from 66% to 80% when 4A molecular sieves were added to the reaction mixture. Treatment of ketone **2.16** with hydroxylamine hydrochloride formed the ketoxime derivative **2.19** in excellent yields, which underwent hydrogenation with 10% Palladium on carbon with a shaker hydrogenation apparatus (parr) at 60 pounds per square inch (psi) and gave **2.17** and diastereomer **2.18** in 53% yield in a 2.1 to 1 diastereomeric ratio (*dr*) favoring the desired amine **2.17**, shown in Scheme 2.6.



Scheme 2.6: Optimized Conditions for the Synthesis of Enantiopure bis-THF Amine **2.17**

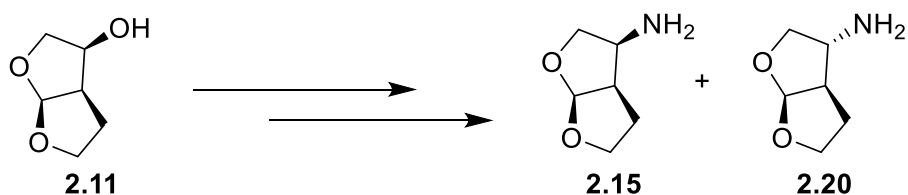
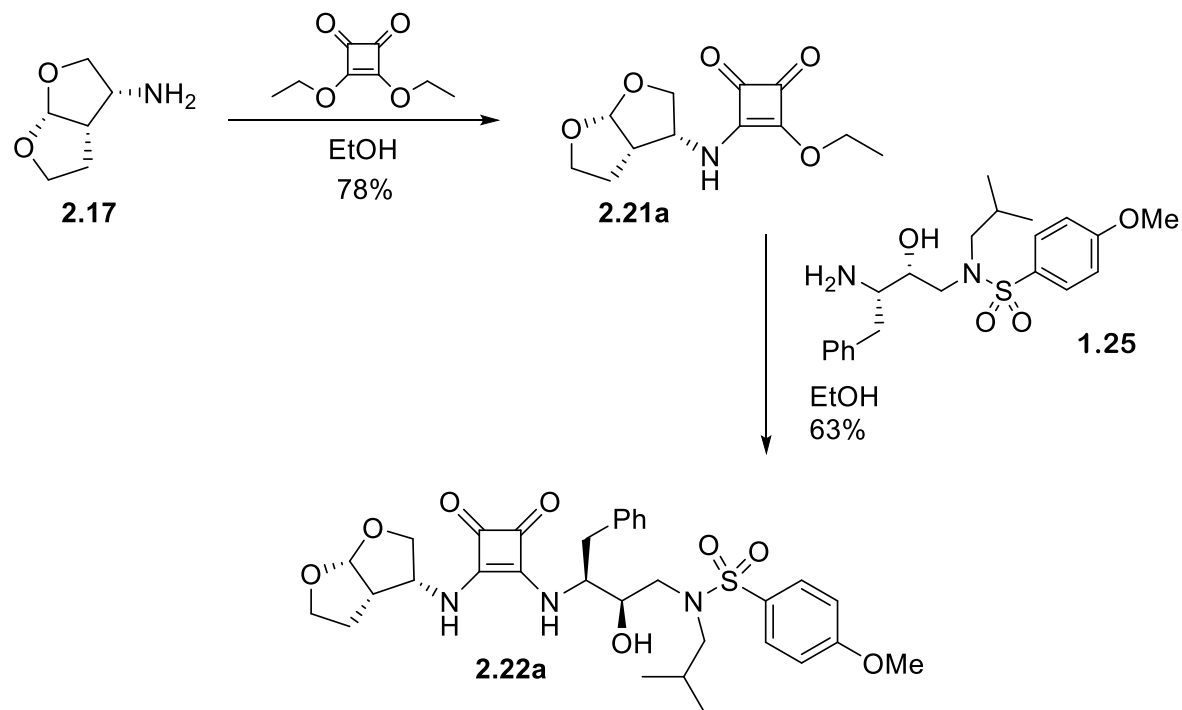


Figure 2.4: Synthesis of Optically Active Amine **2.15**

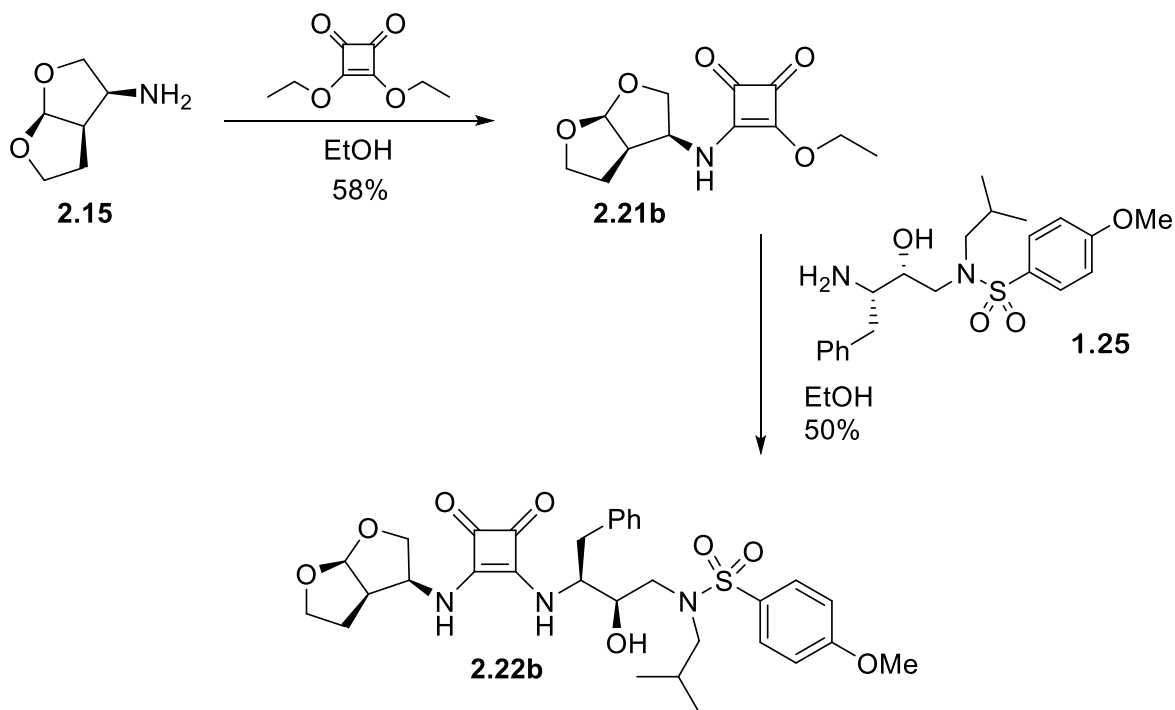
The corresponding enantiomer **2.15** was easily synthesized by swapping out **2.9** with its enantiomer **2.11** and exposing it to the same conditions outlined in Scheme 2.6, structures are shown in Figure 2.4.

With pure optically active bis-THF amine **2.17** and **2.15** in hand the HIV-1 protease inhibitors were finally assembled. Bis-THF amine **2.17** was added to diethyl squarate in ethanol and resulted in a successful mixed squaramide species **2.21a** in 78% yield. **2.21a** was further subjected to known isostere amine **1.25** in ethanol to produce the desired final inhibitor **2.22a** in 63% yield, shown in Scheme 2.7. The same sequence of reactions was applied to enantiomer **2.15**. Bis-THF amine **2.15** was added to diethyl squarate in ethanol and resulted in the coupled mixed

squaramide **2.21b** in 58%. Final inhibitor **2.22b** was produced easily in 63% yield by coupling **2.21b** and isostere amine **1.25** in ethanol, shown in Scheme 2.8.

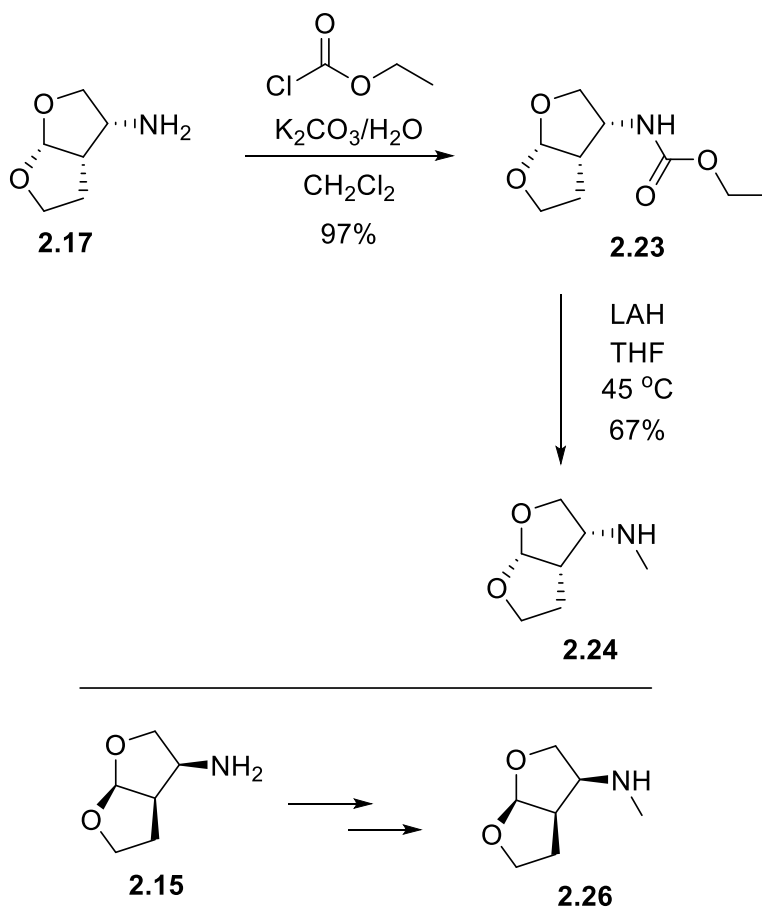


Scheme 2.7: Synthesis of Final Inhibitor **2.22a**



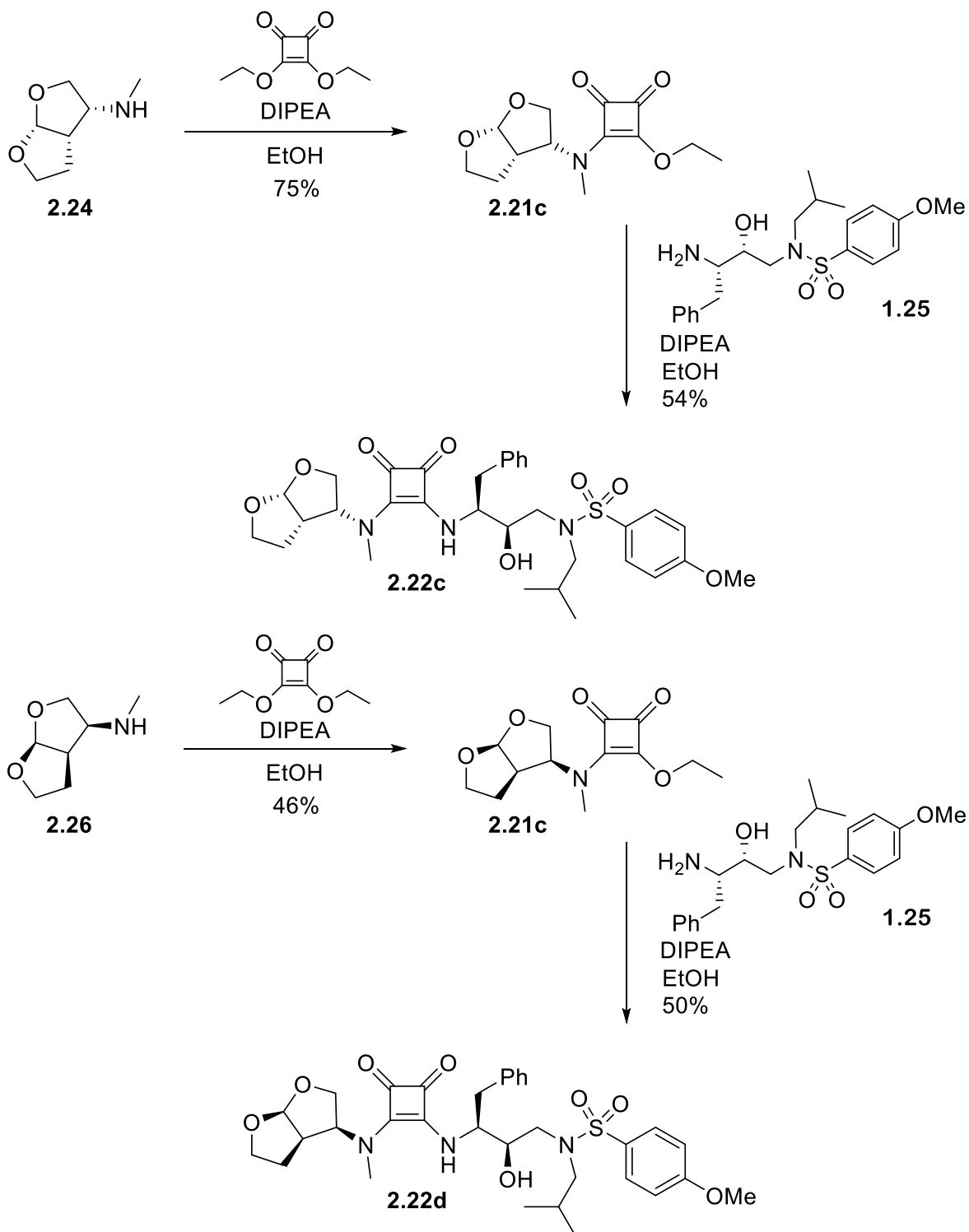
Scheme 2.8: Synthesis of Final Inhibitor **2.22b**

The next phase of this work was to vary the initial HIV-1 protease inhibitor slightly, it was here that both bis-THF amine moieties **2.17** were exposed ethyl chloroformate and potassium carbonate and water to form carbamic acid ethyl ester **2.23** and **2.25** in 70-97% yield. Carbamic acid ethyl esters **2.23** and **2.25** were then subjected to lithium aluminum hydride (LAH) reducing conditions yield the desired methylated amine **2.24** and **2.26**, outlined in Scheme 2.9.



Scheme 2.9: Synthesis of bis-THF Methylamine **2.24** and **2.26**

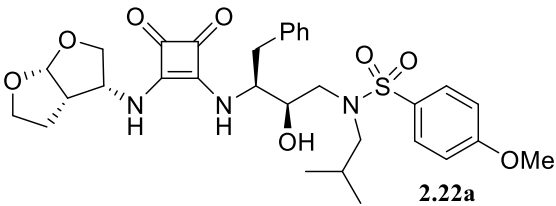
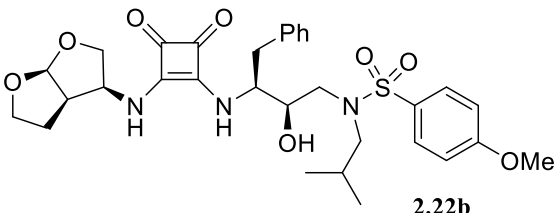
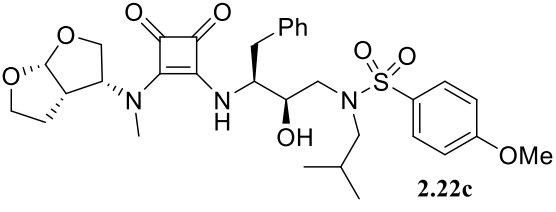
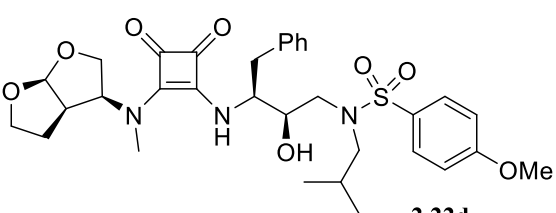
It was here that both enantiomeric bis-THF methyl amines **2.24** and **2.26** were subjected to diethyl squarate in ethanol and diisopropylethylamine (DIPEA) to result in the needed mixed squaramate species **2.21c** and **2.21d** in 75% yield and 46% yield. **2.21c** and **2.21d** were further subjected to known isostere amine **1.25** in ethanol and DIPEA to produce desired final inhibitors **2.22c** in 54% yield and **2.22d** in 50%, shown in Scheme 2.10

Scheme 2.10: Synthesis of Final Inhibitor **2.22c** and **2.22d**

2.2.2.2 Biological Evaluation

All new inhibitors were evaluated first in an HIV-1 protease inhibitory assay based on the known protocol described by Toth and Marshall.¹¹⁸ The enzyme inhibition K_i values can be seen in Table 2.1. The antiviral activity of each PIs was then determined by a known MTT assay that calculates IC_{50} values. Thus, the inhibitors were exposed to HIV_{NL4-3} infected MT-4 cell lines and the minimum concentration that was required to reduce the viral replication by 50% is the reported IC_{50} value. Viral replication was measured by the inhibition of the p24 Gag protein production.¹¹⁹ The results are shown in Table 2.1

Table 2.1: HIV-1 Proteases Inhibitory and Antiviral Activity of Inhibitors **2.22a-d**

| Entry | Inhibitor | K_i (nM) ^a | IC_{50} (nM) ^b |
|-------|---|-------------------------|-----------------------------|
| 1. |  2.22a | 54.8 | >1000 |
| 2. |  2.22b | 5.6 | >1000 |
| 3. |  2.22c | 4.5 | >1000 |
| 4. |  2.22d | 201 | >1000 |

^aThe K_i values are mean values of at least four experiments. Standard error in all cases were less than 7%. Darunavir exhibited $K_i = 16$ pM. ^bHuman T-lymphocytes (MT-4) cells (10^5 /mL) were exposed to 100 TCID₅₀ of HIV-1 and were cultured in the presence of each PI. The IC_{50} values are means of at least three experiments. The IC_{50} of DRV and SQV were 3.2 nM and 21 nM. Standard error in all cases was less than 5%.

2.2.3 Discussion

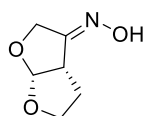
Investigation of the biological data showed that the incorporation of bis squaramide did not disrupt the inhibitor from binding to wild type HIV-1 protease, however, all inhibitors **2.22a-d** showed no significant antiviral activity which suggests these inhibitors fail to cross the cell membrane. Firstly, the stereochemical requirement was examined and results show that inhibitor **2.22a** with the (3*R*,3*aS*,6*aR*) stereochemical define bis-THF amine ligand was less potent than its enantiomer **2.22b** with the (3*S*,3*aR*,6*aS*). Inhibitor **2.22a** exhibited an enzyme inhibitory K_i of 54.6 nM and inhibitor **2.22b** K_i value of 5.6 nM. This 10-fold difference of K_i shows that the PR enzyme prefers the stereo reference of **2.22b**'s (3*S*,3*aR*,6*aS*). Interestingly, the stereo preference was the opposite of what was expected. In order to further explore the squaramide feature further, *N*-Methyl ligands were designed and examined. Analysis of enantiomeric **2.22c** and **2.22d** showed a different pattern in the activity. Inhibitor **2.22c** with the 3*R*,3*aS*,6*aR* stereochemical define bis-THF methyl amine showed an enzyme inhibition K_i of 4.5 nM and inhibitor **2.22d** K_i value of 201 nM. The 200-fold difference of K_i between **2.22c** and **2.22d** shows that the PR enzyme prefers the stereo preference of **2.22c**'s (3*R*, 3*aS*, 6*aR*) and these values agree with previous literature. When comparing **2.22b** and **2.22c**, there was an improvement of enzyme inhibition K_i from 5.6 to 4.5 nM. This suggests that the P2 pocket was able to accommodate the larger squaramide moiety and methylation of inhibitor **2.22c** appears to make the best interaction with the active site than **2.22a**, **2.22b**, and **2.22d**. In can be concluded that the bis-THF amine stereochemical configuration was crucial for activity.

2.3 Conclusion

Our focus on integrating a unique squaramide feature as the P2 ligand led to the design, synthesis, and evaluation of a series of novel inhibitors. A short and enantiomeric synthesis of derived bis squaramides inhibitors was achieved through a key oxime intermediate and simple coupling of various amines allowed derivation to be easy and effective. Inhibitor **2.22c** demonstrated the highest enzymatic potency with a K_i of 4.6 nM. With the current SAR and respectable K_i values it can be assumed this class does make strong interactions in the active site. Furthermore, design and synthesis of incorporating a wider range of squaramide containing inhibitors are envisioned.

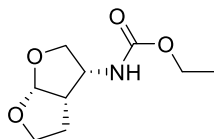
2.4 Experimental Section

All moisture-sensitive reactions were carried out in oven-dried glassware under an argon atmosphere. All chemicals and reagents were obtained from commercial suppliers and were used without further purification. Anhydrous solvents were obtained as follows: Dichloromethane was distilled from calcium hydride under argon. Tetrahydrofuran was distilled from sodium metal/benzophenone under argon. All other solvents were reagent grade. Flash column chromatography was performed with 230-400 mesh silica gel. Thin layer chromatography was carried out using TLC silica gel 60 F254 plates. ^1H NMR and ^{13}C NMR spectra were recorded on a Bruker AV-III-400, Bruker DRX500, or Bruker AV-III-800 with chemical shifts reported in ppm (δ). Characteristic splitting patterns are as follows: s = singlet, d = doublet, t = triplet, q = quartet, m = multiplet, dd = doublet of doublets, ddd = doublet of doublet of doublets, td = triplet of doublets, dq = doublet of quartets, brs = broad singlet, app = apparent. Optical rotations were measured with a Perkin Elmer Series 341 Polarimeter, with a sodium source lamp. Low-resolution mass spectra were collected on a Waters 600 LCMS. High-resolution mass spectra were collected by the Purdue University Campus-Wide Mass Spectrometry Center.



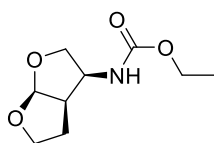
(3aS,6aR,E)-tetrahydrofuro[2,3-b]furan-3(2H)-one oxime (**2.19**)

To a clear solution of ketone **2.16** (20.5 mg, 0.160 mmol) in ethanol (1 mL) was added hydroxylamine hydrochloride (22.2 mg, 0.320 mmol) and pyridine (45 μL , 0.560 mmol). After 20 minutes of stirring at room temperature, the mixture was concentrated via rotary evaporation. The crude product was purified by silica gel column chromatography (30 % EtOAc in hexane) to afford **2.19** (22.0 mg, 96%). R_f = 0.6 (60% EtOAc in hexane); ^1H NMR (400 MHz, Chloroform- d) δ (ppm): 8.87 (d, J = 14.2 Hz, 8H), 5.88 (dd, J = 7.5, 5.0 Hz, 8H), 4.72 – 4.57 (m, 12H), 4.53 – 4.37 (m, 6H), 4.16 – 3.96 (m, 9H), 3.82 (ddd, J = 11.1, 8.8, 5.7 Hz, 9H), 3.62 (ddt, J = 9.4, 4.6, 2.1 Hz, 3H), 3.41 (dd, J = 8.5, 5.3 Hz, 6H), 2.33 – 2.07 (m, 20H), 2.04 (s, 1H). ^{13}C NMR (101 MHz, CDCl_3) δ 164.14, 162.71, 109.06, 108.83, 68.21, 68.16, 67.62, 67.22, 44.74, 43.00, 32.82, 29.79.



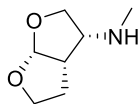
Ethyl ((3*R*,3*aS*,6*aR*)-hexahydrofuro[2,3-*b*]furan-3-yl)carbamate (2.23)

To a stirring solution of bis-THF **2.17** (2 mg, 0.016 mmol) amine in dry DCM (0.5 mL) was added ethyl chloroformate (2 mg, 0.02 mmol). After 10 minutes of stirring at room temperature was added K₂CO₃ (9.6 mg, 0.07 mmol) and H₂O (0.5 mL). Let stir for an additional hour. Reaction mixture was added to a separatory funnel and extracted with DCM. Dried organic layer with NaSO₄. Concentrated via rotary evaporation. The residue purified by silica gel column chromatography (20 % EtOAc in hexane) to afford **2.23** (3 mg, 97%). ¹H NMR (500 MHz, Chloroform-*d*) δ 5.84 (d, *J* = 5.2 Hz, 1H), 4.16 (q, *J* = 7.1 Hz, 2H), 4.07 (t, *J* = 8.3 Hz, 1H), 3.99 – 3.92 (m, 1H), 3.92 – 3.83 (m, 2H), 3.00 (s, 1H), 2.14 – 2.03 (m, 2H), 1.85 (d, *J* = 12.8 Hz, 1H), 1.32 – 1.21 (m, 3H).



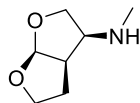
Ethyl ((3*S*,3*aR*,6*aS*)-hexahydrofuro[2,3-*b*]furan-3-yl)carbamate (2.25)

To a stirring solution of bis-THF **2.15** (15 mg, 0.12 mmol) amine in dry DCM (1.0 mL) was added ethyl chloroformate (16 mg, 0.15 mmol). After 10 minutes of stirring at room temperature was added K₂CO₃ (72 mg, 0.52 mmol) and H₂O (2. mL). Let stir for an additional hour. Reaction mixture was added to a separatory funnel and extracted with DCM. Dried organic layer with NaSO₄. Concentrated via rotary evaporation. The residue purified by silica gel column chromatography (20 % EtOAc in hexane) to afford **2.25** (16 mg, 70%). ¹H NMR (500 MHz, Chloroform-*d*) δ 5.78 (d, *J* = 5.0 Hz, 1H), 5.00 (s, 1H), 4.14 – 4.05 (m, 3H), 4.02 (dd, *J* = 9.9, 4.4 Hz, 1H), 3.89 (ddd, *J* = 10.0, 5.5, 2.1 Hz, 2H), 3.76 (d, *J* = 9.8 Hz, 1H), 2.78 – 2.72 (m, 1H), 2.26 – 2.15 (m, 1H), 1.85 (d, *J* = 4.8 Hz, 1H), 1.24 (dd, *J* = 9.0, 4.9 Hz, 3H).



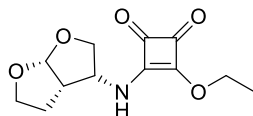
(3*R*,3*aS*,6*aR*)-N-methylhexahydrofuro[2,3-*b*]furan-3-amine (2.24)

To a stirring solution of carbamic acid ethyl ester **2.23** (31 mg, 0.15 mmol) in dry THF (2.0 mL) was added LAH (18 mg, 0.46 mmol) at 0 °C. After 10 minutes of stirring the reaction mixture was heated to 45 °C for two hours. The reaction was cooled down to 0 °C and ethyl acetate was added. Reaction was stirred for an additional 30 minutes. Reaction mixture was filtered over celite and rinsed with ethyl acetate. Concentrated via rotary evaporation. The residue purified by silica gel column chromatography (80 % EtOAc in hexane) to afford **2.24** (14 mg, 67%). ¹H NMR (500 MHz, Chloroform-*d*) δ 5.78 (d, *J* = 5.0 Hz, 1H), 3.94 (dd, *J* = 9.6, 4.5 Hz, 1H), 3.92 – 3.88 (m, 1H), 3.88 – 3.82 (m, 2H), 3.79 (ddd, *J* = 9.6, 1.9, 0.9 Hz, 1H), 3.03 (dt, *J* = 4.2, 1.8 Hz, 1H), 2.70 – 2.62 (m, 1H), 2.42 (s, 3H), 2.21 – 2.10 (m, 1H), 1.76 (ddt, *J* = 13.3, 6.0, 3.9 Hz, 1H).



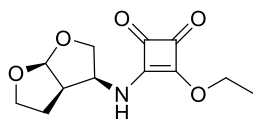
(3*S*,3*aR*,6*aS*)-N-methylhexahydrofuro[2,3-*b*]furan-3-amine (2.26)

To a stirring solution of carbamic acid ethyl ester **2.25** (16 mg, 0.08 mmol) in dry THF (1.0 mL) was added LAH (11 mg, 0.28 mmol) at 0 °C. After 10 minutes of stirring the reaction mixture was heated to 45 °C for two hours. The reaction was cooled down to 0 °C and ethyl acetate was added. Reaction was stirred for an additional 30 minutes. Reaction mixture was filtered over celite and rinsed with ethyl acetate. Concentrated via rotary evaporation. The residue purified by silica gel column chromatography (1 % MeOH in DCM) to afford **2.26** (7 mg, 60%). ¹H NMR (500 MHz, Methanol-*d*₄) δ 5.77 (d, *J* = 5.0 Hz, 1H), 4.07 – 3.98 (m, 2H), 3.87 (dd, *J* = 8.5, 5.2 Hz, 2H), 3.56 (t, *J* = 5.2 Hz, 1H), 2.97 (dt, *J* = 9.4, 4.1 Hz, 1H), 2.64 (s, 3H), 2.31 – 2.16 (m, 1H), 1.51 (d, *J* = 14.3 Hz, 1H).



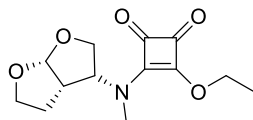
3-ethoxy-4-(((3R,3aS,6aR)-hexahydrofuro[2,3-b]furan-3-yl)amino)cyclobut-3-ene-1,2-dione (2.21a)

To a solution of Bis-THF amine **2.15** (7.3 mg, 0.057 mmol) in ethanol (1.0 mL) was added diethylsquarate (10 mg, 0.062 mmol). After two days of stirring that reaction mixture at room temperature the reaction was concentrated via rotary evaporation. The crude product was purified by silica gel column chromatography (60 % EtOAc in hexane) to afford **2.21a** (11 mg, 78%). ¹H NMR (500 MHz, Chloroform-*d*) δ 6.98 (s, 1H), 5.94 – 5.81 (m, 1H), 4.78 (s, 2H), 4.09 (dd, *J* = 10.3, 4.0 Hz, 1H), 3.91 (dt, *J* = 9.4, 4.8 Hz, 2H), 2.94 (s, 1H), 2.26 (dt, *J* = 12.9, 9.2 Hz, 1H), 1.86 (s, 1H), 1.46 (t, *J* = 6.9 Hz, 3H). ¹³C NMR (126 MHz, Chloroform-*d*) δ 189.07, 183.08, 178.11, 171.52, 108.51, 72.80, 70.00, 68.30, 61.17, 50.52, 29.77, 15.83.



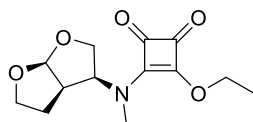
3-ethoxy-4-(((3S,3aR,6aS)-hexahydrofuro[2,3-b]furan-3-yl)amino)cyclobut-3-ene-1,2-dione (2.21b)

To a solution of Bis-THF amine **2.15** (9 mg, 0.070 mmol) in ethanol (1.0 mL) was added diethylsquarate (13 mg, 0.077 mmol). After two days of stirring that reaction mixture at room temperature the reaction was concentrated via rotary evaporation. The crude product was purified by silica gel column chromatography (60 % EtOAc in hexane) to afford **2.21b** (10 mg, 58%). ¹H NMR (500 MHz, Chloroform-*d*) δ 6.84 (s, 1H), 5.87 (d, *J* = 5.1 Hz, 1H), 4.78 (t, *J* = 7.7 Hz, 2H), 3.95 – 3.87 (m, 3H), 2.92 (s, 1H), 2.25 (dq, *J* = 13.3, 8.8 Hz, 1H), 1.46 (td, *J* = 7.1, 2.3 Hz, 3H).



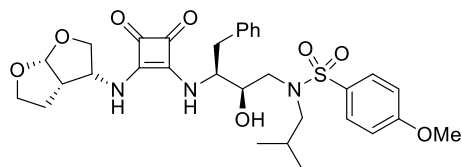
3-ethoxy-4-(((3R,3aS,6aR)-hexahydrofuro[2,3-b]furan-3-yl)(methyl)amino)cyclobut-3-ene-1,2-dione (2.21c)

To a solution of Bis-THF methyl amine **2.24** (9 mg, 0.070 mmol) in ethanol (1.0 mL) was added diethylsquarate (13 mg, 0.077 mmol) and DIPEA (24 mg, 0.186 mmol). After two days of stirring the reaction mixture at room temperature the reaction was then concentrated via rotary evaporation. The crude product was purified by silica gel column chromatography (60 % EtOAc in hexane) to afford **2.21b**. ^1H NMR (500 MHz, Chloroform-*d*) δ 5.87 (d, J = 5.0 Hz, 1H), 5.19 (d, J = 5.6 Hz, 1H), 4.77 (p, J = 6.8 Hz, 2H), 4.16 – 4.06 (m, 2H), 4.02 (d, J = 11.1 Hz, 1H), 3.94 (td, J = 8.4, 3.2 Hz, 1H), 3.90 – 3.82 (m, 1H), 3.29 (s, 1H), 3.10 (s, 2H), 2.95 – 2.83 (m, 1H), 2.30 – 2.16 (m, 1H), 2.06 (ddd, J = 15.6, 6.9, 3.4 Hz, 1H), 1.94 – 1.86 (m, 1H), 1.46 (t, J = 7.1 Hz, 3H).



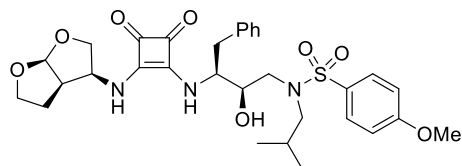
3-ethoxy-4-(((3S,3aR,6aS)-hexahydrofuro[2,3-b]furan-3-yl)(methyl)amino)cyclobut-3-ene-1,2-dione (2.21d)

To a solution of Bis-THF methyl amine **2.26** (2 mg, 0.015 mmol) in ethanol (0.5 mL) was added diethylsquarate (8 mg, 0.046 mmol) and DIPEA (3 μL , 0.186 mmol). After two days of stirring the reaction mixture at room temperature the reaction was concentrated via rotary evaporation. The crude product was purified by silica gel column chromatography (60 % EtOAc in hexane) to afford **2.21b** (2 mg, 46%). ^1H NMR (500 MHz, Chloroform-*d*) δ 5.70 (d, J = 4.9 Hz, 1H), 5.12 (s, 1H), 4.79 (qd, J = 7.1, 1.8 Hz, 2H), 4.14 (dd, J = 10.0, 6.5 Hz, 1H), 4.09 – 3.92 (m, 1H), 3.35 (s, 1H), 3.25 (s, 1H), 2.11 – 1.92 (m, 1H), 1.84 (d, J = 9.9 Hz, 1H), 1.47 (t, J = 7.1 Hz, 3H).



N-((2*R*,3*S*)-3-((2-(((3*R*,3*aS*,6*aR*)-hexahydrofuro[2,3-*b*]furan-3-yl)amino)-3,4-dioxocyclobut-1-en-1-yl)amino)-2-hydroxy-4-phenylbutyl)-*N*-isobutyl-4-methoxybenzenesulfonamide (2.22a)

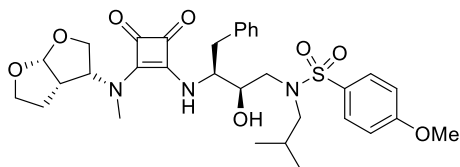
To a solution of Bis-THF mixed squarate **2.21a** (11 mg, 0.044 mmol) in ethanol (1 mL) was added isostere amine **1.25** (13 mg, 0.039 mmol). After two days of stirring the reaction mixture at room temperature the reaction was concentrated via rotary evaporation. The crude product was purified by silica gel column chromatography (5 % MeOH in DCM) to afford **2.22a** (7 mg, 63%). ¹H NMR (500 MHz, Chloroform-*d*) δ 7.55 (d, *J* = 8.6 Hz, 3H), 7.27 (s, 3H), 7.13 (dd, *J* = 8.8, 6.1 Hz, 3H), 7.07 (d, *J* = 7.1 Hz, 4H), 6.90 – 6.83 (m, 3H), 5.66 (d, *J* = 4.9 Hz, 2H), 5.19 (s, 1H), 4.99 (s, 2H), 4.37 (d, *J* = 3.9 Hz, 2H), 3.92 (d, *J* = 7.3 Hz, 4H), 3.90 (s, 14H), 3.84 (dt, *J* = 8.4, 4.5 Hz, 3H), 3.80 – 3.73 (m, 6H), 3.66 (d, *J* = 10.1 Hz, 2H), 3.53 (s, 1H), 3.22 (dd, *J* = 3.4, 1.8 Hz, 6H), 2.96 (dd, *J* = 14.2, 4.6 Hz, 3H), 2.77 (d, *J* = 7.6 Hz, 3H), 2.67 (dd, *J* = 14.0, 9.7 Hz, 3H), 2.09 (ddt, *J* = 18.3, 9.1, 5.1 Hz, 3H), 1.91 (d, *J* = 7.1 Hz, 2H), 1.83 – 1.71 (m, 4H), 1.12 (s, 7H), 0.74 (t, *J* = 6.3 Hz, 9H). ¹³C NMR (126 MHz, Chloroform-*d*) δ 183.01, 182.66, 167.57, 166.83, 163.23, 137.14, 129.23, 129.17, 128.37, 126.57, 114.25, 109.07, 77.34, 77.09, 76.83, 68.11, 57.95, 55.44, 49.20, 49.03, 48.86, 48.69, 48.52, 48.35, 48.23, 35.93, 29.49, 29.31, 26.75, 19.72, 19.62. LRMS-ESI (*m/z*): 636.3 [M+Na], HRMS-ESI: 614.2526 [M+H].



N-((2*R*,3*S*)-3-((2-(((3*S*,3*aR*,6*aS*)-hexahydrofuro[2,3-*b*]furan-3-yl)amino)-3,4-dioxocyclobut-1-en-1-yl)amino)-2-hydroxy-4-phenylbutyl)-*N*-isobutyl-4-methoxybenzenesulfonamide (2.22b)

To a solution of Bis-THF mixed squarate **2.21b** (10 mg, 0.040 mmol) in ethanol (1 mL) was added isostere amine **1.25** (14 mg, 0.036 mmol). After two days of stirring the reaction mixture at room

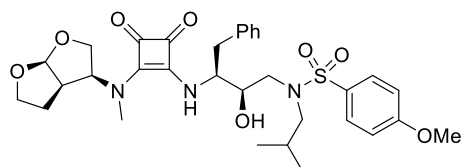
temperature the reaction mixture was concentrated via rotary evaporation. The crude product was purified by silica gel column chromatography (5 % MeOH in DCM) to afford **2.22b** (12 mg, 50%). ¹H NMR (500 MHz, Methanol-*d*₄) δ 7.72 (d, *J* = 8.9 Hz, 3H), 7.28 – 7.14 (m, 7H), 7.05 (d, *J* = 8.9 Hz, 3H), 5.77 (d, *J* = 5.0 Hz, 2H), 4.43 (s, 1H), 4.35 (s, 1H), 4.04 (dd, *J* = 10.9, 4.5 Hz, 2H), 3.98 – 3.90 (m, 2H), 3.86 (s, 4H), 3.84 (s, 1H), 3.84 – 3.75 (m, 3H), 3.41 (dt, *J* = 14.4, 4.9 Hz, 2H), 3.34 (s, 1H), 3.29 (s, 6H), 3.23 (dd, *J* = 13.9, 3.9 Hz, 2H), 3.08 (dd, *J* = 13.7, 8.2 Hz, 2H), 2.96 (dd, *J* = 14.9, 8.0 Hz, 2H), 2.81 (ddd, *J* = 21.3, 11.4, 5.5 Hz, 4H), 2.74 – 2.66 (m, 2H), 2.22 (d, *J* = 8.7 Hz, 1H), 2.19 (s, 1H), 2.06 – 1.94 (m, 3H), 1.93 – 1.83 (m, 2H), 0.89 (dd, *J* = 29.4, 6.7 Hz, 9H). ¹³C NMR (126 MHz, Chloroform-*d*) δ 182.48, 182.06, 168.01, 166.41, 163.20, 137.81, 130.28, 129.19, 128.02, 126.17, 113.96, 108.39, 72.62, 67.63, 60.41, 58.68, 57.65, 54.81, 52.37, 51.01, 35.81, 29.05, 26.68, 19.06. LRMS-ESI (*m/z*): 636.3 [M+Na], HRMS-ESI: 614.2523 [M+H].



N-((2R,3S)-3-(((3R,3aS,6aR)-hexahydrofuro[2,3-b]furan-3-yl)(methyl)amino)-3,4-dioxocyclobut-1-en-1-yl)amino)-2-hydroxy-4-phenylbutyl)-N-isobutyl-4-methoxybenzenesulfonamide (2.22c**)**

To a solution of Bis-THF methyl squarate **2.21c** (1.5 mg, 0.006 mmol) in ethanol (0.5 mL) was added isostere amine **1.25** (2.5 mg, 0.06 mmol) and DIPEA (2 μL, 0.19 mmol). After three days of stirring the reaction mixture at room temperature the reaction was concentrated via rotary evaporation. The crude product was purified by silica gel column chromatography (5 % MeOH in DCM) to afford **2.22c** (3 mg, 54%). ¹H NMR (500 MHz, Chloroform-*d*) δ 7.69 (d, *J* = 8.9 Hz, 1H), 7.33 – 7.19 (m, 10H), 7.03 – 6.97 (m, 2H), 5.99 (s, 1H), 5.86 (d, *J* = 5.0 Hz, 1H), 4.09 (dd, *J* = 10.9, 6.0 Hz, 2H), 3.97 – 3.87 (m, 6H), 3.87 – 3.79 (m, 1H), 3.23 – 3.14 (m, 2H), 3.08 (s, 4H), 3.08 – 2.94 (m, 2H), 2.82 (dd, *J* = 13.5, 7.1 Hz, 2H), 2.23 – 2.11 (m, 1H), 2.07 – 1.89 (m, 3H), 1.28 – 1.19 (m, 5H), 0.88 (dd, *J* = 6.6, 2.3 Hz, 8H). ¹³C NMR (126 MHz, Chloroform-*d*) δ 183.01, 182.66, 167.57, 166.83, 163.23, 137.14, 129.55, 129.31, 129.26, 128.71, 126.89, 114.49, 109.07,

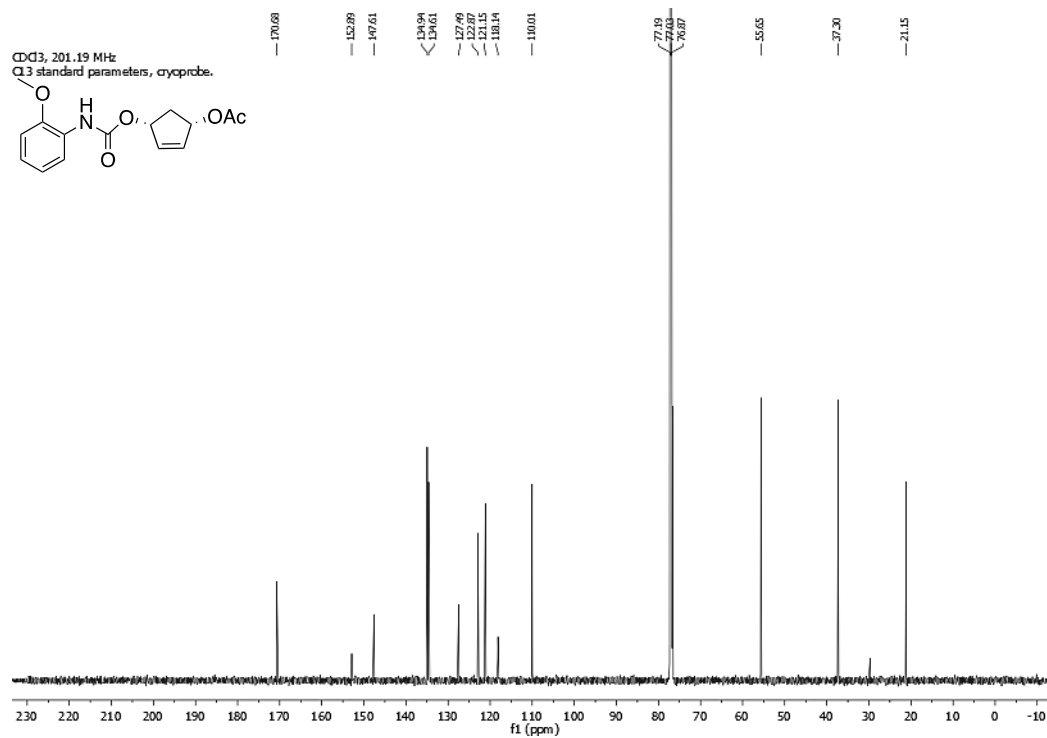
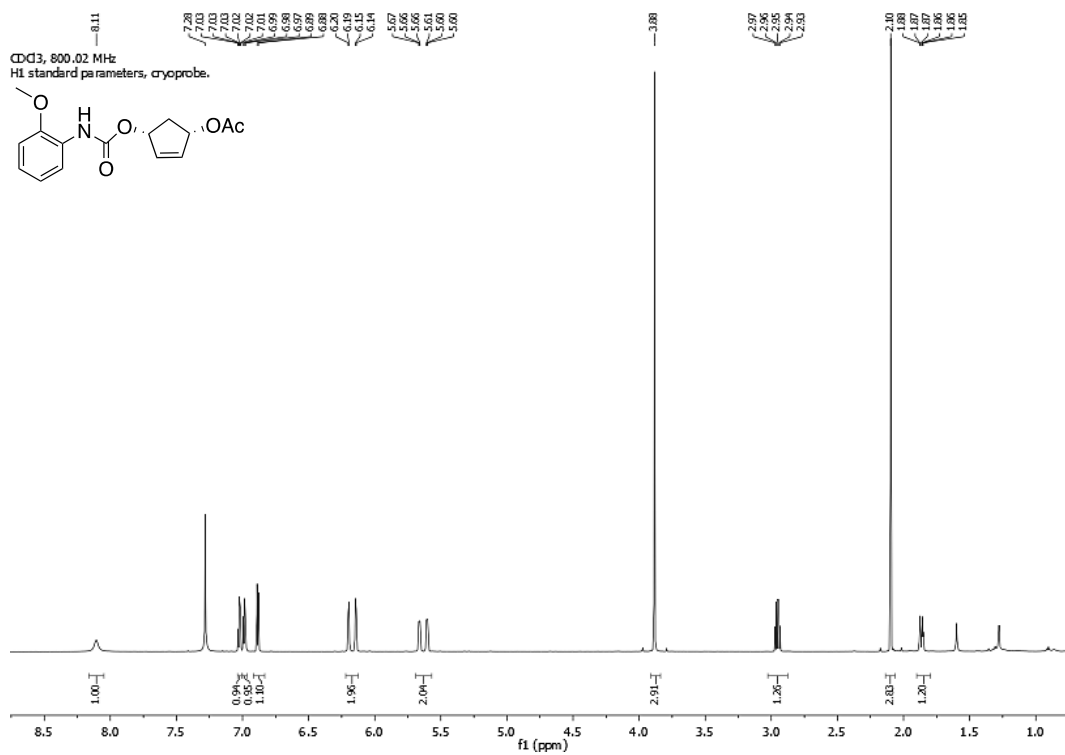
72.16, 71.13, 68.30, 65.68, 59.07, 58.45, 55.97, 55.68, 52.38, 48.80, 36.10, 30.91, 29.70, 27.07, 20.14, 20.02. LRMS-ESI (m/z): 628.58 [M+H], HRMS-ESI: 628.2682 [M+H].

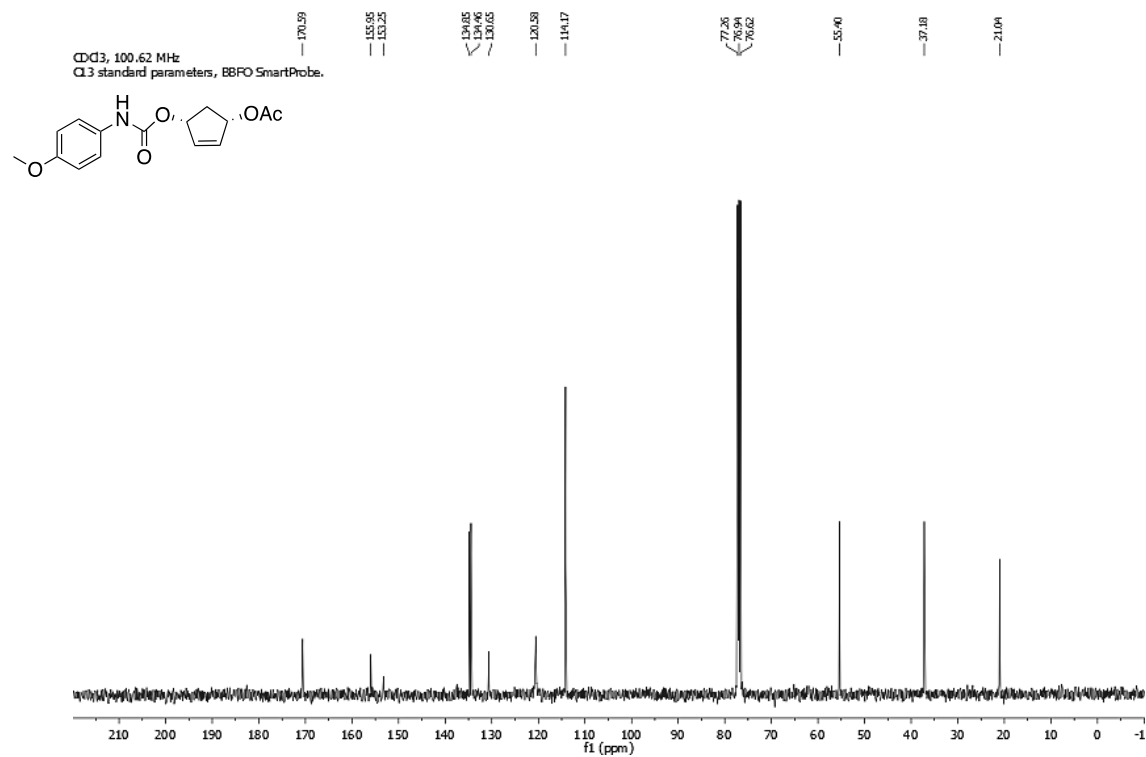
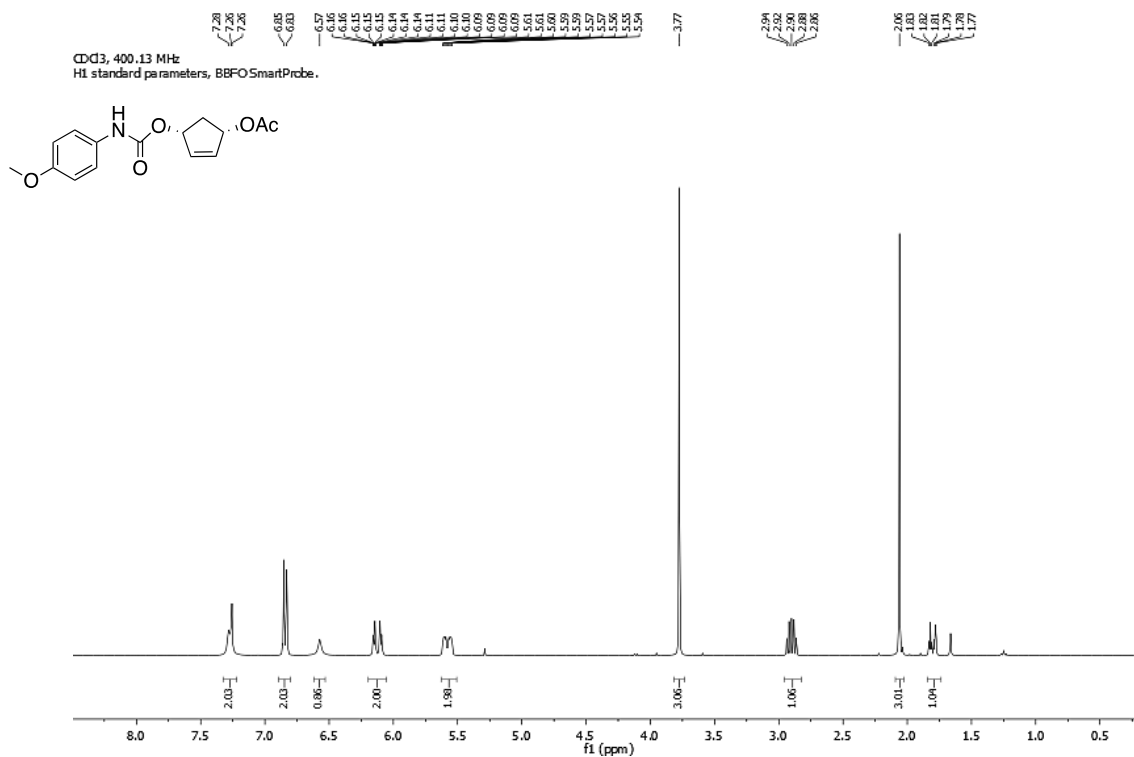


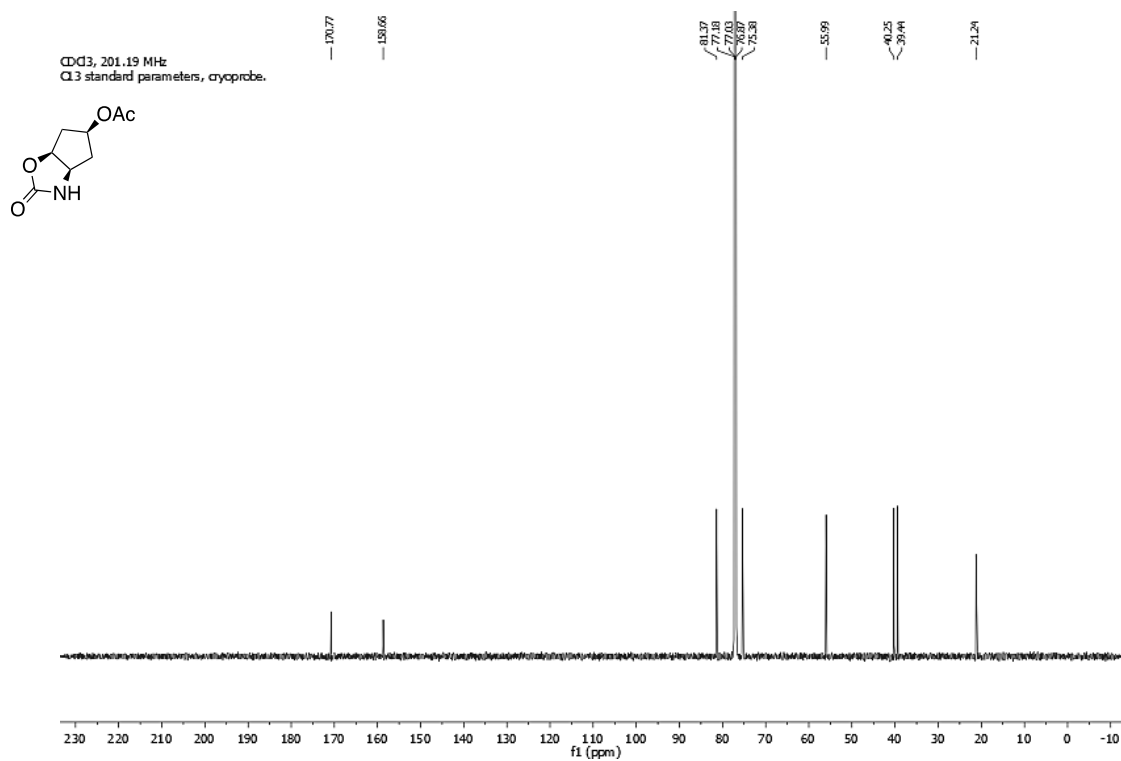
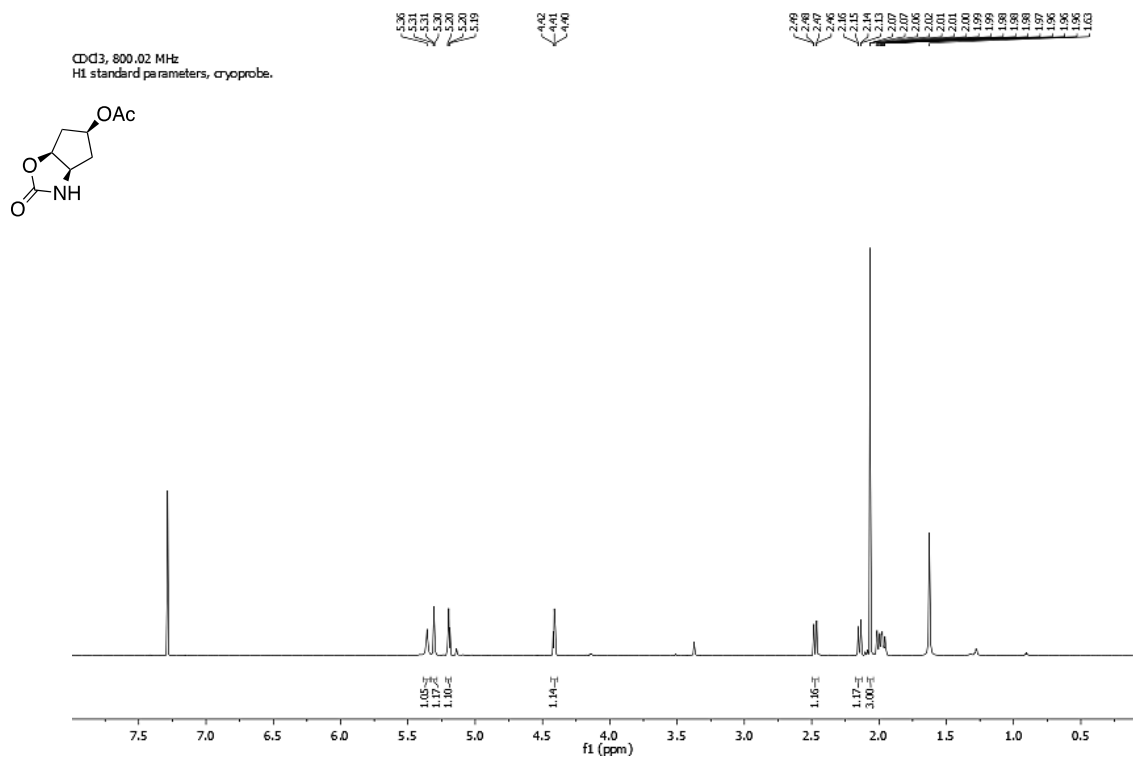
N-((2*R*,3*S*)-3-((2-(((3*S*,3*aR*,6*aS*)-hexahydrofuro[2,3-*b*]furan-3-yl)(methyl)amino)-3,4-dioxocyclobut-1-en-1-yl)amino)-2-hydroxy-4-phenylbutyl)-*N*-isobutyl-4-methoxybenzenesulfonamide (2.22d)

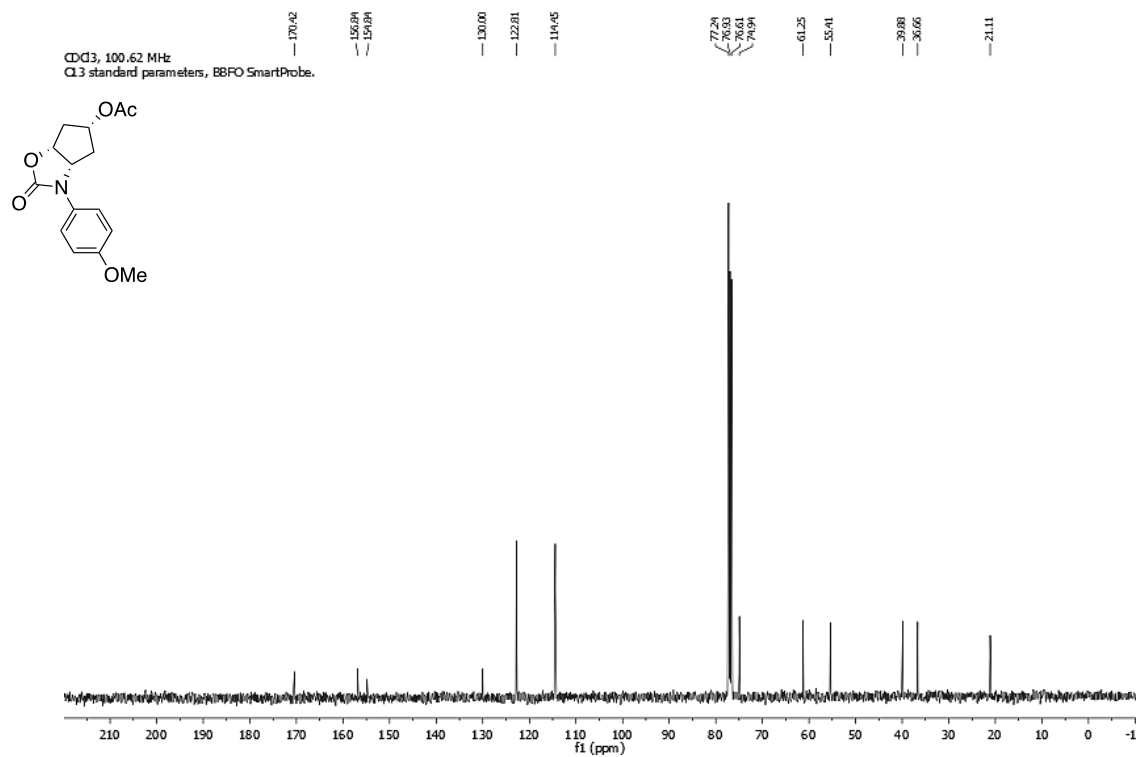
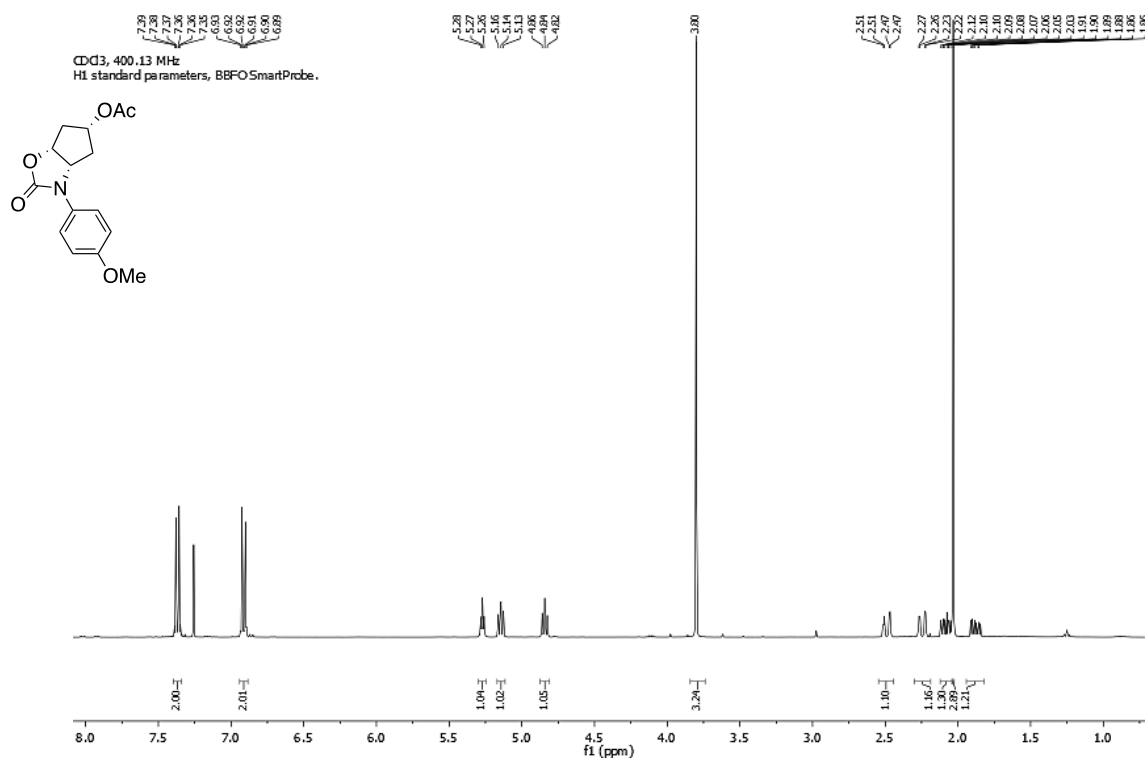
To a solution of Bis-THF methyl squarate **2.21d** (2 mg, 0.006 mmol) in ethanol (0.5 mL) was added isostere amine **1.25** (2.3 mg, 0.057 mmol) and DIPEA (2 μ L, 0.18 mmol). After three days of stirring the reaction mixture at room temperature the reaction was concentrated via rotary evaporation. The crude product was purified by silica gel column chromatography (5 % MeOH in DCM) to afford **2.22d** (2 mg, 50%). ^1H NMR (400 MHz, Chloroform-*d*) δ (ppm): 7.71 (d, J = 8.9 Hz, 2H), 7.36 – 7.17 (m, 6H), 7.00 (d, J = 8.9 Hz, 2H), 6.32 (d, J = 9.5 Hz, 1H), 5.64 (d, J = 5.3 Hz, 1H), 4.80 (brd s, 1H), 4.52 (brd s, 1H), 4.15 – 4.06 (m, 2H), 4.01 (dd, J = 10.5, 5.0 Hz, 1H), 3.95 (td, J = 8.6, 3.6 Hz, 1H), 3.92 – 3.85 (m, 4H), 3.49 (s, 1H), 3.36 (s, 1H), 3.28 (s, 1H), 3.22 (d, 1H), 3.14 – 3.02 (m, 2H), 2.98 (dd, J = 13.5, 7.8 Hz, 1H), 2.92 – 2.83 (m, 2H), 2.04 (s, 1H), 1.96 (dt, J = 13.7, 6.9 Hz, 2H), 1.75 (dt, J = 18.6, 9.2 Hz, 2H), 1.70 – 1.52 (m, 3H), 1.30 – 1.21 (m, 4H), 0.88 (d, J = 6.6 Hz, 6H). ^{13}C NMR (126 MHz, Chloroform-*d*) δ 183.37, 182.56, 168.36, 166.98, 163.21, 137.23, 129.66, 129.34, 129.21, 128.72, 126.84, 114.47, 109.32, 72.16, 69.31, 67.23, 61.15, 60.38, 58.99, 58.49, 55.67, 52.12, 48.13, 35.99, 35.13, 29.69, 27.03, 25.63, 20.13, 20.03, 14.18. LRMS-ESI (m/z): 628.58 [M+H], HRMS-ESI: 628.2692 [M+H].

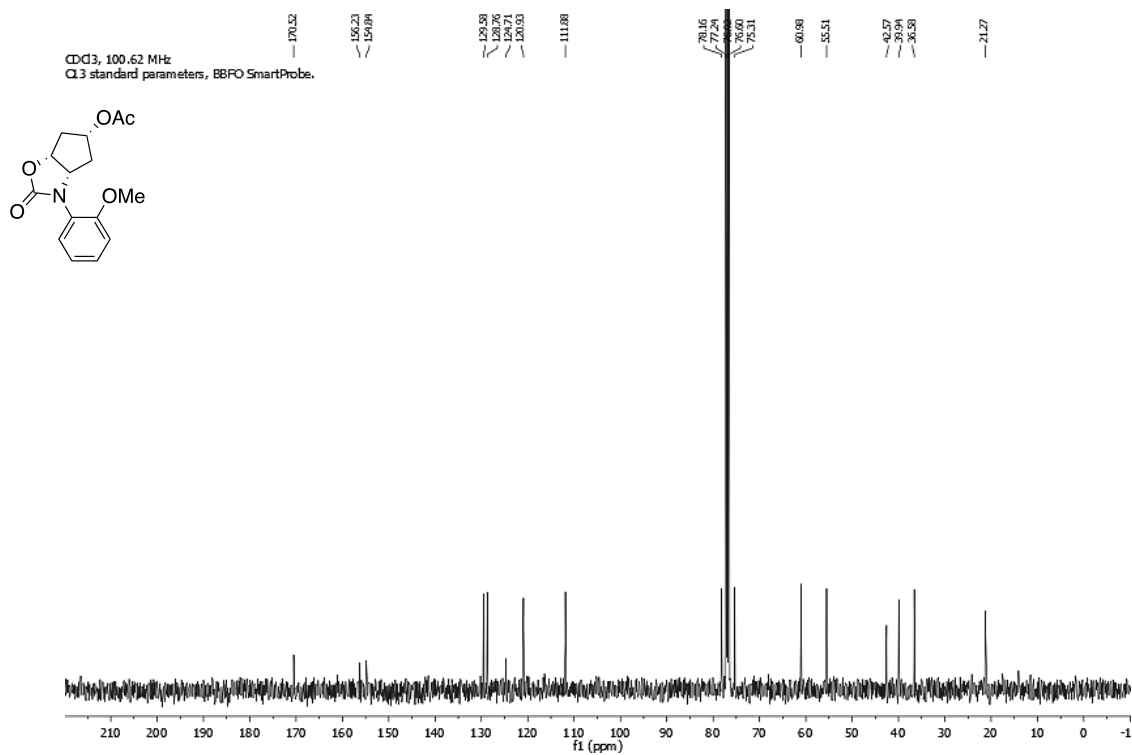
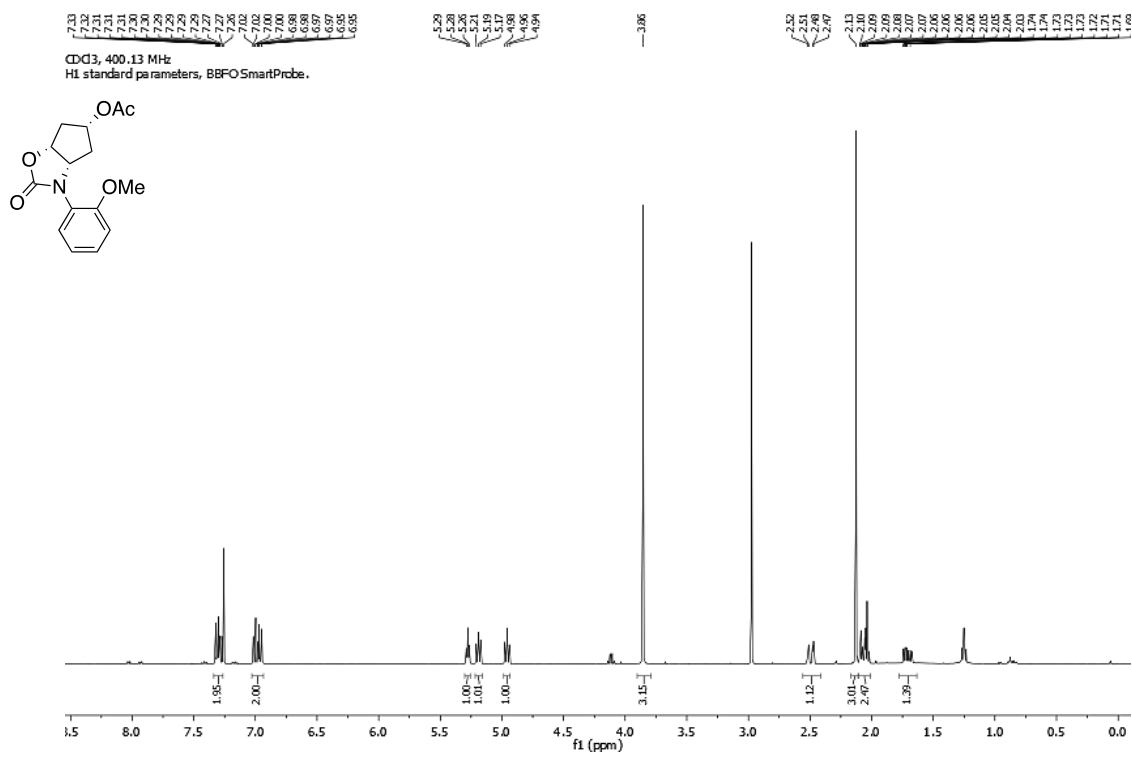
APPENDIX: NMR SPECTRA

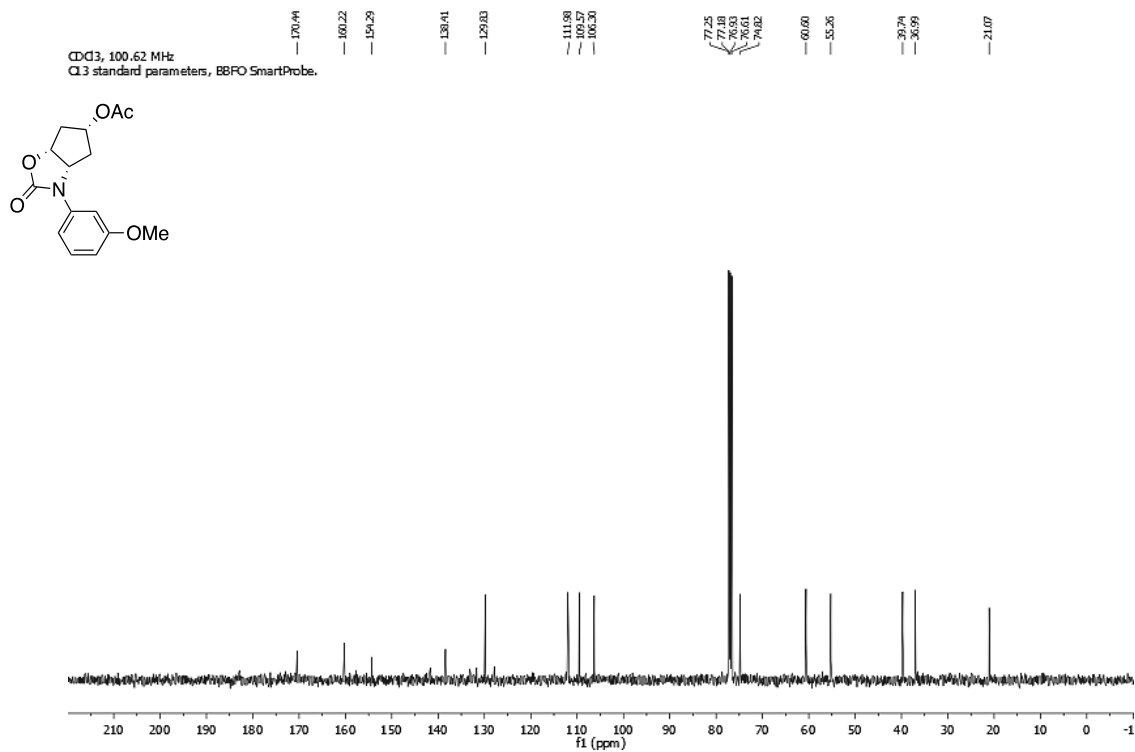
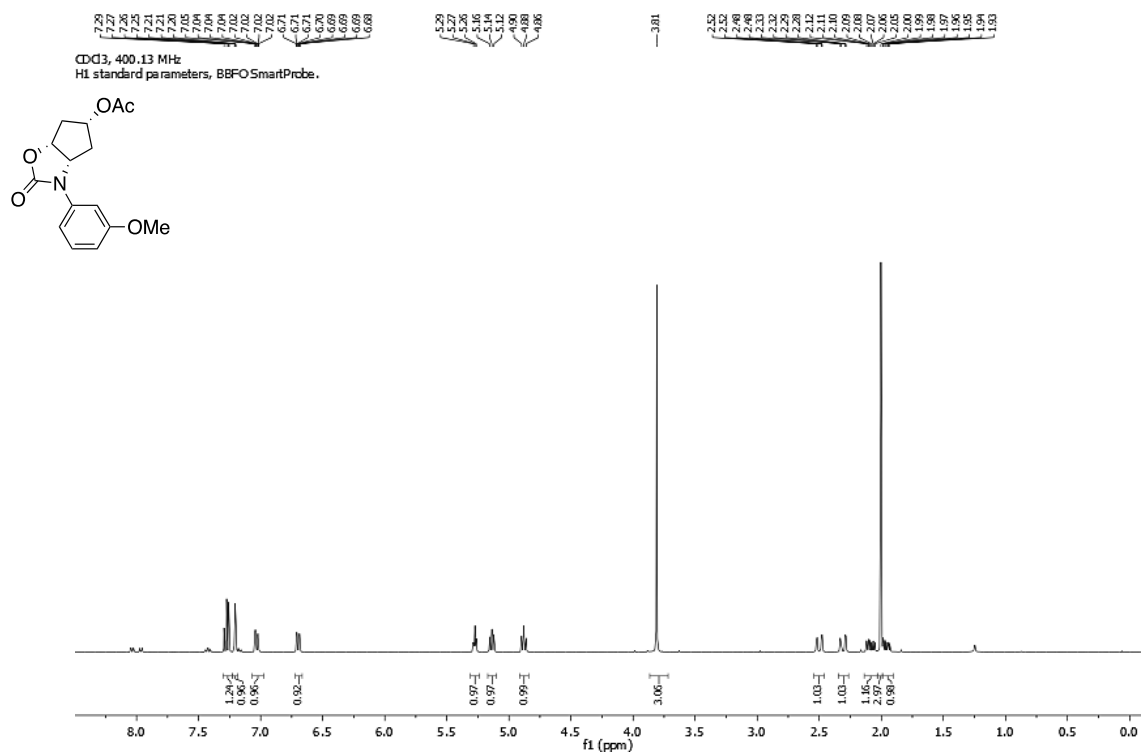


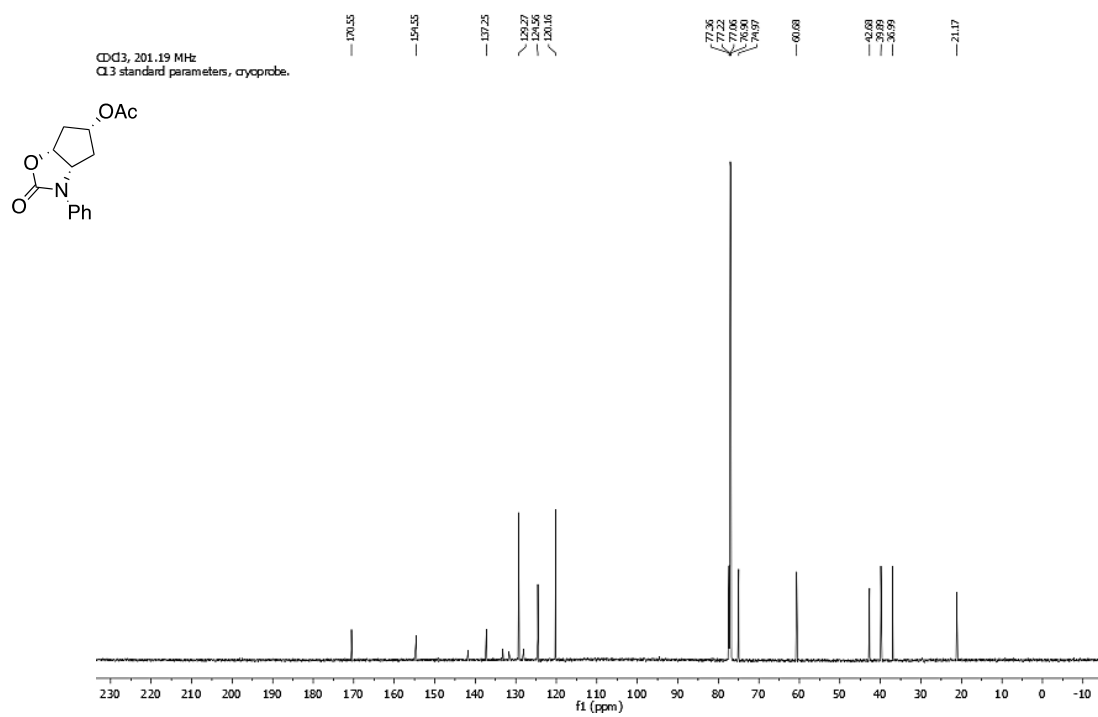


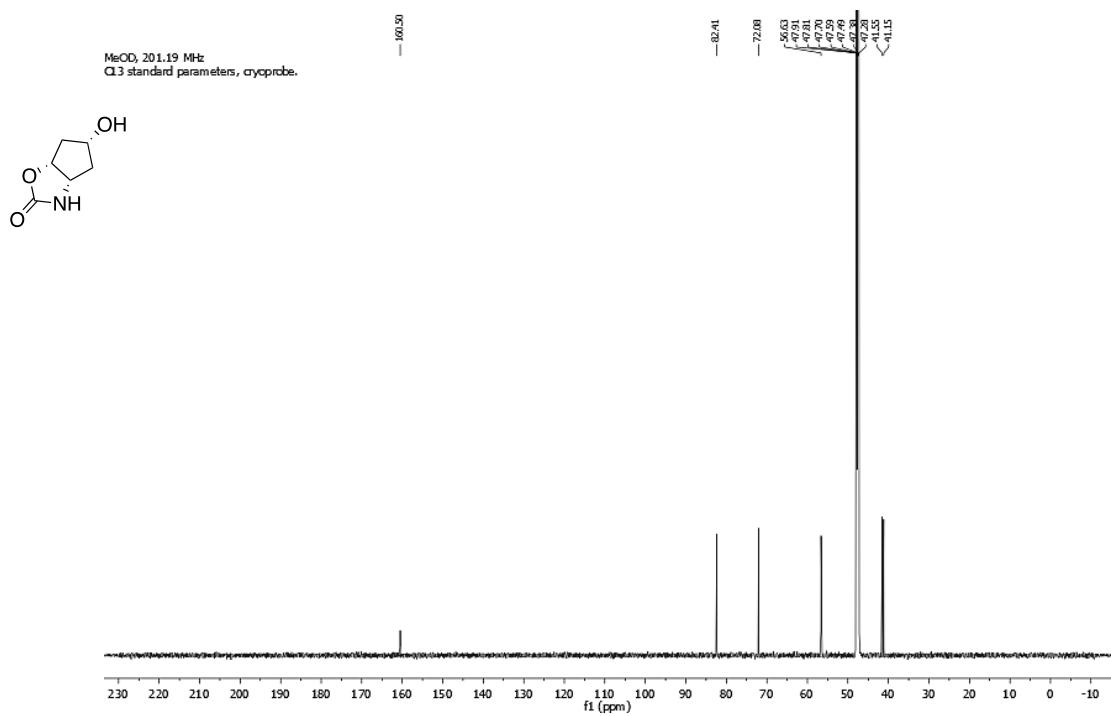


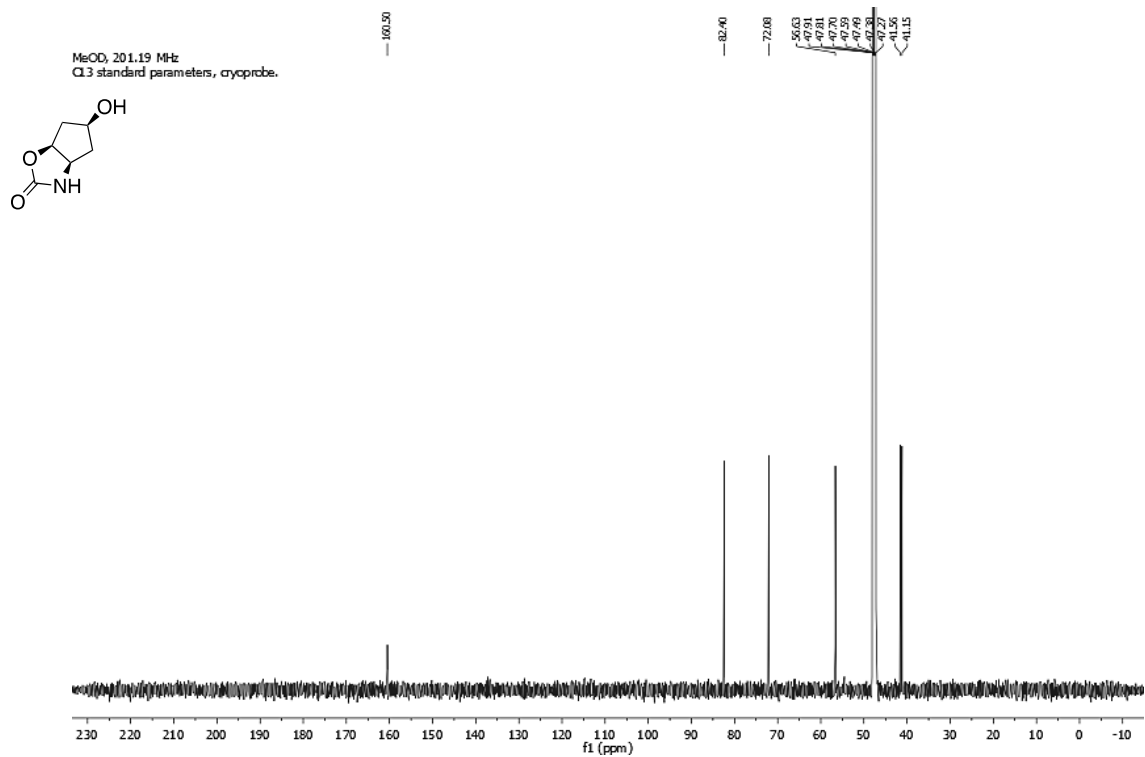
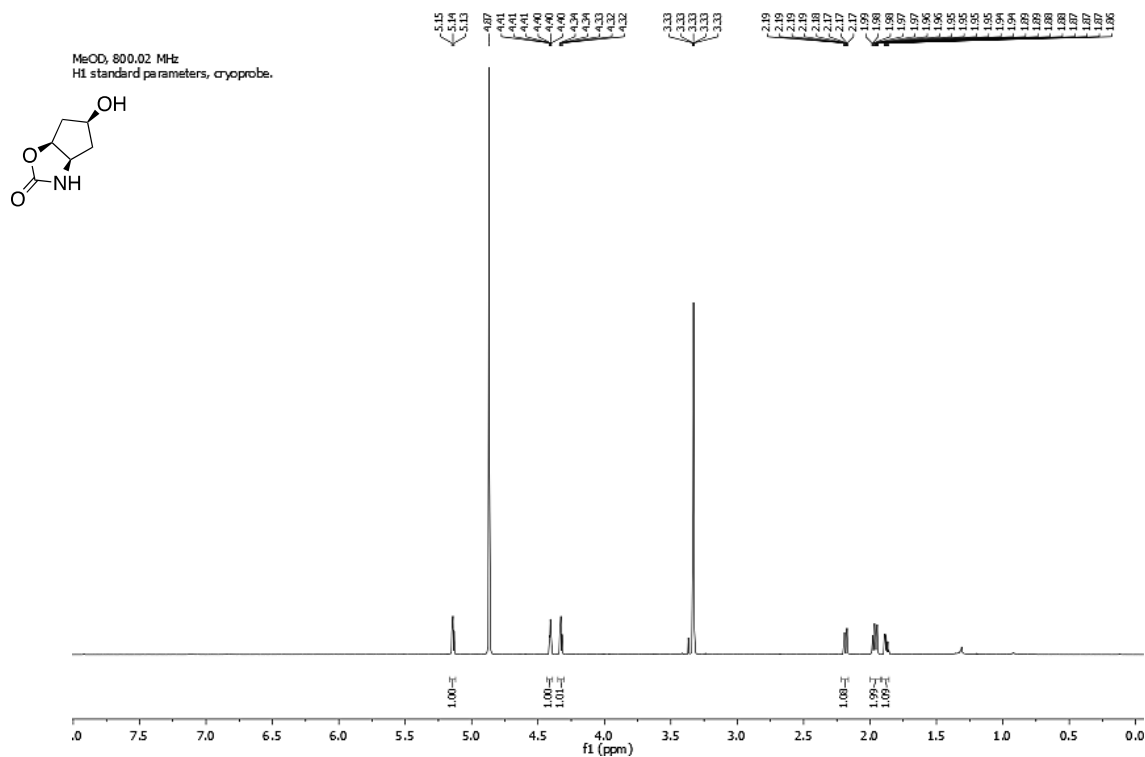


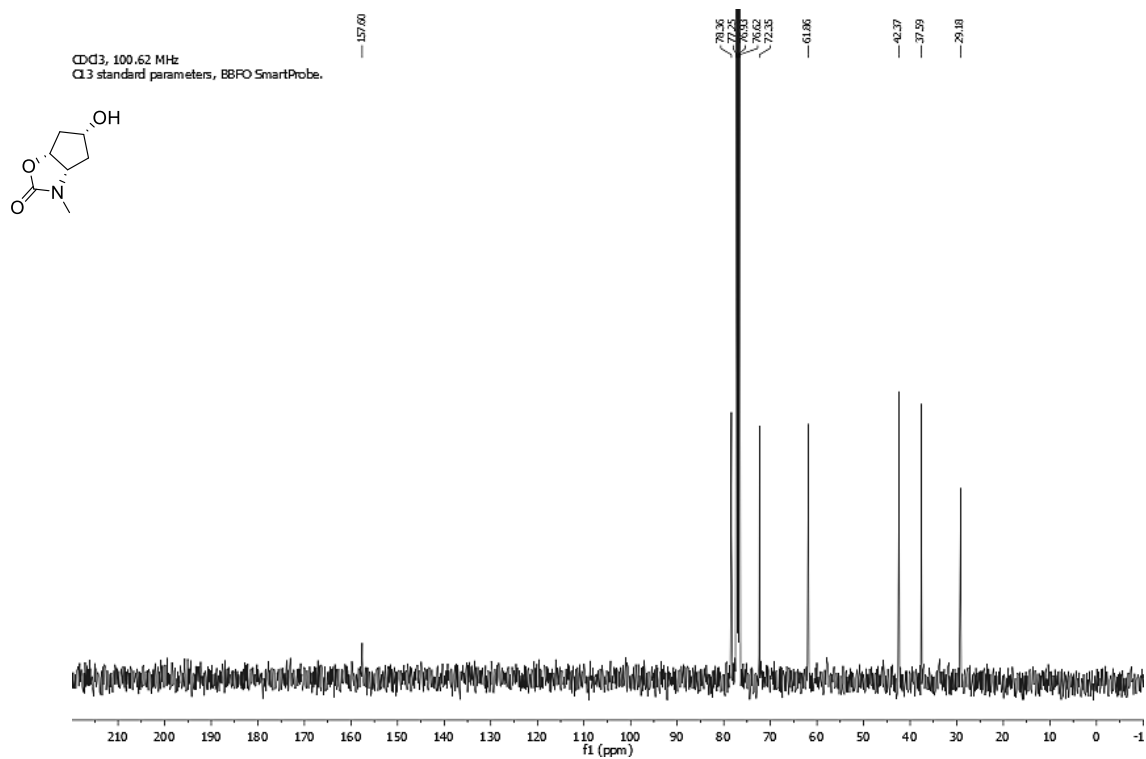
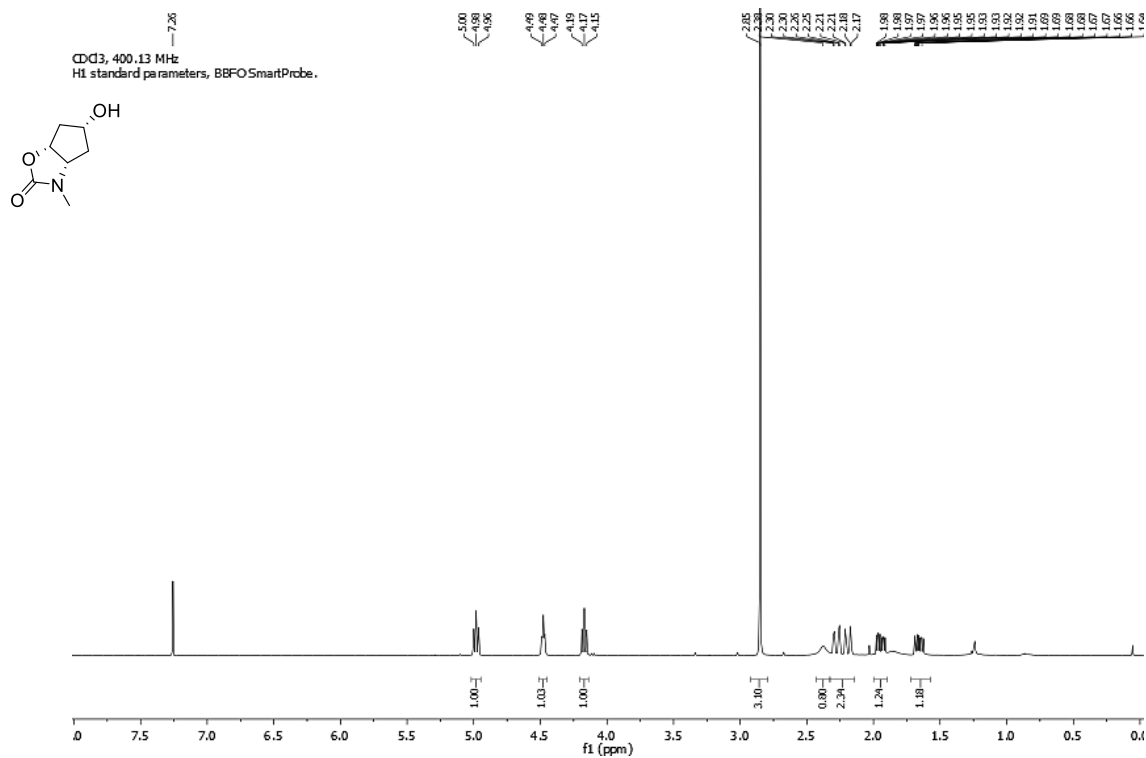


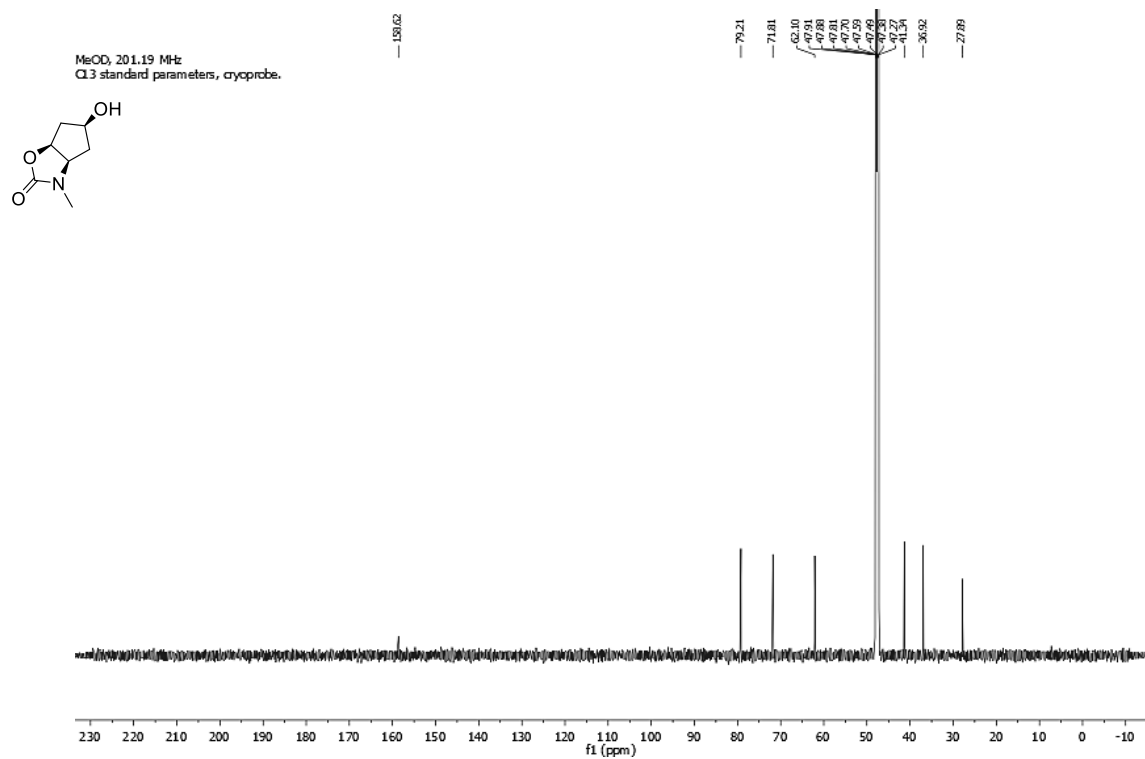
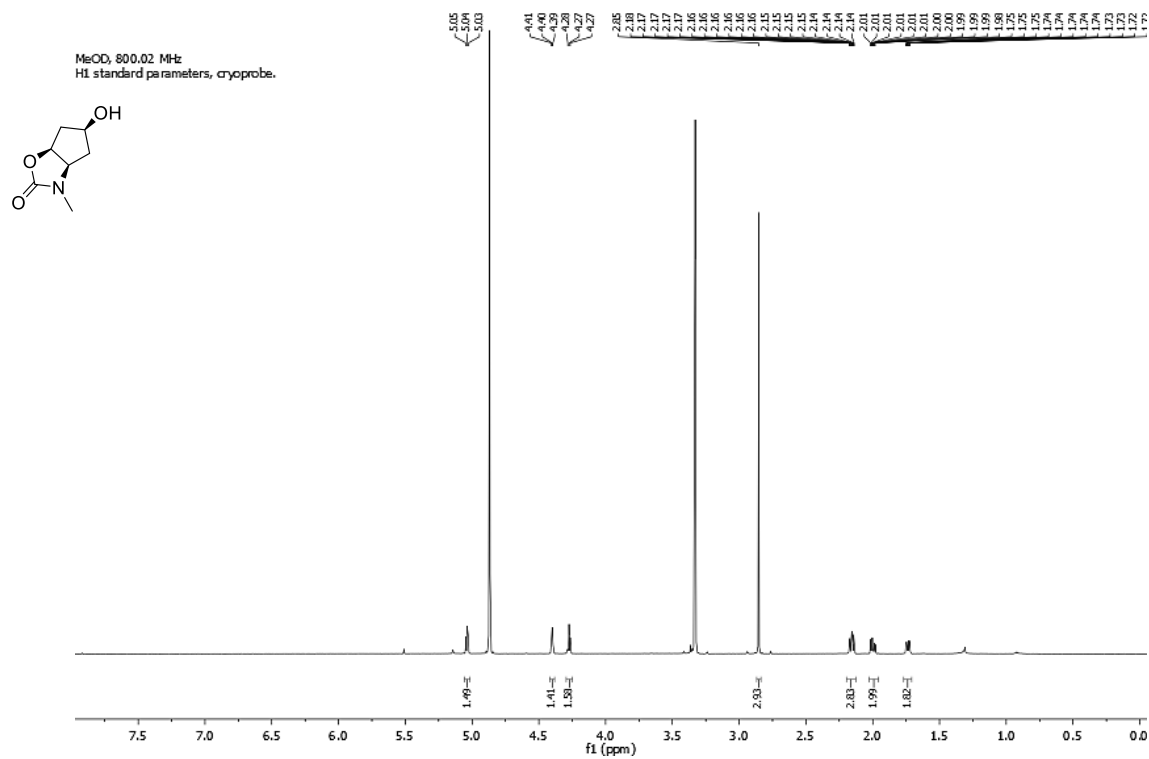


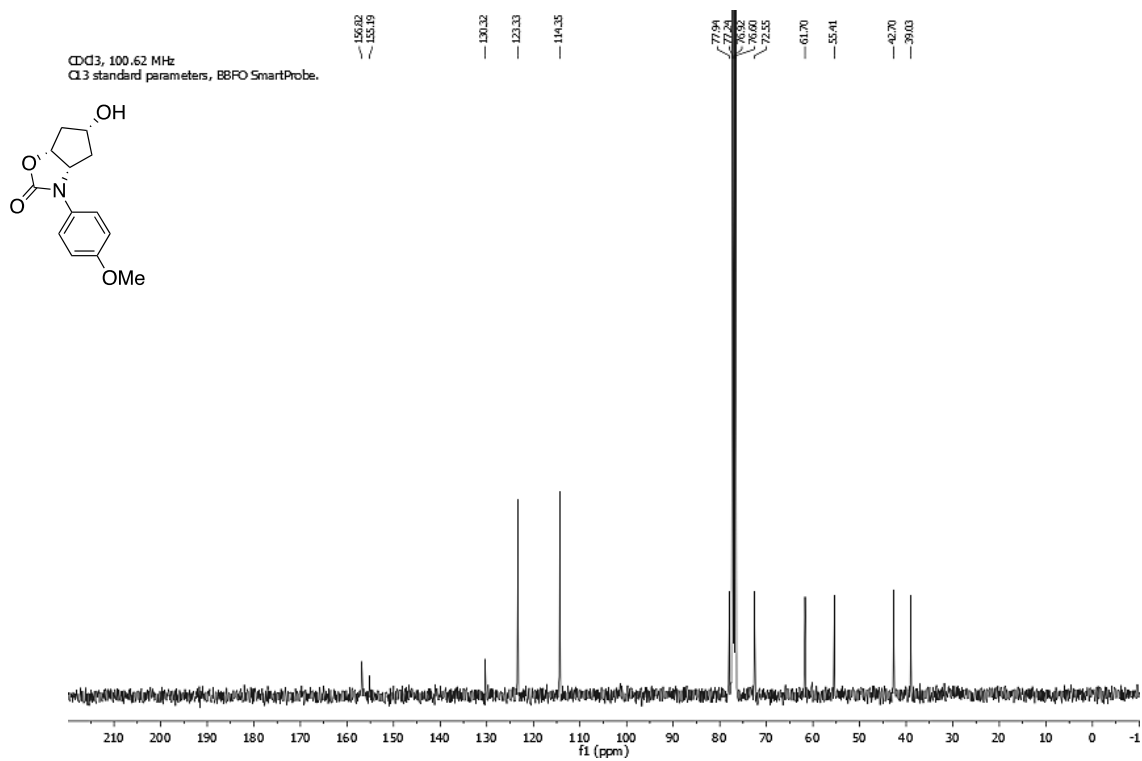
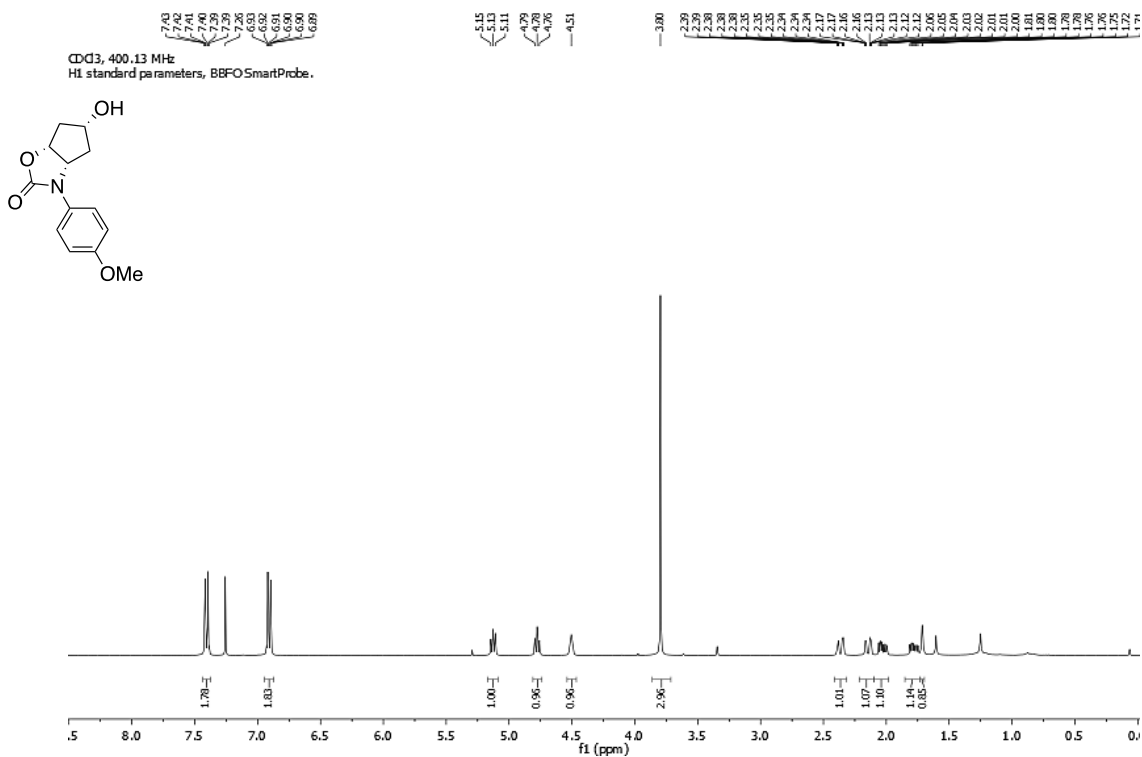


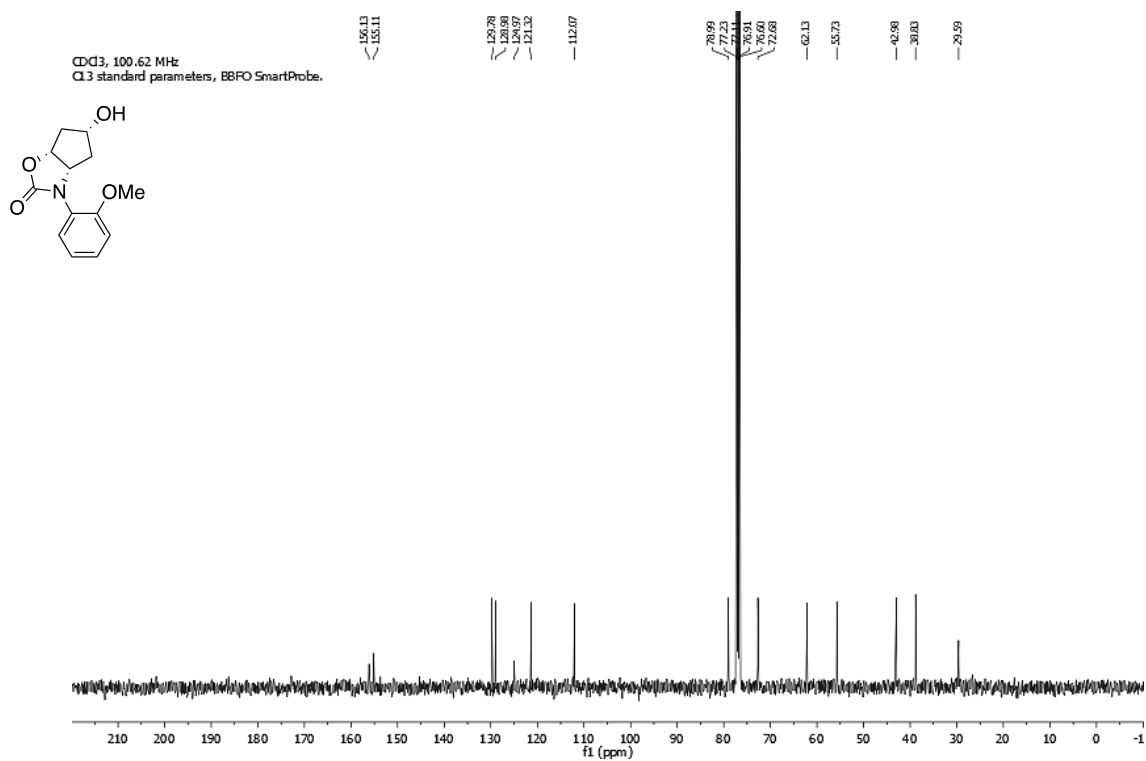
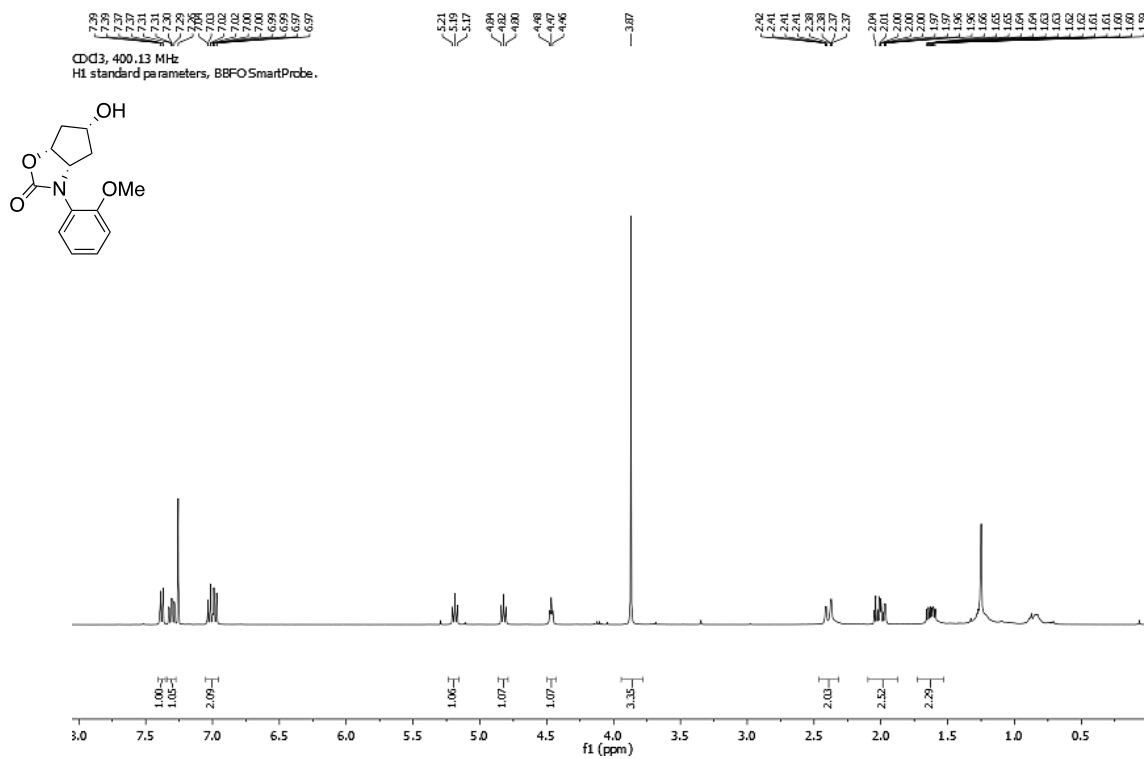


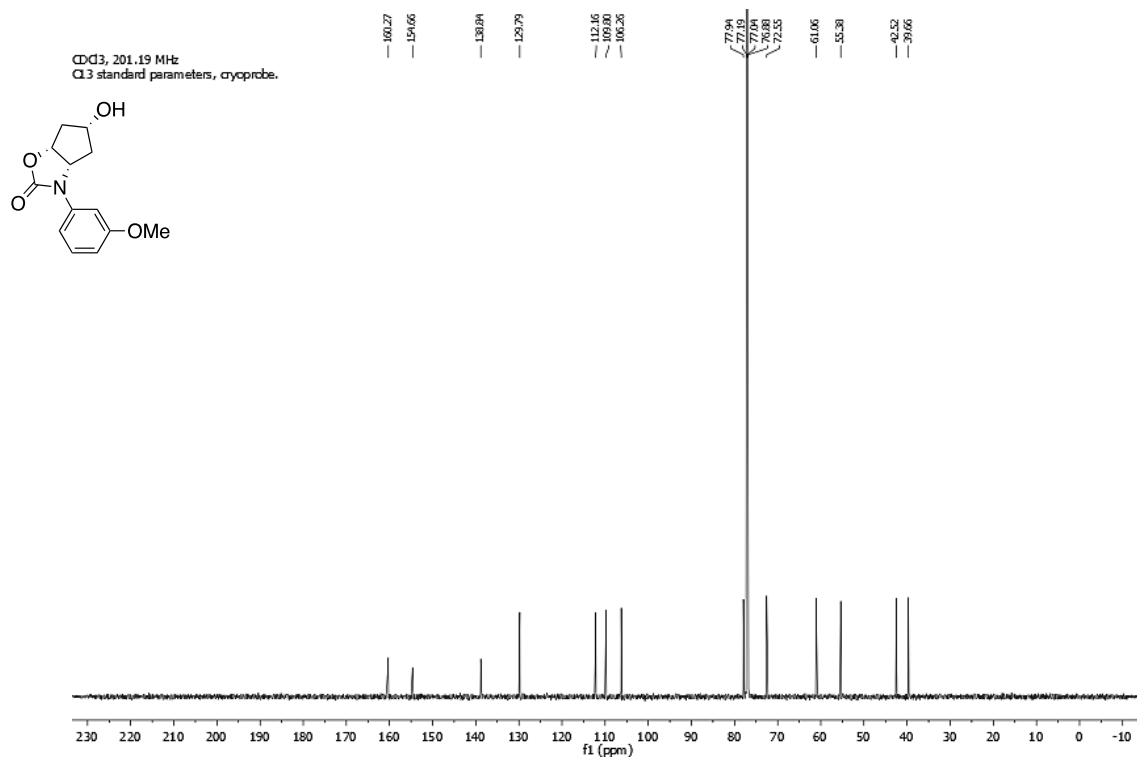
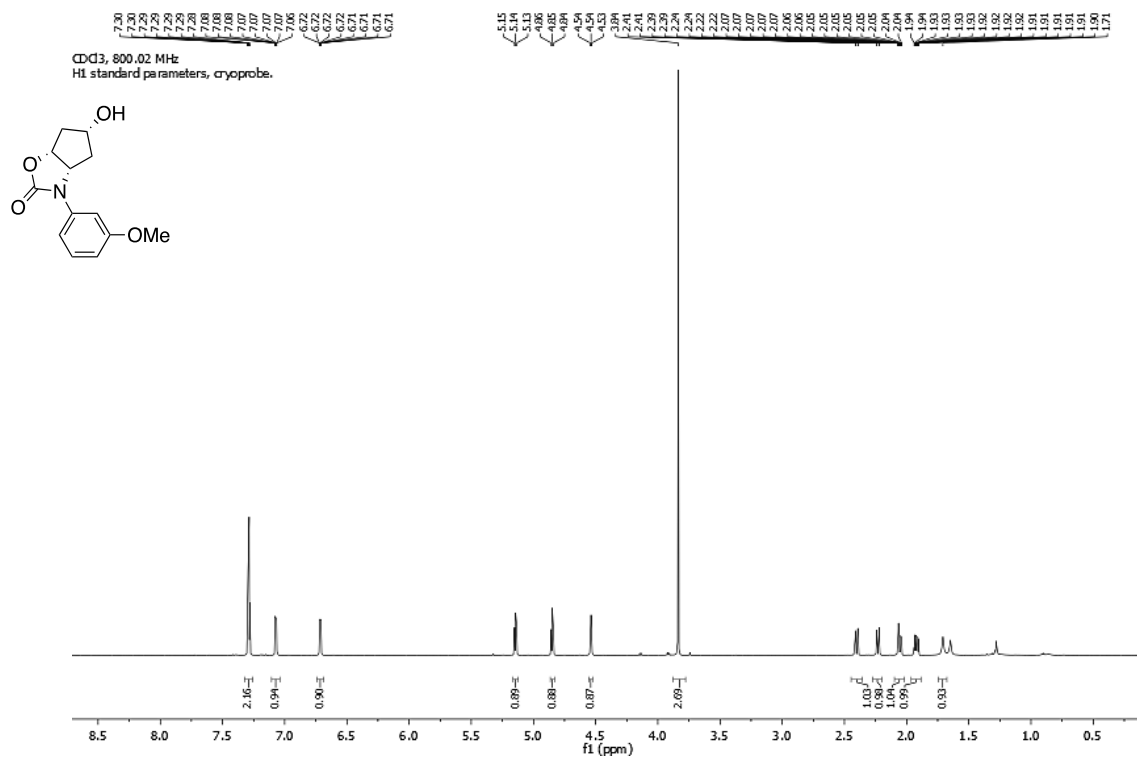


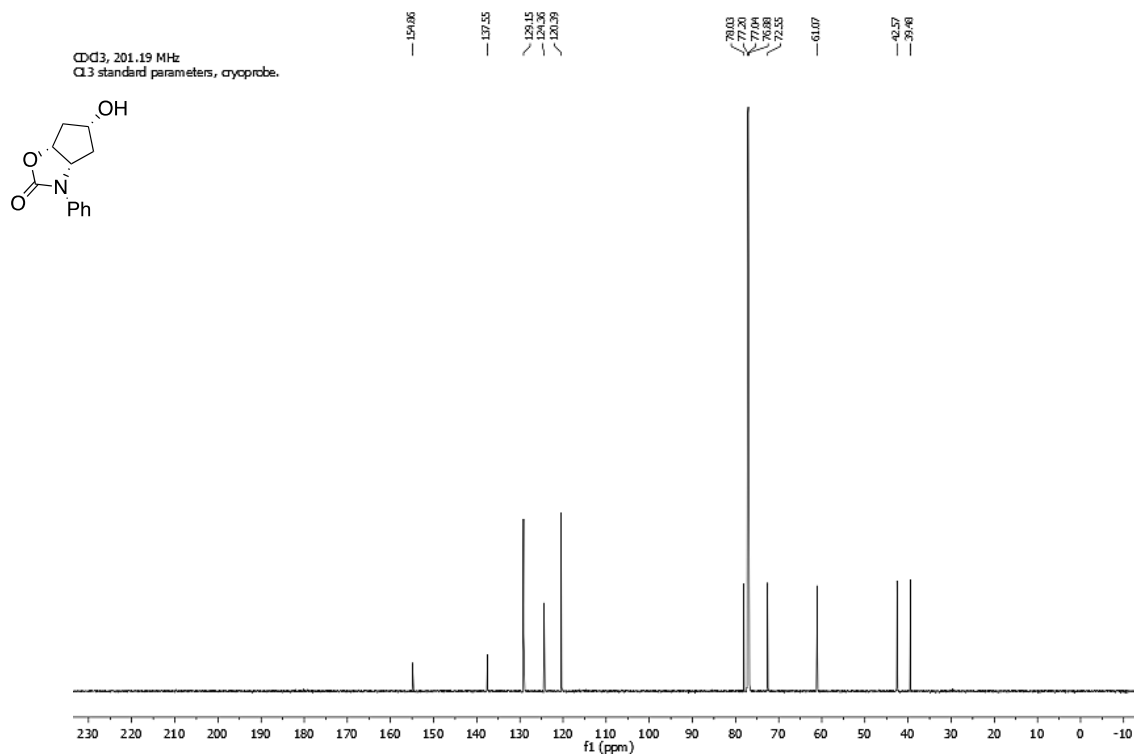
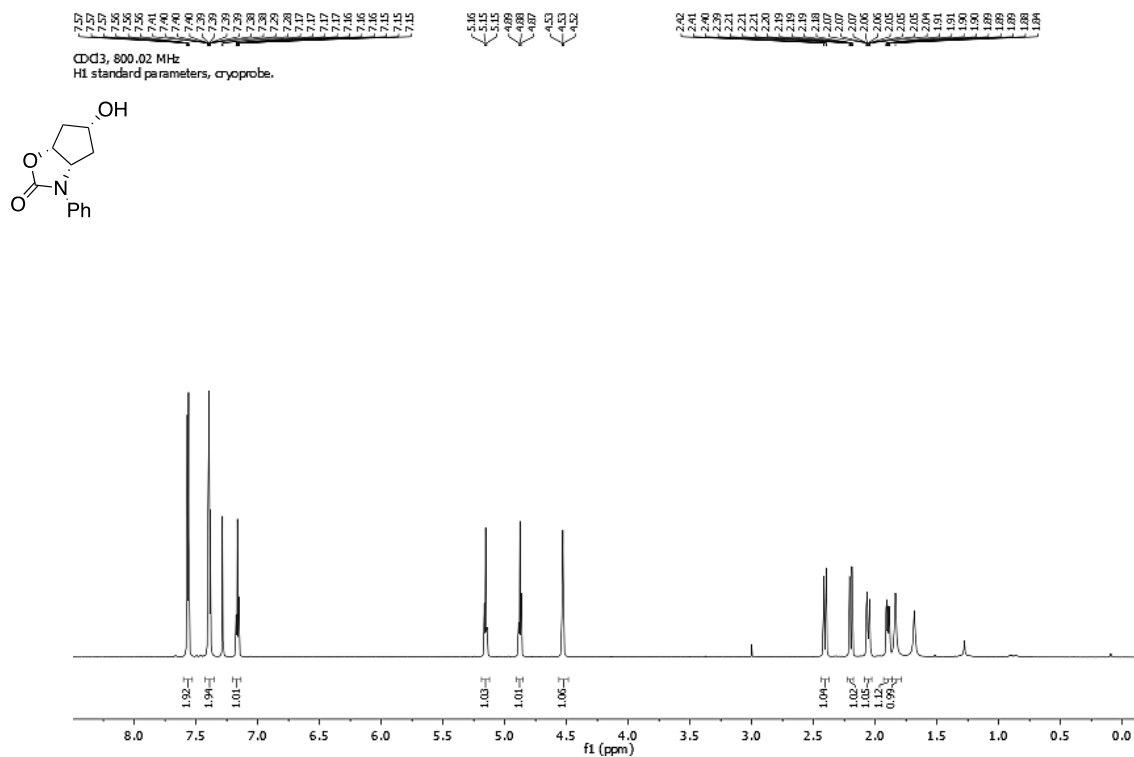


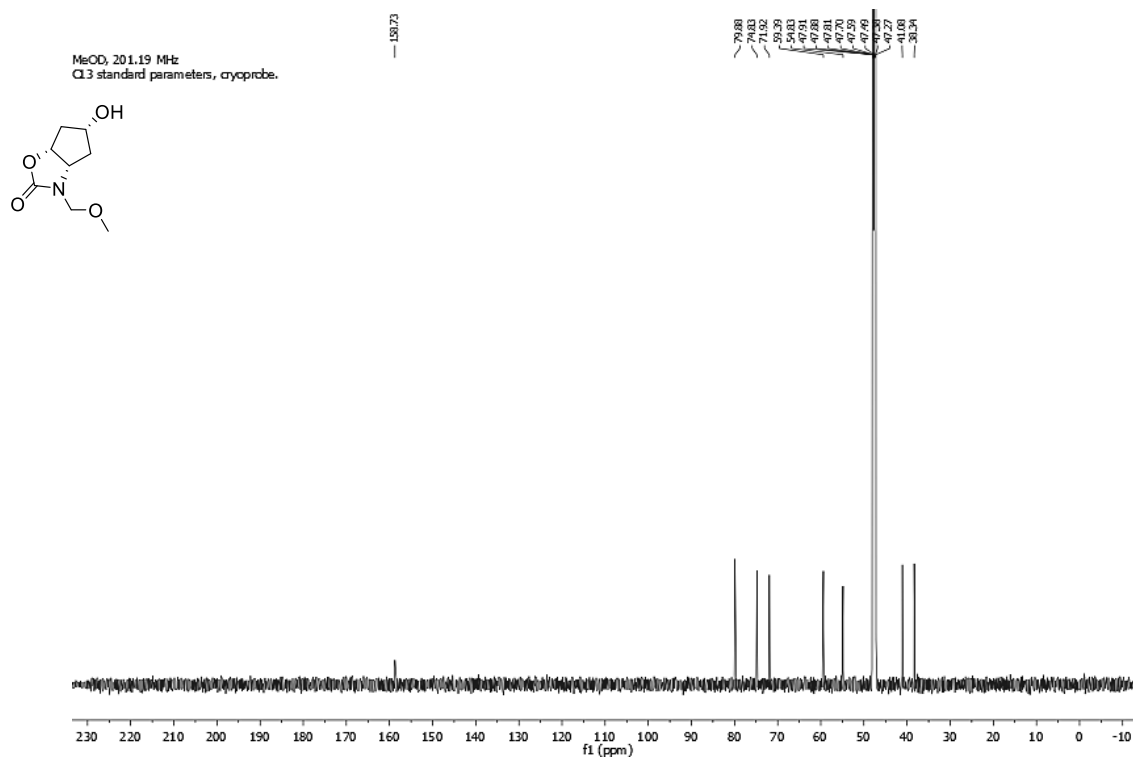


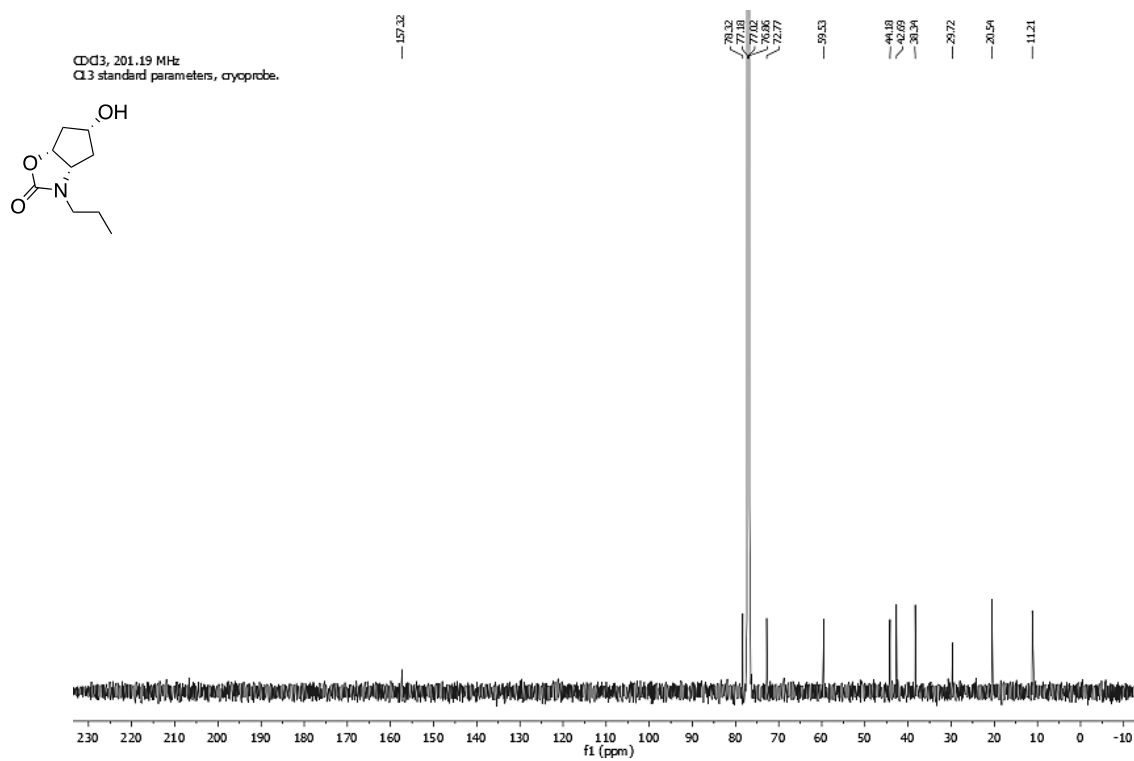
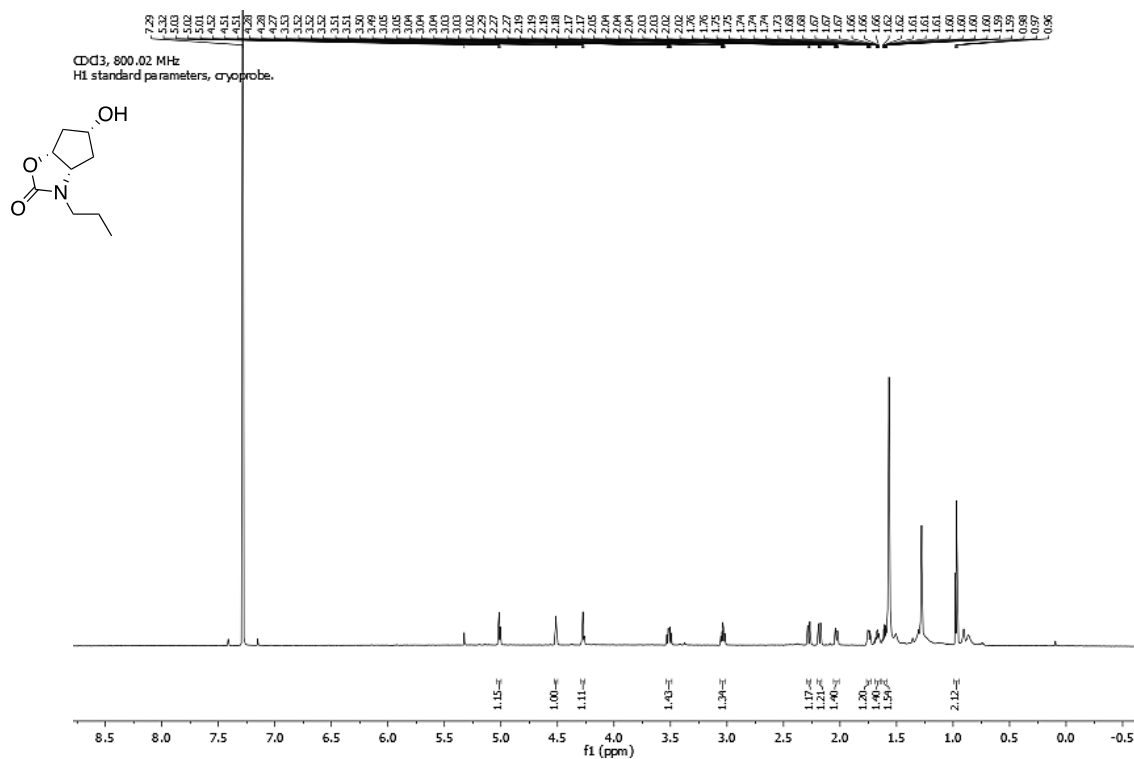


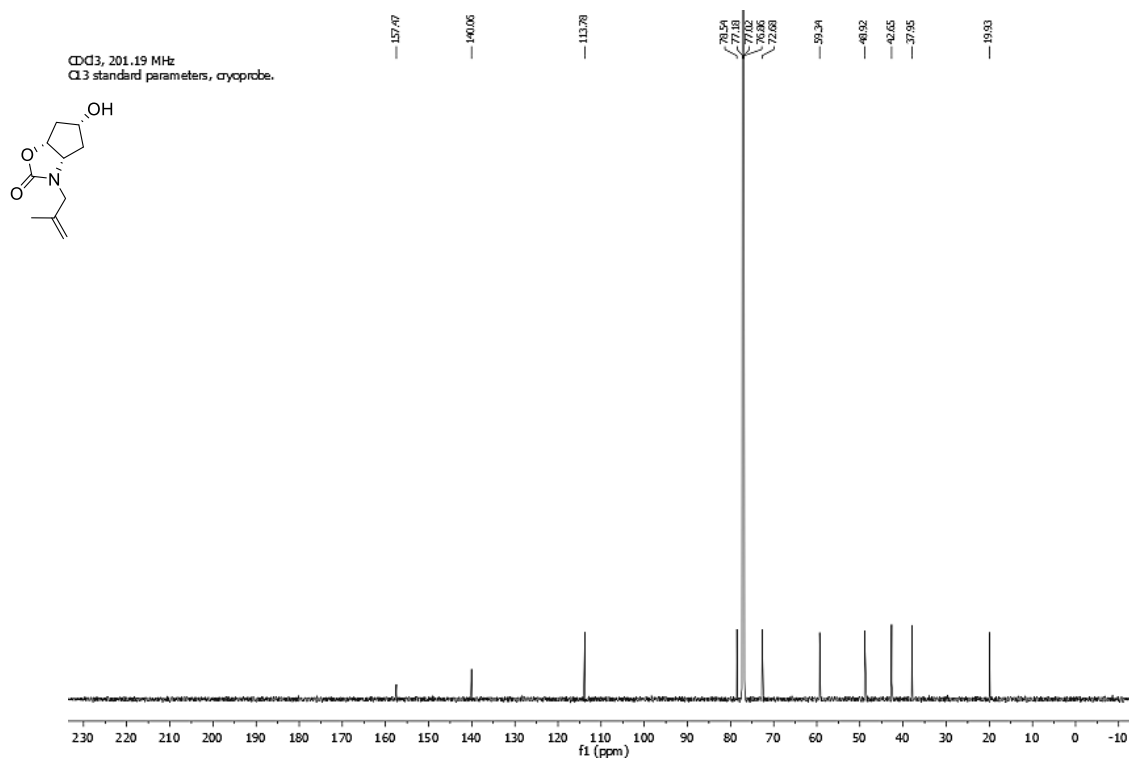
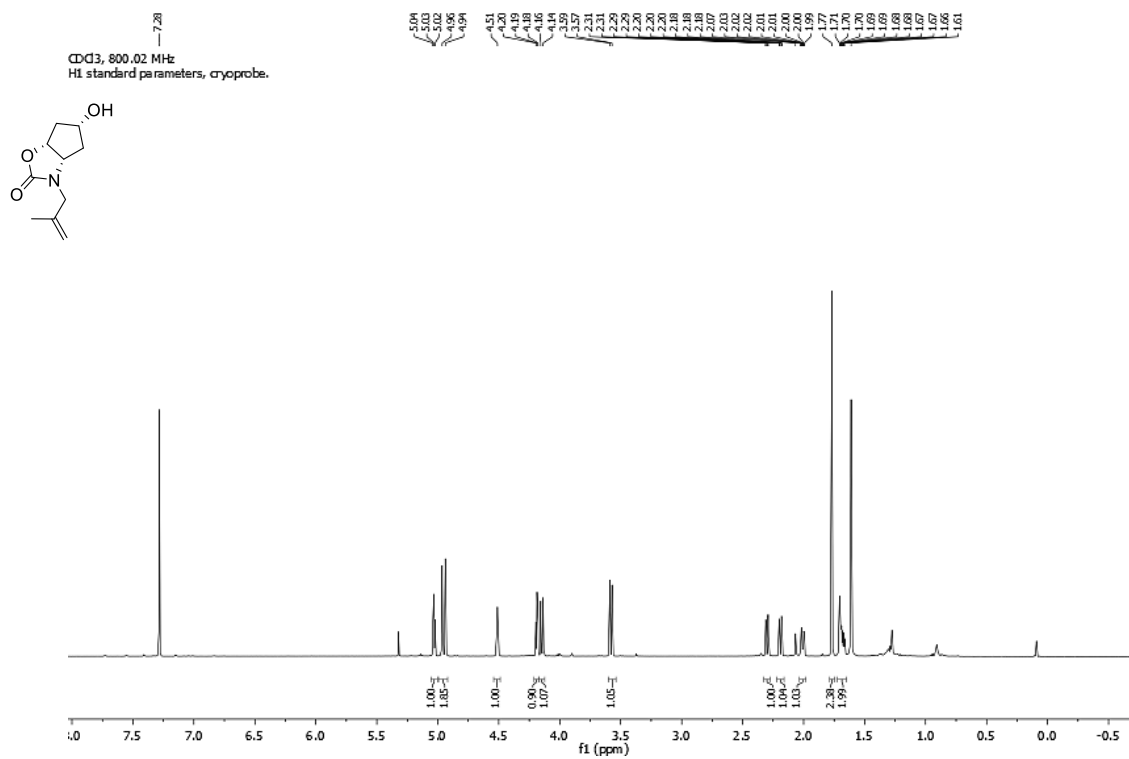


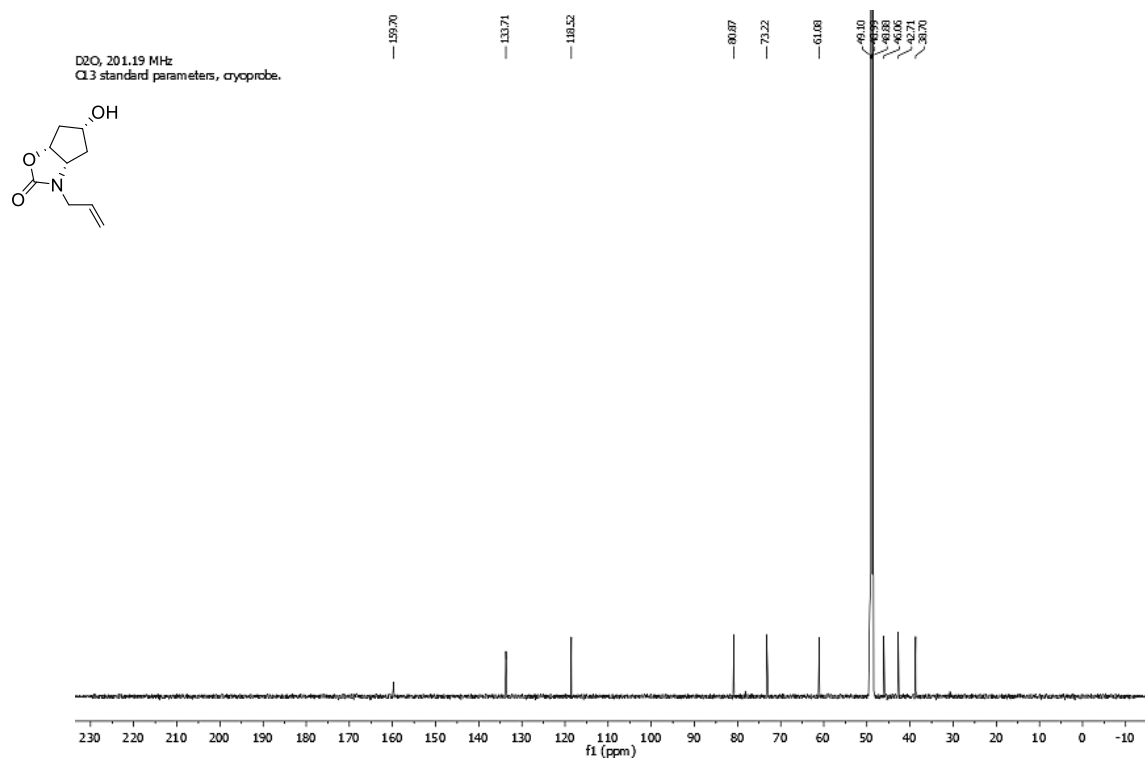
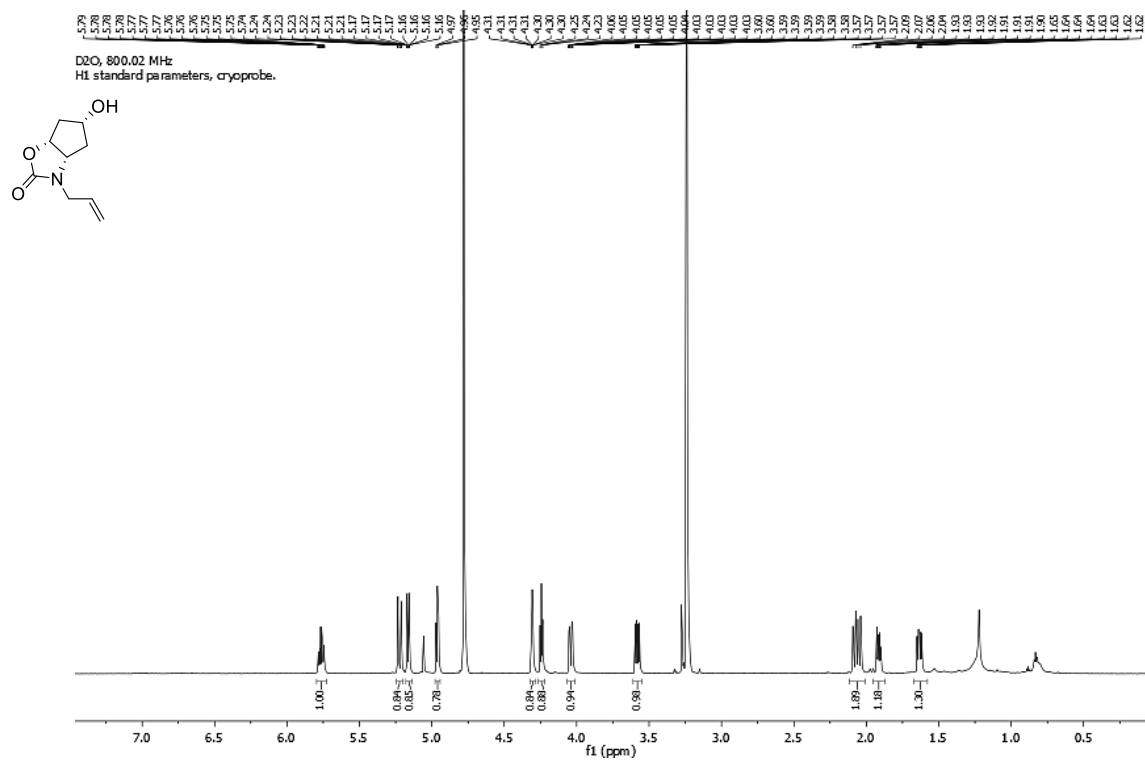


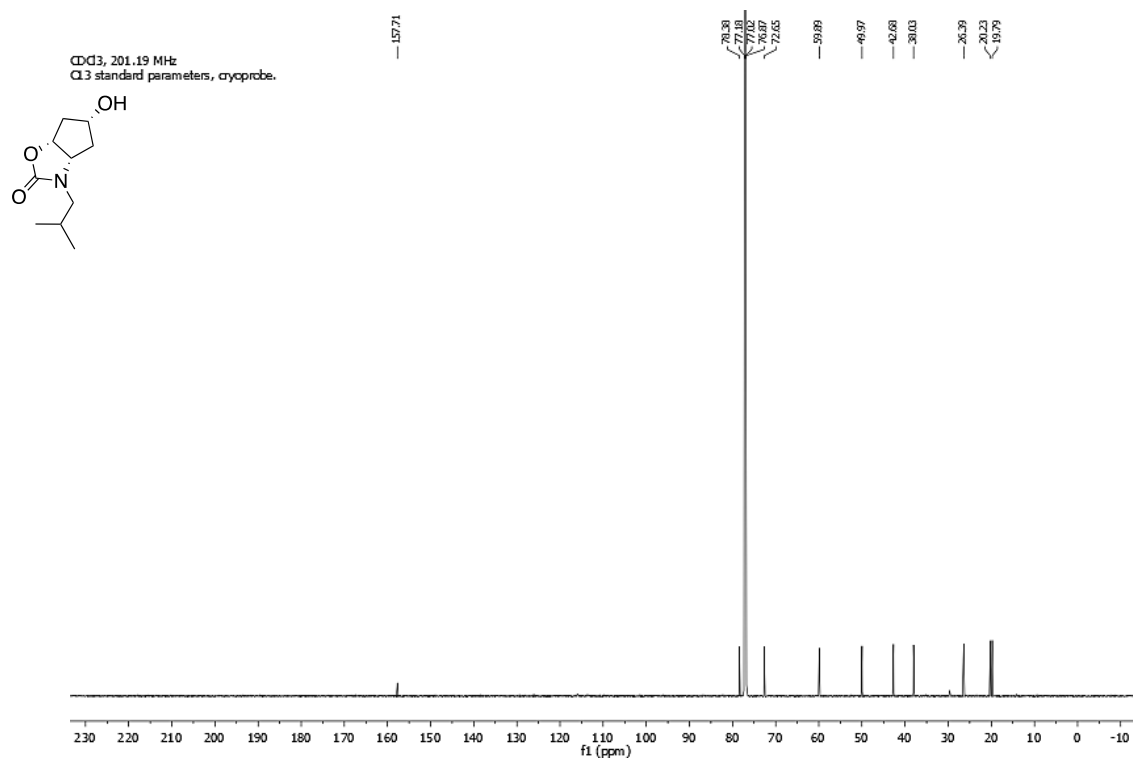
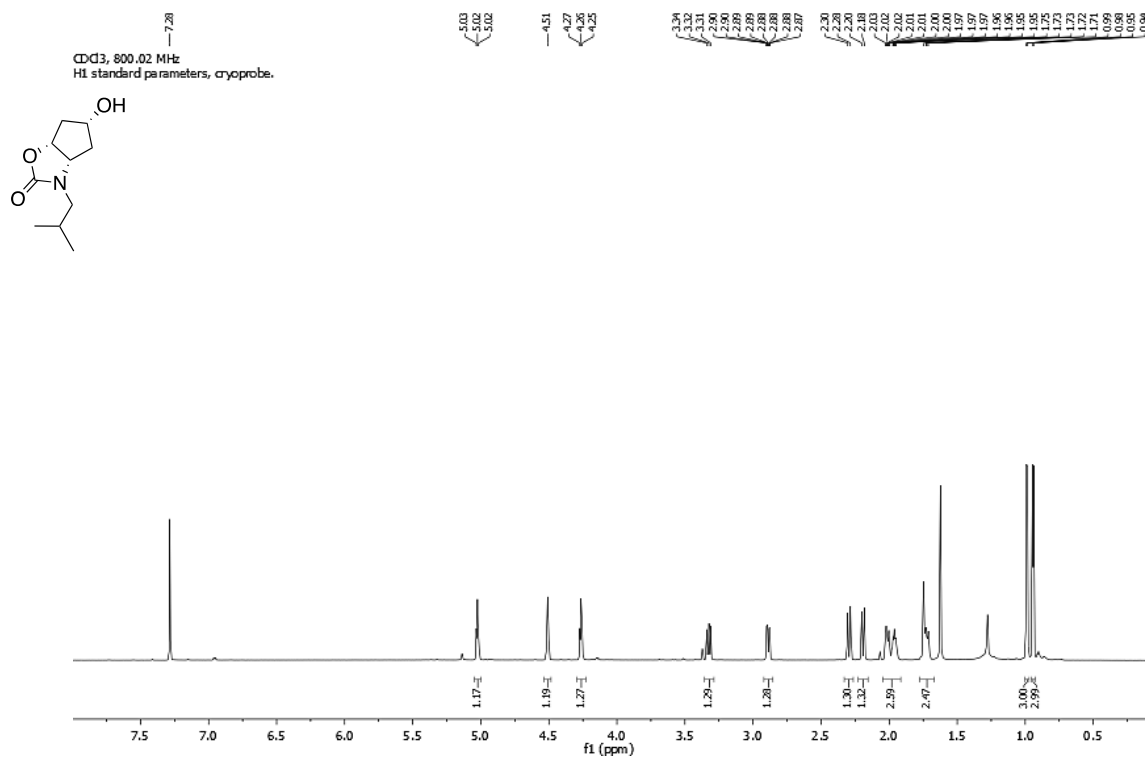


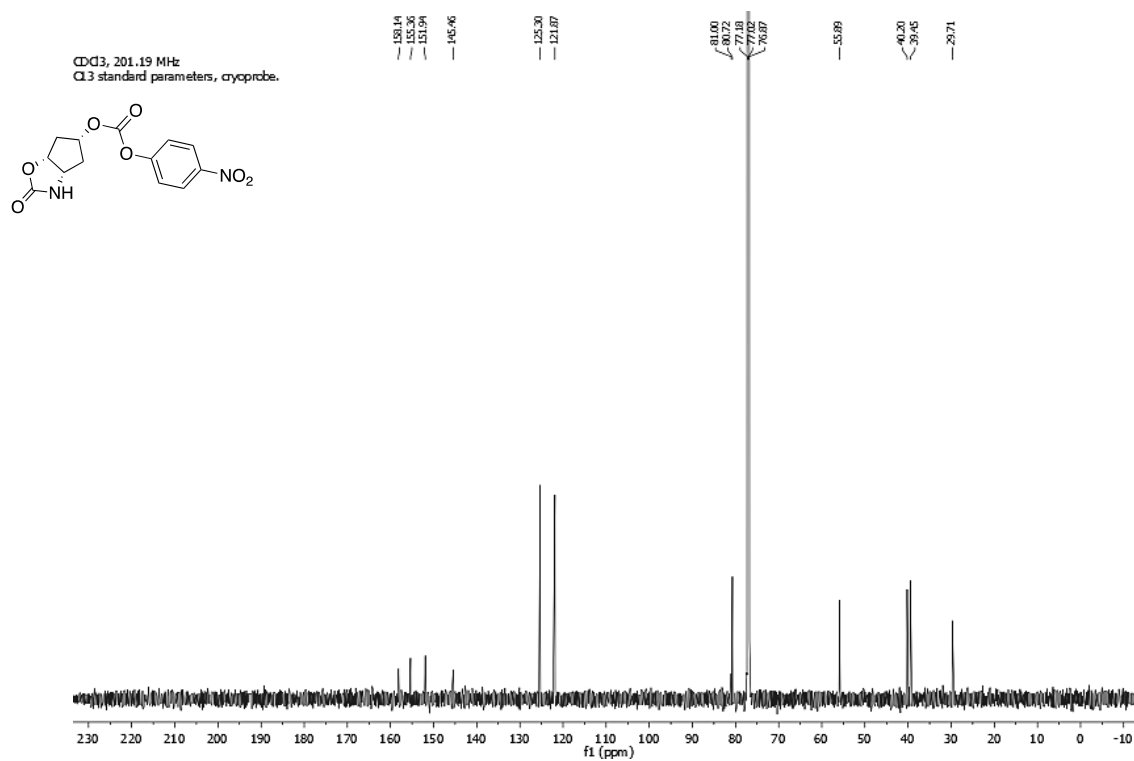
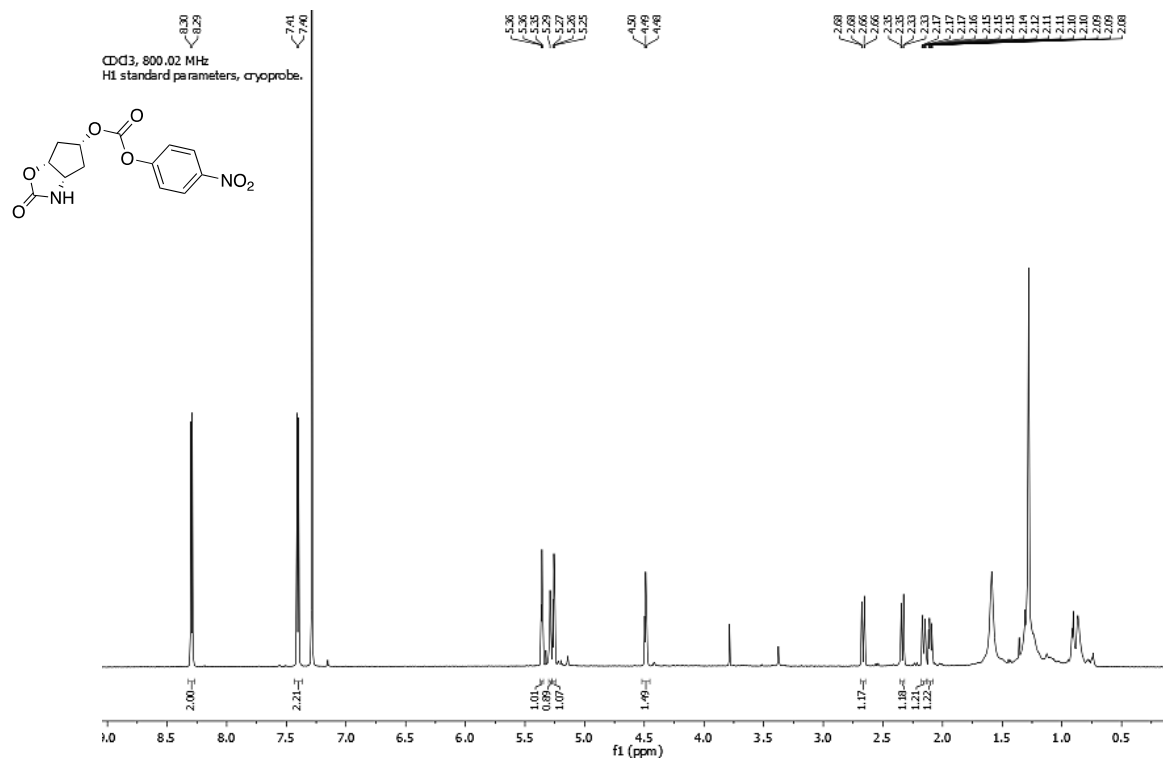


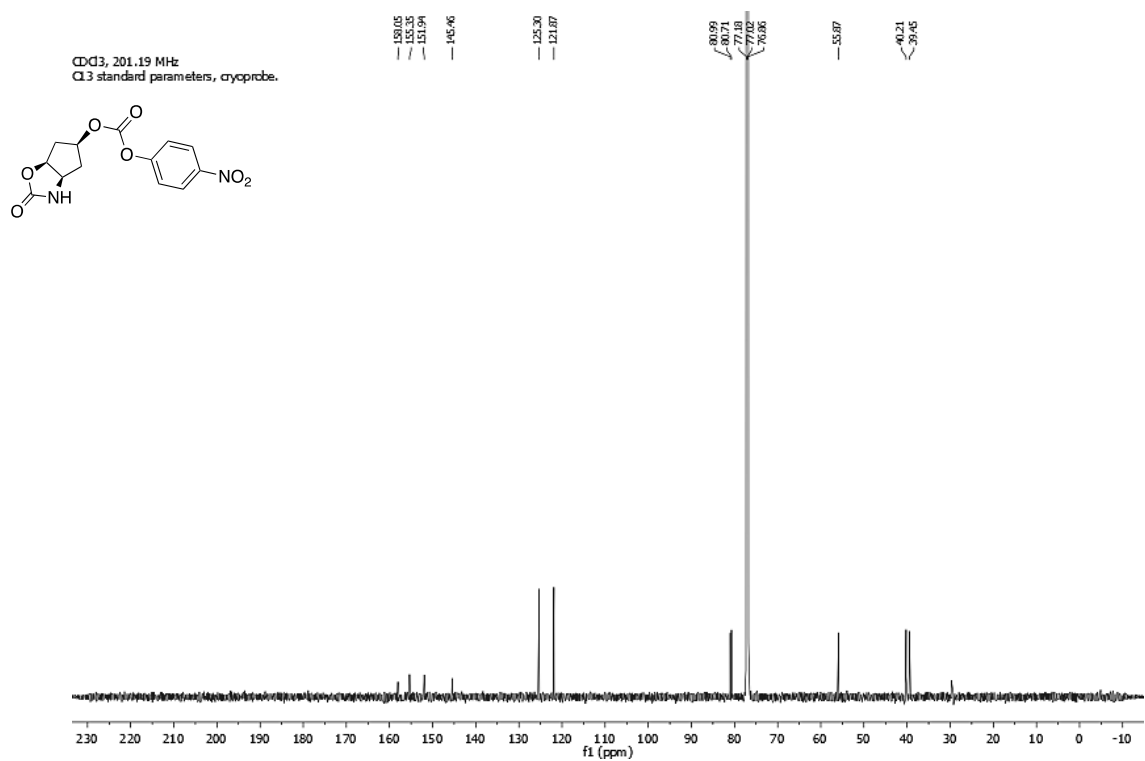
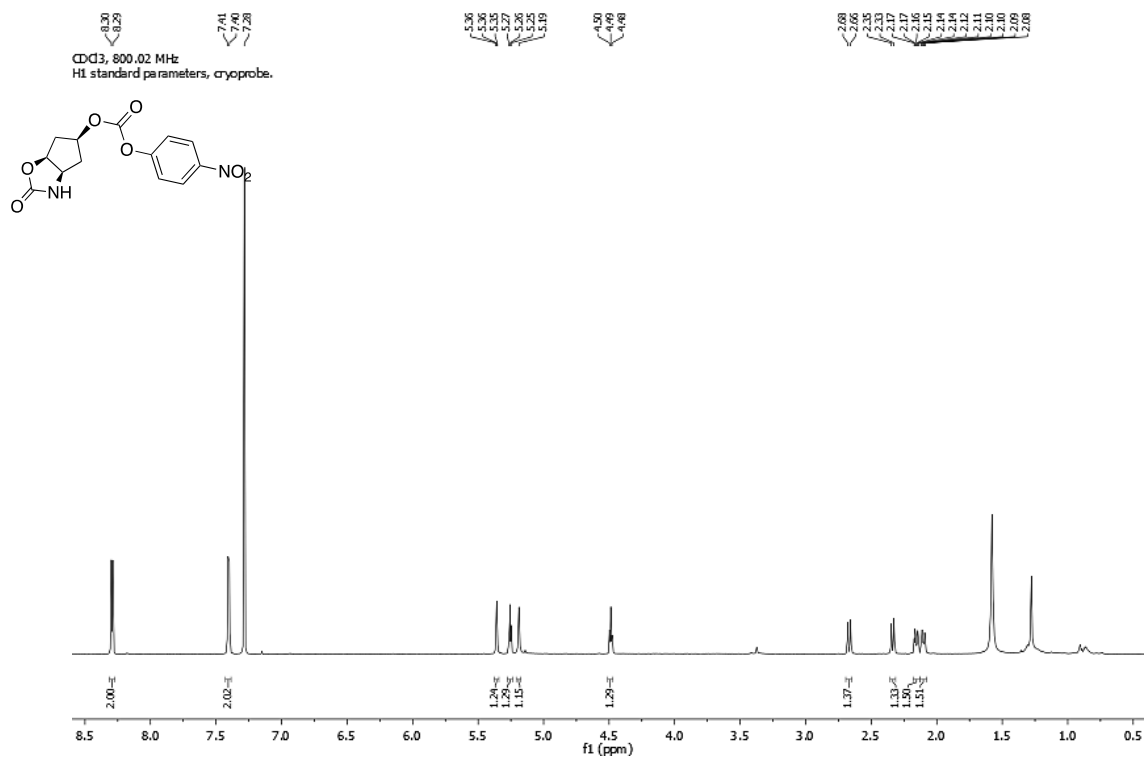


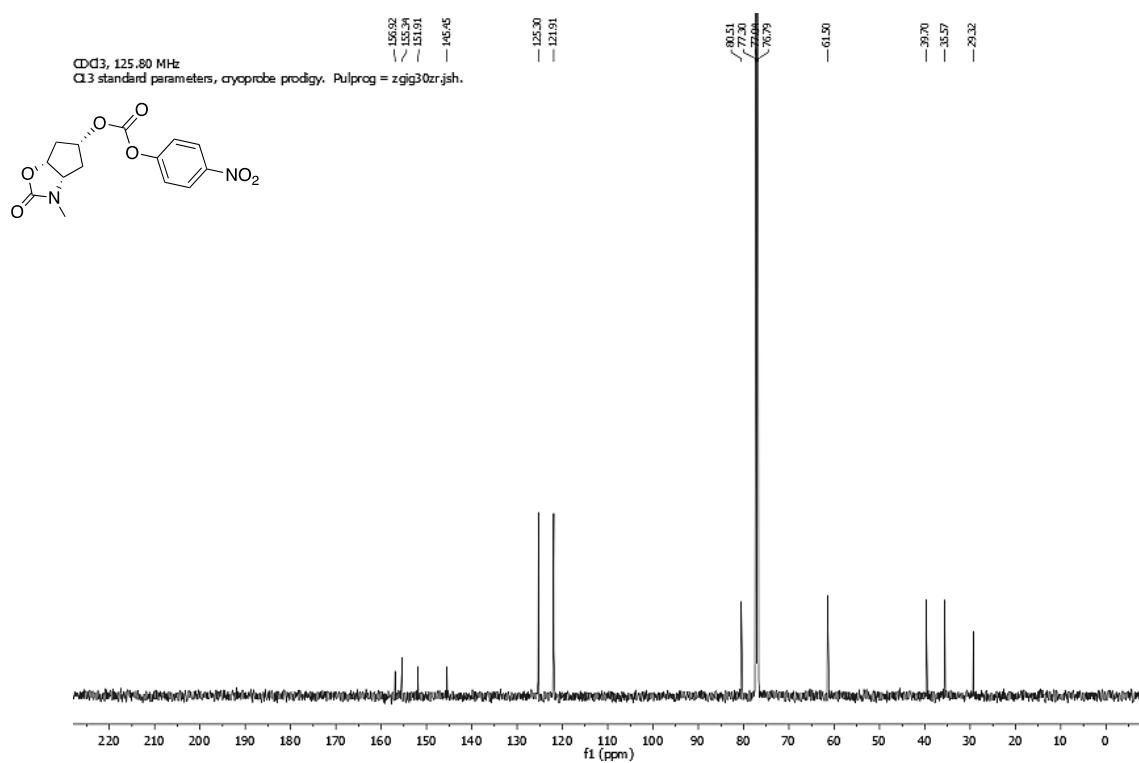
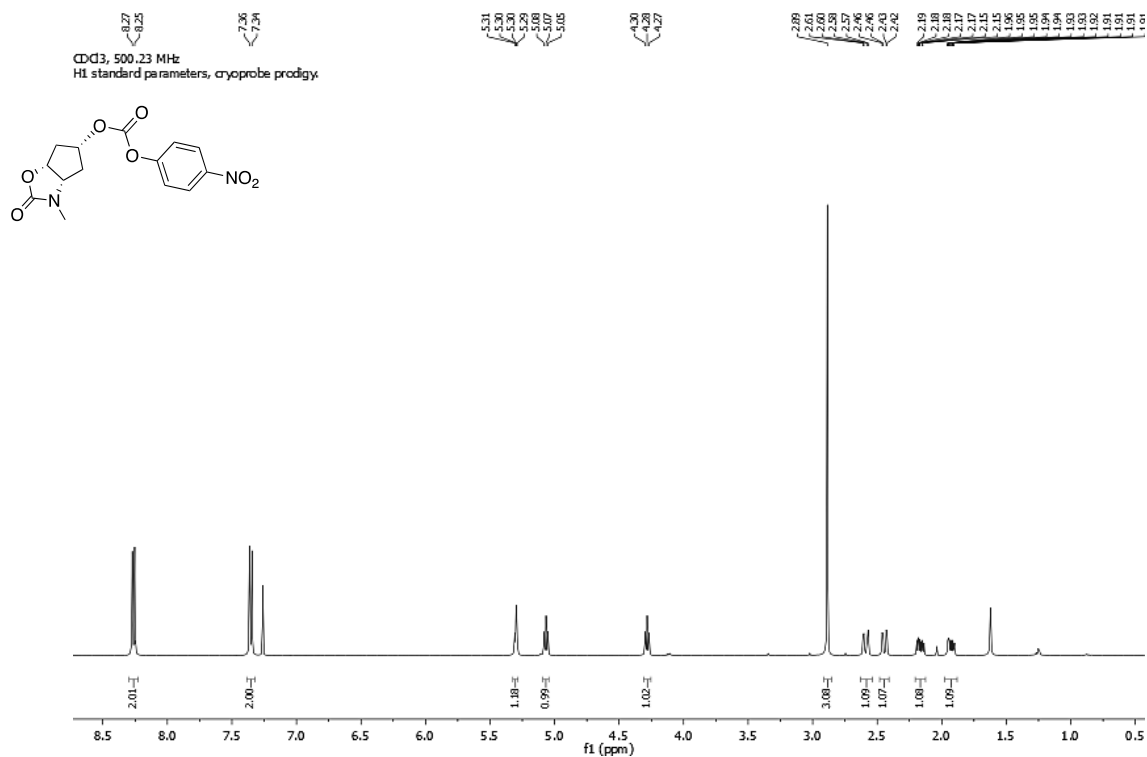


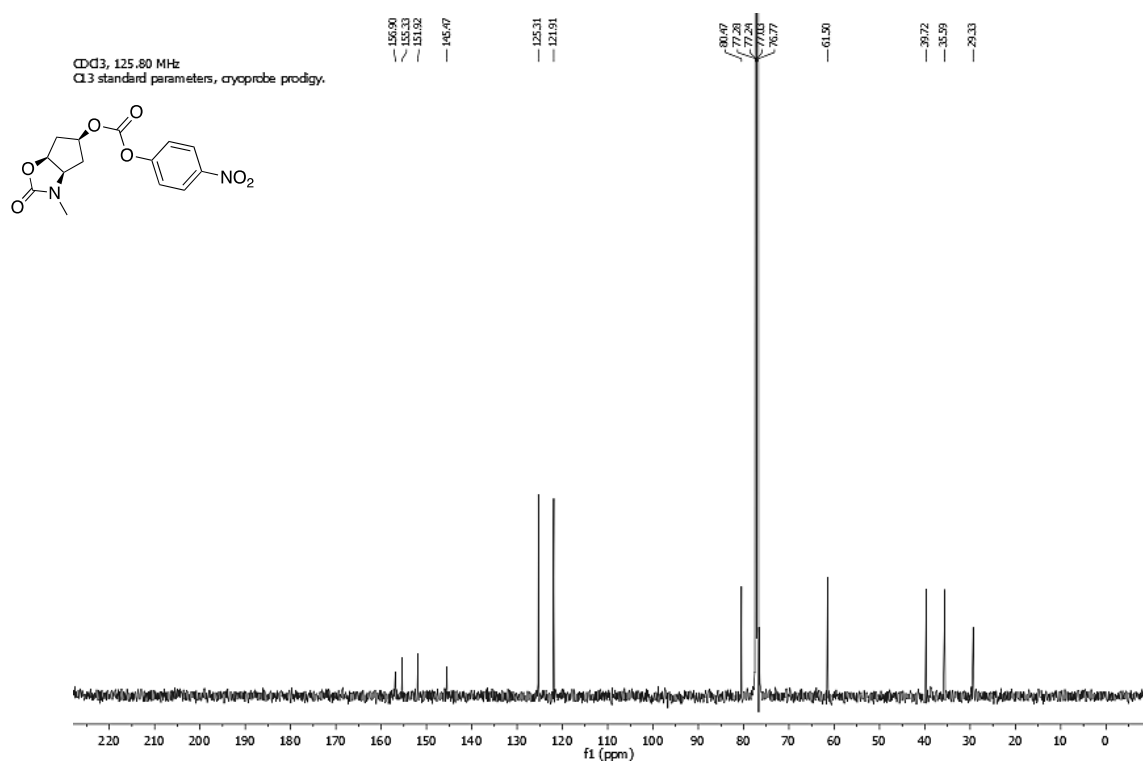
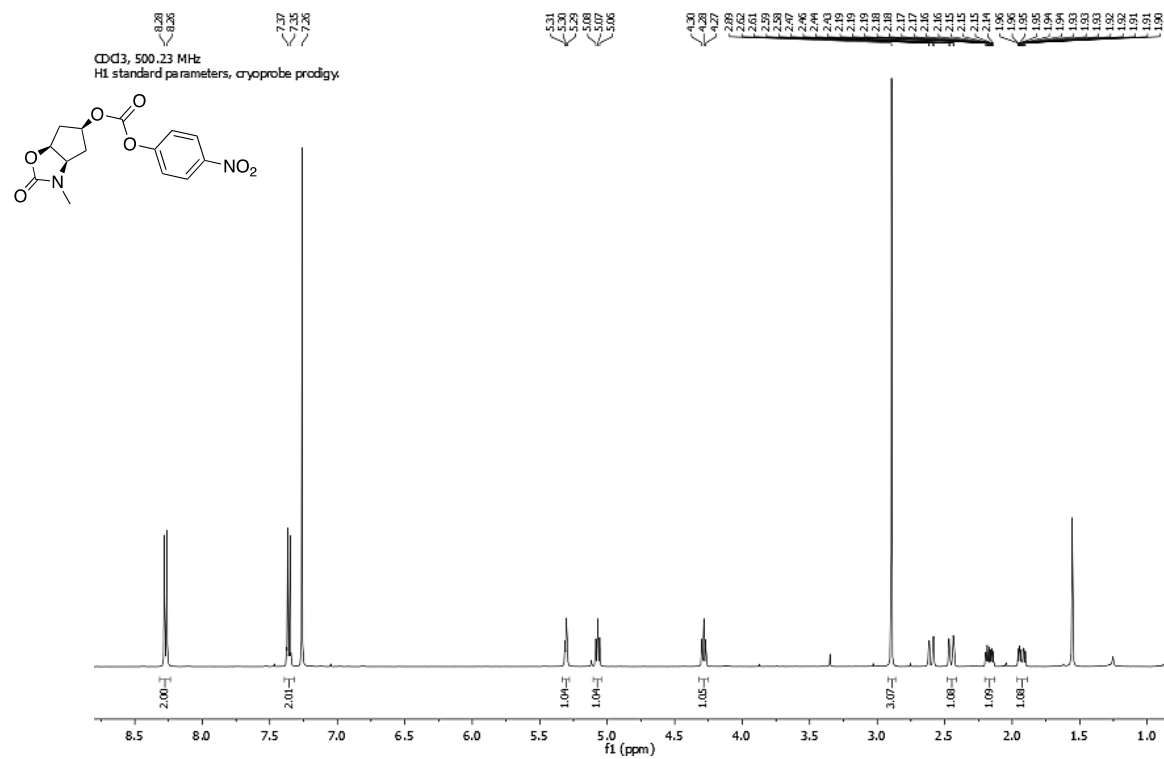


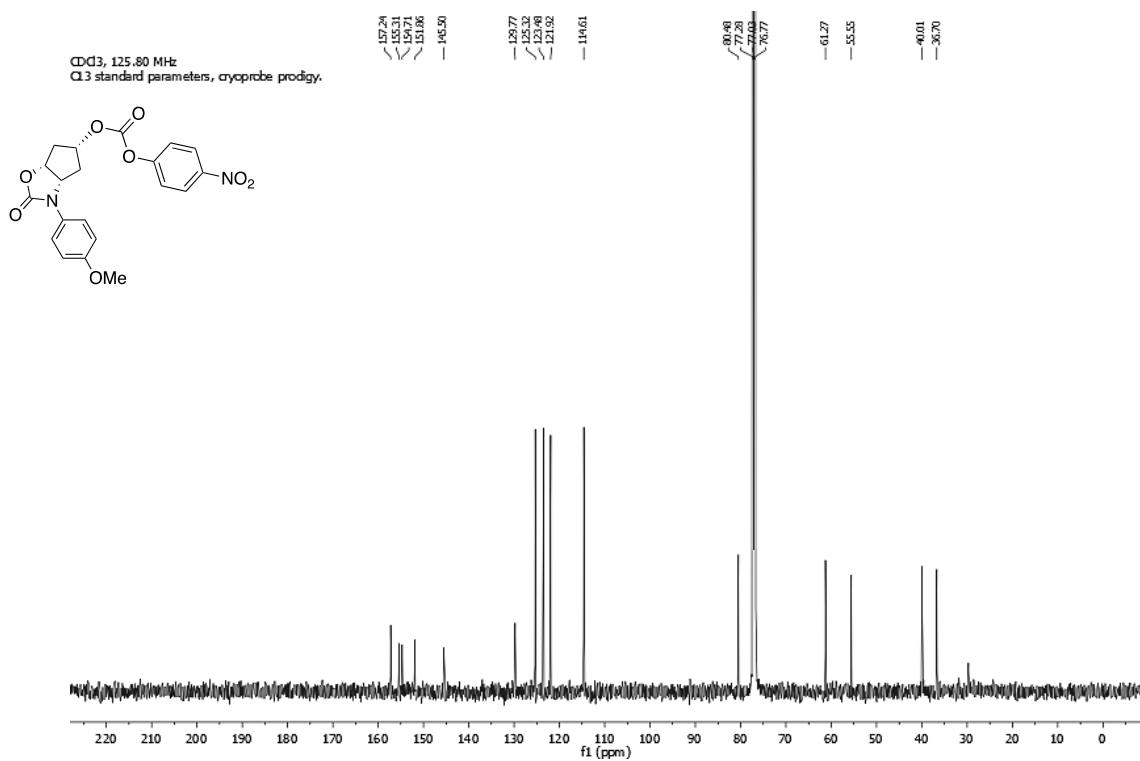
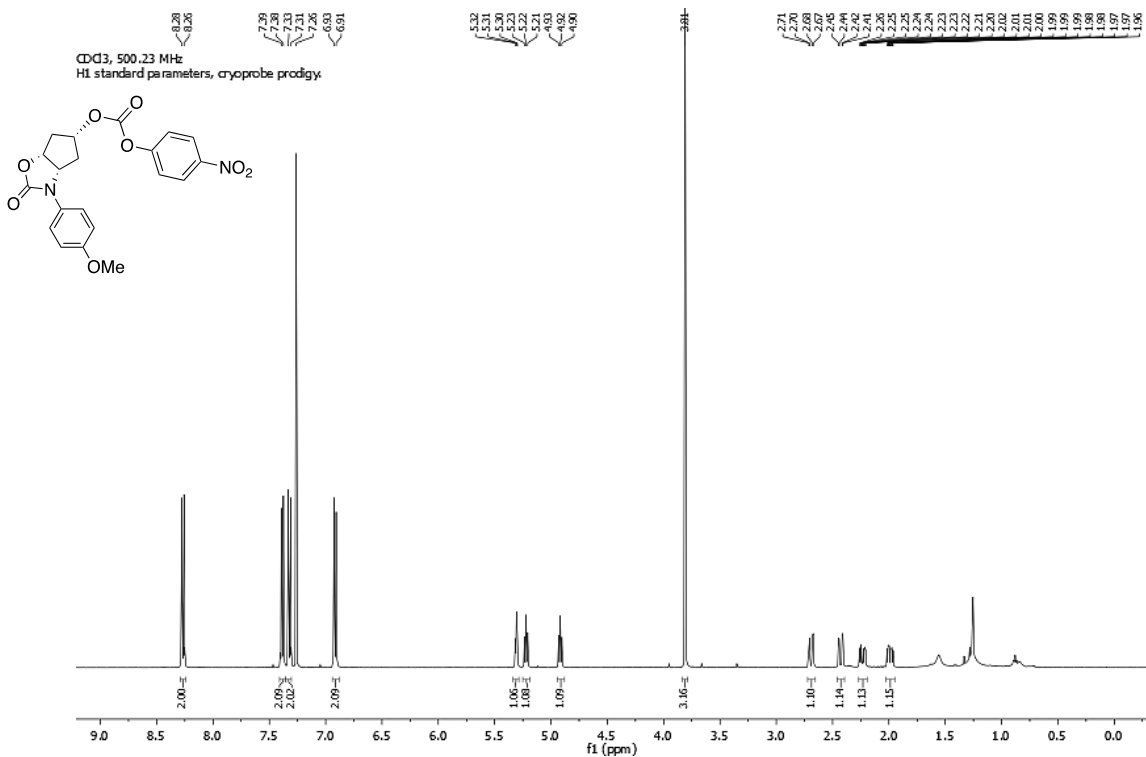


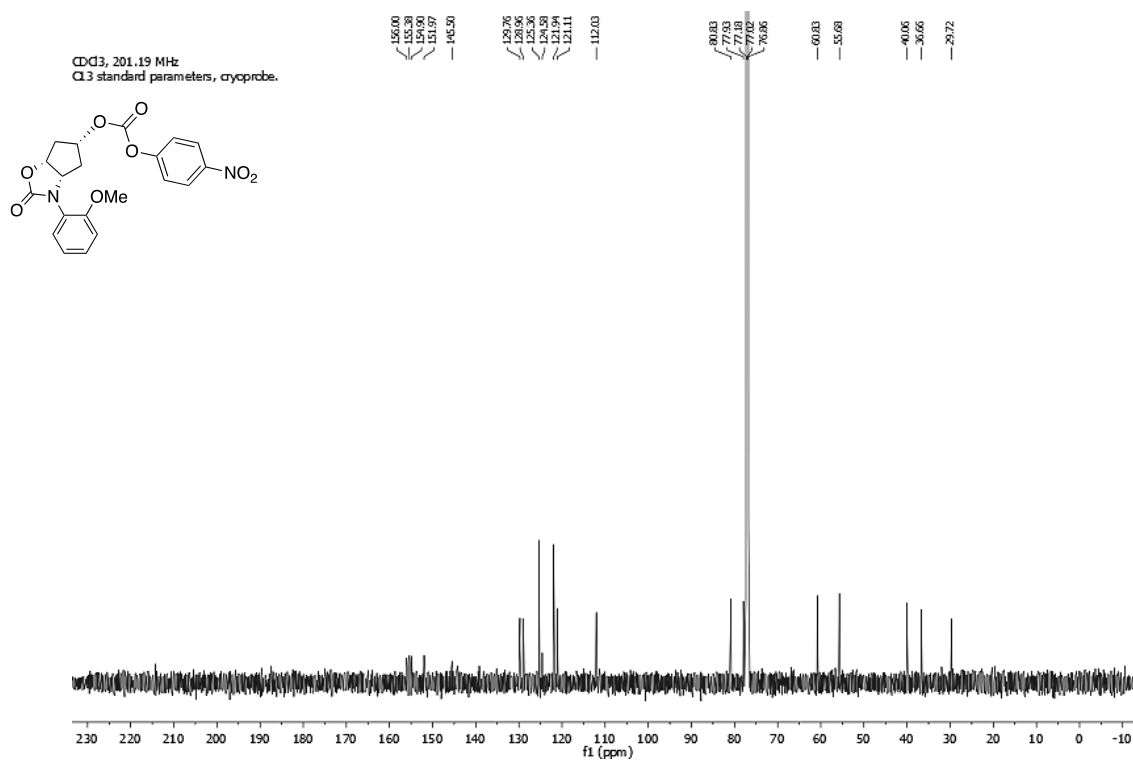


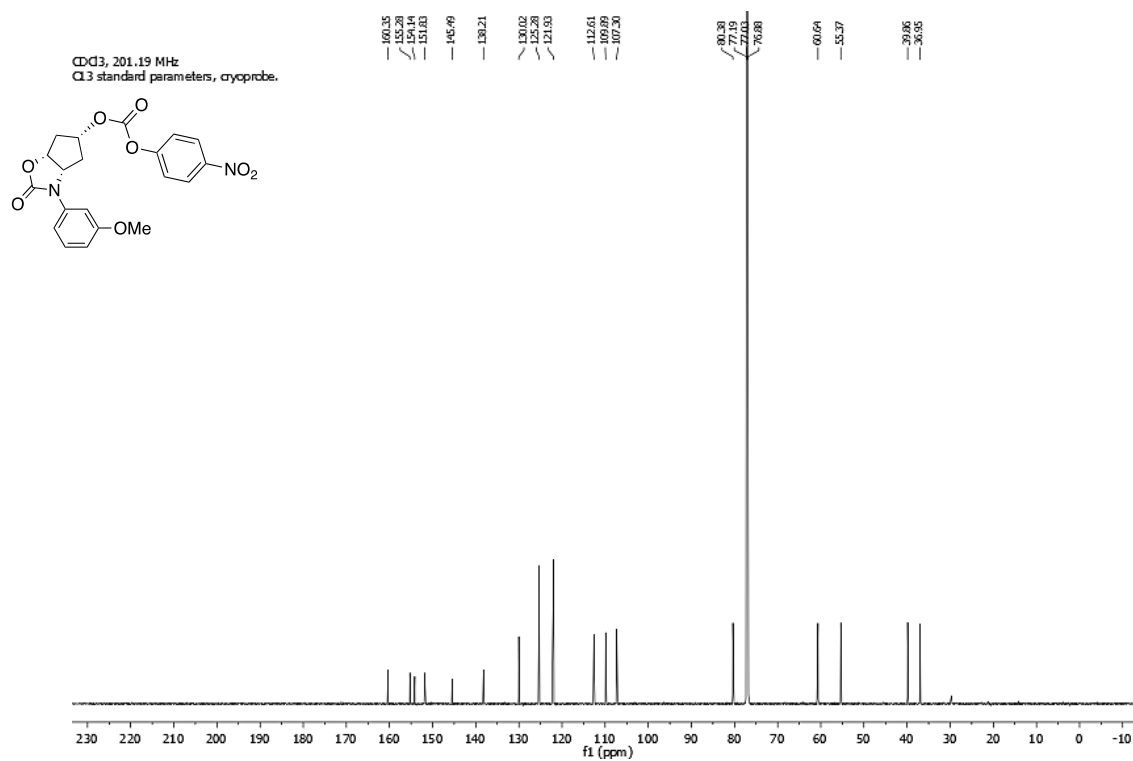
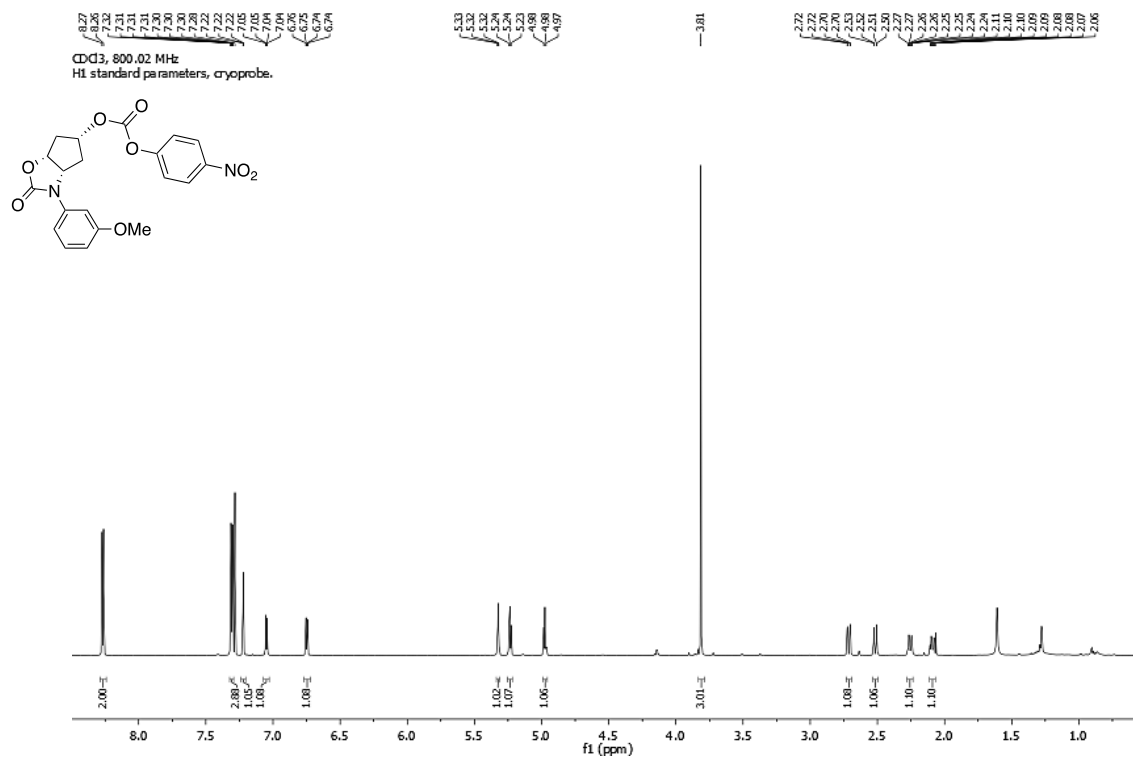


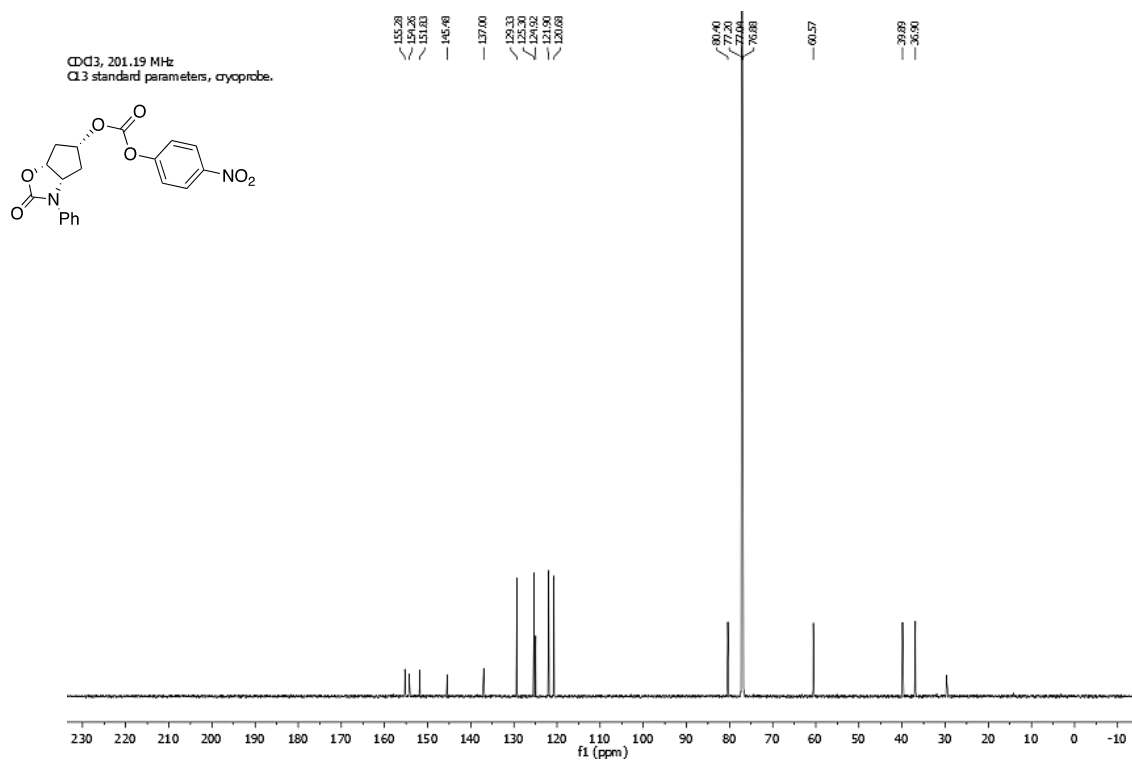
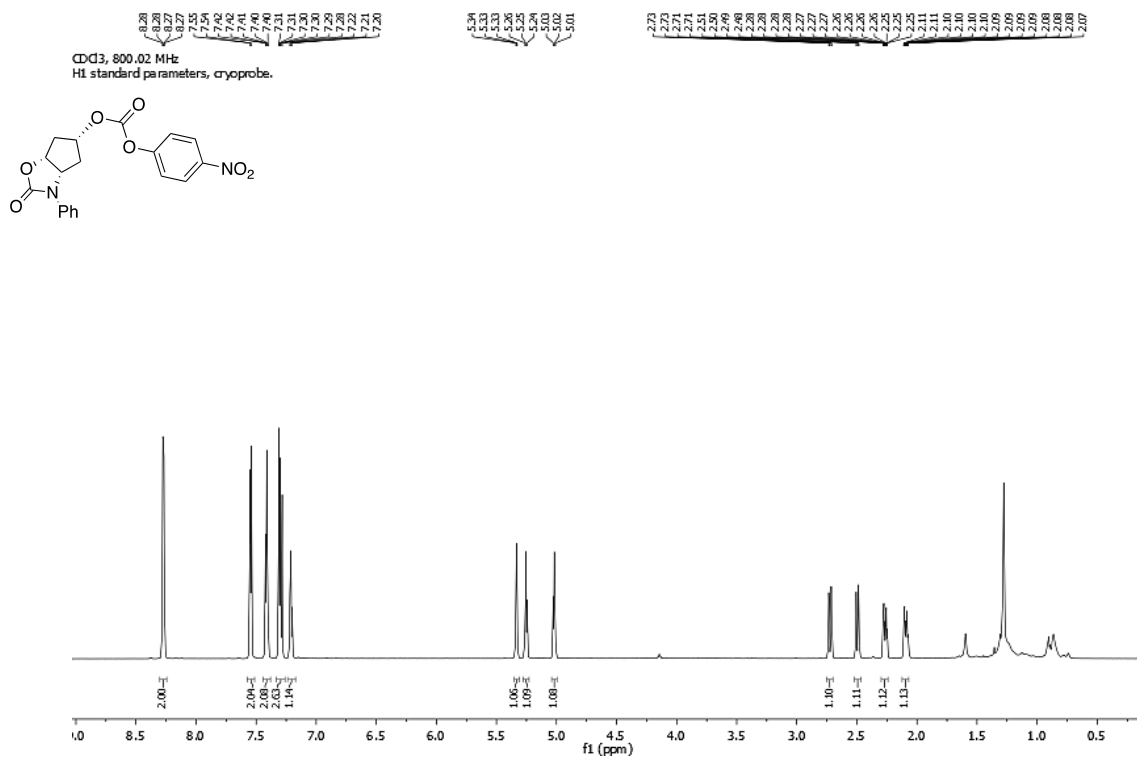


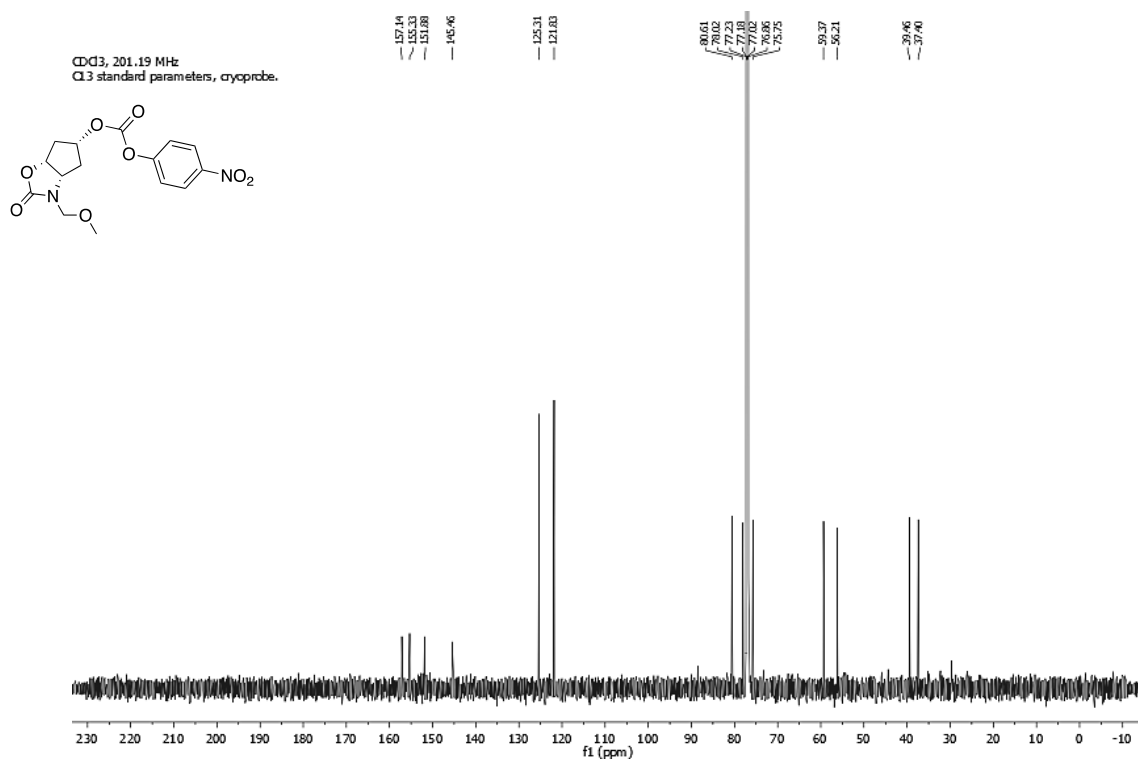
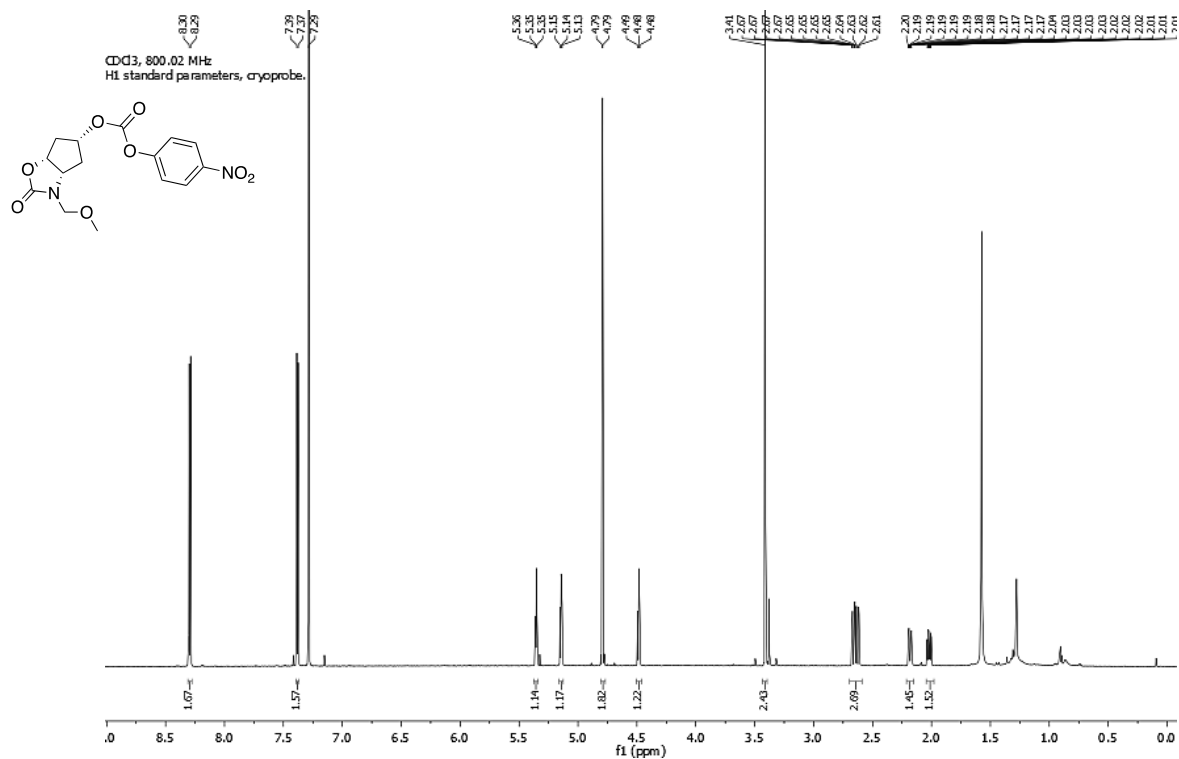


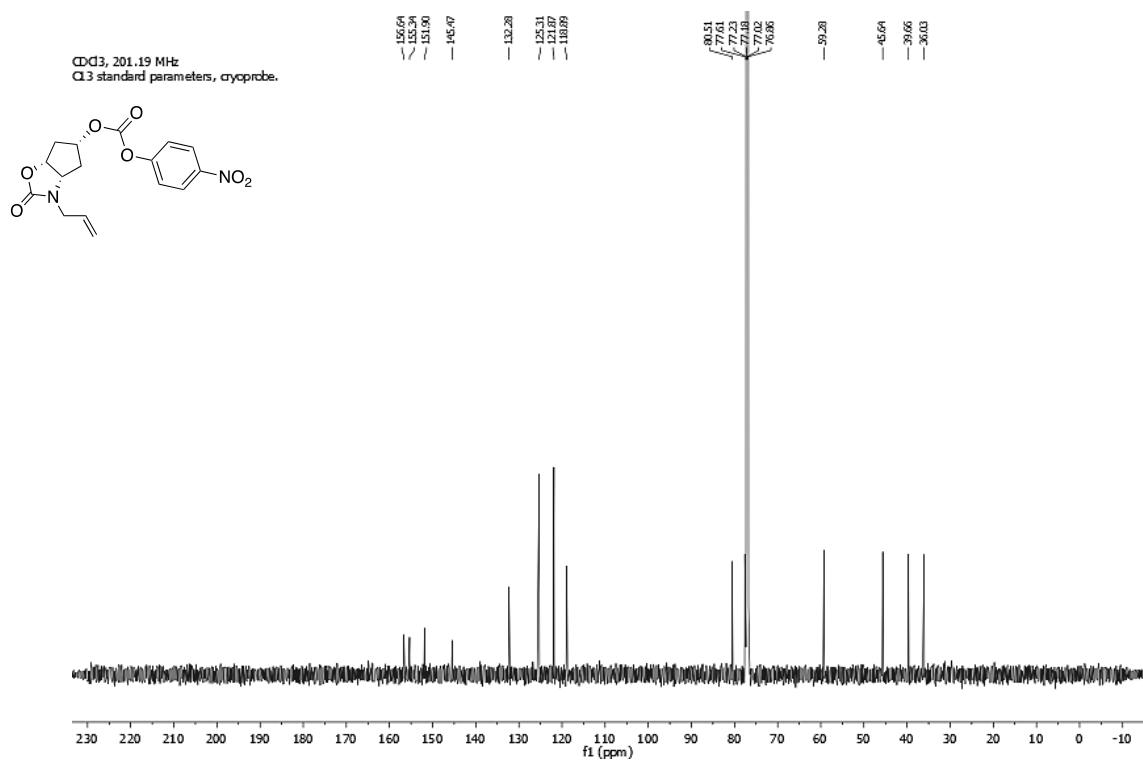
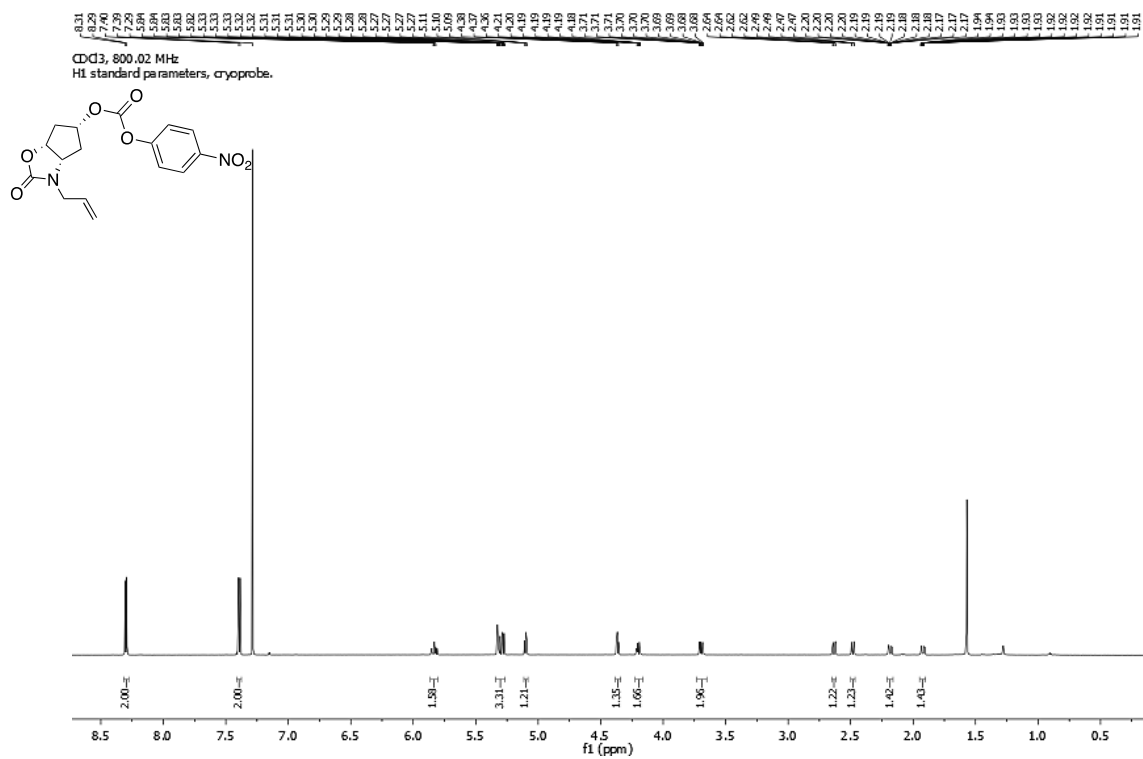


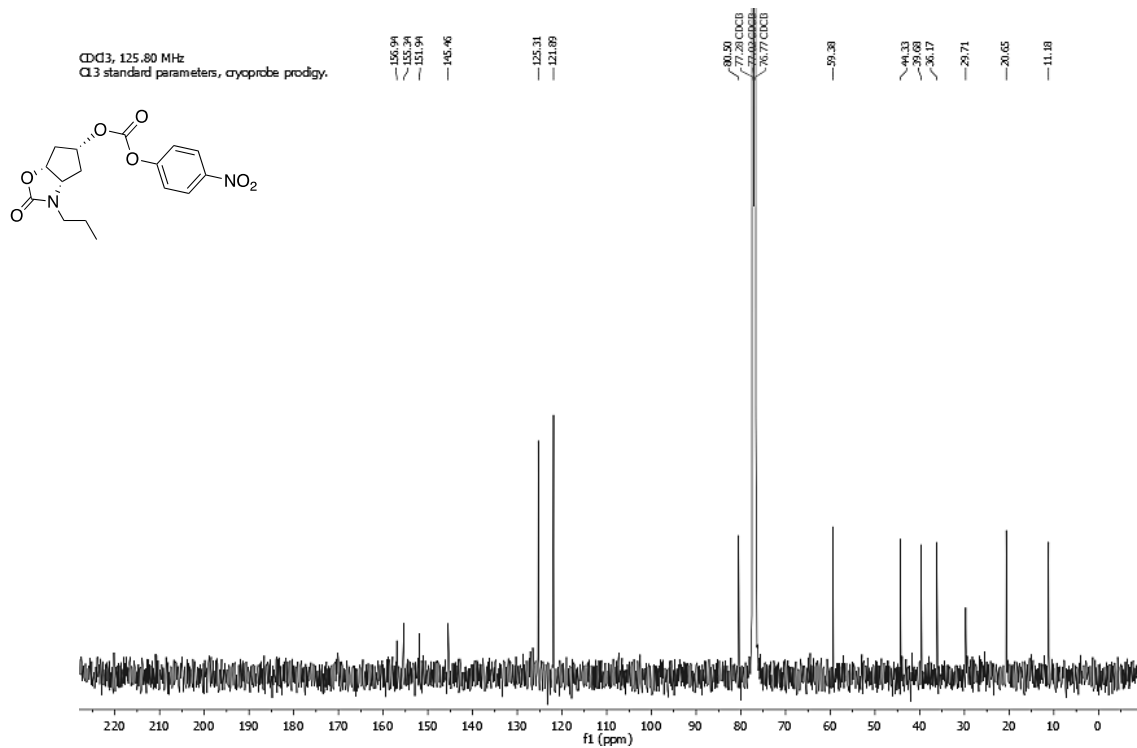
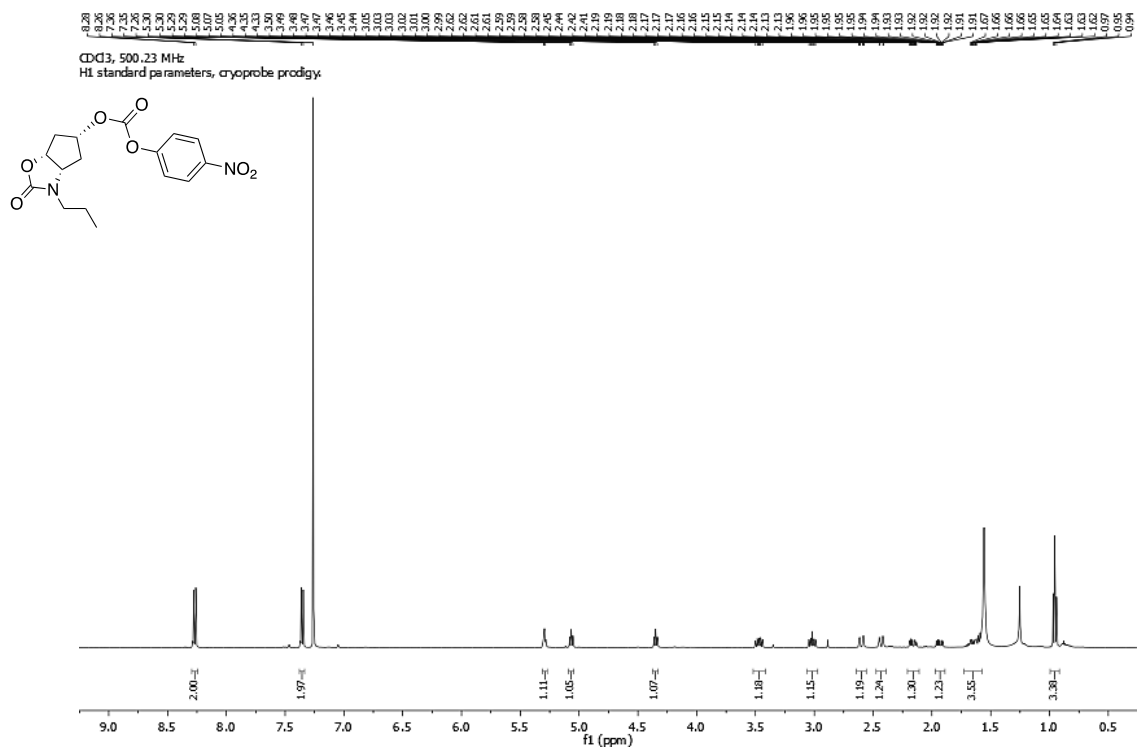


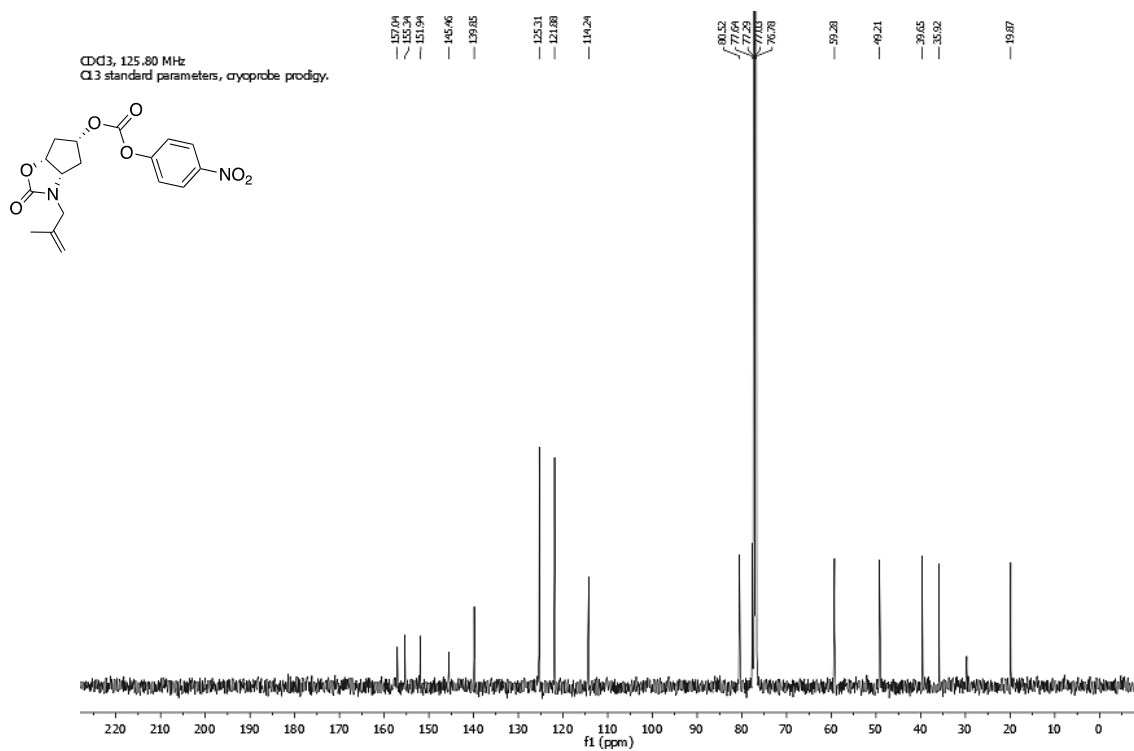
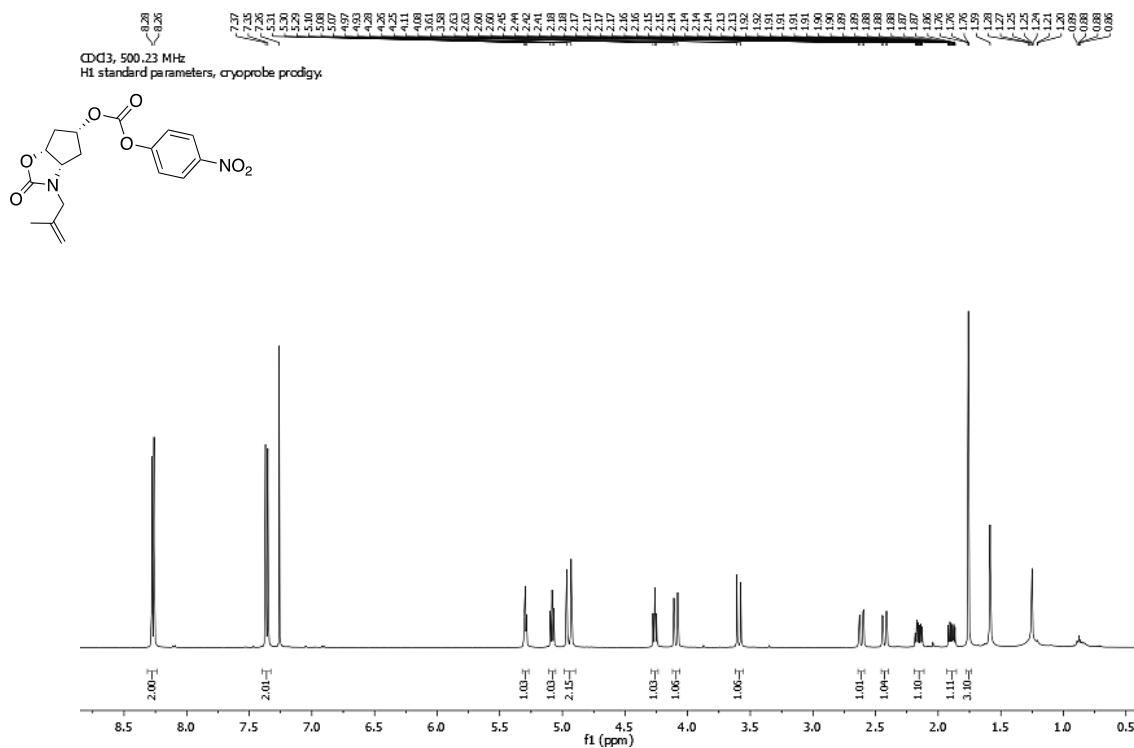


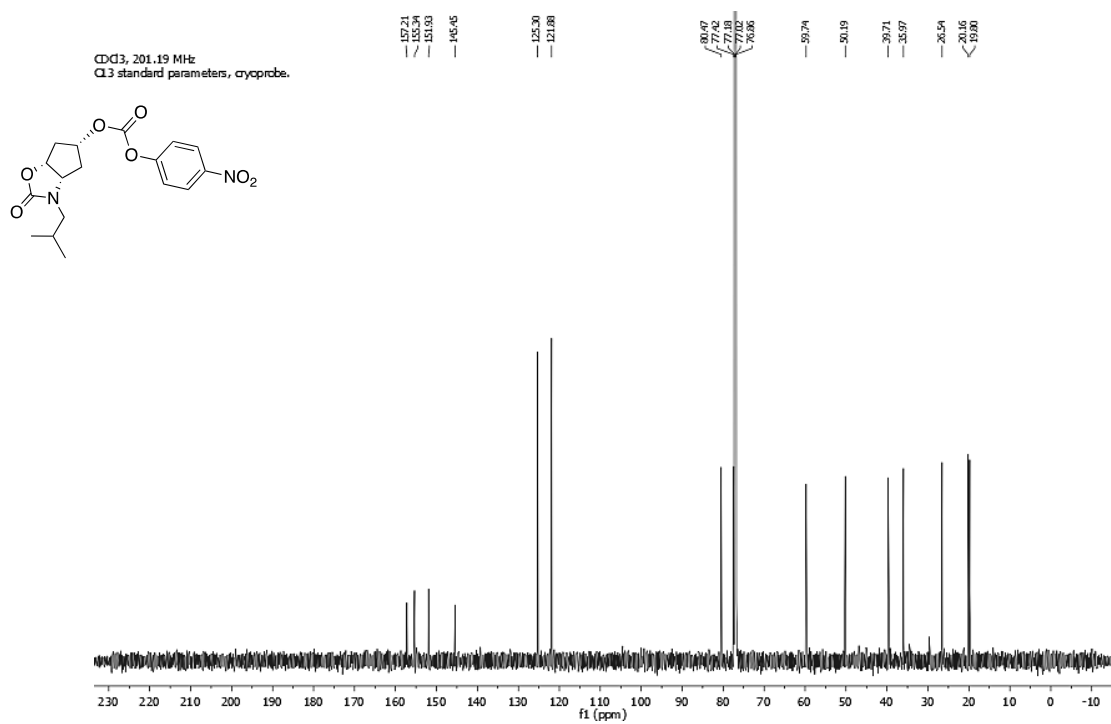
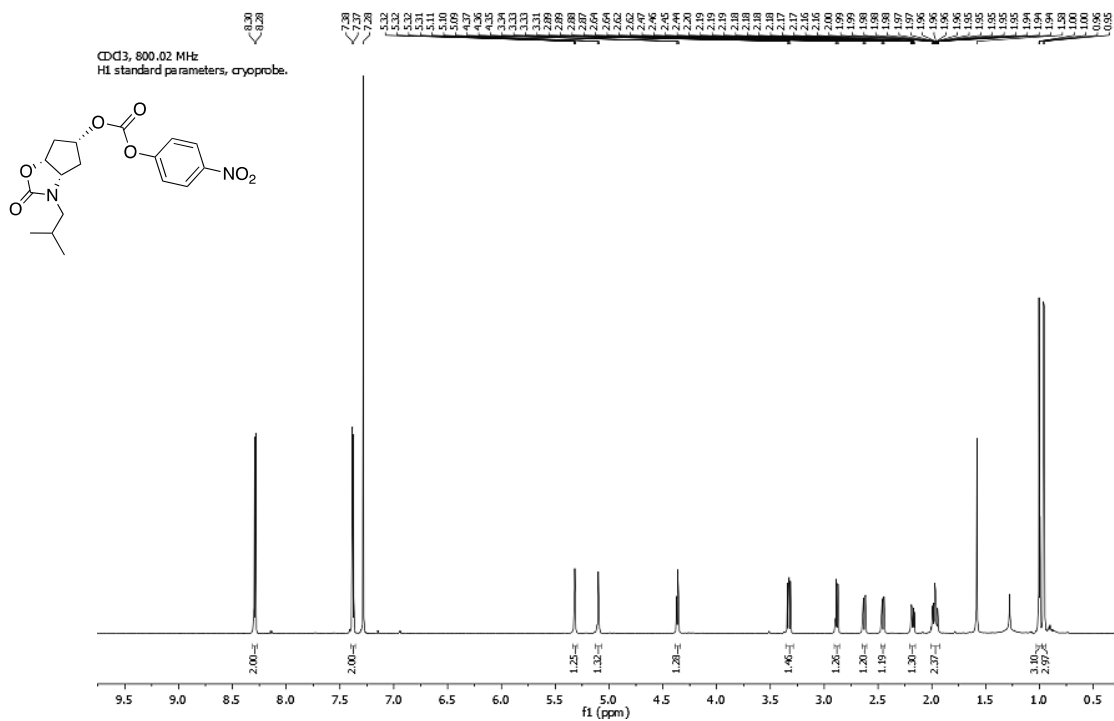


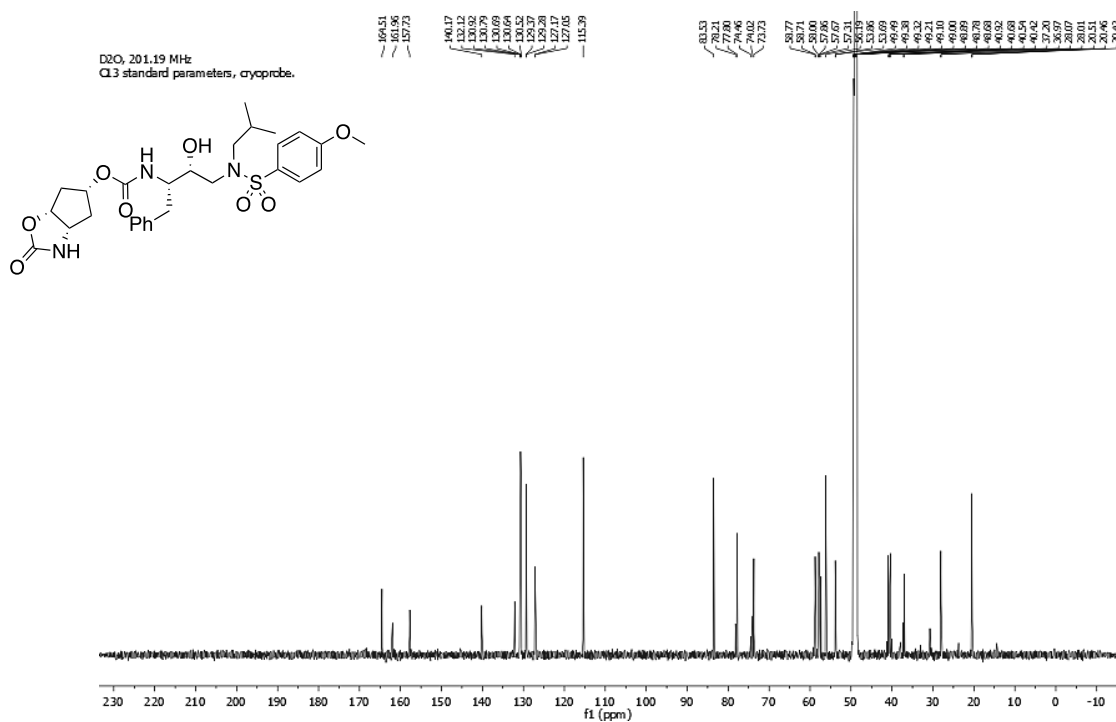
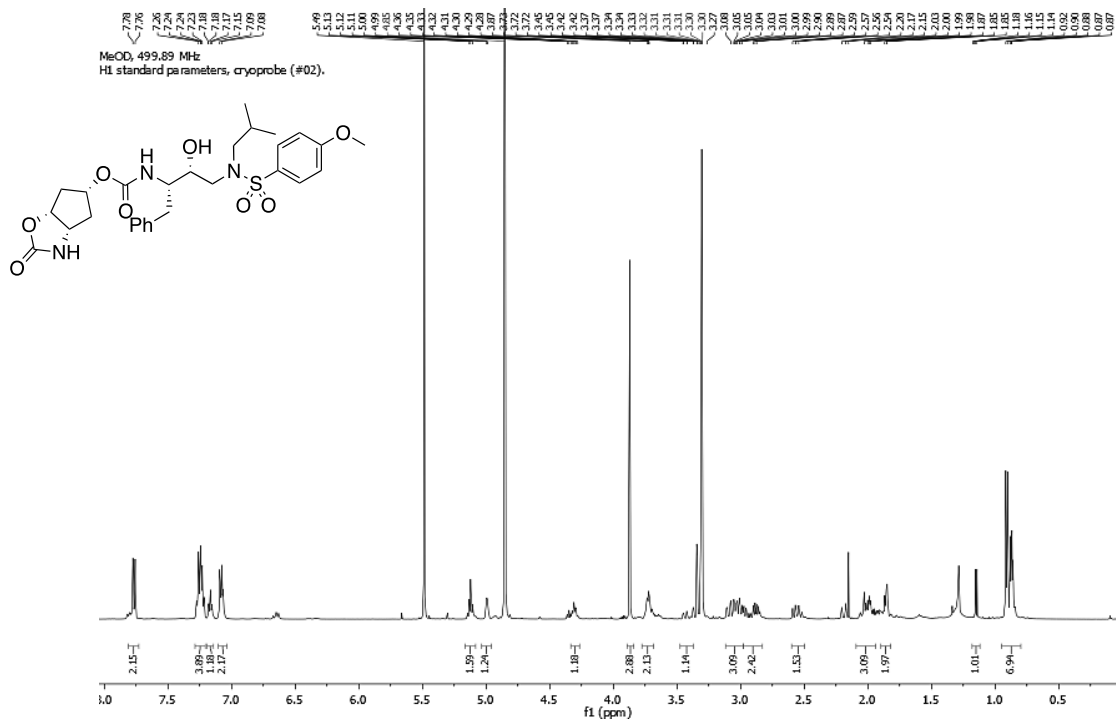


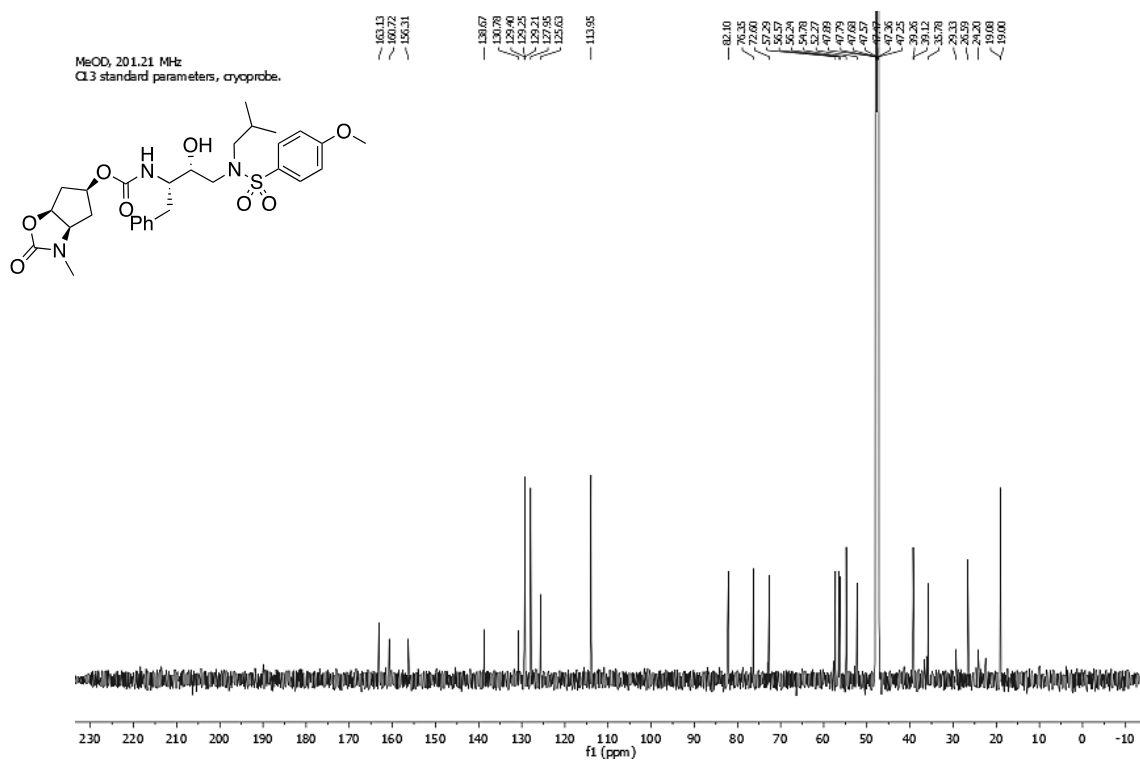
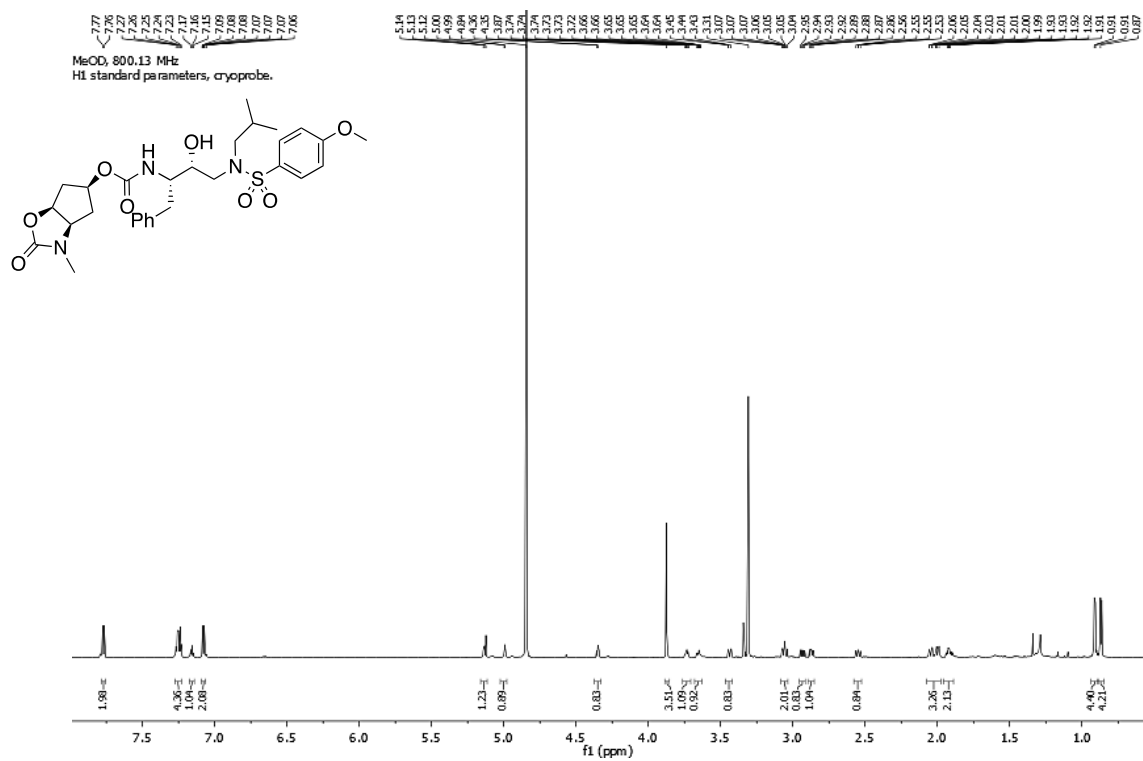


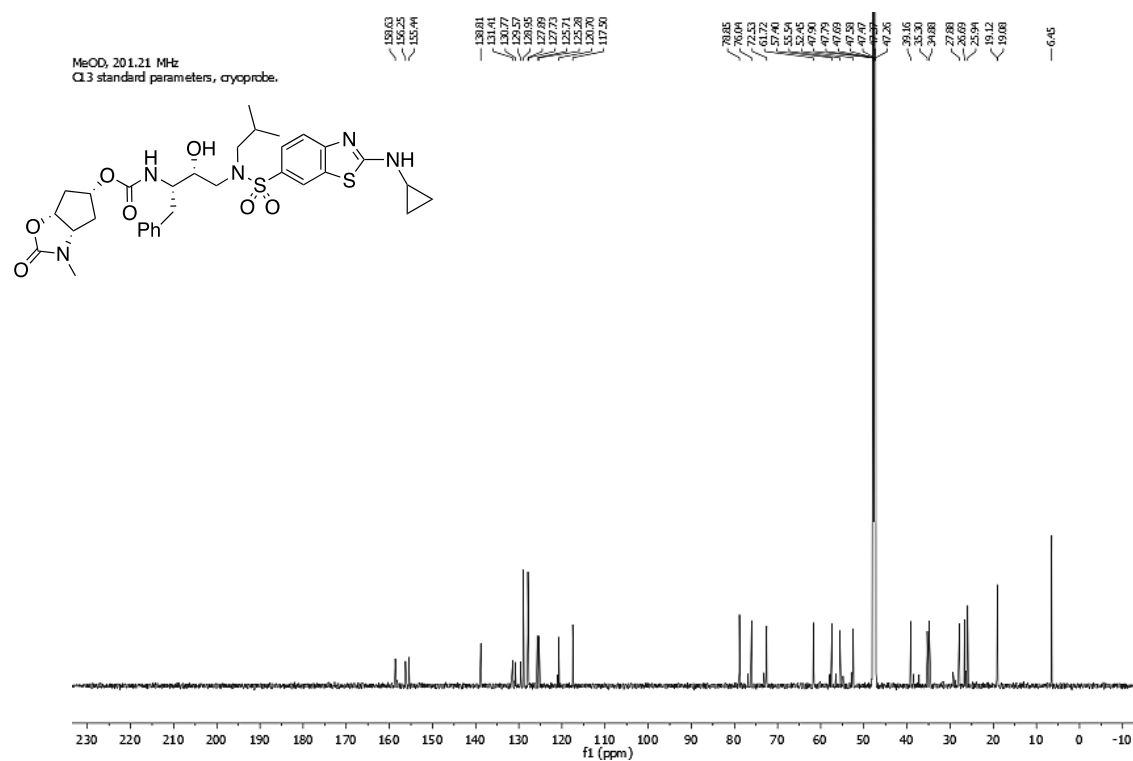
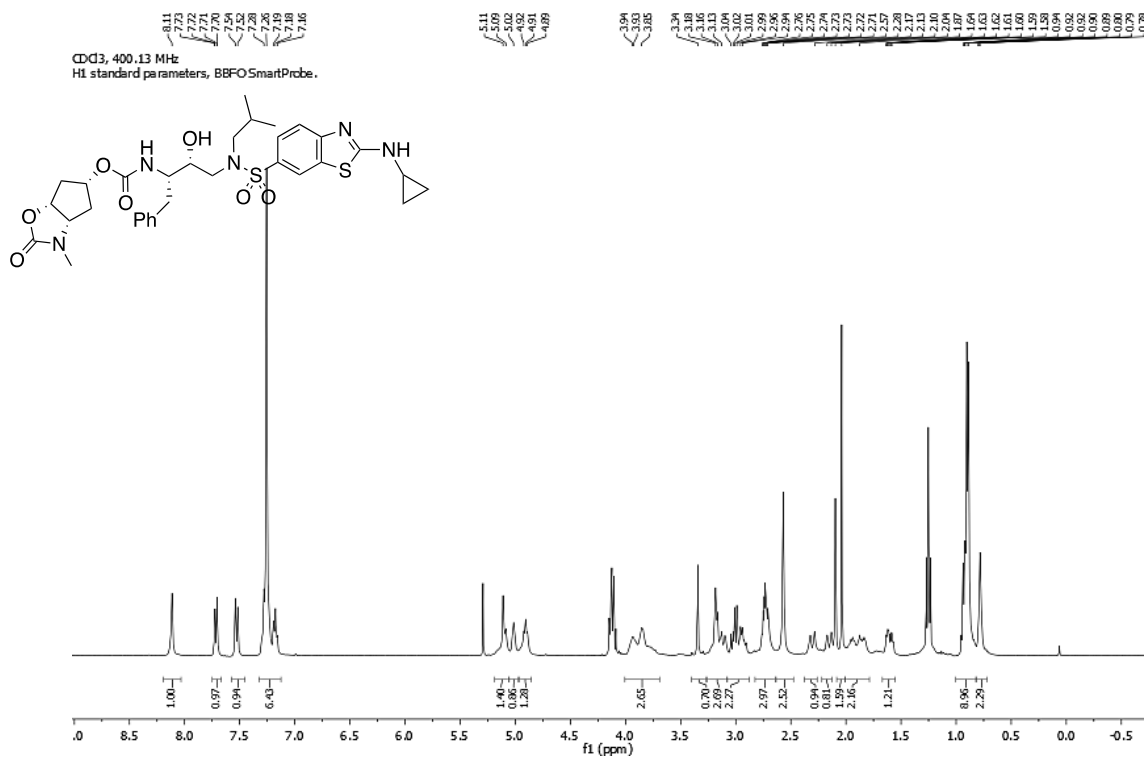


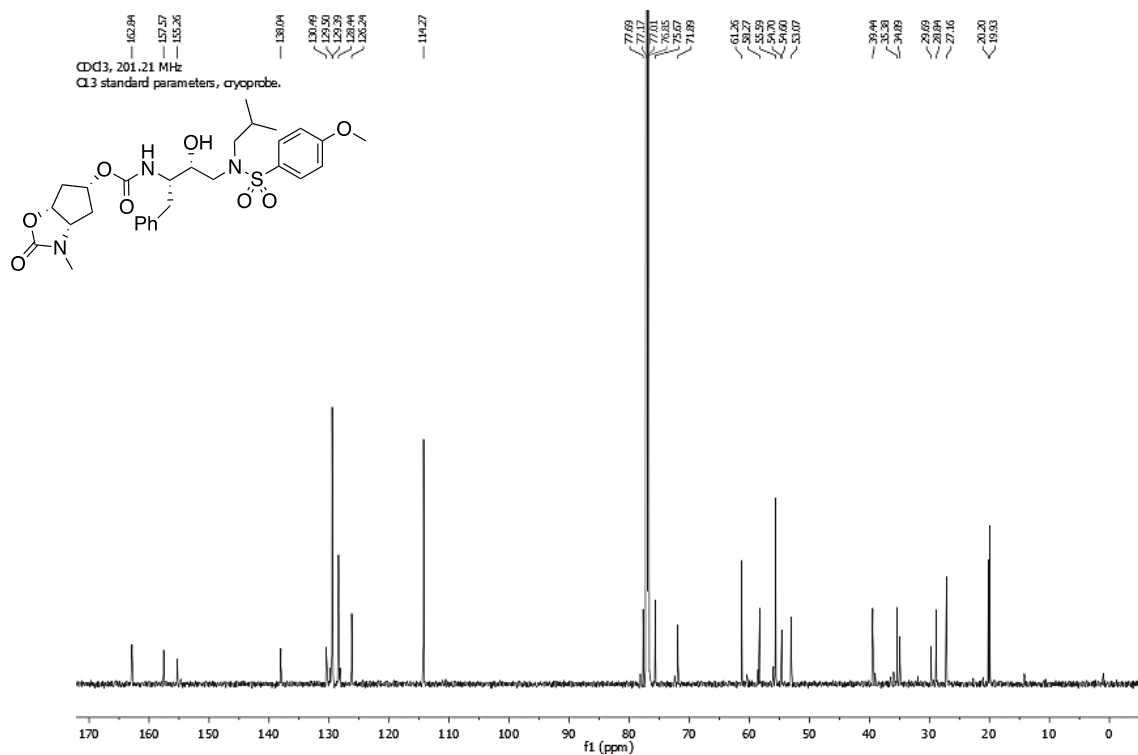
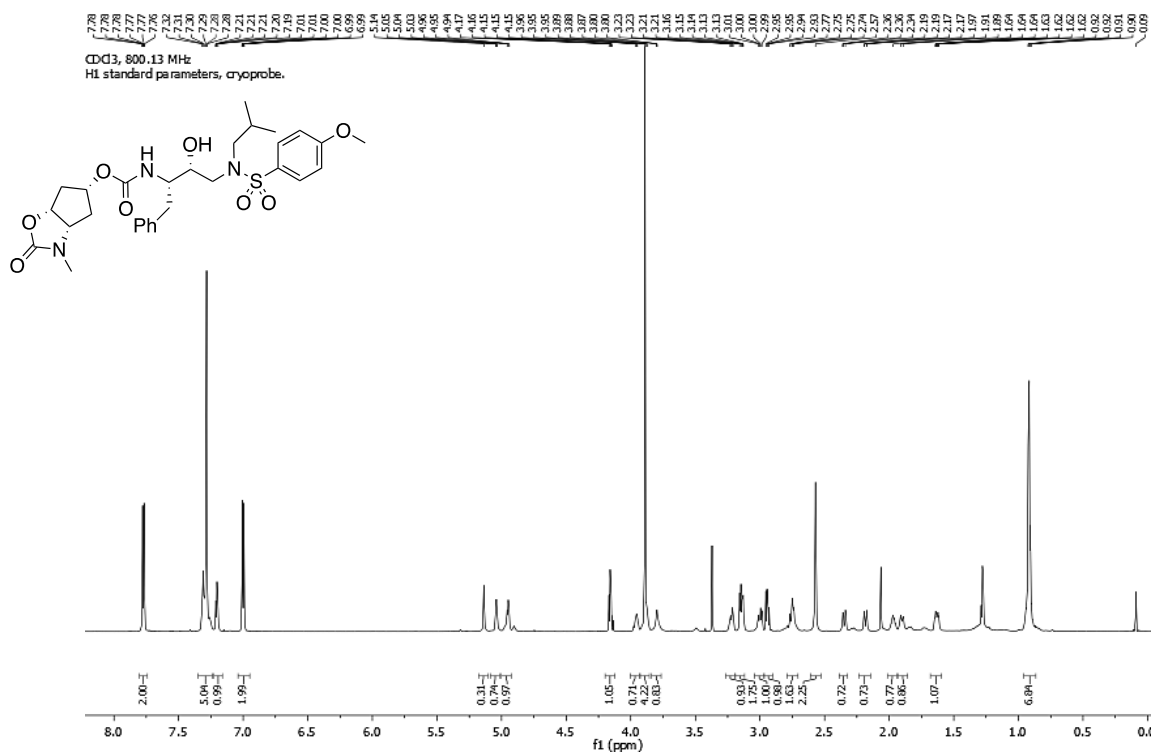


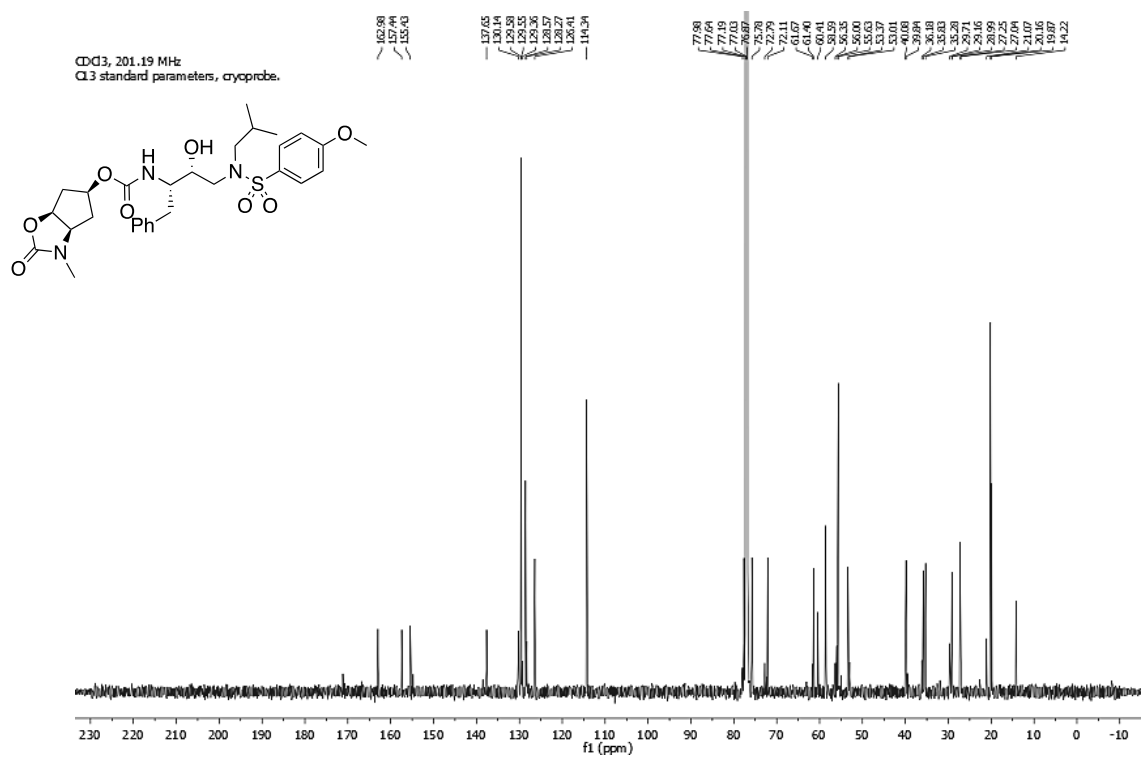
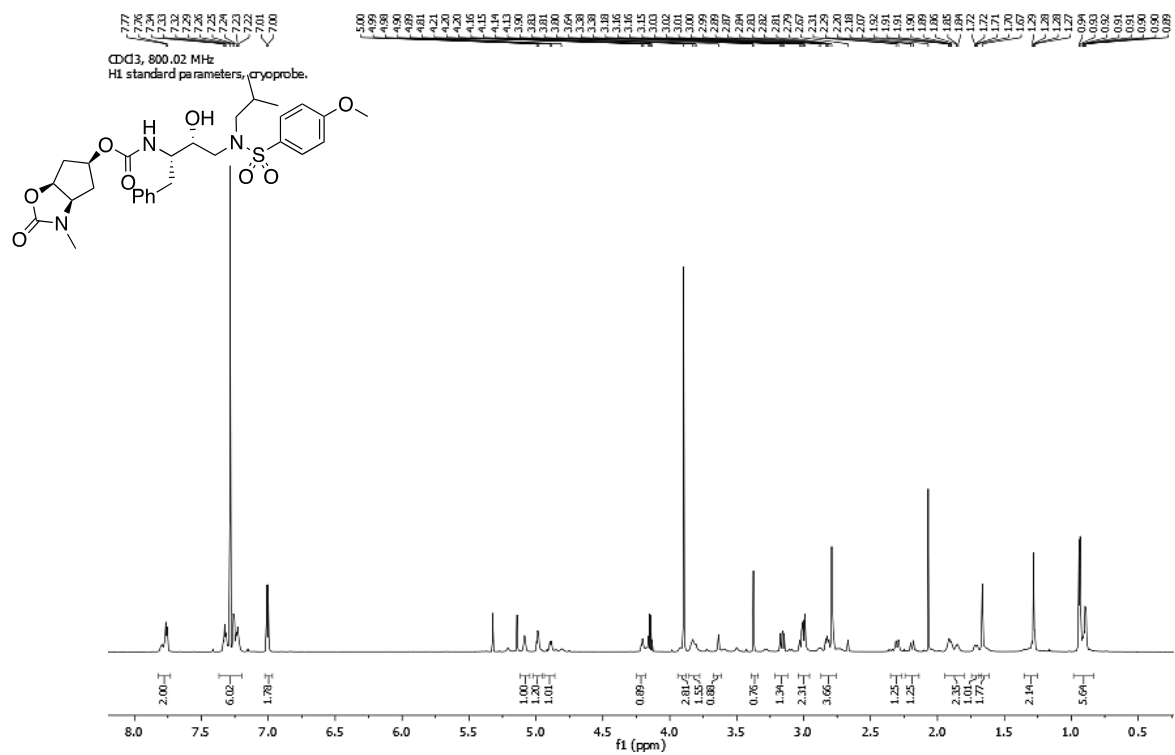


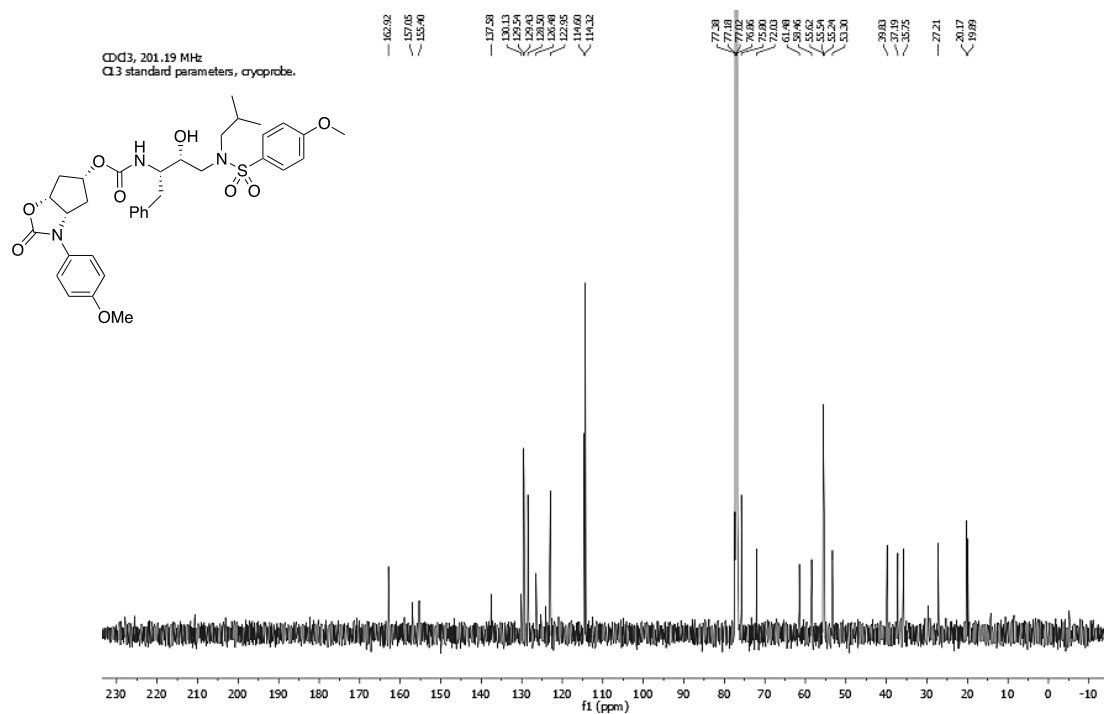


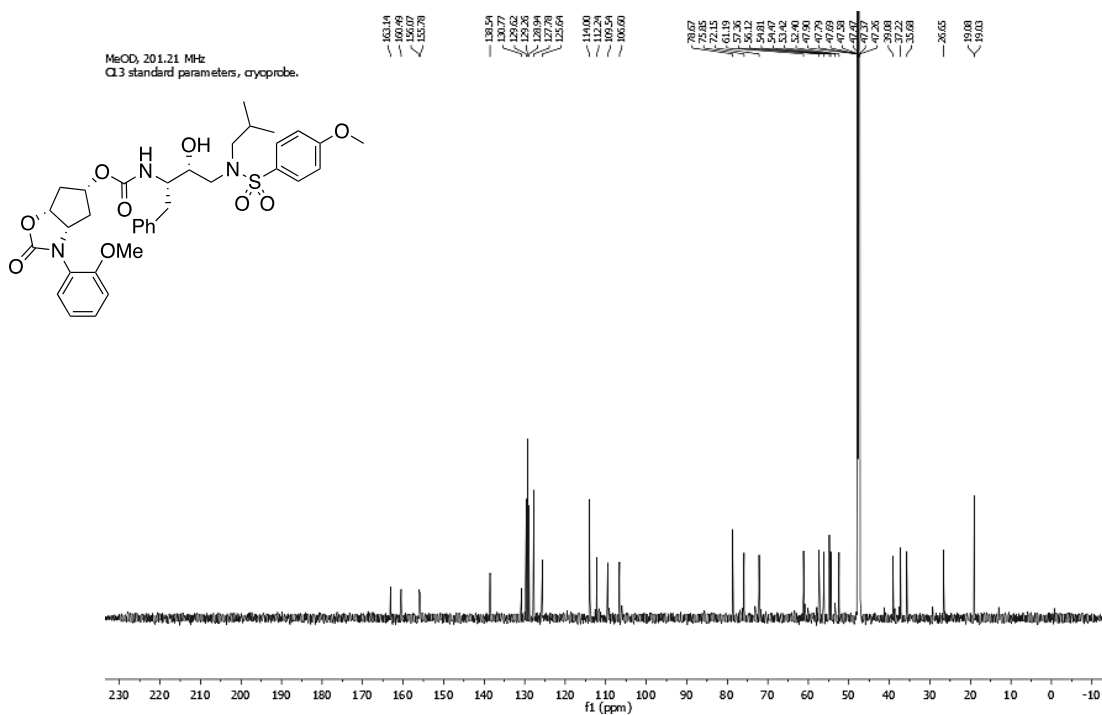
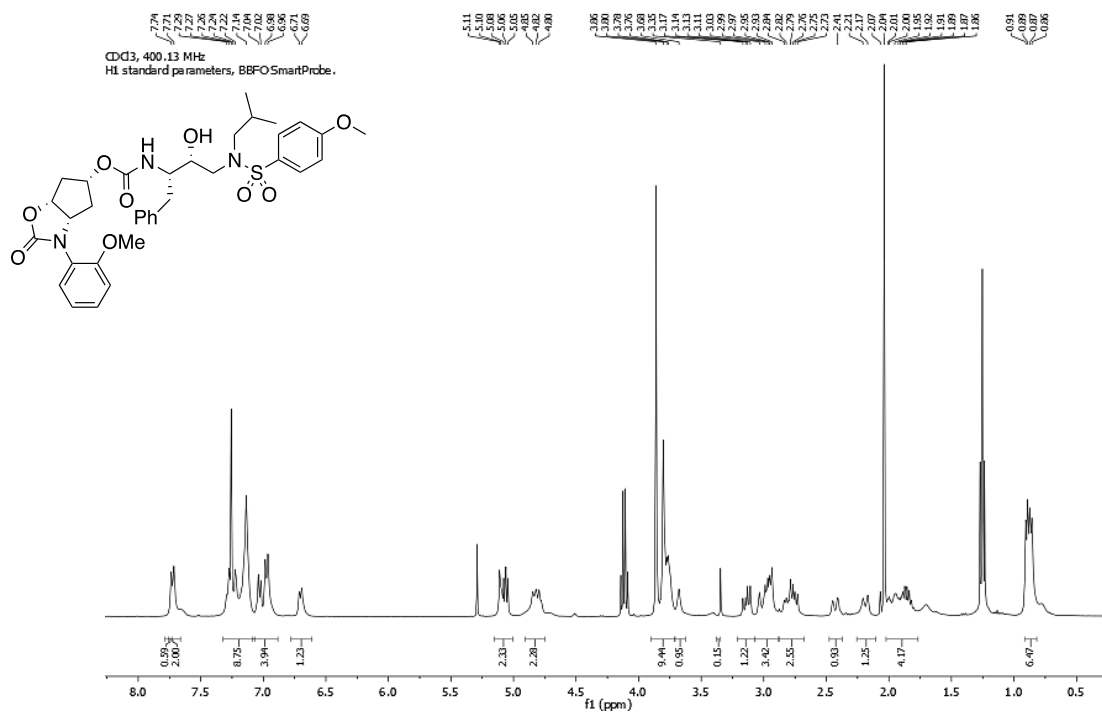


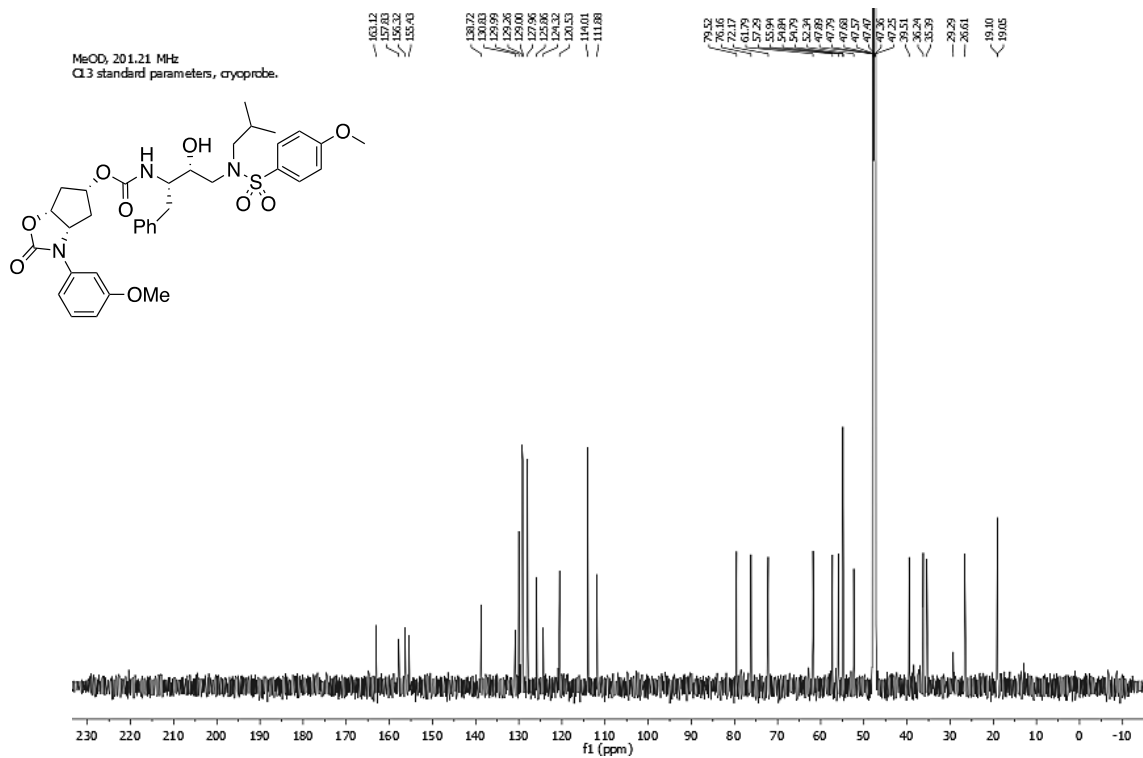
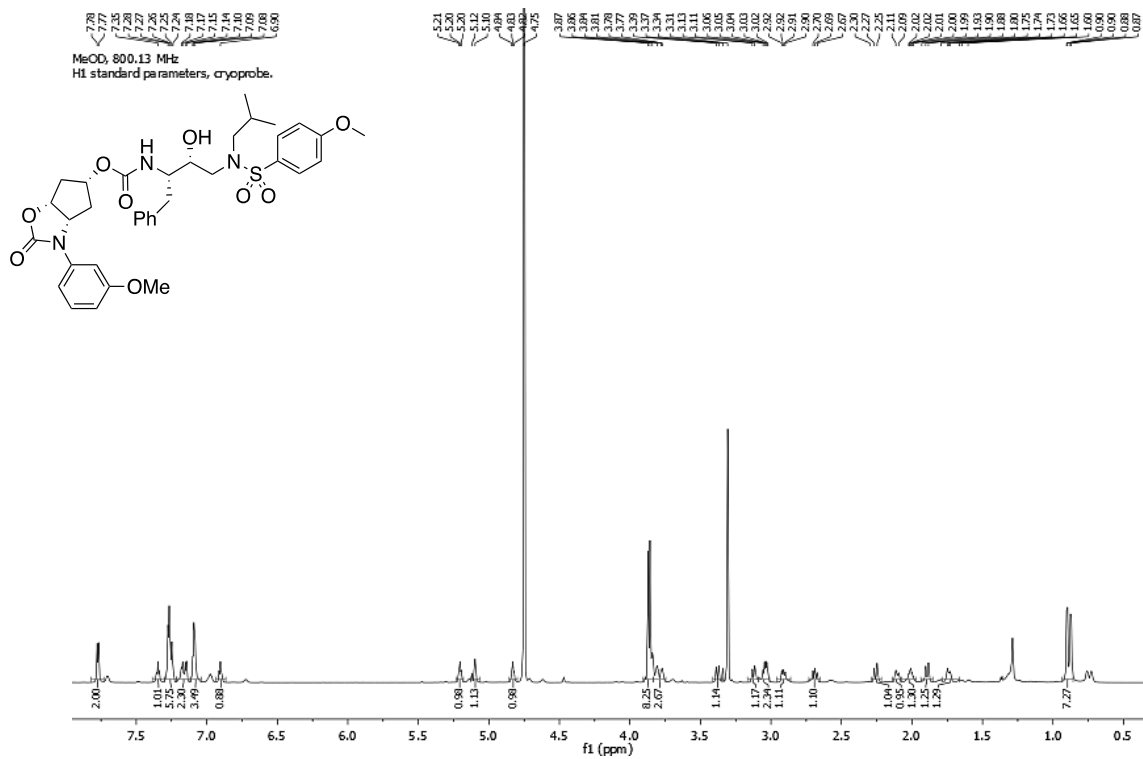


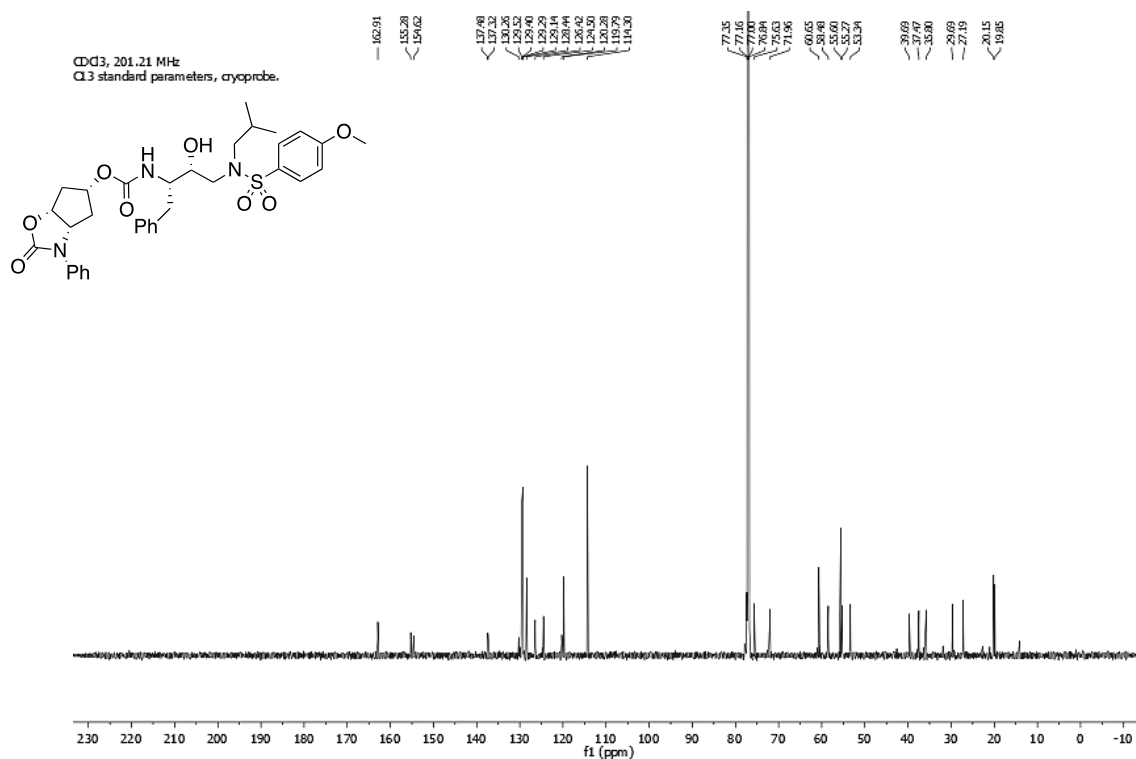
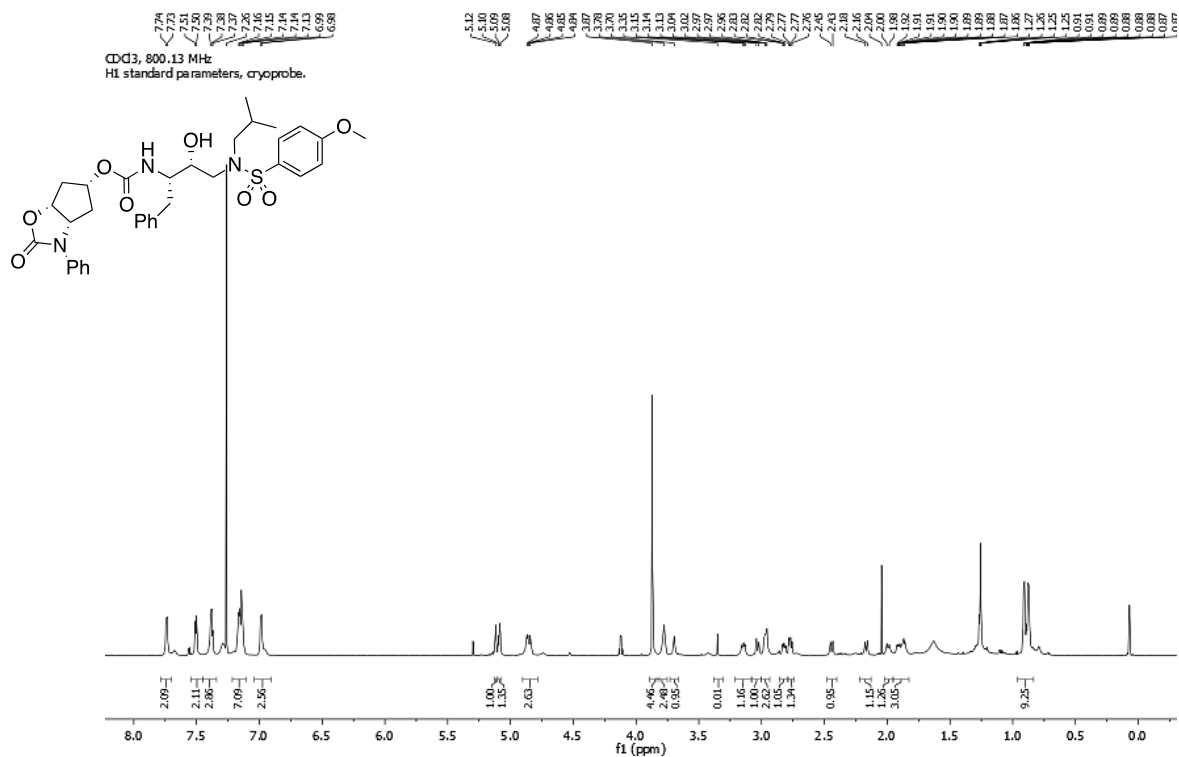


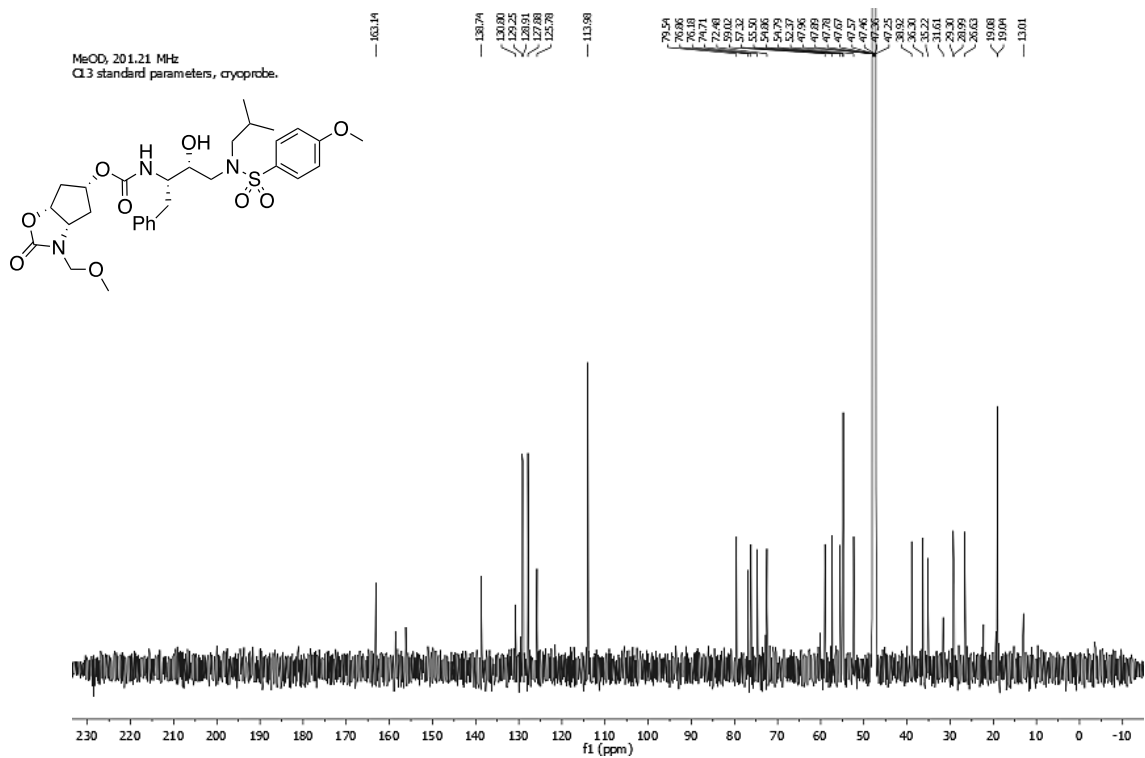
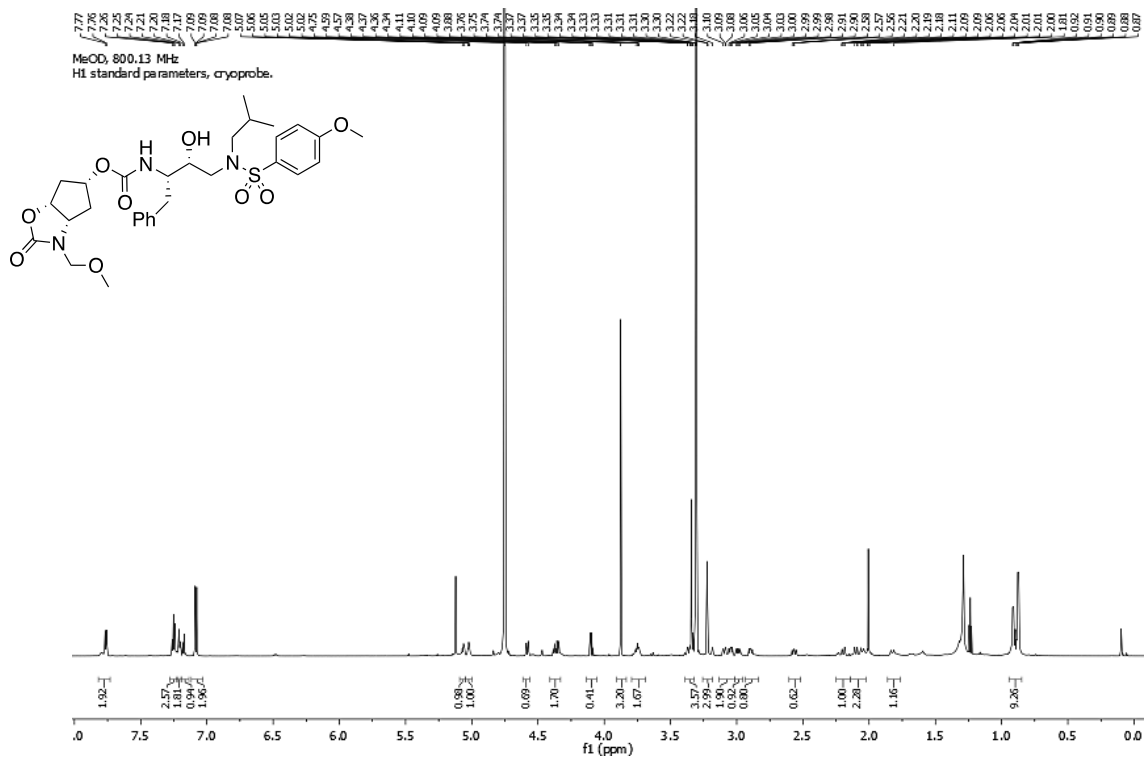


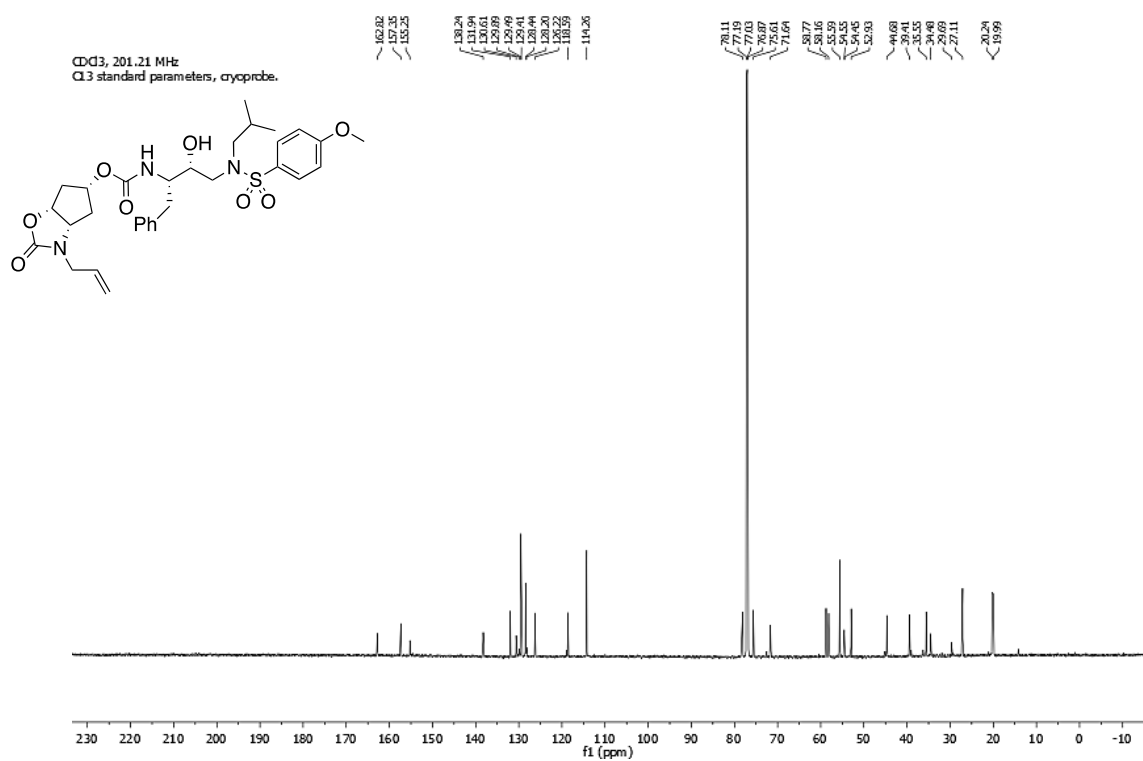
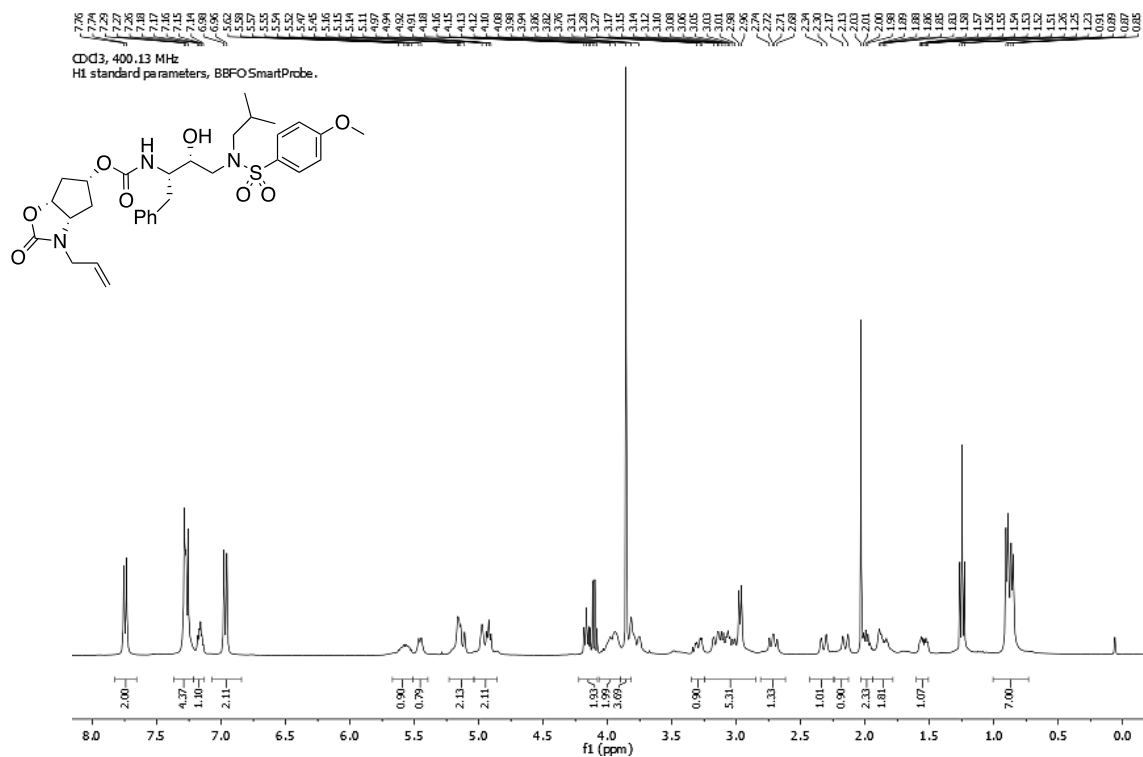


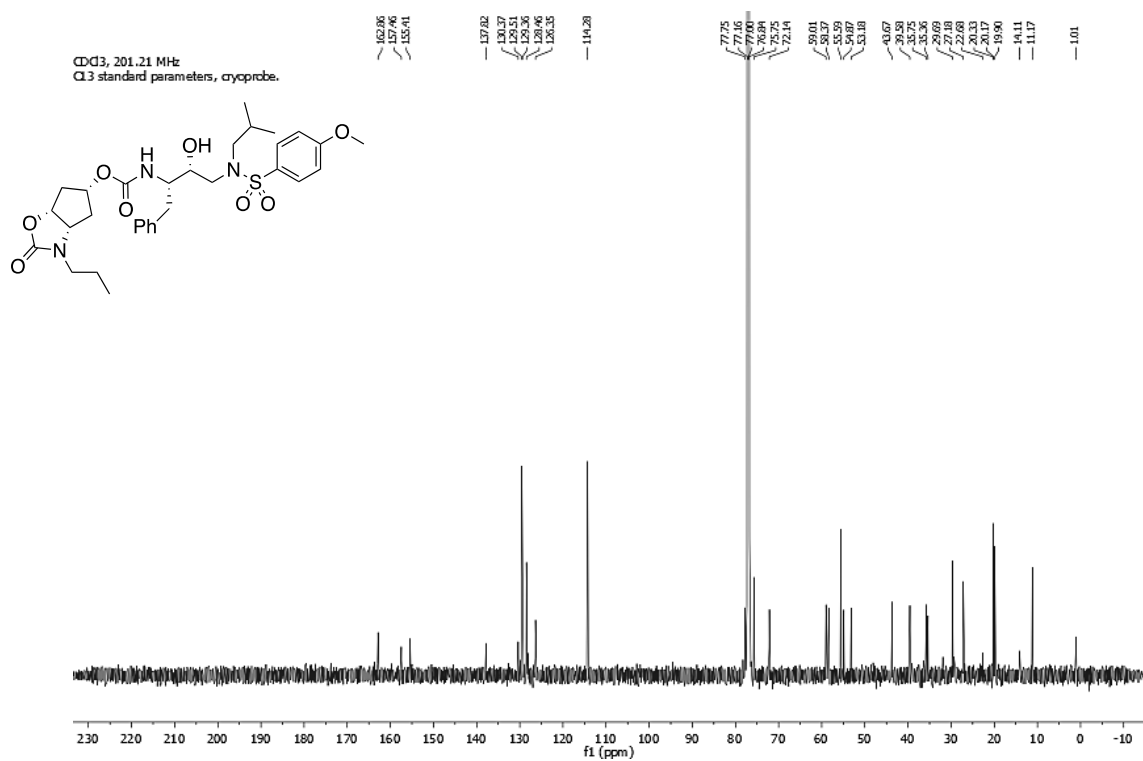


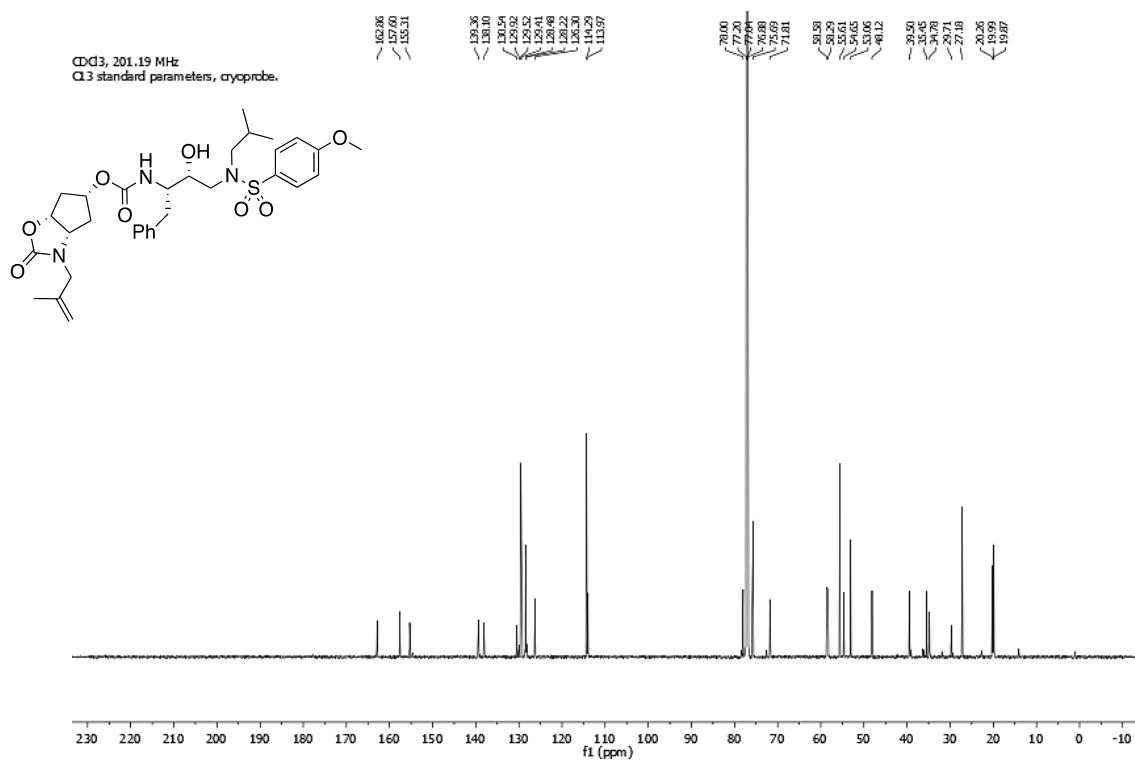
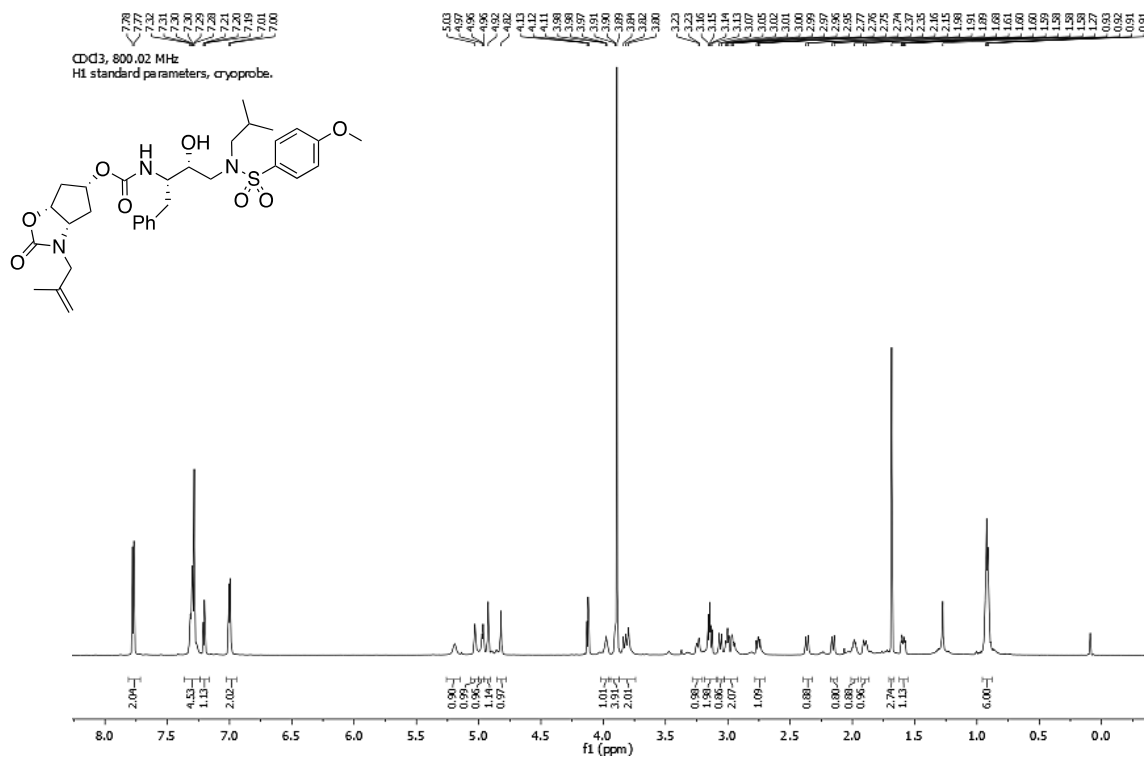


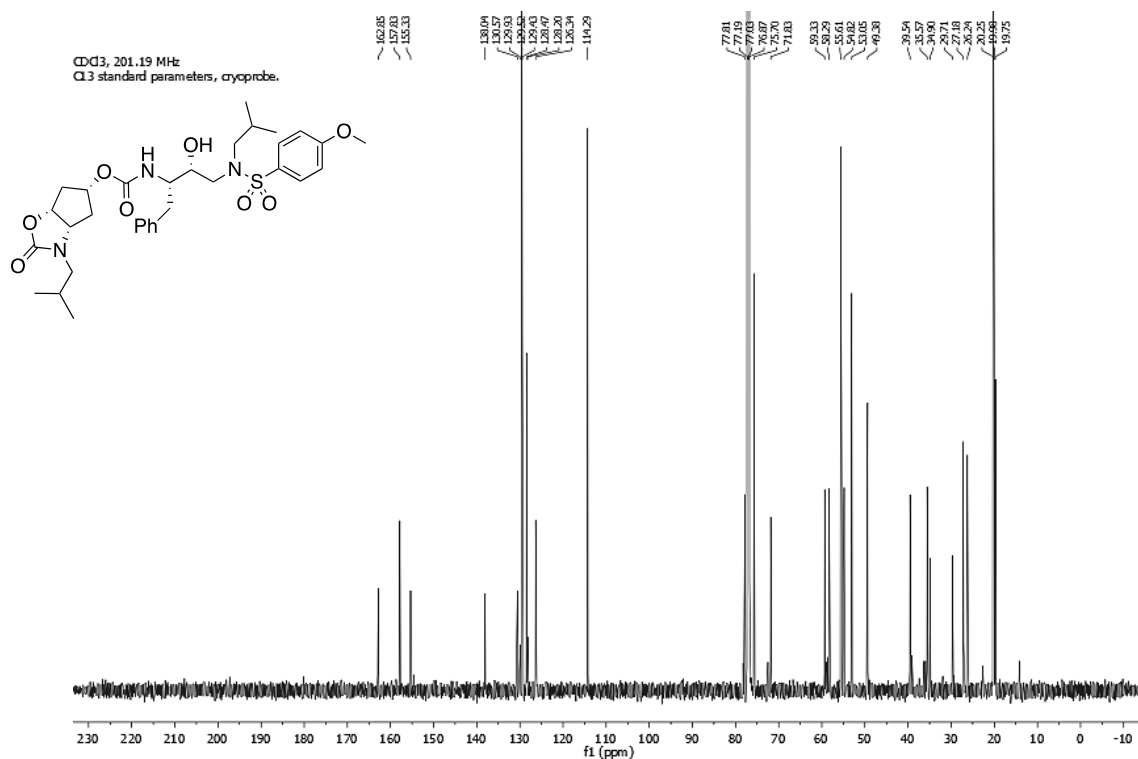
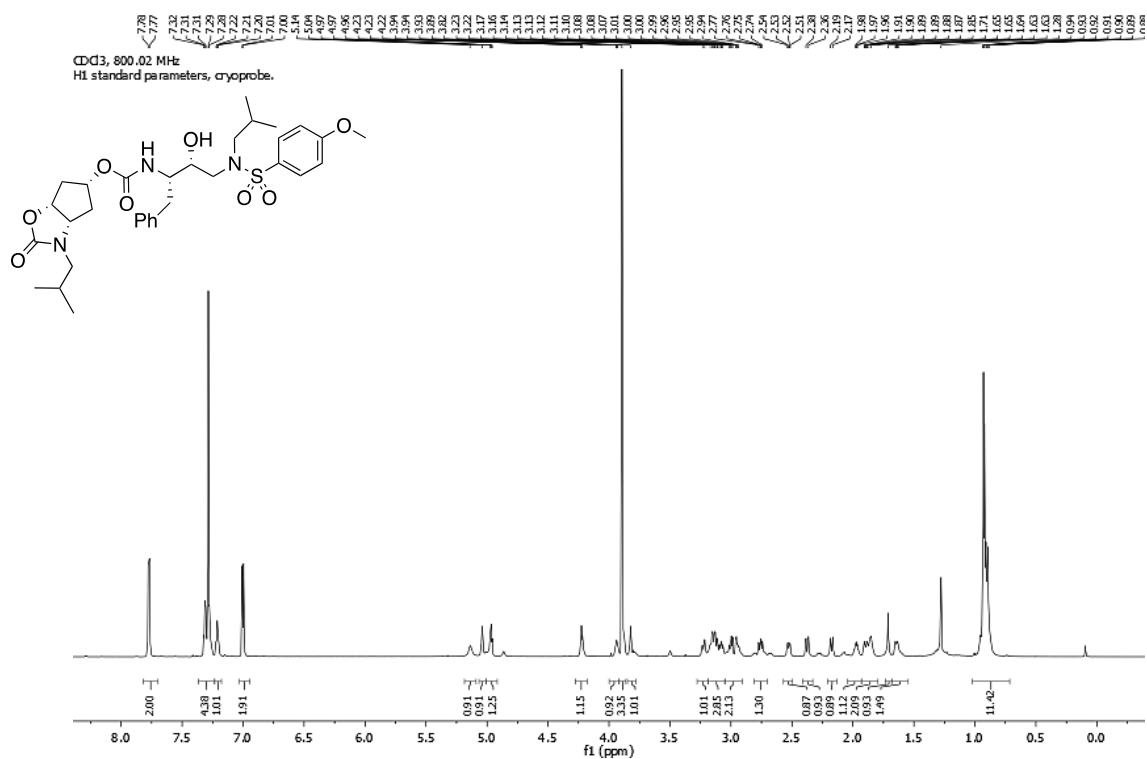


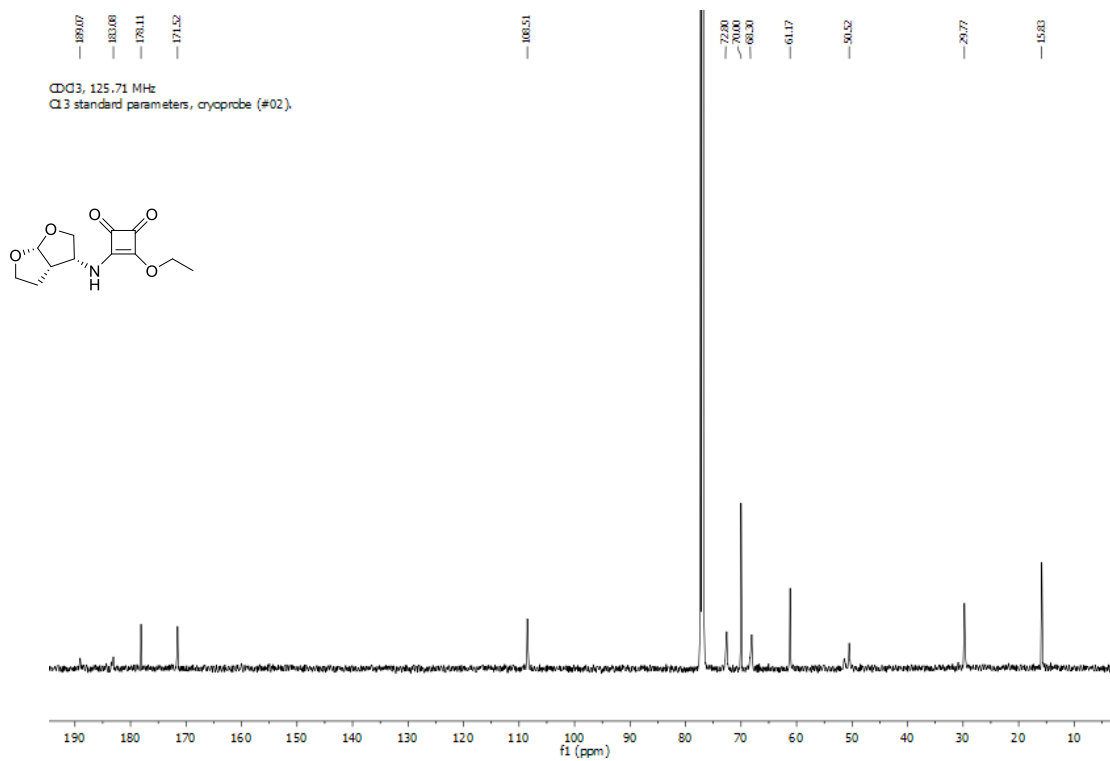
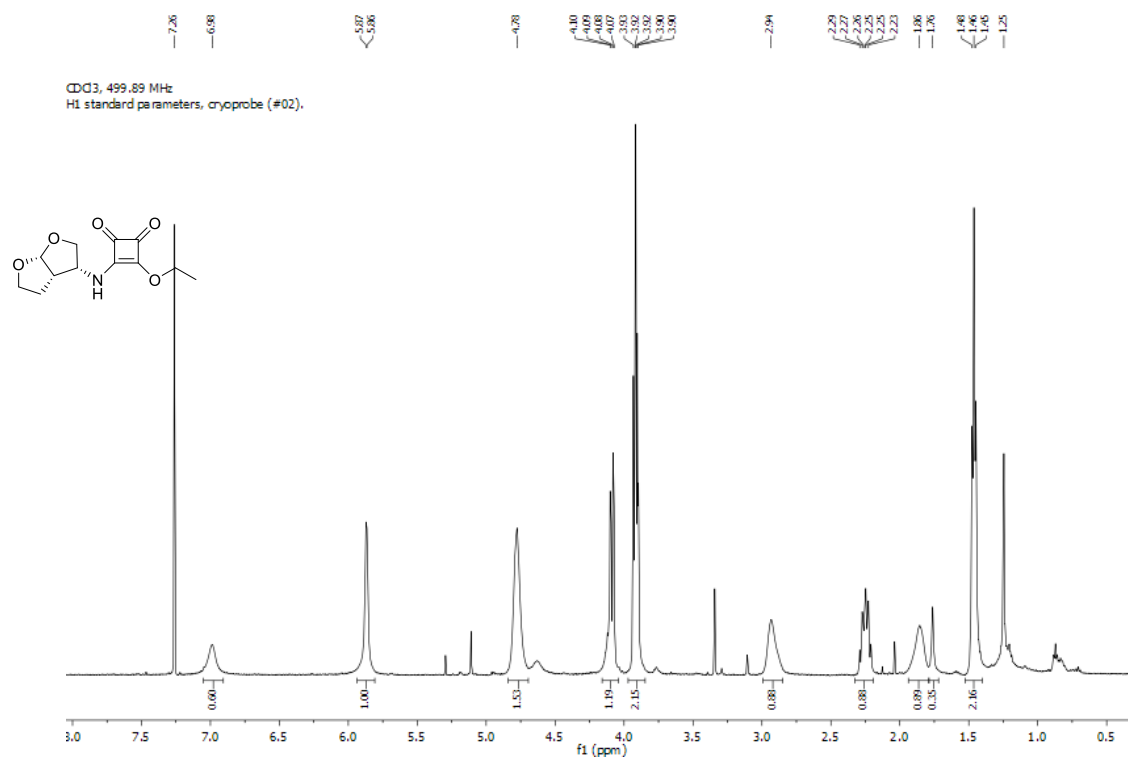


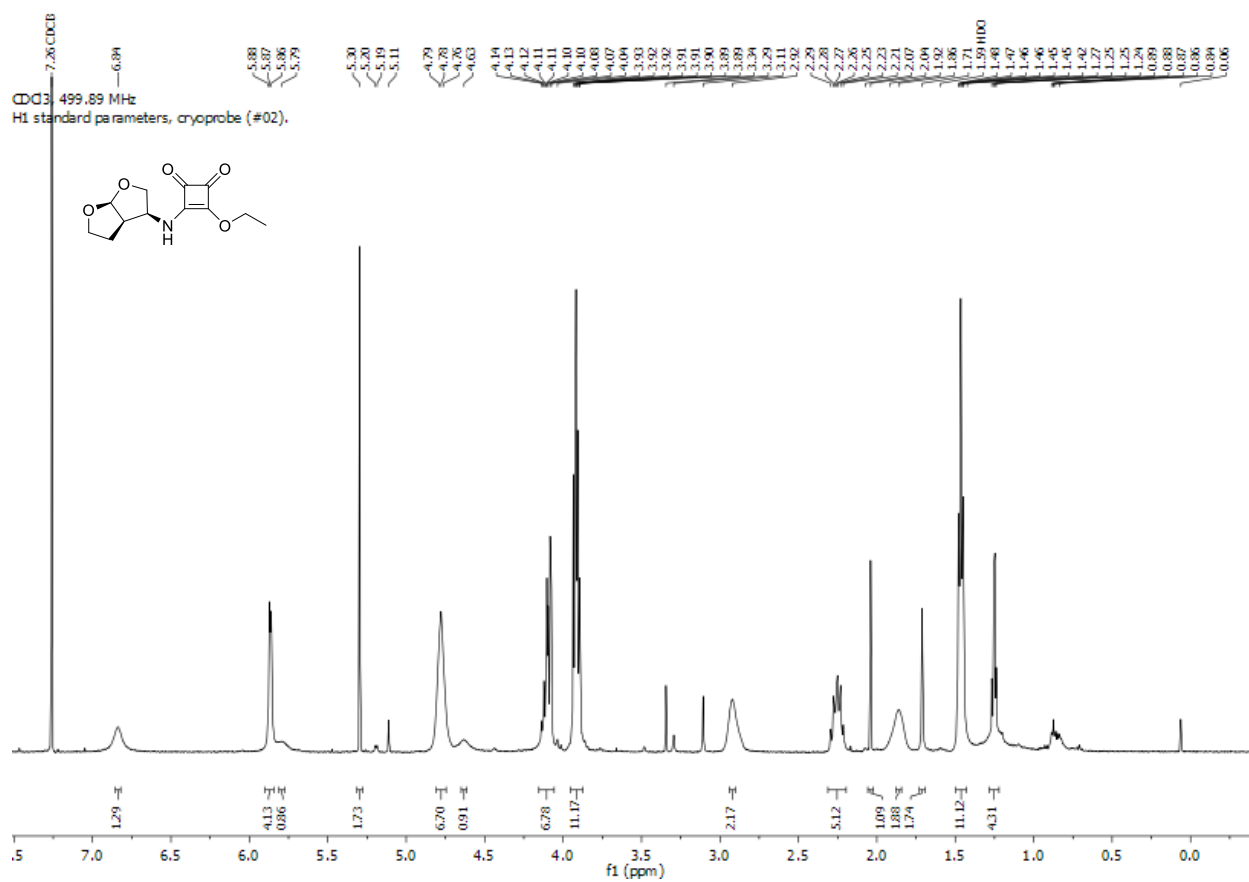


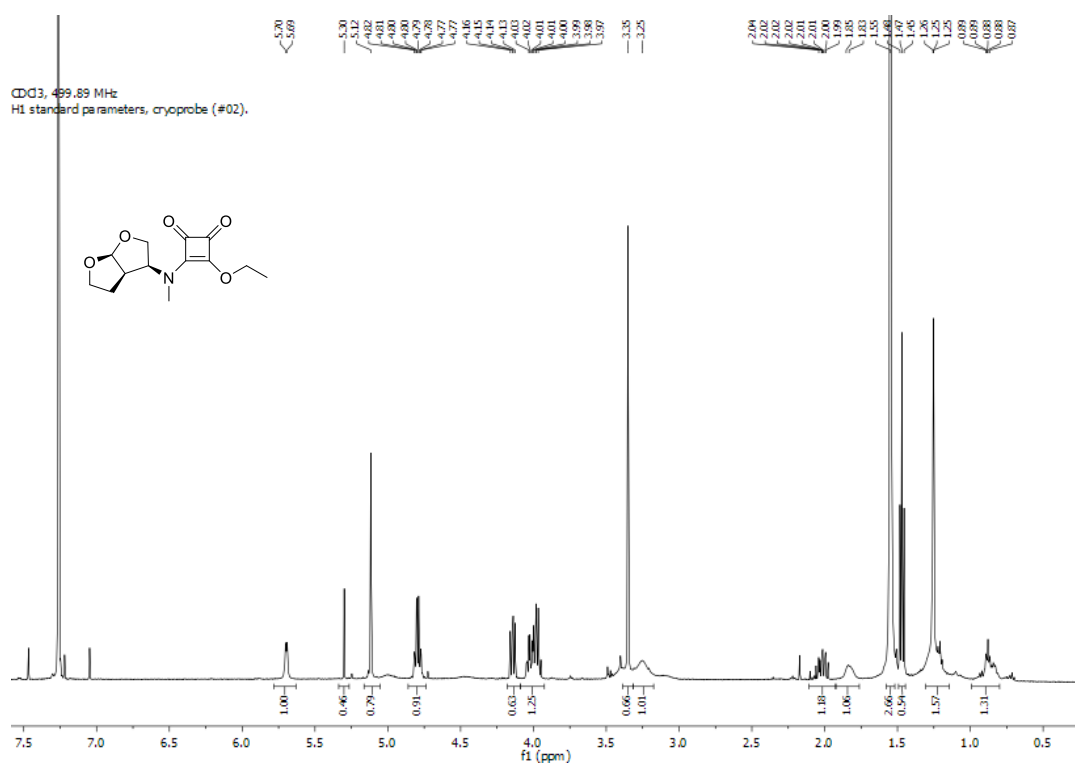
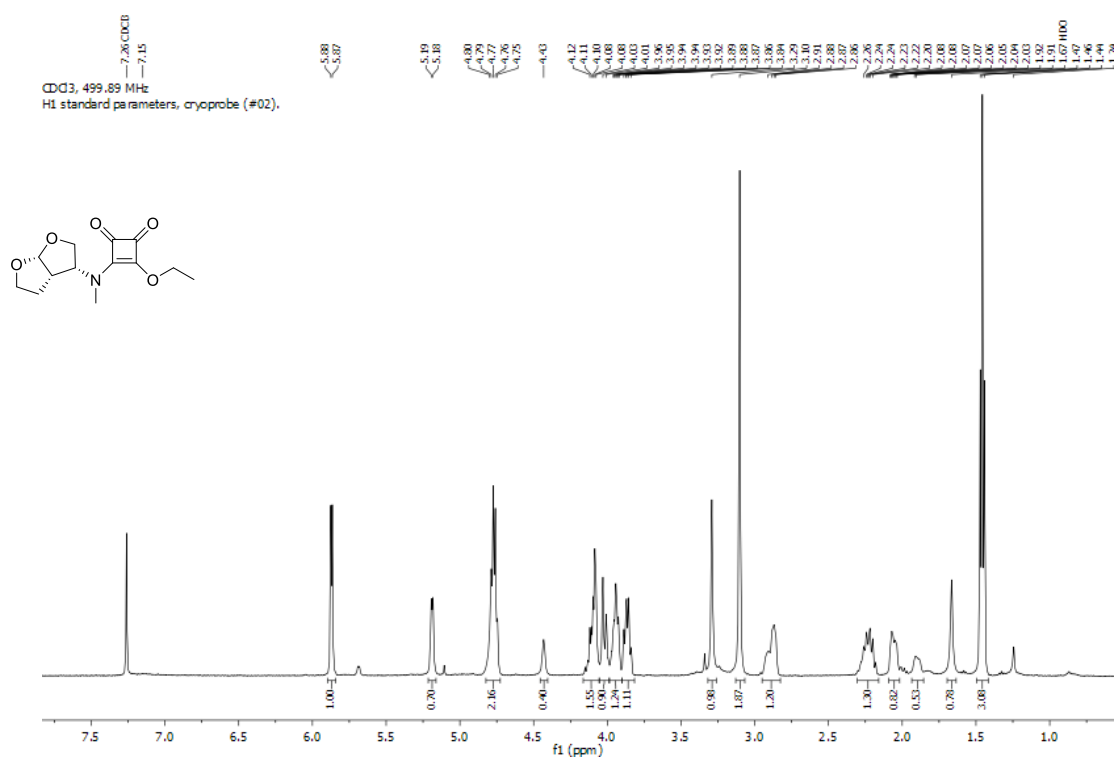


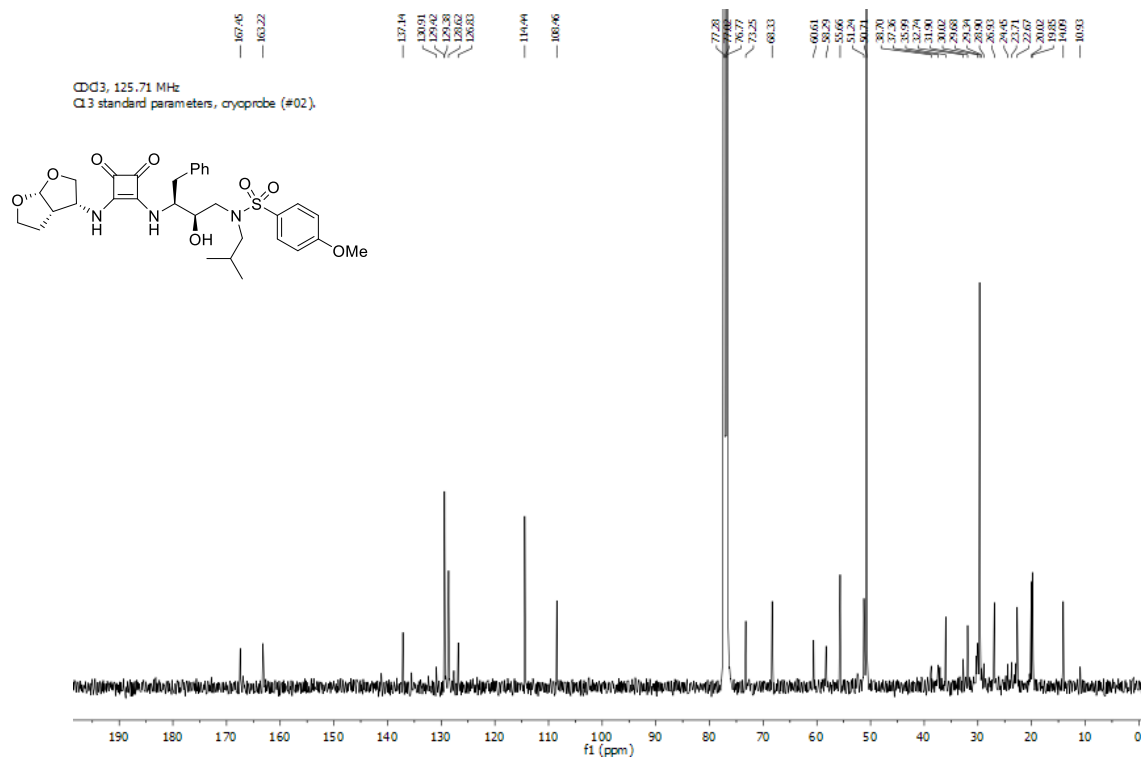
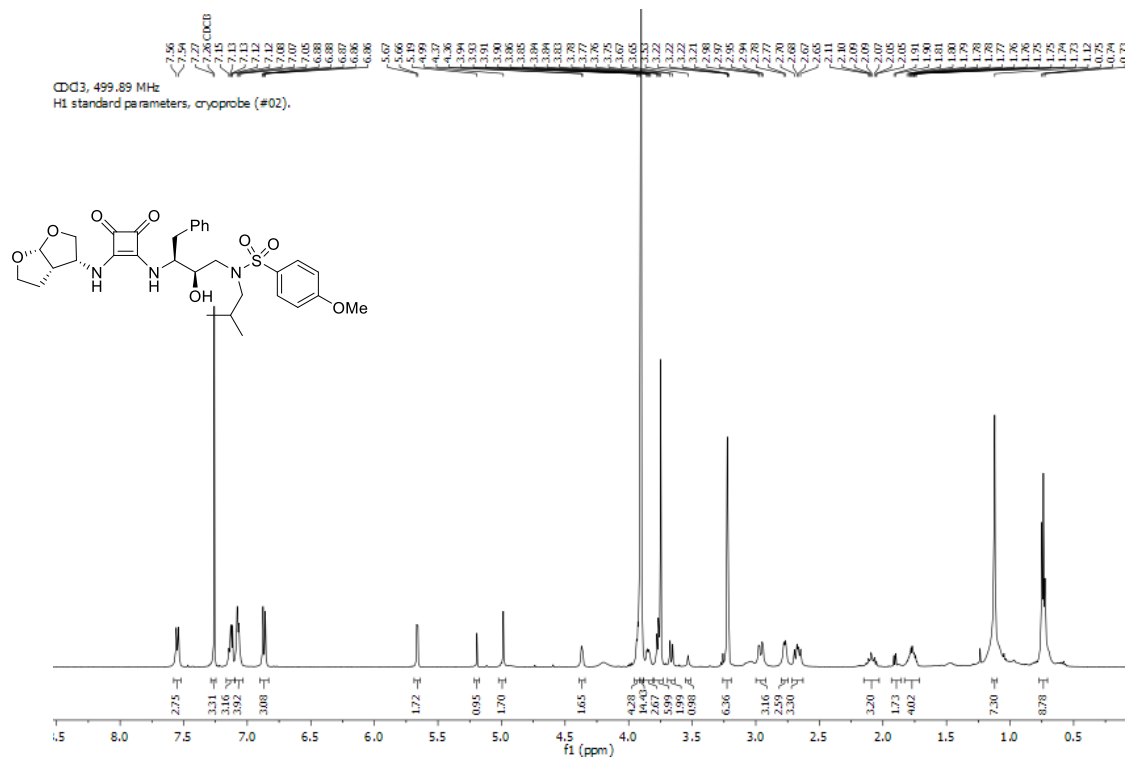


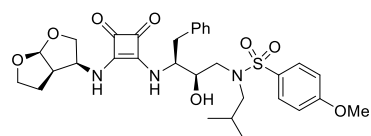
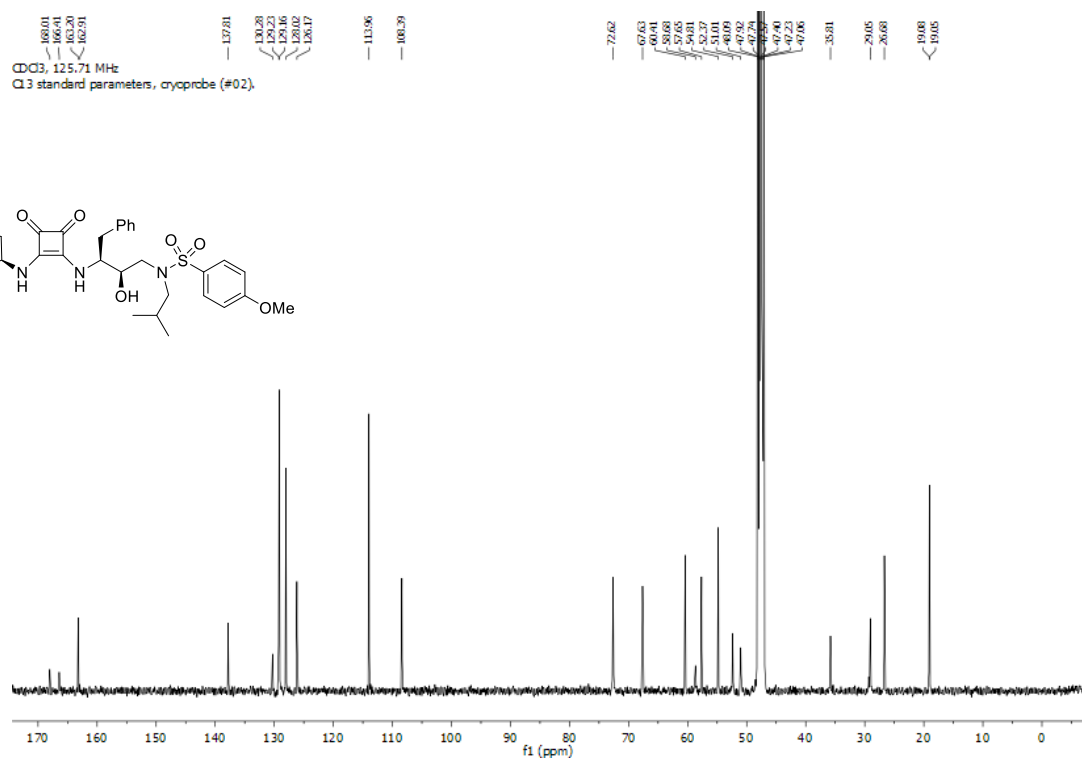
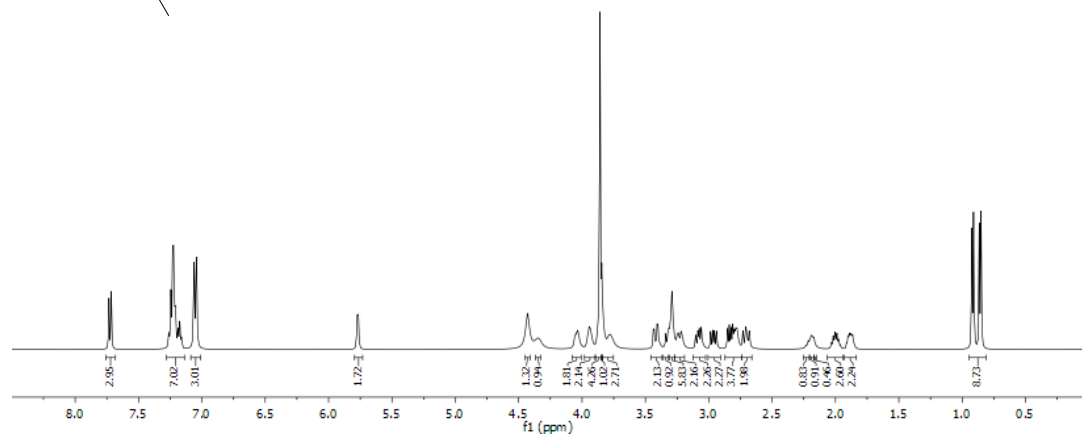
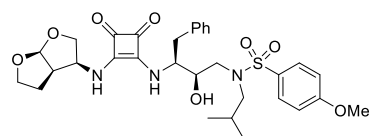
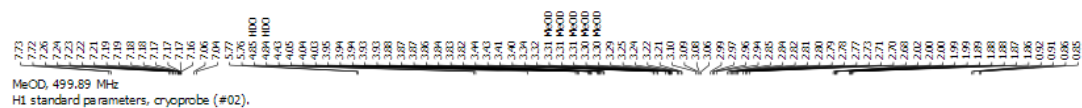


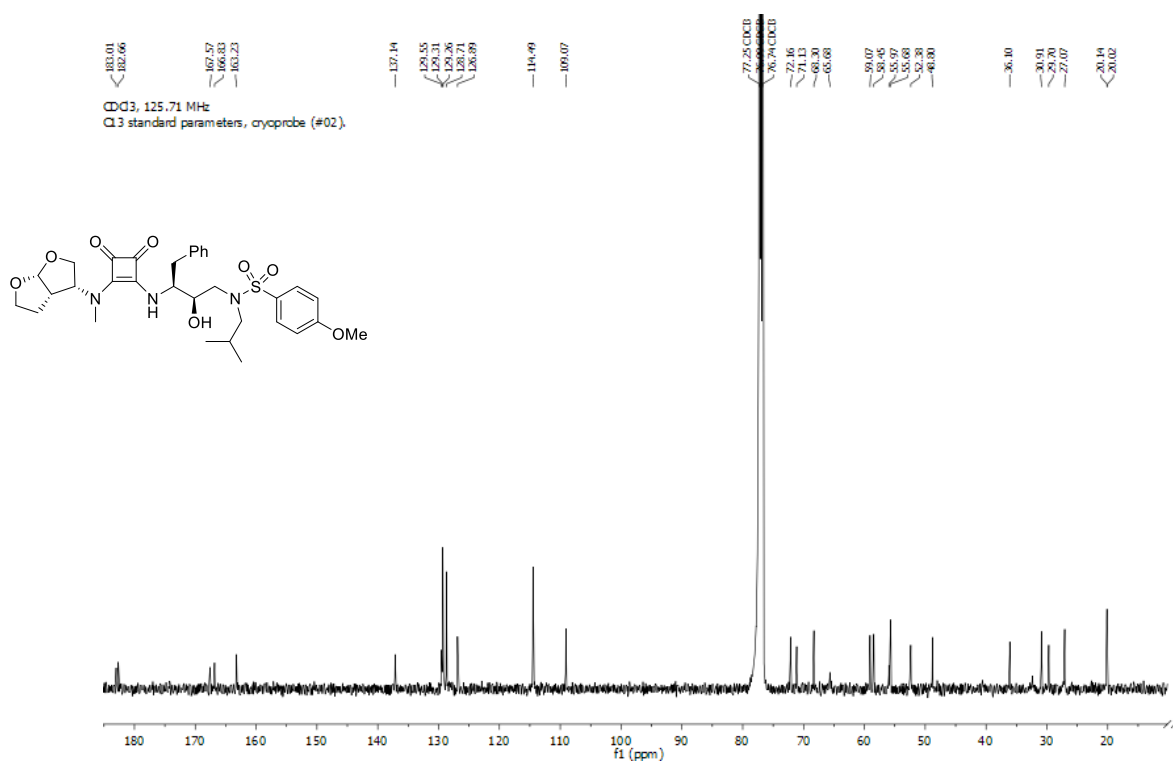
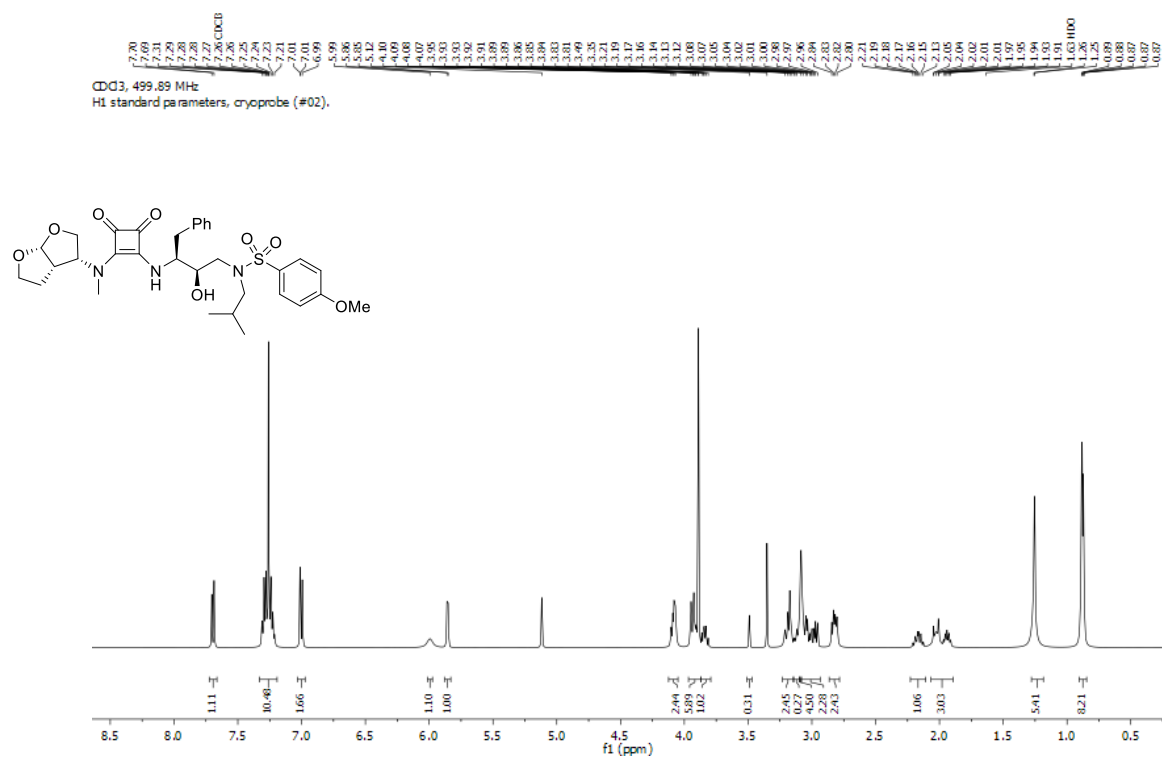


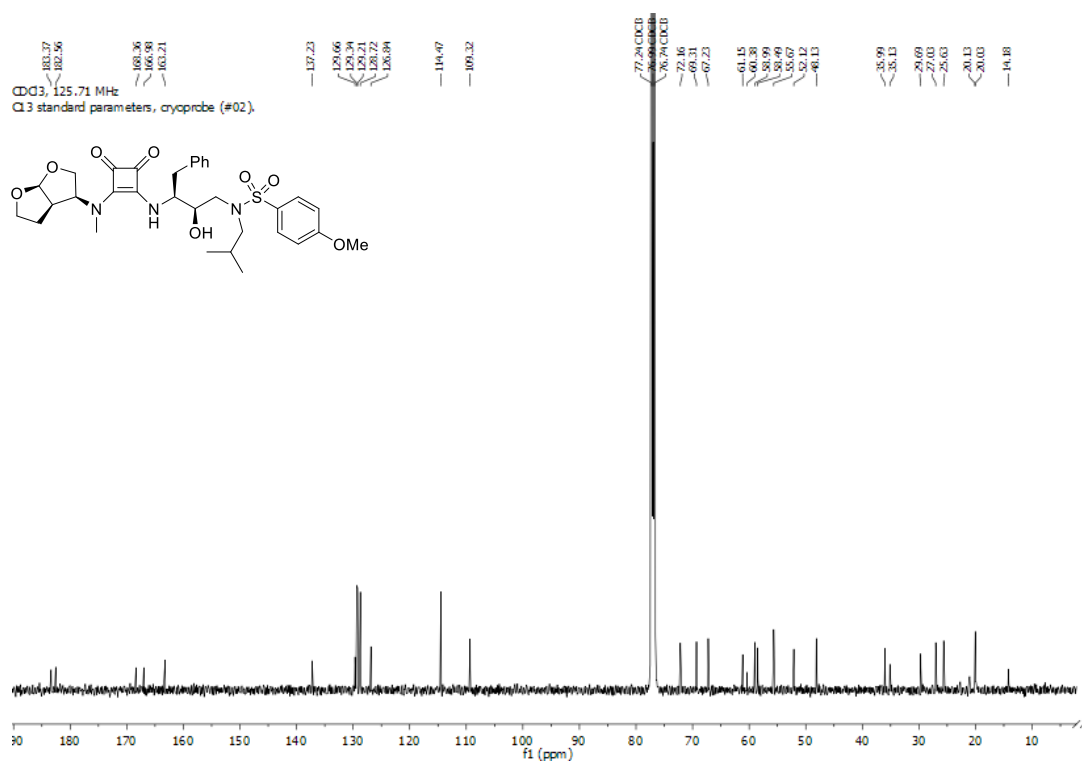












REFERENCES

1. Centers for Disease Control and Prevention. Pneumocystis pneumonia--Los Angeles. 1981. *MMWR Morb Mortal Wkly Rep* **1996**, 45 (34), 729-33.
2. Centers for Disease Control and Prevention., Update on acquired immune deficiency syndrome (AIDS)--United States. *MMWR Morb Mortal Wkly Rep* **1982**, 31 (37), 507-8, 513-4.
3. Centers for Disease Control and Prevention. Update on acquired immune deficiency syndrome (AIDS) among patients with hemophilia A. *MMWR Morb Mortal Wkly Rep* **1982**, 31 (48), 644-6, 652.
4. Barre-Sinoussi, F.; Chermann, J.; Rey, F.; Nugeyre, M.; Chamaret, S.; Gruest, J.; Dauguet, C.; Axler-Blin, C.; Vezinet-Brun, F.; Rouzioux, C.; Rozenbaum, W.; Montagnier, L., Isolation of a T-lymphotropic retrovirus from a patient at risk for acquired immune deficiency syndrome (AIDS). *Science* **1983**, 220 (4599), 868-871.
5. Montagnier, L., Lymphadenopathy-associated virus: from molecular biology to pathogenicity. *Ann Intern Med* **1985**, 103 (5), 689-93.
6. Gallo, R.; Sarin, P.; Gelmann, E.; Robert-Guroff, M.; Richardson, E.; Kalyanaraman, V.; Mann, D.; Sidhu, G.; Stahl, R.; Zolla-Pazner, S.; Leibowitch, J.; Popovic, M., Isolation of human T-cell leukemia virus in acquired immune deficiency syndrome (AIDS). *Science* **1983**, 220 (4599), 865-867.
7. Brown, F., The Classification and Nomenclature of Viruses: Summary of Results of Meetings of the International Committee on Taxonomy of Viruses in Sendai, September 1984. *Intervirology* **1986**, 25 (3), 141-143.
8. Chakrabarti, L.; Guyader, M.; Alizon, M.; Daniel, M. D.; Desrosiers, R. C.; Tiollais, P.; Sonigo, P., Sequence of simian immunodeficiency virus from macaque and its relationship to other human and simian retroviruses. *Nature* **1987**, 328 (6130), 543-547.
9. LeBreton, M.; Yang, O.; Tamoufe, U.; Mpoudi-Ngole, E.; Torimiro, J. N.; Djoko, C. F.; Carr, J. K.; Tassy Prosser, A.; Rimoin, A. W.; Bix, D. L.; Burke, D. S.; Wolfe, N. D., Exposure to wild primates among HIV-infected persons. *Emerging infectious diseases* **2007**, 13 (10), 1579-1582.
10. Huet, T.; Cheynier, R.; Meyerhans, A.; Roelants, G.; Wain-Hobson, S., Genetic organization of a chimpanzee lentivirus related to HIV-1. *Nature* **1990**, 345 (6273), 356-359.

11. Hirsch, V. M.; Olmsted, R. A.; Murphey-Corb, M.; Purcell, R. H.; Johnson, P. R., An African primate lentivirus SIVsm closely related to HIV-2. *Nature* **1989**, 339 (6223), 389-392.
12. Sharp, P. M.; Hahn, B. H., Prehistory of HIV-1. *Nature* **2008**, 455, 605.
13. Sharp, P. M.; Hahn, B. H., Origins of HIV and the AIDS Pandemic. *Cold Spring Harbor Perspectives in Medicine* **2011**, 1 (1).
14. Guyader, M.; Emerman, M.; Sonigo, P.; Clavel, F.; Montagnier, L.; Alizon, M., Genome organization and transactivation of the human immunodeficiency virus type 2. *Nature* **1987**, 326 (6114), 662-669.
15. Hladik, F.; McElrath, M. J., Setting the stage: host invasion by HIV. *Nature Reviews Immunology* **2008**, 8, 447.
16. Cohen, M. S.; Shaw, G. M.; McMichael, A. J.; Haynes, B. F., Acute HIV-1 Infection. *New England Journal of Medicine* **2011**, 364 (20), 1943-1954.
17. Tindall, B.; Cooper, D. A., Primary HIV infection: host responses and intervention strategies. *AIDS* **1991**, 5 (1), 1-14.
18. Belyakov, I. M.; Berzofsky, J. A., Immunobiology of Mucosal HIV Infection and the Basis for Development of a New Generation of Mucosal AIDS Vaccines. *Immunity* **2004**, 20 (3), 247-253.
19. Stebbing, J.; Gazzard, B.; Douek, D. C., Where Does HIV Live? *New England Journal of Medicine* **2004**, 350 (18), 1872-1880.
20. Siegel, M.; Masur, H.; Kovacs, J., Pneumocystis jirovecii Pneumonia in Human Immunodeficiency Virus Infection. *Semin Respir Crit Care Med* **2016**, 37 (2), 243-56.
21. Su, Y. S.; Lu, J. J.; Perng, C. L.; Chang, F. Y., Pneumocystis jirovecii pneumonia in patients with and without human immunodeficiency virus infection. *J Microbiol Immunol Infect* **2008**, 41 (6), 478-82.
22. Smith, M. A.; Brennessel, D. J., Cytomegalovirus. *Infect Dis Clin North Am* **1994**, 8 (2), 427-38.
23. Horsburgh, C. R., Jr., The Pathophysiology of Disseminated Mycobacterium avium Complex Disease in AIDS. *J Infect Dis* **1999**, 179, S461-S465.
24. Quinnan, G. V., Jr.; Masur, H.; Rook, A. H.; Armstrong, G.; Frederick, W. R.; Epstein, J.; Manischewitz, J. F.; Macher, A. M.; Jackson, L.; Ames, J.; et al., Herpesvirus infections in the acquired immune deficiency syndrome. *JAMA* **1984**, 252 (1), 72-7.

25. German Advisory Committee Blood, S. A. o. P. T. b. B., Human Immunodeficiency Virus (HIV). *Transfusion medicine and hemotherapy* **2016**, 43 (3), 203-222.
26. Sierra, S.; Kupfer, B.; Kaiser, R., Basics of the virology of HIV-1 and its replication. *J Clin Virol* **2005**, 34 (4), 233-44.
27. Sundquist, W. I.; Krausslich, H. G., HIV-1 assembly, budding, and maturation. *Cold Spring Harb Perspect Med* **2012**, 2 (7), a006924.
28. King, S. R., HIV: Virology and mechanisms of disease. *Annals of Emergency Medicine* **1994**, 24 (3), 443-449.
29. Musinova, Y. R.; Sheval, E. V.; Dib, C.; Germini, D.; Vassetzky, Y. S., Functional roles of HIV-1 Tat protein in the nucleus. *Cellular and Molecular Life Sciences* **2016**, 73 (3), 589-601.
30. Pollard, V. W.; Malim, M. H., THE HIV-1 REV PROTEIN. *Annual Review of Microbiology* **1998**, 52 (1), 491-532.
31. Rücker, E.; Grivel, J.-C.; Münch, J.; Kirchhoff, F.; Margolis, L., Vpr and Vpu Are Important for Efficient Human Immunodeficiency Virus Type 1 Replication and CD4+ T-Cell Depletion in Human Lymphoid Tissue Ex Vivo. *Journal of Virology* **2004**, 78 (22), 12689-12693.
32. Wilen, C. B.; Tilton, J. C.; Doms, R. W., HIV: cell binding and entry. *Cold Spring Harbor Perspectives in Medicine* 2 (8), a006866.
33. Deng, H.; Liu, R.; Ellmeier, W.; Choe, S.; Unutmaz, D.; Burkhart, M.; Di Marzio, P.; Marmon, S.; Sutton, R. E.; Hill, C. M.; Davis, C. B.; Peiper, S. C.; Schall, T. J.; Littman, D. R.; Landau, N. R., Identification of a major co-receptor for primary isolates of HIV-1. *Nature* **1996**, 381 (6584), 661-6.
34. Feng, Y.; Broder, C. C.; Kennedy, P. E.; Berger, E. A., HIV-1 entry cofactor: functional cDNA cloning of a seven-transmembrane, G protein-coupled receptor. *Science* **1996**, 272 (5263), 872-7.
35. Derdeyn, C. A.; Hunter, E., Viral characteristics of transmitted HIV. *Curr Opin HIV AIDS* **2008**, 3 (1), 16-21.
36. Kitchen, S. G.; Zack, J. A., Distribution of the Human Immunodeficiency Virus Coreceptors CXCR4 and CCR5 in Fetal Lymphoid Organs: Implications for Pathogenesis in Utero. *AIDS Res Hum Retroviruses* **1999**, 15 (2), 143-148.
37. Poveda, E.; Briz, V.; Quinones-Mateu, M.; Soriano, V., HIV tropism: diagnostic tools and implications for disease progression and treatment with entry inhibitors. *AIDS* **2006**, 20 (10), 1359-67.

38. Zhang, L.; He, T.; Talal, A.; Wang, G.; Frankel, S. S.; Ho, D. D., In Vivo Distribution of the Human Immunodeficiency Virus/Simian Immunodeficiency Virus Coreceptors: CXCR4, CCR3, and CCR5. *Journal of Virology* **1998**, 72 (6), 5035-5045.
39. Gomez, C.; Hope, T. J., The ins and outs of HIV replication. *Cellular Microbiology* **2005**, 7 (5), 621-626.
40. National Institute of Allergy and Infectious Diseases. HIV Replication Cycle. <https://www.niaid.nih.gov/diseases-conditions/hiv-replication-cycle> (accessed April 15th, 2019).
41. Marmor, M.; Hertzmark, K.; Thomas, S. M.; Halkitis, P. N.; Vogler, M., Resistance to HIV infection. *Journal of urban health : bulletin of the New York Academy of Medicine* **2006**, 83 (1), 5-17.
42. Anderson, J.; Akkina, R., Complete knockdown of CCR5 by lentiviral vector-expressed siRNAs and protection of transgenic macrophages against HIV-1 infection. *Gene Therapy* **2007**, 14, 1287.
43. Hütter, G.; Nowak, D.; Mossner, M.; Ganepola, S.; Müßig, A.; Allers, K.; Schneider, T.; Hofmann, J.; Kücherer, C.; Blau, O.; Blau, I. W.; Hofmann, W. K.; Thiel, E., Long-Term Control of HIV by CCR5 Delta32/Delta32 Stem-Cell Transplantation. *New England Journal of Medicine* **2009**, 360 (7), 692-698.
44. Gupta, R. K.; Abdul-Jawad, S.; McCoy, L. E.; Mok, H. P.; Peppas, D.; Salgado, M.; Martinez-Picado, J.; Nijhuis, M.; Wensing, A. M. J.; Lee, H.; Grant, P.; Nastouli, E.; Lambert, J.; Pace, M.; Salasc, F.; Monit, C.; Innes, A. J.; Muir, L.; Waters, L.; Frater, J.; Lever, A. M. L.; Edwards, S. G.; Gabriel, I. H.; Olavarria, E., HIV-1 remission following CCR5^{32/32} haematopoietic stem-cell transplantation. *Nature* **2019**.
45. Mitsuya, H.; Weinhold, K. J.; Furman, P. A.; St Clair, M. H.; Lehrman, S. N.; Gallo, R. C.; Bolognesi, D.; Barry, D. W.; Broder, S., 3'-Azido-3'-deoxythymidine (BW A509U): an antiviral agent that inhibits the infectivity and cytopathic effect of human T-lymphotropic virus type III/lymphadenopathy-associated virus in vitro. *Proceedings of the National Academy of Sciences* **1985**, 82 (20), 7096-7100.
46. Fischl, M. A.; Richman, D. D.; Grieco, M. H.; Gottlieb, M. S.; Volberding, P. A.; Laskin, O. L.; Leedom, J. M.; Groopman, J. E.; Mildvan, D.; Schooley, R. T.; Jackson, G. G.; Durack, D. T.; King, D., The Efficacy of Azidothymidine (AZT) in the Treatment of Patients with AIDS and AIDS-Related Complex. *New England Journal of Medicine* **1987**, 317 (4), 185-191.

47. Richman, D.; Rosenthal, A. S.; Skoog, M.; Eckner, R. J.; Chou, T. C.; Sabo, J. P.; Merluzzi, V. J., BI-RG-587 is active against zidovudine-resistant human immunodeficiency virus type 1 and synergistic with zidovudine. *Antimicrobial agents and chemotherapy* **1991**, *35* (2), 305-308.
48. Richman, D. D.; Havlir, D.; Corbeil, J.; Looney, D.; Ignacio, C.; Spector, S. A.; Sullivan, J.; Cheeseman, S.; Barringer, K.; Pauletti, D., Nevirapine resistance mutations of human immunodeficiency virus type 1 selected during therapy. *Journal of Virology* **1994**, *68* (3), 1660-1666.
49. Montaner, J. S. G.; Reiss, P.; Cooper, D.; Vella, S.; Harris, M.; Conway, B.; Wainberg, M. A.; Smith, D.; Robinson, P.; Hall, D.; Myers, M.; Lange, J. M. A.; Group, f. t. I. S., A Randomized, Double-blind Trial Comparing Combinations of Nevirapine, Didanosine, and Zidovudine for HIV-Infected PatientsThe INCAS Trial. *JAMA* **1998**, *279* (12), 930-937.
50. Collier, A. C.; Coombs, R. W.; Schoenfeld, D. A.; Bassett, R. L.; Timpone, J.; Baruch, A.; Jones, M.; Facey, K.; Whitacre, C.; McAuliffe, V. J.; Friedman, H. M.; Merigan, T. C.; Reichman, R. C.; Hooper, C.; Corey, L., Treatment of Human Immunodeficiency Virus Infection with Saquinavir, Zidovudine, and Zalcitabine. *New England Journal of Medicine* **1996**, *334* (16), 1011-1018.
51. National Institute of Allergy and Infectious Diseases. FDA-approved HIV medicines.
52. Nagashima, K. A.; Thompson, D. A.; Rosenfield, S. I.; Maddon, P. J.; Dragic, T.; Olson, W. C., Human immunodeficiency virus type 1 entry inhibitors PRO 542 and T-20 are potently synergistic in blocking virus-cell and cell-cell fusion. *J Infect Dis* **2001**, *183* (7), 1121-5.
53. Tremblay, C. L.; Kollmann, C.; Giguel, F.; Chou, T. C.; Hirsch, M. S., Strong in vitro synergy between the fusion inhibitor T-20 and the CXCR4 blocker AMD-3100. *J Acquir Immune Defic Syndr* **2000**, *25* (2), 99-102.
54. Lalezari, J. P.; Eron, J. J.; Carlson, M.; Cohen, C.; DeJesus, E.; Arduino, R. C.; Gallant, J. E.; Volberding, P.; Murphy, R. L.; Valentine, F.; Nelson, E. L.; Sista, P. R.; Dusek, A.; Kilby, J. M., A phase II clinical study of the long-term safety and antiviral activity of enfuvirtide-based antiretroviral therapy. *AIDS* **2003**, *17* (5), 691-8.
55. Baba, M.; Nishimura, O.; Kanzaki, N.; Okamoto, M.; Sawada, H.; Iizawa, Y.; Shiraishi, M.; Aramaki, Y.; Okonogi, K.; Ogawa, Y.; Meguro, K.; Fujino, M., A small-molecule, nonpeptide CCR5 antagonist with highly potent and selective anti-HIV-1 activity. *Proc Natl Acad Sci U S A* **1999**, *96* (10), 5698-5703.

56. Rosenkilde, M. M.; Gerlach, L.-O.; Jakobsen, J. S.; Skerlj, R. T.; Bridger, G. J.; Schwartz, T. W., Molecular Mechanism of AMD3100 Antagonism in the CXCR4 Receptor: transfer of binding site to the cxcr3 receptor. *Journal of Biological Chemistry* **2004**, 279 (4), 3033-3041.
57. Moore, J. P.; Sattentau, Q. J.; Klasse, P. J.; Burkly, L. C., A monoclonal antibody to CD4 domain 2 blocks soluble CD4-induced conformational changes in the envelope glycoproteins of human immunodeficiency virus type 1 (HIV-1) and HIV-1 infection of CD4+ cells. *Journal of Virology* **1992**, 66 (8), 4784-4793.
58. Emu, B.; Fessel, J.; Schrader, S.; Kumar, P.; Richmond, G.; Win, S.; Weinheimer, S.; Marsolais, C.; Lewis, S., Phase 3 Study of Ibalizumab for Multidrug-Resistant HIV-1. *New England Journal of Medicine* **2018**, 379 (7), 645-654.
59. Steitz, T. A., Hot Papers - Biochemistry - Crystal-Structure at 3.5 Angstrom Resolution of Hiv-1 Reverse-Transcriptase Complexed with an Inhibitor by Kohlstaedt, L.A., Wang, J., Friedman, J.M., Et-Al. *Scientist* **1993**, 7 (17), 16-16.
60. Jacobomolina, A.; Ding, J. P.; Nanni, R. G.; Clark, A. D.; Lu, X. D.; Tantillo, C.; Williams, R. L.; Kamer, G.; Ferris, A. L.; Clark, P.; Hizi, A.; Hughes, S. H.; Arnold, E., Crystal-Structure of Human-Immunodeficiency-Virus Type-1 Reverse-Transcriptase Complexed with Double-Stranded DNA at 3.0 Angstrom Resolution Shows Bent DNA. *Proc Natl Acad Sci U S A* **1993**, 90 (13), 6320-6324.
61. Tanese, N.; Goff, S. P., Domain-Structure of the Moloney Murine Leukemia-Virus Reverse-Transcriptase - Mutational Analysis and Separate Expression of the DNA-Polymerase and RNase-H Activities. *Proc Natl Acad Sci U S A* **1988**, 85 (6), 1777-1781.
62. Namasivayam, V.; Vanangamudi, M.; Kramer, V. G.; Kurup, S.; Zhan, P.; Liu, X.; Kongsted, J.; Byrareddy, S. N., The Journey of HIV-1 Non-Nucleoside Reverse Transcriptase Inhibitors (NNRTIs) from Lab to Clinic. *Journal of Medicinal Chemistry* **2018**.
63. Cihlar, T.; Ray, A. S., Nucleoside and nucleotide HIV reverse transcriptase inhibitors: 25 years after zidovudine. *Antiviral Research* **2010**, 85 (1), 39-58.
64. Furman, P. A.; Fyfe, J. A.; Stclair, M. H.; Weinhold, K.; Rideout, J. L.; Freeman, G. A.; Lehrman, S. N.; Bolognesi, D. P.; Broder, S.; Mitsuya, H.; Barry, D. W., Phosphorylation of 3'-Azido-3'-Deoxythymidine and Selective Interaction of the 5'-Triphosphate with Human-Immunodeficiency-Virus Reverse-Transcriptase. *Proc Natl Acad Sci U S A* **1986**, 83 (21), 8333-8337.

65. Sarafianos, S. G.; Clark, A. D.; Das, K.; Tuske, S.; Birktoft, J. J.; Ilankumaran, P.; Ramesha, A. R.; Sayer, J. M.; Jerina, D. M.; Boyer, P. L.; Hughes, S. H.; Arnold, E., Structures of HIV-1 reverse transcriptase with pre- and post-translocation AZTMP-terminated DNA. *Embo Journal* **2002**, *21* (23), 6614-6624.
66. Sluis-Cremer, N.; Tachedjian, G., Mechanisms of inhibition of HIV replication by non-nucleoside reverse transcriptase inhibitors. *Virus Research* **2008**, *134* (1-2), 147-156.
67. Adams, J.; Patel, N.; Mankaryous, N.; Tadros, M.; Miller, C. D., Nonnucleoside Reverse Transcriptase Inhibitor Resistance and the Role of the Second-Generation Agents. *Annals of Pharmacotherapy* **2010**, *44* (1), 157-165.
68. Hazuda, D.; Iwamoto, M.; Wenning, L., Emerging Pharmacology: Inhibitors of Human Immunodeficiency Virus Integration. *Annual Review of Pharmacology and Toxicology* **2009**, *49*, 377-394.
69. Espeseth, A. S.; Felock, P.; Wolfe, A.; Witmer, M.; Grobler, J.; Anthony, N.; Egbertson, M.; Melamed, J. Y.; Young, S.; Hamill, T.; Cole, J. L.; Hazuda, D. J., HIV-1 integrase inhibitors that compete with the target DNA substrate define a unique strand transfer conformation for integrase. *Proc Natl Acad Sci U S A* **2000**, *97* (21), 11244-11249.
70. Tozser, J.; Oroszlan, S., Proteolytic Events of HIV-1 Replication as Targets for Therapeutic Intervention. *Current Pharmaceutical Design* **2003**, *9* (22), 1803-1815.
71. Kohl, N. E.; Emini, E. A.; Schleif, W. A.; Davis, L. J.; Heimbach, J. C.; Dixon, R. A. F.; Scolnick, E. M.; Sigal, I. S., Active Human Immunodeficiency Virus Protease Is Required for Viral Infectivity. *Proc Natl Acad Sci U S A* **1988**, *85* (13), 4686-4690.
72. Craig, J. C.; Duncan, I. B.; Hockley, D.; Grief, C.; Roberts, N. A.; Mills, J. S., Antiviral properties of Ro 31-8959, an inhibitor of human immunodeficiency virus (HIV) proteinase. *Antiviral Res* **1991**, *16* (4), 295-305.
73. Robbins, A. H.; Coman, R. M.; Bracho-Sanchez, E.; Fernandez, M. A.; Gilliland, C. T.; Li, M.; Agbandje-McKenna, M.; Wlodawer, A.; Dunn, B. M.; McKenna, R., Structure of the unbound form of HIV-1 subtype A protease: comparison with unbound forms of proteases from other HIV subtypes. *Acta crystallographica. Section D, Biological crystallography* **2010**, *66*, 233-242.
74. Brik, A.; Wong, C.-H., HIV-1 protease: mechanism and drug discovery. *Organic & Biomolecular Chemistry* **2003**, *1* (1), 5-14.
75. Gustchina, A.; Weber, I. T., Comparison of inhibitor binding in HIV-1 protease and in non-viral aspartic proteases: the role of the flap. *FEBS Lett* **1990**, *269* (1), 269-72.

76. Miller, M.; Schneider, J.; Sathyanarayana, B. K.; Toth, M. V.; Marshall, G. R.; Clawson, L.; Selk, L.; Kent, S. B.; Wlodawer, A., Structure of complex of synthetic HIV-1 protease with a substrate-based inhibitor at 2.3 Å resolution. *Science* **1989**, *246* (4934), 1149-52.
77. Brik, A.; Wong, C. H., HIV-1 protease: mechanism and drug discovery. *Organic & Biomolecular Chemistry* **2003**, *1* (1), 5-14.
78. Gustchina, A.; Sansom, C.; Prevost, M.; Richelle, J.; Wodak, S. Y.; Wlodawer, A.; Weber, I. T., Energy calculations and analysis of HIV-1 protease-inhibitor crystal structures. *Protein Engineering, Design and Selection* **1994**, *7* (3), 309-316.
79. Ghosh, A. K.; Osswald, H. L.; Prato, G., Recent Progress in the Development of HIV-1 Protease Inhibitors for the Treatment of HIV/AIDS. *Journal of Medicinal Chemistry* **2016**, *59* (11), 5172-5208.
80. Krohn, A.; Redshaw, S.; Ritchie, J. C.; Graves, B. J.; Hatada, M. H., Novel binding mode of highly potent HIV-proteinase inhibitors incorporating the (R)-hydroxyethylamine isostere. *Journal of Medicinal Chemistry* **1991**, *34* (11), 3340-3342.
81. Tie, Y.; Kovalevsky, A. Y.; Boross, P.; Wang, Y.-F.; Ghosh, A. K.; Tozser, J.; Harrison, R. W.; Weber, I. T., Atomic resolution crystal structures of HIV-1 protease and mutants V82A and I84V with saquinavir. *Proteins: Structure, Function, and Bioinformatics* **2007**, *67* (1), 232-242.
82. Kempf, D. J.; Marsh, K. C.; Denissen, J. F.; McDonald, E.; Vasavanonda, S.; Flentge, C. A.; Green, B. E.; Fino, L.; Park, C. H.; Kong, X. P., ABT-538 is a potent inhibitor of human immunodeficiency virus protease and has high oral bioavailability in humans. *Proceedings of the National Academy of Sciences* **1995**, *92* (7), 2484-2488.
83. Kumar, G. N.; Rodrigues, A. D.; Buko, A. M.; Denissen, J. F., Cytochrome P450-mediated metabolism of the HIV-1 protease inhibitor ritonavir (ABT-538) in human liver microsomes. *Journal of Pharmacology and Experimental Therapeutics* **1996**, *277* (1), 423-431.
84. Vacca, J. P.; Dorsey, B. D.; Schleif, W. A.; Levin, R. B.; McDaniel, S. L.; Darke, P. L.; Zugay, J.; Quintero, J. C.; Blahy, O. M.; Roth, E., L-735,524: an orally bioavailable human immunodeficiency virus type 1 protease inhibitor. *Proceedings of the National Academy of Sciences* **1994**, *91* (9), 4096-4100.
85. Kaldor, S. W.; Kalish, V. J.; Davies, J. F.; Shetty, B. V.; Fritz, J. E.; Appelt, K.; Burgess, J. A.; Campanale, K. M.; Chirgadze, N. Y.; Clawson, D. K.; Dressman, B. A.; Hatch, S. D.; Khalil, D. A.; Kosa, M. B.; Lubbehusen, P. P.; Muesing, M. A.; Patick, A. K.; Reich, S. H.; Su, K. S.; Tatlock, J. H., Viracept (Nelfinavir Mesylate, AG1343): A Potent, Orally Bioavailable Inhibitor of HIV-1 Protease. *Journal of Medicinal Chemistry* **1997**, *40* (24), 3979-3985.

86. Kim, E. E.; Baker, C. T.; Dwyer, M. D.; Murcko, M. A.; Rao, B. G.; Tung, R. D.; Navia, M. A., Crystal structure of HIV-1 protease in complex with VX-478, a potent and orally bioavailable inhibitor of the enzyme. *Journal of the American Chemical Society* **1995**, *117* (3), 1181-1182.
87. Sham, H. L.; Kempf, D. J.; Molla, A.; Marsh, K. C.; Kumar, G. N.; Chen, C.-M.; Kati, W.; Stewart, K.; Lal, R.; Hsu, A.; Betebenner, D.; Korneyeva, M.; Vasavanonda, S.; McDonald, E.; Saldivar, A.; Wideburg, N.; Chen, X.; Niu, P.; Park, C.; Jayanti, V.; Grabowski, B.; Granneman, G. R.; Sun, E.; Japour, A. J.; Leonard, J. M.; Plattner, J. J.; Norbeck, D. W., ABT-378, a Highly Potent Inhibitor of the Human Immunodeficiency Virus Protease. *Antimicrobial agents and chemotherapy* **1998**, *42* (12), 3218-3224.
88. Robinson, B. S.; Riccardi, K. A.; Gong, Y.-f.; Guo, Q.; Stock, D. A.; Blair, W. S.; Terry, B. J.; Deminie, C. A.; Djang, F.; Colonno, R. J.; Lin, P.-f., BMS-232632, a Highly Potent Human Immunodeficiency Virus Protease Inhibitor That Can Be Used in Combination with Other Available Antiretroviral Agents. *Antimicrobial agents and chemotherapy* **2000**, *44* (8), 2093-2099.
89. Doyon, L.; Tremblay, S.; Bourgon, L.; Wardrop, E.; Cordingley, M. G., Selection and characterization of HIV-1 showing reduced susceptibility to the non-peptidic protease inhibitor tipranavir. *Antiviral Research* **2005**, *68* (1), 27-35.
90. Ghosh, A. K.; Kincaid, J. F.; Cho, W.; Walters, D. E.; Krishnan, K.; Hussain, K. A.; Koo, Y.; Cho, H.; Rudall, C.; Holland, L.; Buthod, J., Potent HIV protease inhibitors incorporating high-affinity P2-ligands and (R)-(hydroxyethylamino)sulfonamide isostere. *Bioorg Med Chem Lett* **1998**, *8* (6), 687-690.
91. Organization, W. H., Global action plan on HIV drug resistance 2017–2021. **2017**.
92. Das, K.; Arnold, E., HIV-1 reverse transcriptase and antiviral drug resistance. Part 1. *Current Opinion in Virology* **2013**, *3* (2), 111-118.
93. Turner, D.; Schapiro, J. M.; Brenner, B. G.; Wainberg, M. A., The influence of protease inhibitor resistance profiles on selection of HIV therapy in treatment-naïve patients. *Antiviral Therapy* **2004**, *9* (3), 301-314.
94. Ghosh, A. K.; Anderson, D. D.; Weber, I. T.; Mitsuya, H., Enhancing Protein Backbone Binding—A Fruitful Concept for Combating Drug-Resistant HIV. *Angewandte Chemie International Edition* **2012**, *51* (8), 1778-1802.
95. Ghosh, A. K.; Chapsal, B. D.; Weber, I. T.; Mitsuya, H., Design of HIV Protease Inhibitors Targeting Protein Backbone: An Effective Strategy for Combating Drug Resistance. *Accounts of Chemical Research* **2008**, *41* (1), 78-86.
96. Cihlar, T.; Fordyce, M., Current status and prospects of HIV treatment. *Current Opinion in Virology* **2016**, *18*, 50-56.

97. Koh, Y.; Amano, M.; Towata, T.; Danish, M.; Leshchenko-Yashchuk, S.; Das, D.; Nakayama, M.; Tojo, Y.; Ghosh, A. K.; Mitsuya, H., In vitro selection of highly darunavir-resistant and replication-competent HIV-1 variants by using a mixture of clinical HIV-1 isolates resistant to multiple conventional protease inhibitors. *Journal of Virology* **2010**, *84* (22), 11961-11969.
98. Ghosh, A. K.; Sridhar, P. R.; Leshchenko, S.; Hussain, A. K.; Li, J.; Kovalevsky, A. Y.; Walters, D. E.; Wedekind, J. E.; Grum-Tokars, V.; Das, D.; Koh, Y.; Maeda, K.; Gatanaga, H.; Weber, I. T.; Mitsuya, H., Structure-Based Design of Novel HIV-1 Protease Inhibitors To Combat Drug Resistance. *Journal of Medicinal Chemistry* **2006**, *49* (17), 5252-5261.
99. Ghosh, A. K.; Gemma, S.; Takayama, J.; Baldrige, A.; Leshchenko-Yashchuk, S.; Miller, H. B.; Wang, Y.-F.; Kovalevsky, A. Y.; Koh, Y.; Weber, I. T.; Mitsuya, H., Potent HIV-1 protease inhibitors incorporating meso-bicyclic urethanes as P2-ligands: structure-based design, synthesis, biological evaluation and protein-ligand X-ray studies. *Organic & Biomolecular Chemistry* **2008**, *6* (20), 3703-3713.
100. Ghosh, A. K.; Chapsal, B. D.; Steffey, M.; Agniswamy, J.; Wang, Y.-F.; Amano, M.; Weber, I. T.; Mitsuya, H., Substituent effects on P2-cyclopentyltetrahydrofuranyl urethanes: design, synthesis, and X-ray studies of potent HIV-1 protease inhibitors. *Bioorg Med Chem Lett* **2012**, *22* (6), 2308-2311.
101. Parai, M. K.; Huggins, D. J.; Cao, H.; Nalam, M. N. L.; Ali, A.; Schiffer, C. A.; Tidor, B.; Rana, T. M., Design, Synthesis, and Biological and Structural Evaluations of Novel HIV-1 Protease Inhibitors To Combat Drug Resistance. *Journal of Medicinal Chemistry* **2012**, *55* (14), 6328-6341.
102. Gao, B.-L.; Zhang, C.-M.; Yin, Y.-Z.; Tang, L.-Q.; Liu, Z.-P., Design and synthesis of potent HIV-1 protease inhibitors incorporating hydroxyprolinamides as novel P2 ligands. *Bioorg Med Chem Lett* **2011**, *21* (12), 3730-3733.
103. Ali, A.; Reddy, G. S. K. K.; Nalam, M. N. L.; Anjum, S. G.; Cao, H.; Schiffer, C. A.; Rana, T. M., Structure-Based Design, Synthesis, and Structure–Activity Relationship Studies of HIV-1 Protease Inhibitors Incorporating Phenylloxazolidinones. *Journal of Medicinal Chemistry* **2010**, *53* (21), 7699-7708.
104. He, M.; Zhang, H.; Yao, X.; Eckart, M.; Zuo, E.; Yang, M., Design, Biologic Evaluation, and SAR of Novel Pseudo-peptide Incorporating Benzheterocycles as HIV-1 Protease Inhibitors. *Chemical Biology & Drug Design* **2010**, *76* (2), 174-180.
105. Grubbs, R. H.; Chang, S., Recent advances in olefin metathesis and its application in organic synthesis. *Tetrahedron* **1998**, *54* (18), 4413-4450.
106. Guan, Y.; Bissantz, C.; Bergstrom, D. E.; Link, A., 1,2,4-Trisubstituted Cyclopentanes as Platforms for Diversity. *Archiv der Pharmazie* **2012**, *345* (9), 677-686.

107. Voorhees, V.; Adams, R., The use of the oxides of platinum for the catalytic reduction of organic compounds. *Journal of the American Chemical Society* **1922**, *44* (6), 1397-1405.
108. Mitsunobu, O., *The Use of Diethyl Azodicarboxylate and Triphenylphosphine in Synthesis and Transformation of Natural Products*. 1981; Vol. 1981, p 1-28.
109. Ghosh, A. K.; Bilcer, G.; Schiltz, G., Syntheses of FDA Approved HIV Protease Inhibitors. *Synthesis* **2001**, *2001* (15), 2203-2229.
110. Kaneko, C.; Sugimoto, A.; Tanaka, S., A Facile One-step Synthesis of cis-2-Cyclopentene- and cis-2-Cyclohexene-1,4-diols from the Corresponding Cyclodienes. *Synthesis* **1974**, *1974* (12), 876-877.
111. Johnson, C. R.; Bis, S. J., Enzymatic asymmetrization of meso-2-cycloalken-1,4-diols and their diacetates in organic and aqueous media. *Tetrahedron Letters* **1992**, *33* (48), 7287-7290.
112. Deardorff, D. R.; Windham, C. Q.; Craney, C. L., Enantioselective hydrolysis of cis-3,5-diacetoxycyclopentene: (1R,4S)-(+)-4-hydroxy-2-cyclopentenyl acetate - (4-cyclopentene-1,3-diol, monoacetate, (1R-cis)-). *Organic Synthesis, Vol 73* **1996**, *73*, 25-35.
113. Nicolaou, K. C.; Baran, P. S.; Zhong, Y. L.; Vega, J. A., Novel IBX-Mediated Processes for the Synthesis of Amino Sugars and Libraries Thereof. *Angewandte Chemie International Edition* **2000**, *39* (14), 2525-2529.
114. Nicolaou, K. C.; Baran, P. S.; Zhong, Y. L.; Barluenga, S.; Hunt, K. W.; Kranich, R.; Vega, J. A., Iodine(V) Reagents in Organic Synthesis. Part 3. New Routes to Heterocyclic Compounds via o-Iodoxybenzoic Acid-Mediated Cyclizations: Generality, Scope, and Mechanism. *Journal of the American Chemical Society* **2002**, *124* (10), 2233-2244.
115. Frigerio, M.; Santagostino, M.; Sputore, S., A User-Friendly Entry to 2-Iodoxybenzoic Acid (IBX). *The Journal of Organic Chemistry* **1999**, *64* (12), 4537-4538.
116. Knapp, S.; Kukkola, P. J.; Sharma, S.; Dhar, T. G. M.; Naughton, A. B. J., Amino alcohol and amino sugar synthesis by benzoylcarbamate cyclization. *The Journal of Organic Chemistry* **1990**, *55* (22), 5700-5710.
117. Ghosh, A. K.; Rao, K. V.; Nyalapatla, P. R.; Osswald, H. L.; Martyr, C. D.; Aoki, M.; Hayashi, H.; Agniswamy, J.; Wang, Y.-F.; Bulut, H.; Das, D.; Weber, I. T.; Mitsuya, H., Design and Development of Highly Potent HIV-1 Protease Inhibitors with a Crown-Like Oxotricyclic Core as the P2-Ligand To Combat Multidrug-Resistant HIV Variants. *Journal of Medicinal Chemistry* **2017**, *60* (10), 4267-4278.
118. Toth, M. V.; Marshall, G. R., A Simple, Continuous Fluorometric Assay for Hiv Protease. *International Journal of Peptide and Protein Research* **1990**, *36* (6), 544-550.

119. Koh, Y.; Nakata, H.; Maeda, K.; Ogata, H.; Bilcer, G.; Devasamudram, T.; Kincaid, J. F.; Boross, P.; Wang, Y.-F.; Tie, Y.; Volarath, P.; Gaddis, L.; Harrison, R. W.; Weber, I. T.; Ghosh, A. K.; Mitsuya, H., Novel bis-Tetrahydrofuranylurethane-Containing Nonpeptidic Protease Inhibitor (PI) UIC-94017 (TMC114) with Potent Activity against Multi-PI-Resistant Human Immunodeficiency Virus In Vitro. *Antimicrobial agents and chemotherapy* **2003**, 47 (10), 3123-3129.
120. Amano, M.; Tojo, Y.; Salcedo-Gómez, P. M.; Campbell, J. R.; Das, D.; Aoki, M.; Xu, C.-X.; Rao, K. V.; Ghosh, A. K.; Mitsuya, H., GRL-0519, a Novel Oxatricyclic Ligand-Containing Nonpeptidic HIV-1 Protease Inhibitor (PI), Potently Suppresses Replication of a Wide Spectrum of Multi-PI-Resistant HIV-1 Variants - In Vitro. *Antimicrobial agents and chemotherapy* **2013**, 57 (5), 2036-2046.
121. Ghosh, A. K.; Williams, J. N.; Ho, R. Y.; Simpson, H. M.; Hattori, S.-i.; Hayashi, H.; Agniswamy, J.; Wang, Y.-F.; Weber, I. T.; Mitsuya, H., Design and Synthesis of Potent HIV-1 Protease Inhibitors Containing Bicyclic Oxazolidinone Scaffold as the P2 Ligands: Structure–Activity Studies and Biological and X-ray Structural Studies. *Journal of Medicinal Chemistry* **2018**, 61 (21), 9722-9737.
122. Tie, Y.; Boross, P. I.; Wang, Y.-F.; Gaddis, L.; Hussain, A. K.; Leshchenko, S.; Ghosh, A. K.; Louis, J. M.; Harrison, R. W.; Weber, I. T., High resolution crystal structures of HIV-1 protease with a potent non-peptide inhibitor (UIC-94017) active against multi-drug-resistant clinical strains. *Journal of Molecular Biology* **2004**, 338 (2), 341-352.
123. Mahalingam, B.; Louis, J. M.; Hung, J.; Harrison, R. W.; Weber, I. T., Structural implications of drug-resistant mutants of HIV-1 protease: High-resolution crystal structures of the mutant protease/substrate analogue complexes. *Proteins: Structure, Function, and Bioinformatics* **2001**, 43 (4), 455-464.
124. Kovalevsky, A. Y.; Liu, F.; Leshchenko, S.; Ghosh, A. K.; Louis, J. M.; Harrison, R. W.; Weber, I. T., Ultra-high resolution crystal structure of HIV-1 protease mutant reveals two binding sites for clinical inhibitor TMC114. *Journal of Molecular Biology* **2006**, 363 (1), 161-173.
125. Ian Storer, R.; Aciro, C.; Jones, L. H., Squaramides: physical properties, synthesis and applications. *Chemical Society Reviews* **2011**, 40 (5), 2330-2346.
126. Chauhan, P.; Mahajan, S.; Kaya, U.; Hack, D.; Enders, D., Bifunctional Amine-Squaramides: Powerful Hydrogen-Bonding Organocatalysts for Asymmetric Domino/Cascade Reactions. *Advanced Synthesis & Catalysis* **2015**, 357 (2-3), 253-281.
127. Kijima, H.; Isobe, Y.; Kiuchi, Y.; Kajita, S.; Saito, T.; Fukushima, K.; Sato, M.; Kimura, M.; Kaneda, Y.; Akashi, T., *Effect of a histamine H2-receptor antagonist pibutidine hydrochloride on the healing of acetic acid-induced gastric ulcer*. 1999; Vol. 27, p 61-68.

128. Cavanagh, R. L.; Buyniski, J. P., Effect of BMY-25368, a potent and long-acting histamine H₂-receptor antagonist, on gastric secretion and aspirin-induced gastric lesions in the dog. *Alimentary Pharmacology & Therapeutics* **1989**, 3 (3), 299-313.
129. Kinney, W. A.; Abou-Gharbia, M.; Garrison, D. T.; Schmid, J.; Kowal, D. M.; Bramlett, D. R.; Miller, T. L.; Tasse, R. P.; Zaleska, M. M.; Moyer, J. A., Design and Synthesis of [2-(8,9-Dioxo-2,6-diazabicyclo[5.2.0]non-1(7)-en-2-yl)- ethyl]phosphonic Acid (EAA-090), a Potent N-Methyl-d-aspartate Antagonist, via the Use of 3-Cyclobutene-1,2-dione as an Achiral α -Amino Acid Bioisostere. *Journal of Medicinal Chemistry* **1998**, 41 (2), 236-246.
130. Dwyer, M. P.; Yu, Y.; Chao, J.; Aki, C.; Chao, J.; Biju, P.; Girijavallabhan, V.; Rindgen, D.; Bond, R.; Mayer-Ezel, R.; Jakway, J.; Hipkin, R. W.; Fossetta, J.; Gonsiorek, W.; Bian, H.; Fan, X.; Terminelli, C.; Fine, J.; Lundell, D.; Merritt, J. R.; Rokosz, L. L.; Kaiser, B.; Li, G.; Wang, W.; Stauffer, T.; Ozgur, L.; Baldwin, J.; Taveras, A. G., Discovery of 2-Hydroxy-N,N-dimethyl-3-{2-[[*(R)*]-1-(5-methylfuran-2-yl)propyl]amino}-3,4-dioxocyclobut-1-enylamino}benzamide (SCH 527123): A Potent, Orally Bioavailable CXCR2/CXCR1 Receptor Antagonist. *Journal of Medicinal Chemistry* **2006**, 49 (26), 7603-7606.
131. Salchow, K.; Bond, M.; Evans, S.; Press, N.; Charlton, S.; Hunt, P.; Bradley, M., A common intracellular allosteric binding site for antagonists of the CXCR2 receptor. *British Journal of Pharmacology* **2010**, 159 (7), 1429-1439.
132. Olmo, F.; Rotger, C.; Ramírez-Macías, I.; Martínez, L.; Marín, C.; Carreras, L.; Urbanová, K.; Vega, M.; Chaves-Lemaur, G.; Sampedro, A.; Rosales, M. J.; Sánchez-Moreno, M.; Costa, A., Synthesis and Biological Evaluation of N,N'-Squaramides with High in Vivo Efficacy and Low Toxicity: Toward a Low-Cost Drug against Chagas Disease. *Journal of Medicinal Chemistry* **2014**, 57 (3), 987-999.
133. Ghosh, A. K.; Chen, Y., Synthesis and optical resolution of high affinity P2-ligands for HIV-1 protease inhibitors. *Tetrahedron Letters* **1995**, 36 (4), 505-508.
134. Griffith, W. P.; Ley, S. V.; Whitcombe, G. P.; White, A. D., Preparation and use of tetra-n-butylammonium per-ruthenate (TBAP reagent) and tetra-n-propylammonium per-ruthenate (TPAP reagent) as new catalytic oxidants for alcohols. *Journal of the Chemical Society, Chemical Communications* **1987**, (21), 1625-1627.

VITA

Jacqueline N. Williams was born in November of 1993 in Detroit, MI. She graduated high school from Lakeview High School in St. Clair Shores, MI in 2011. During that time she also dual enrolled at Macomb Community College in Warren, MI from the summer of 2009 to 2011. This preliminary college exposure introduced her to the field of organic chemistry. She then attended Grand Valley State University in Grand Rapids, MI, for her undergraduate education. Here, she began to further her chemical education and was introduced to organic chemistry and biochemistry research techniques. In 2014, she earned her Bachelor of Science in Chemistry where she moved to West Lafayette, IN to start her graduate work at Purdue University. She joined the research group of Professor Arun K. Ghosh and focused on structure-based approach for the development of HIV-1 protease inhibitors for the treatment of HIV/AIDS.

PUBLICATION

Design and Synthesis of Potent HIV-1 Protease Inhibitors Containing Bicyclic Oxazolidinone Scaffold as the P2 Ligands: Structure–Activity Studies and Biological and X-ray Structural Studies

Arun K. Ghosh,^{*,†,‡} Jacqueline N. Williams,[†] Rachel Y. Ho,[†] Hannah M. Simpson,[†] Shin-ichiro Hattori,[§] Hironori Hayashi,[§] Johnson Agniswamy,[‡] Yuan-Fang Wang,[‡] Irene T. Weber,^{‡,||} and Hiroaki Mitsuya^{§,||,⊥}

[†]Department of Chemistry and Department of Medicinal Chemistry, Purdue University, 560 Oval Drive, West Lafayette, Indiana 47907, United States

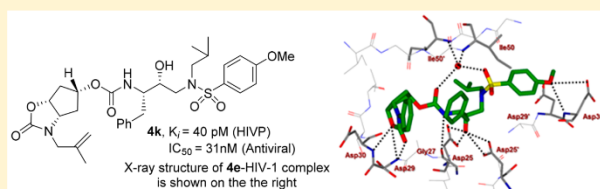
[‡]Department of Biology, Molecular Basis of Disease, Georgia State University, Atlanta, Georgia 30303, United States

[§]Department of Refractory Viral Infections, National Center for Global Health and Medicine Research Institute, Tokyo 162-8655, Japan

^{||}Departments of Infectious Diseases and Hematology, Kumamoto University Graduate School of Biomedical Sciences, Kumamoto 860-8556, Japan

[⊥]Experimental Retrovirology Section, HIV and AIDS Malignancy Branch, National Cancer Institute, National Institutes of Health, Bethesda, Maryland 20892, United States

Supporting Information



ABSTRACT: We have designed, synthesized, and evaluated a new class of potent HIV-1 protease inhibitors with novel bicyclic oxazolidinone derivatives as the P2 ligand. We have developed an enantioselective synthesis of these bicyclic oxazolidinones utilizing a key *o*-iodoxybenzoic acid mediated cyclization. Several inhibitors displayed good to excellent activity toward HIV-1 protease and significant antiviral activity in MT-4 cells. Compound 4k has shown an enzyme K_i of 40 pM and antiviral IC_{50} of 31 nM. Inhibitors 4k and 4l were evaluated against a panel of highly resistant multidrug-resistant HIV-1 variants, and their fold-changes in antiviral activity were similar to those observed with darunavir. Additionally, two X-ray crystal structures of the related inhibitors 4a and 4e bound to HIV-1 protease were determined at 1.22 and 1.30 Å resolution, respectively, and revealed important interactions in the active site that have not yet been explored.

INTRODUCTION

The development of combined antiretroviral therapy (cART) has dramatically improved the treatment of human immunodeficiency virus type 1 (HIV-1) infections and acquired immunodeficiency syndrome (AIDS).^{1,2} HIV-1 protease inhibitors (PIs) are a critically important class of antiretroviral medications in cART.^{3,4} HIV-1 protease plays an essential role in the HIV life cycle and is a primary target for HIV/AIDS treatment.^{5,6} PIs block the ability of HIV-1 protease to cleave polyproteins and prevent the formation of mature virions.^{7,8} While cART drastically improved the course of HIV management and reduced the mortality and morbidity rates of HIV-1 infected individuals, the early FDA-approved PIs

suffer from the traditional problems of peptide-like drugs including poor absorption, metabolic instability, and a number of other debilitating side effects.^{9,10} Perhaps the most alarming problem is the emergence of drug resistance which renders these therapies ineffective.^{11,12} Darunavir (DRV) is the latest FDA-approved PI and is the only PI-drug recommended as a first-line therapy.^{13,14} DRV exhibits a high genetic barrier to resistance and is used for both treatment-experienced and treatment-naïve patients with HIV-1 infection and AIDS.^{15,16} DRV exhibits a dual mechanism of action as (1) an inhibitor of

Received: August 3, 2018
Published: October 24, 2018

catalytically important dimeric HIV-1 protease and (2) an inhibitor of the dimerization of protease monomers.^{17,18} The present first-line cART with boosted PI-based drugs and integrase-inhibitor bound regimens are effective against developing multidrug-resistant HIV-1 variants over an extended period of time. However, there are limitations with regard to drug related side effects, toxicity, and rapid emergence of drug-resistant variants for some patient groups. Therefore, potent and more effective HIV-1 protease inhibitors are necessary for the long-term success of cART.

DRV incorporates a privileged P2 ligand, 3(R),3a(S),6a(R)-bis-tetrahydrofuranyurethane (bis-THF), on an (R)-(hydroxyethylamino)sulfonamide isostere (1, Figure 1).^{19,20}

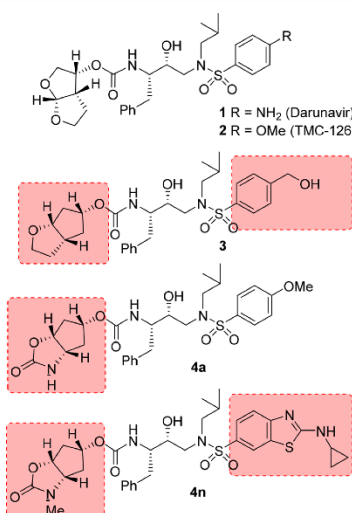


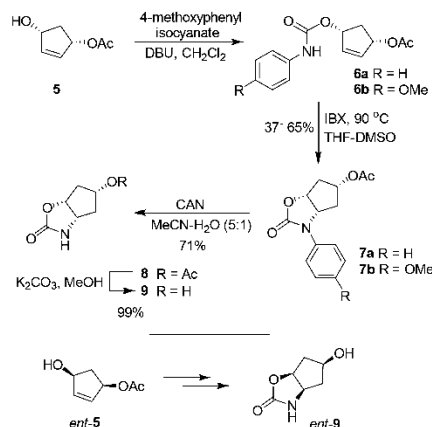
Figure 1. Structures of HIV-1 protease inhibitors 1–4.

The X-ray structural studies of DRV-bound HIV-1 protease revealed a network of hydrogen bonds with backbone atoms like a molecular crab throughout the S2 and S2' subsites.^{21,22} In particular, both oxygens on the bis-THF P2 ligand formed a pair of strong hydrogen bonds with the backbone amide NHs of Asp30 and Asp29. Furthermore, the 4-aminobenzene-sulfonamide P2' ligand also formed a strong hydrogen bond with the Asp30 backbone amide NH. These ligand-binding site interactions are responsible for DRV's superb antiviral and drug-resistance properties. Further modulation of ligand-binding site interactions in the active site of HIV-1 protease led us to develop a range of very potent PIs effective against multidrug-resistant HIV-1 variants.^{23,24} In particular, we have designed inhibitor 3 containing a cyclopentanyltetrahydrofuran (Cp-THF) as the P2 ligand. Upon the basis of the X-ray structure of DRV-bound HIV-1 protease, we now speculate that a bicyclic oxazolidinone derivative can mimic the hydrogen-bonding interactions as well as the van der Waals interactions of the bis-THF and Cp-THF ligands in PIs 1–3 in the S2 subsite. We describe here the design and synthesis of a new class of HIV-1 protease inhibitors that incorporate stereochemically defined bicyclic oxazolidinone scaffolds as the P2 ligands.

CHEMISTRY

For initial investigation, we planned to synthesize an unsubstituted oxazolidinone ligand as represented in inhibitor 4a. The synthesis of the requisite bicyclic oxazolidinone ligand in inhibitor 4a in the optically active form is shown in Scheme 1. Multigram quantities of optically active (1*R*,4*S*)-*cis*-4-

Scheme 1. Synthesis of Bicyclic Oxazolidinone Ligands 9

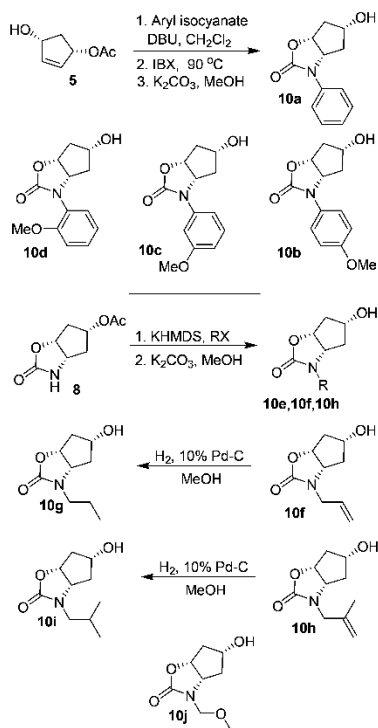


acetoxy-2-cyclopenten-1-ol (–)-5 were prepared from cyclopentadiene using procedures described previously.^{25,26} We utilized a 2-iodoxybenzoic acid (IBX) mediated cyclization protocol developed by Nicolaou and Baran for the synthesis of the bicyclic oxazolidinone ligand.²⁷ Thus, monoacetate 5 was treated with phenyl isocyanate or 4-methoxyphenyl isocyanate and a catalytic amount (10 mol %) of DBU in CH₂Cl₂ at 23 °C for 4 h to provide carbamate derivatives 6a and 6b, respectively, in 81% yield. Treatment of these aryl carbamates with IBX in a mixture (10:1) of THF and DMSO at 90 °C for 24 h afforded oxazolidinones 7a and 7b, respectively, in 37–65% yields. Both *N*-aryl oxazolidinones were obtained as a single isomer (by ¹H NMR analysis). The cleavage of the *p*-methoxyphenyl group on 7b was accomplished by treatment with ceric ammonium nitrate (CAN) in a mixture (5:1) of acetonitrile and water at 23 °C for 1 h to afford the acetate derivative 8 in 71% yield. Removal of the acetate group in 8 with K₂CO₃ in methanol provided the optically active 5-hydroxyhexahydro-2*H*-cyclopenta[*d*]oxazol-2-one 9 in near quantitative yield. To investigate the stereochemical effect on the ligand-binding site interactions, we have also prepared the corresponding enantiomeric oxazolidinone, ent-9. This was prepared from the known optically active (1*S*,4*R*)-*cis*-4-acetoxy-2-cyclopenten-1-ol, ent-5 using the steps as described for compound 9.

For the structure–activity relationship studies, we have prepared a number of substituted oxazolidinone derivatives. Upon the basis of our initial X-ray structure of DRV-bound HIV-1 protease-based models, it appeared that (3*aS*,5*R*,6*aR*)-5-hydroxyhexahydro-2*H*-cyclopenta[*d*]oxazol-2-one stereochemistry would be well-accommodated by the HIV-1 protease active site.²¹ Our preliminary studies of the unsubstituted oxazolidinone-derived inhibitors revealed the preference for the (3*aS*,5*R*,6*aR*)-oxazolidinone stereochemistry as in inhibitor

4a over the enantiomeric ligand in compound **4b**. The synthesis of various substituted oxazolidinone derivatives is shown in Scheme 2. For the synthesis of *N*-phenyl and

Scheme 2. Synthesis of Substituted Oxazolidinone Ligand Alcohols

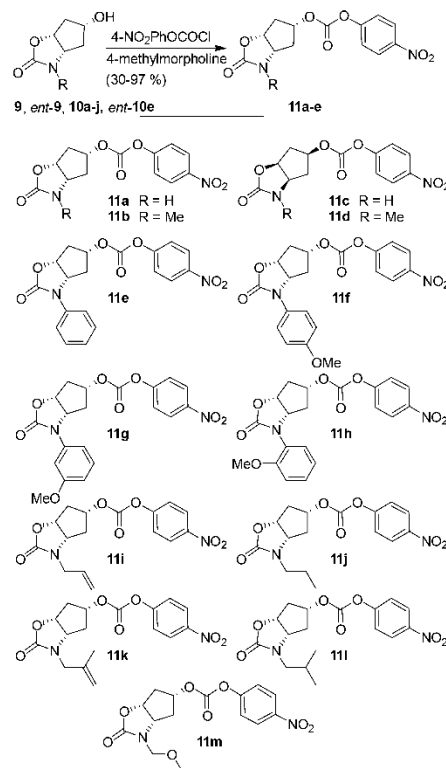


substituted phenyl oxazolidinones, optically active (1*R*,4*S*)-*cis*-4-acetoxy-2-cyclopenten-1-ol **5** was reacted with various aryl isocyanates in the presence of DBU to provide the respective carbamates. IBX-mediated cyclization of these carbamates at 90 °C in a mixture (10:1) of THF and DMSO provided the corresponding bicyclic oxazolidinone derivatives.²⁷ Removal of the acetate group by exposure to K₂CO₃ in methanol at 23 °C afforded the phenyl-substituted oxazolidinone ligand alcohols **10a–d**. For the synthesis of various aliphatic *N*-alkyl derivatives, acetoxy oxazolidinone derivative **8** was alkylated with various alkyl halides. As shown, oxazolidinone **8** was reacted with KHMDS in CH₃CN at 0 °C and the resulting anion was treated with MeI and the reaction mixture was warmed to 23 °C for 1 h to provide the *N*-Me derivative **10e** in 80% isolated yield. Saponification of the resulting ester afforded *N*-Me ligand alcohol **10e** in near quantitative yield. The corresponding enantiomeric *N*-Me derivative *ent*-**10** was prepared from *ent*-**9**. Similarly, *N*-alkylation with allyl iodide followed by removal of the acetate group furnished *N*-allyl derivative **10f** in 60% yield over two steps. Catalytic hydrogenation of **10f** in the presence of catalytic amount of 10% Pd–C in methanol under a hydrogen-filled balloon

furnished the *N*-propyl derivative **10g** in 86% yield. Similarly, alkylation of **8** with 3-bromo-2-methylpropene followed by removal of the acetate provided ligand alcohol **10h** in 84% yield. Catalytic hydrogenation of **10h** furnished saturated ligand alcohol **10i** in 92% yield. For the introduction of the methoxymethyl side chain in ligand alcohol, oxazolidinone **8** was alkylated with KHMDS and chloromethyl methyl ether in THF at 0–23 °C for 1 h, providing the corresponding alkylated product. Removal of acetate group gave ligand alcohol **10j** in 33% yield over two steps.

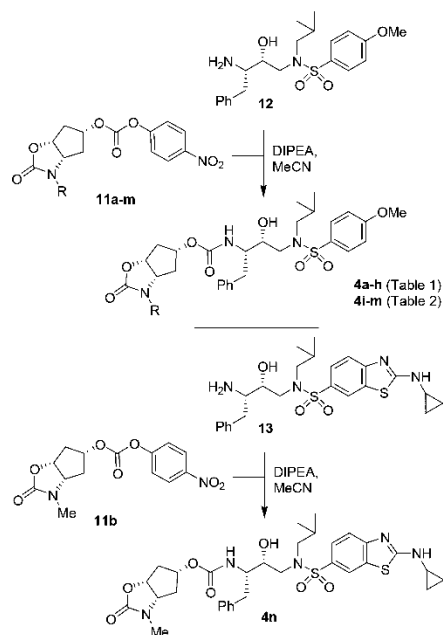
The diverse optically active ligand alcohols **9**, *ent*-**9**, **10a–j**, and *ent*-**10e** were converted to the corresponding activated mixed carbonates.²⁸ As shown in Scheme 3, treatment of ligand alcohols with 4-nitrophenyl chloroformate and 4-methylmorpholine in CH₂Cl₂ at 0 °C for 12 h provided carbonates **11a–m** in good to excellent yields (30–97%).

Scheme 3. Synthesis of Activated Carbonates of Oxazolidinone Ligands



The syntheses of various inhibitors containing hydroxyethylaminesulfonamide isosteres with 4-methoxysulfonamide as the P2' ligands are shown in Scheme 4. Reaction of known amine **12**²⁸ with activated carbonate **11a** provided inhibitor **4a** in good yield. Similarly, reaction of carbonates **11b–m** and amine **12** provided inhibitors **4b–m**. Inhibitor **4n**

Scheme 4. Synthesis of HIV-1 Protease Inhibitors 4a–n



was prepared by reaction of known amine **13**²⁹ and carbonate **11b** as described above.

RESULTS AND DISCUSSION

We first evaluated all new inhibitors in an HIV-1 protease inhibitory assay according to the protocol described by Toth and Marshall.³⁰ Inhibitors that displayed potent K_i values (<1 nM), were then selected for further evaluation in an antiviral assay in MT-4 human T-lymphocytes exposed to HIV-1_{NL4-3}, and the antiviral assay was carried out as described previously.¹⁵ Inhibitor structures and biological results are shown in Tables 1 and 2. As can be seen in Table 1, inhibitor **4a** with (3*S*,5*R*,6*R*)-2-oxohexahydro-2*H*-cyclopenta[*d*]-5-oxazolyl urethane as the P2 ligand exhibited very potent enzyme inhibitory and antiviral activity. The corresponding enantiomeric ligand in inhibitor **4b** showed an over 1000-fold reduction of enzyme inhibitory activity. Also, this inhibitor did not exhibit any appreciable antiviral activity. We then examined the effect of an *N*-alkyl group and stereochemical effects on potency. Inhibitor **4c** containing (3*S*,5*R*,6*R*)-oxazolidinone with an *N*-Me group showed an enzyme inhibitory K_i of 0.03 nM. This inhibitor showed slight improvement of antiviral activity (36 nM, entry 3). Inhibitor **4d**, containing the enantiomeric *N*-Me oxazolidinone derivative, displayed substantial reduction of enzyme inhibitory as well as antiviral activity. This result is consistent with activity observed for the unsubstituted ligand in inhibitor **4b** (entry 2). The stereochemical preference for (3*S*,5*R*,6*R*)-oxazolidinone is also consistent with our preliminary models. All further SAR studies were carried out with (3*S*,5*R*,6*R*)-oxazolidinone derived compounds. We then examined the effect of steric

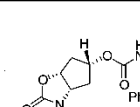
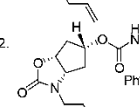
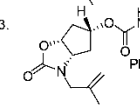
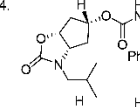
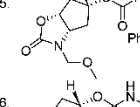
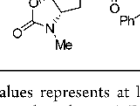
Table 1. HIV-1 Protease Inhibitory and Antiviral Activity of PIs 4a–h

| Entry | Inhibitor | K_i (nM) ^a | IC ₅₀ (nM) ^b |
|-------|-----------|-------------------------|------------------------------------|
| 1. | | 0.0012 | 48.3 |
| 2. | | 1.33 | >1000 |
| 3. | | 0.03 | 36 |
| 4. | | 0.16 | 436 |
| 5. | | 0.33 | >1000 |
| 6. | | 0.63 | >1000 |
| 7. | | 92.8 | >1000 |
| 8. | | 0.08 | 251 |

^a K_i values represents at least four data points. Standard error in all cases was less than 7%. Darunavir exhibited $K_i = 16$ pM. ^bValues are the mean of at least three experiments. Standard error in all cases was less than 5%. Darunavir exhibited antiviral IC₅₀ = 3.2 nM, saquinavir IC₅₀ = 21 nM.

bulk on the oxazolidinone nitrogen. Incorporation of an *N*-phenyl derivative in inhibitor **4e** (entry 5) resulted in significant loss of enzyme inhibitory activity. This inhibitor also displayed no appreciable antiviral activity. To promote hydrogen bonding interactions in the S2 subsite of HIV-1 protease, we incorporated a methoxy substituent on the *N*-phenyl ring. As shown, both *p*-methoxy and *m*-methoxy derivatives show reduction of enzymatic K_i values, particularly

Table 2. HIV-1 Protease Inhibitory and Antiviral Activity of PIs 4i–n

| Entry | Inhibitor | K_i (nM) ^a | IC ₅₀ (nM) ^b |
|-------|---|-------------------------|------------------------------------|
| 1. |  | 0.016 | 369 |
| 2. |  | 0.14 | 447 |
| 3. |  | 0.04 | 31 |
| 4. |  | 0.16 | 41 |
| 5. |  | 0.016 | 84 |
| 6. |  | 0.19 | 28 |

^a K_i values represents at least four data points. Standard error in all cases was less than 7%. Darunavir exhibited $K_i = 16$ pM. ^bValues are the mean of at least three experiments. Standard error in all cases was less than 5%. Darunavir exhibited antiviral IC₅₀ = 3.2 nM, saquinavir IC₅₀ = 21 nM.

for inhibitor 4g (entry 7). Inhibitor 4h with a 2-methoxy substituent on the *N*-phenyl ring, showed an improvement in enzyme inhibitory and antiviral activity (entry 8).

We then investigated the effect of a sterically demanding alkyl chain on the oxazolidinone ring. The results are shown in

Table 2. Inhibitor 4i with an *N*-allyl oxazolidinone as the P2 ligand showed a comparable enzyme inhibitory K_i as the *N*-methyl derivative 4c (entry 3). However, there is a 10-fold reduction of antiviral activity compared to the corresponding *N*-methyl derivative 4c. The corresponding inhibitor 4j with *N*-propyl side chain showed a 10-fold reduction of HIV-1 protease inhibitory activity compared to *N*-allyl derivative 4i. There was a slight reduction of antiviral activity as well. Incorporation of a sterically demanding branched chain *N*-methylallyl group in inhibitor 4k resulted in good enzyme inhibitory activity as well as antiviral activity with an IC₅₀ value of 31 nM (entry 3). Inhibitor 4l with a saturated isobutyl side chain resulted in slight reduction of both enzyme K_i and antiviral activity compared to inhibitor 4k (entry 4). We have introduced an *N*-methoxymethyl side chain in an effort to promote hydrogen bonding with the methoxyl oxygen in the S2 subsite. Inhibitor 4m showed very potent enzyme inhibitory activity. We recently demonstrated the potency enhancing effect of the cyclopropylaminobenzothiazole group as a P2' ligand as it forms additional hydrogen bonding and van der Waals interactions in the S2' subsite. We, therefore, synthesized inhibitor 4n with a *N*-methyloxazolidinone as the P2 ligand and cyclopropylaminobenzothiazole as the P2' ligand. However, there was no significant change in potency for this inhibitor compared to inhibitor 4c (entry 3, Table 1) with a 4-methoxyphenylsulfonamide as the P2' ligand.

PIs continue to be an important in current ART regimens, and in particular, they are extensively used for the treatment of naive and experienced HIV/AIDS patients. However, heavily ART regimen-experienced HIV/AIDS patients show drug failure with current PIs including DRV.^{31,32} Therefore, one of the main design objectives is to develop new PIs that maintain potency against a variety of existing multi-PI-resistant HIV-1 variants. In preliminary studies, we examined the activity of two potent oxazolidinone containing PIs 4k and 4l against a panel of HIV-1 variants that had been selected in vitro with three widely used FDA-approved PIs, ATV, LPV, and APV. Each of these HIV-1 variants was selected in vitro by propagating HIV-1_{NL4-3} in the presence of increasing concentrations of each PI (up to 5 μ M) in MT-4 cells as described by us previously.^{31,33}

The viruses used in the present work were obtained, propagated, and titrated as described by us previously.³⁴ Also, the IC₅₀ values were determined as previously described and the names of HIV-1 strains used are described in the very left

Table 3. Comparison of the Antiviral Activity of 4k and 4l and Other PIs against Highly PI-Resistant HIV-1 Variants

| virus ^a | mean IC ₅₀ \pm SD (nM) ^b | | | | | |
|-------------------------------------|--|-------------|-----------------|--------------------|-------------------|------------------|
| | LPV | APV | ATV | DRV | 4k | 4l |
| HIV-1 _{NL4-3} | 6.0 \pm 0.09 | 431 \pm 3 | 0.89 \pm 0.02 | 3.5 \pm 0.09 | 23 \pm 0.1 | 40 \pm 1 |
| HIV-1 _{ATV^RSPM} | 311 \pm 6 | >1000 | >1000 | 19 \pm 2 (5) | 36 \pm 2 (1) | 33 \pm 2 (1) |
| HIV-1 _{LPV^RSPM} | >1000 | >1000 | 293 \pm 4 | 301 \pm 0.2 (86) | >1000 | 615 \pm 8 (15) |
| HIV-1 _{APV^RSPM} | 218 \pm 1 | >1000 | 2.0 \pm 0.08 | 129 \pm 3 (37) | 261 \pm 15 (11) | 309 \pm 4 (7) |
| HIV-1 _{DRV^RP20} | >1000 | >1000 | >1000 | 169 \pm 15 | >1000 | >1000 |
| HIV-1 _{DRV^RP30} | >1000 | >1000 | >1000 | 426 \pm 26 | >1000 | >1000 |
| HIV-1 _{DRV^RP51} | >1000 | >1000 | >1000 | >1000 | >1000 | >1000 |

^aThe amino acid substitutions identified in the protease-encoding region compared to the wild-type HIV-1_{NL4-3} were L23I, E34Q, K43I, M46I, I50L, G51A, L63P, A71V, V82A, T91A in HIV-1_{ATV^RSPM}; L10F, M46I, I54V, V82A in HIV-1_{LPV^RSPM} or L10F, M46I, I50V, I85V in HIV-1_{APV^RSPM}.

^bThe IC₅₀ (50% effective concentration) values were determined by using MT-4 cells as target cells. MT-4 cells (10⁵/mL) were exposed to 100 TCID₅₀ values of each HIV-1, and the inhibition of p24 Gag protein production by each drug was used as an end point. All assays were conducted in duplicate, and the data shown represent mean values (\pm SD) derived from the results of two independent experiments.

column of Table 3.³⁴ The results are shown in Table 3. As can be seen, PI APV lost significant activity against all multidrug-resistant HIV-1 variants. LPV also lost activity against the three HIV-1 variants. DRV showed relatively better results; however, it too failed to block replication of each of these three variants very effectively. DRV exhibited an IC_{50} value fold-change ranging from 5- to 86-fold. While both oxazolidinone-based new PIs **4k** and **4l** are significantly less potent than DRV, both PIs maintained good activity against all three HIV-1 variants compared to wild-type HIV_{NL4-3}. Inhibitor **4l** showed antiviral activity with IC_{50} values ranging from 33 nM to 615 nM. In particular, its fold-changes in activity are better than any other PIs examined. Both PIs **4k** and **4l** maintained full antiviral activity against highly ATV-resistant HIV-1 variants. While DRV was relatively less potent against HIV-1_{DRV P20} with an IC_{50} value of 169 nM, both oxazolidinone-derived inhibitors **4k** and **4l** failed to block the replication of a highly DRV-resistant HIV-1 variants. In general, oxazolidinone-derived inhibitors showed low cytotoxicity (CC_{50}) values in MT-4 cells. The CC_{50} values were determined as previously described.³⁴ The selectivity index of selected inhibitors is shown in Table 4. In general, our detailed X-ray crystallo-

graphed a single conformation of the inhibitor **4e**. The overall backbones of the two protease dimers were very similar to that of the PR/DRV complex with a RMSD of 0.20 and 0.24 Å for 198 equivalent C α atoms in the complexes with **4a** and **4e**, respectively.^{21,36} The **4a**-bound protease showed the largest shift of approximately 1.0 Å for flap residue Phe53, which may result from the hydrogen bond between the urethane nitrogen of P2 ligand and the carbonyl oxygen of Gly48 in the adjacent β strand of the flap. In contrast, the largest disparity of approximately 0.8 Å at Gly48 in the **4e**-bound protease is likely caused by steric hindrance of the additional phenyl group of P2. The key interactions of inhibitors **4a** and **4e** with HIV-1 protease are highlighted in a stereoview of the active sites in Figures 2 and 3, respectively. Both inhibitors form a water-mediated tetracoordinated hydrogen bonding interaction involving the inhibitor carbonyl oxygen and one of the oxygens of the sulfonamide functionality with amides of Ile50 and Ile50' in the flaps. Such interactions have been observed for many other HIV-1 protease inhibitors.^{3,21,22} With the exception of the P2 ligand, the inhibitors retain the majority of hydrogen bonds observed between DRV and the main chain atoms of the protease. The oxazolidin-2-one P2 group of both inhibitors is embedded between the amide of Asp29 and the carbonyl oxygen of Gly48. The two oxygens of the oxazolidinone group form good hydrogen bond interactions with the amide NH of Asp29 at 3.1–3.2 Å and 2.8–2.9 Å distances for the ring oxygen and the carbonyl oxygen, respectively. The P2 urethane NH of the major conformation of inhibitor **4a** forms a good hydrogen bond with the main chain carbonyl oxygen of Gly48 with distance of 3.0 Å, although the distance lengthened to 3.5 Å, for the minor conformation.

The larger P2 group of **4e** exhibits hydrophobic, C–H $\cdots\pi$, and hydrogen bond interactions with the protease (Figure 4). The phenyl group is sandwiched between the carbonyl oxygen atom of Gly48 and the guanidinium group of Arg8' and forms several C–H $\cdots\pi$ interactions with shortest interatomic distances of 2.8 and 3.5 Å with Gly48 and Arg8', respectively. These short hydrophobic interactions of **4e** are associated with a shift of Gly48 and may be responsible for the higher K_i of this inhibitor compared to that of **4a**. The cyclopentoxazolone group of both inhibitors has van der Waals contacts with Val32, Ile47, Ile50', and Ile84 similar to those seen for the bis-THF P2 ligand of DRV.^{21,22} A comparison of the ligand binding

Table 4. Selectivity Index for Selected Inhibitors^a

| inhibitor | CC_{50} (μ M) | selectivity index ^a |
|-----------|----------------------|--------------------------------|
| 4a | >100 | >2070 |
| 4c | >100 | >2778 |
| 4d | >100 | >229 |
| 4k | >100 | >3226 |
| 4l | >100 | >2439 |
| 4n | 43 | 1536 |

^aEach selectivity index denotes a ratio of CC_{50} to IC_{50} .

graphic studies of structurally related inhibitor **4e**-bound HIV-1 protease provided molecular insight into the binding features responsible for its properties.³⁵

The X-ray structures of wild-type HIV-1 protease cocrystallized with inhibitors **4a** (GRL-034-17A) and **4e** (GRL-042-17A) were refined to resolutions of 1.22 and 1.30 Å resolution with R/R_{free} of 15.5/18.8 and 15.0/18.2%, respectively. The protease dimer complexed with **4a** bound two alternative orientations of inhibitor in the active site cavity with 0.7/0.3 relative occupancy, while the other protease structure

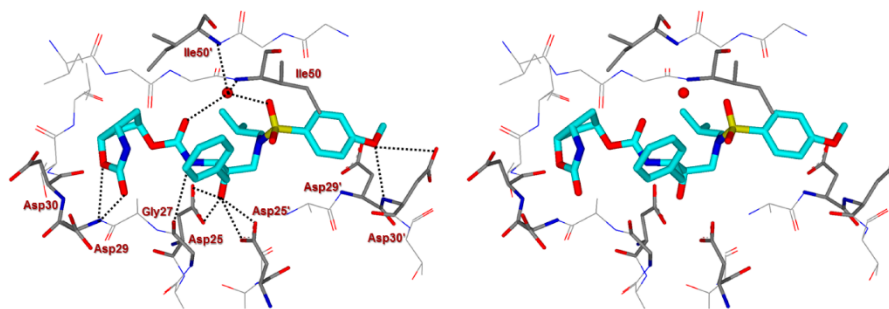


Figure 2. Stereoview of the X-ray crystal structure of inhibitor **4a** (turquoise) in the active site of HIV-1 protease (PDB code 6E9A). The oxazolidinone P2 ligand makes hydrogen-bonding and van der Waals interactions in the S2 subsite. All key hydrogen bonds are shown as black dotted lines.

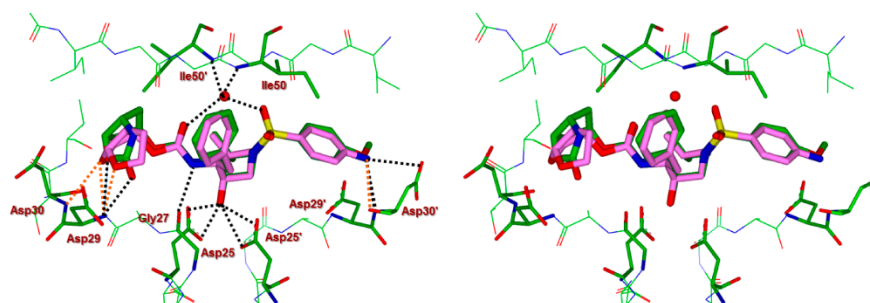


Figure 3. Stereoview of the overlay of X-ray crystal structures of inhibitor **4a** (green) and DRV (magenta) in the active site of HIV-1 protease (PDB code 6E9A for **4a** and PDB code 2IEN for DRV). Both P2 and P2' ligands make strong hydrogen bonds in the S2 subsite. All key hydrogen bonds are shown as black dotted lines for **4a** and orange dotted lines for DRV.

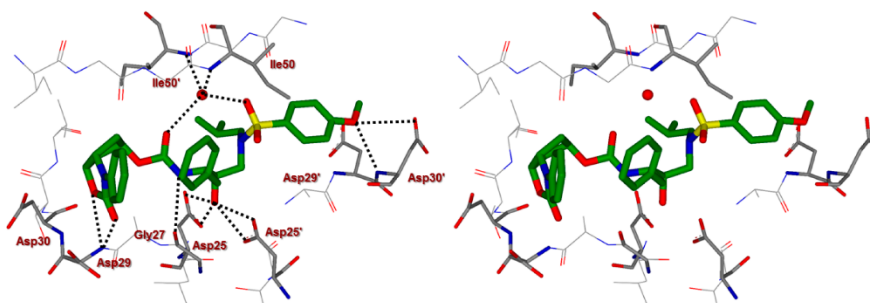


Figure 4. Stereoview of the X-ray crystal structure of inhibitor **4e** (green) in the active site of HIV-1 protease (PDB code 6E7J). The oxazolinone P2 ligand makes hydrogen-bonding and van der Waals interactions in the S2 subsite. All key hydrogen bonds are shown as black dotted lines.

interactions of the bis-THF ligand of darunavir and the oxazolidinone ligand of inhibitor **4a** in the HIV-1 protease active site is shown in the stereoview of Figure 3. The figure was created based upon the X-ray structures of DRV-bound and **4a**-bound HIV-1 protease. It appears that the bis-THF ligand in DRV makes additional hydrogen bonding interactions with the backbone amide NH of Asp30. However, van der Waals interactions of both bicyclic scaffolds are comparable. The bicyclic oxazolidinone moiety for both inhibitors **4a** and **4e** make similar hydrogen bonding interactions in the active site. These interactions contribute to the high enzyme affinity and antiviral activity of the majority of the oxazolidinone-derived inhibitors in our current studies.

CONCLUSION

In summary, we have designed and synthesized a new class of HIV-1 protease inhibitors incorporating bicyclic oxazolidinone as the P2 ligand. We demonstrated that the ligand stereochemistry is very important for potency. Inhibitor **4a** with (3*a*,5*R*,6*a**R*)-oxazolidinone stereochemistry is significantly more potent than the corresponding inhibitor with the enantiomeric ligand. We have examined various *N*-aryl and *N*-alkyl oxazolidinone derivatives to improve potency. It turns out that *N*-alkyl oxazolidinones with small aliphatic alkyl groups can be accommodated by the active site. The *N*-methyl, *N*-isobutenyl, and *N*-isobutyl derivatives **4c**, **4k**, and **4l**, respectively, have shown excellent enzyme inhibitory and

antiviral activity. Inhibitors **4k** and **4l** were evaluated against a panel of multidrug-resistant HIV-1 variants. While both compounds are less potent than darunavir, its fold-changes in activity were similar to those observed with other approved PIs. Both inhibitors **4k** and **4l** maintained near full antiviral potency against ATV-resistant HIV-1 variants. However, these PIs failed to block the replication of highly DRV-resistant HIV-1 variants. The bicyclic oxazolidinones contain three asymmetric centers, and various ligands were synthesized efficiently from readily available, optically active *cis*-4-acetoxycyclopenten-1-ol by formation of the aryl carbamate followed by an IBX-mediated cyclization reaction developed by Nicolaou and Baran. Our X-ray structural studies of inhibitor **4a**- and **4e**-bound HIV-1 protease provided molecular insight into their ligand-binding site interactions. As it turns out, the oxazolidinone oxygen forms a strong hydrogen bonding interaction with Asp29 backbone amide NH. The bicyclic scaffold and the *N*-phenyl ring form van der Waals interactions with residues in the S2 site. The preliminary results of these oxazolidinone-derived inhibitors are very encouraging, and we plan to carry out optimization of ligand-binding site interactions and improve inhibitor potency. Further structural modifications are in progress in our laboratories.

EXPERIMENTAL METHODS

All moisture-sensitive reactions were carried out in oven-dried glassware under an argon atmosphere unless otherwise stated. Anhydrous solvents were obtained as follows: Tetrahydrofuran was

distilled from sodium metal/benzophenone under argon. Dichloromethane was distilled from calcium hydride under argon. All other solvents were reagent grade. Column chromatography was performed using Silicycle SiliFlash F60 230–400 mesh silica gel. Thin layer chromatography was carried out using EMD Millipore TLC silica gel 60 F254 plates. ^1H NMR and ^{13}C NMR spectra were recorded on a Bruker AV-III-400, Bruker DRX500, or Bruker AV-III-800. Low-resolution mass spectra were collected on an LCMS. High-resolution mass spectra were collected by the Purdue University Campus-Wide Mass Spectrometry Center. HPLC analysis and purification were done on an Agilent 1100 series instrument using a YMC Pack ODS-A column of 4.6 mm i.d. for analysis and either 10 mm i.d. or 20 mm i.d. for purification. The purity of all test compounds was determined by HPLC analysis to be $\geq 95\%$ pure.

(3aS,5R,6aR)-2-Oxohexahydro-2H-cyclopenta[d]oxazol-5-yl ((2S,3R)-3-Hydroxy-4-((N-isobutyl-4-methoxyphenyl)sulfonamido)-1-phenylbutan-2-yl)carbamate (4a). To a stirred solution of activated carbonate **11a** (16 mg, 0.05 mmol) in dry acetonitrile (1.5 mL) were added N_2N -diisopropylethylamine (56 μL , 0.3 mmol) and isostere amine **12** (23 mg, 0.06 mmol) at 23 °C under argon atmosphere. The reaction mixture was stirred for 48 h. Upon completion, solvent was removed under reduced pressure. The crude product was purified by silica gel column chromatography (80% EtOAc in hexane) to afford **4a** (13 mg, 44%): ^1H NMR (500 MHz, CD_3OD) δ 7.77 (d, J = 8.8 Hz, 2H), 7.24 (dd, J = 8.9, 6.1 Hz, 4H), 7.19–7.14 (m, 1H), 7.08 (d, J = 8.9 Hz, 2H), 5.12 (t, J = 6.7 Hz, 1H), 5.03–4.96 (m, 1H), 4.33–4.27 (m, 1H), 3.87 (s, 3H), 3.78–3.68 (m, 2H), 3.48–3.37 (m, 1H), 3.03 (ddd, J = 20.0, 13.1, 9.7 Hz, 3H), 2.98–2.83 (m, 2H), 2.57 (dd, J = 13.7, 10.4 Hz, 1H), 2.09–1.94 (m, 3H), 1.90–1.82 (m, 2H), 1.16 (dd, J = 10.7, 6.3 Hz, 1H), 0.95–0.80 (m, 7H). ^{13}C NMR (201 MHz, CDCl_3) δ 162.9, 158.8, 155.5, 138.4, 137.5, 129.6, 128.4, 126.3, 114.3, 81.4, 81.2, 72.8, 58.6, 57.9, 55.6, 54.8, 52.2, 40.0, 39.2, 36.4, 35.9, 29.7, 27.2, 27.1, 20.2, 19.9. LRMS (ESI) m/z : $[\text{M} + \text{H}]^+$ 576.2. HRMS (ESI) m/z : $[\text{M} + \text{Na}]^+$ calcd $\text{C}_{28}\text{H}_{37}\text{N}_5\text{O}_8\text{SNa}$ 598.2194; found 598.2185.

(3aR,5S,6aS)-2-Oxohexahydro-2H-cyclopenta[d]oxazol-5-yl ((2S,3R)-3-Hydroxy-4-((N-isobutyl-4-methoxyphenyl)sulfonamido)-1-phenylbutan-2-yl)carbamate (4b). Compound **11c** (4.8 mg, 0.02 mmol) was treated with isostere amine **12** (7 mg, 0.02 mmol) by following the same procedure outlined for inhibitor **4a** to give inhibitor **4b** (5.3 mg, 60%): ^1H NMR (800 MHz, CD_3OD) δ 7.77 (d, J = 8.9 Hz, 2H), 7.29–7.21 (m, 4H), 7.16 (tt, J = 7.0, 1.7 Hz, 1H), 7.08 (d, J = 8.9 Hz, 2H), 5.16–5.11 (m, 1H), 4.99 (t, J = 4.5 Hz, 1H), 4.35 (t, J = 7.1 Hz, 1H), 3.87 (s, 3H), 3.80–3.72 (m, 1H), 3.65 (ddd, J = 10.5, 6.8, 3.6 Hz, 1H), 3.44 (dd, J = 15.0, 3.0 Hz, 1H), 3.34 (d, J = 10.8 Hz, 1H), 3.10–3.02 (m, 2H), 2.93 (dd, J = 15.0, 8.6 Hz, 1H), 2.87 (dd, J = 13.6, 7.1 Hz, 1H), 2.55 (dd, J = 13.7, 10.6 Hz, 1H), 2.09–1.96 (m, 3H), 1.96–1.88 (m, 2H), 1.29 (s, 2H), 0.91 (d, J = 6.5 Hz, 3H), 0.87 (d, J = 6.6 Hz, 3H). ^{13}C NMR (201 MHz, CD_3OD) δ 163.1, 160.7, 156.3, 138.7, 130.8, 129.4, 129.3, 129.2, 128.0, 125.6, 114.0, 82.1, 76.4, 72.6, 57.3, 56.6, 56.2, 54.8, 52.3, 39.3, 39.1, 35.8, 26.6, 19.1, 19.0. LRMS (ESI) m/z : $[\text{M} + \text{H}]^+$ 576.2. HRMS (ESI) m/z : $[\text{M} + \text{Na}]^+$ calcd $\text{C}_{28}\text{H}_{37}\text{N}_5\text{O}_8\text{SNa}$ 598.2194; found 598.2189.

(3aS,5R,6aR)-3-Methyl-2-oxohexahydro-2H-cyclopenta[d]oxazol-5-yl ((2S,3R)-3-Hydroxy-4-((N-isobutyl-4-methoxyphenyl)sulfonamido)-1-phenylbutan-2-yl)carbamate (4c). Compound **11b** (7.5 mg, 0.02 mmol) was treated with isostere amine **12** (10.4 mg, 0.03 mmol) by following the same procedure outlined for inhibitor **4a** to give inhibitor **4c** (3.5 mg, 88%): ^1H NMR (800 MHz, CDCl_3) δ 7.80–7.74 (m, 2H), 7.35–7.24 (m, 4H), 7.23–7.16 (m, 1H), 7.04–6.95 (m, 2H), 5.04 (t, J = 4.3 Hz, 1H), 4.95 (q, J = 9.3, 6.9 Hz, 1H), 4.20–4.12 (m, 1H), 3.96 (dq, J = 9.8, 4.4 Hz, 1H), 3.89 (s, 3H), 3.79 (q, J = 17.3, 10.2 Hz, 1H), 3.22 (dd, J = 14.4, 4.2 Hz, 1H), 3.14 (dd, J = 14.9, 8.3 Hz, 2H), 3.00 (dd, J = 13.5, 8.0 Hz, 1H), 2.94 (dd, J = 13.5, 7.1 Hz, 1H), 2.75 (dd, J = 14.2, 10.1 Hz, 2H), 2.57 (s, 3H), 2.39–2.32 (m, 1H), 2.18 (dd, J = 15.1, 3.0 Hz, 1H), 1.97 (p, J = 6.7 Hz, 1H), 1.90 (dt, J = 15.7, 5.5 Hz, 1H), 1.63 (ddd, J = 15.5, 6.6, 4.0 Hz, 1H), 0.92 (t, J = 6.9 Hz, 6H). ^{13}C NMR (201 MHz, CDCl_3) δ 162.8, 157.6, 155.3, 138.0, 130.5, 129.5, 129.4, 128.4, 126.2, 114.3, 77.7, 75.7, 71.9, 61.3, 58.3, 55.6, 54.7, 54.6, 53.1, 39.4,

35.4, 34.9, 29.7, 28.8, 27.2, 20.2, 19.9. LRMS (ESI) m/z : $[\text{M} + \text{H}]^+$ 590.3. HRMS (ESI) m/z : $[\text{M} + \text{H}]^+$ calcd $\text{C}_{29}\text{H}_{40}\text{N}_5\text{O}_8\text{S}$ 590.2531; found 590.2525.

(3aR,5S,6aS)-3-Methyl-2-oxohexahydro-2H-cyclopenta[d]oxazol-5-yl ((2S,3R)-3-Hydroxy-4-((N-isobutyl-4-methoxyphenyl)sulfonamido)-1-phenylbutan-2-yl)carbamate (4d). Compound **11d** (4.9 mg, 0.02 mmol) was treated with isostere amine **12** (6.8 mg, 0.02 mmol) by following the same procedure outlined for inhibitor **4a** to give inhibitor **4d** (6.1 mg, 68%): ^1H NMR (800 MHz, CDCl_3) δ 7.76 (d, J = 8.4 Hz, 2H), 7.35–7.19 (m, 5H), 7.01 (d, J = 8.8 Hz, 2H), 5.08 (s, 1H), 4.99 (t, J = 6.7 Hz, 1H), 4.89 (d, J = 8.8 Hz, 1H), 4.23–4.18 (m, 1H), 3.90 (s, 3H), 3.82 (d, J = 19.1 Hz, 1H), 3.64 (s, 1H), 3.38 (s, 1H), 3.16 (dd, J = 15.0, 9.1 Hz, 1H), 3.05–2.96 (m, 2H), 2.82 (dd, J = 13.6, 7.6 Hz, 1H), 2.79 (s, 3H), 2.30 (d, J = 15.4 Hz, 1H), 2.19 (d, J = 15.9 Hz, 1H), 1.91 (dd, J = 15.5, 5.4 Hz, 1H), 1.88–1.82 (m, 1H), 1.74–1.69 (m, 1H), 1.67 (s, 2H), 0.92 (dd, J = 35.7, 6.6 Hz, 6H). ^{13}C NMR (201 MHz, CDCl_3) δ 163.0, 157.4, 155.4, 137.7, 130.1, 129.6, 129.5, 128.6, 128.3, 126.4, 114.3, 77.6, 75.8, 72.1, 61.4, 58.6, 56.0, 55.6, 53.4, 39.8, 35.8, 35.3, 29.7, 29.2, 29.0, 27.3, 27.0, 20.2, 19.9. LRMS (ESI) m/z : $[\text{M} + \text{H}]^+$ 590.6. HRMS (ESI) m/z : $[\text{M} + \text{Na}]^+$ calcd $\text{C}_{29}\text{H}_{39}\text{N}_5\text{O}_8\text{SNa}$ 612.2350; found 612.2358.

(3aS,5R,6aR)-2-Oxo-3-phenylhexahydro-2H-cyclopenta[d]oxazol-5-yl ((2S,3R)-3-Hydroxy-4-((N-isobutyl-4-methoxyphenyl)sulfonamido)-1-phenylbutan-2-yl)carbamate (4e). Compound **11e** (8 mg, 0.02 mmol) was treated with isostere amine **12** (9.3 mg, 0.02 mmol) by following the same procedure outlined for inhibitor **4a** to give inhibitor **4e** (6.1 mg, 45%): ^1H NMR (800 MHz, CDCl_3) δ 7.74 (d, J = 8.4 Hz, 2H), 7.54–7.46 (m, 2H), 7.44–7.35 (m, 2H), 7.15 (dt, J = 16.1, 5.6 Hz, 6H), 6.99 (d, J = 8.4 Hz, 2H), 5.12 (q, J = 3.5 Hz, 1H), 5.09 (t, J = 6.7 Hz, 1H), 4.91–4.82 (m, 2H), 3.87 (s, 3H), 3.78 (s, 2H), 3.70 (s, 1H), 3.14 (dd, J = 14.9, 8.1 Hz, 1H), 3.06–3.00 (m, 1H), 2.97 (dd, J = 14.4, 6.8 Hz, 2H), 2.82 (dd, J = 13.4, 6.8 Hz, 1H), 2.77 (dd, J = 13.9, 8.2 Hz, 1H), 2.48–2.41 (m, 1H), 2.21–2.14 (m, 1H), 1.99 (d, J = 15.8 Hz, 1H), 1.63 (s, 2H), 0.89 (dd, J = 29.2, 6.4 Hz, 6H). ^{13}C NMR (201 MHz, CDCl_3) δ 162.9, 155.3, 154.6, 137.5, 137.3, 130.3, 129.5, 129.4, 129.3, 128.4, 126.4, 124.5, 120.3, 119.8, 114.3, 75.6, 72.0, 60.7, 58.5, 55.6, 55.3, 53.3, 39.7, 37.5, 35.8, 29.7, 27.2, 20.2, 19.9. LRMS (ESI) m/z : $[\text{M} + \text{Na}]^+$ 674.2. HRMS (ESI) m/z : $[\text{M} + \text{Na}]^+$ calcd $\text{C}_{33}\text{H}_{41}\text{N}_5\text{O}_8\text{SNa}$ 674.2507; found 674.2497.

(3aS,5R,6aR)-3-(4-Methoxyphenyl)-2-oxohexahydro-2H-cyclopenta[d]oxazol-5-yl ((2S,3R)-3-Hydroxy-4-((N-isobutyl-4-methoxyphenyl)sulfonamido)-1-phenylbutan-2-yl)carbamate (4f). Compound **11f** (3.9 mg, 0.01 mmol) was treated with isostere amine **12** (4.2 mg, 0.01 mmol) by following the same procedure outlined for inhibitor **4a** to give inhibitor **4f** (2.7 mg, 47%): ^1H NMR (800 MHz, CDCl_3) δ 7.72 (dd, J = 33.8, 8.5 Hz, 2H), 7.34 (d, J = 9.2 Hz, 2H), 7.20 (dd, J = 24.4, 7.4 Hz, 4H), 6.97 (dd, J = 22.4, 8.5 Hz, 3H), 6.90 (t, J = 7.9 Hz, 2H), 5.12 (s, 1H), 5.11–5.06 (m, 2H), 4.97 (d, J = 9.2 Hz, 1H), 4.76 (t, J = 7.5 Hz, 1H), 3.87 (s, 3H), 3.81 (s, 3H), 3.15 (dd, J = 15.0, 8.7 Hz, 1H), 3.06 (d, J = 15.0 Hz, 1H), 3.02–2.88 (m, 2H), 2.82 (ddd, J = 34.6, 16.1, 8.6 Hz, 2H), 2.43 (d, J = 15.9 Hz, 1H), 2.22 (s, 1H), 2.16 (d, J = 15.3 Hz, 1H), 1.96 (tt, J = 15.8, 4.6 Hz, 2H), 1.91–1.78 (m, 2H), 0.95–0.85 (m, 6H). ^{13}C NMR (201 MHz, CDCl_3) δ 162.9, 157.1, 155.2, 137.6, 130.3, 130.1, 129.5, 129.4, 128.5, 126.5, 123.0, 114.6, 114.3, 77.4, 77.2, 77.0, 76.9, 75.8, 72.0, 61.5, 58.5, 55.6, 55.5, 55.2, 53.3, 39.8, 37.2, 35.8, 27.2, 20.2, 19.9. LRMS (ESI) m/z : $[\text{M} + \text{H}]^+$ 682.2. HRMS (ESI) m/z : $[\text{M} + \text{H}]^+$ calcd $\text{C}_{33}\text{H}_{44}\text{N}_5\text{O}_8\text{SNa}$ 682.2793; found 682.2800.

(3aS,5R,6aR)-3-(3-Methoxyphenyl)-2-oxohexahydro-2H-cyclopenta[d]oxazol-5-yl ((2S,3R)-3-Hydroxy-4-((N-isobutyl-4-methoxyphenyl)sulfonamido)-1-phenylbutan-2-yl)carbamate (4g). Compound **11g** (13.6 mg, 0.03 mmol) was treated with isostere amine **12** (14.7 mg, 0.04 mmol) by following the same procedure outlined for inhibitor **4a** to give inhibitor **4g** (13.1 mg, 58%): ^1H NMR (800 MHz, CD_3OD) δ 7.77 (d, J = 7.9 Hz, 2H), 7.35 (t, J = 7.7 Hz, 1H), 7.26 (dd, J = 14.5, 7.2 Hz, 4H), 7.16 (dd, J = 22.0, 7.2 Hz, 2H), 7.09 (t, J = 7.2 Hz, 3H), 6.91 (s, 1H), 5.23–5.17 (m, 1H), 5.10 (s, 1H), 4.85–4.80 (m, 1H), 3.89–3.85 (m, 6H), 3.84 (s, 1H), 3.82–3.75 (m, 2H), 3.38 (d, J = 15.2 Hz, 1H), 3.12 (d, J = 14.3 Hz, 1H),

3.04 (dt, $J = 13.1, 7.2$ Hz, 2H), 2.91 (dd, $J = 13.4, 7.0$ Hz, 1H), 2.72–2.65 (m, 1H), 2.26 (d, $J = 15.8$ Hz, 1H), 2.10 (d, $J = 15.9$ Hz, 1H), 2.05–1.96 (m, 1H), 1.89 (d, $J = 15.3$ Hz, 1H), 1.74 (dd, $J = 13.9, 7.0$ Hz, 1H), 0.89 (dd, $J = 21.6, 6.2$ Hz, 6H). ^{13}C NMR (201 MHz, CD_3OD) δ 163.1, 157.8, 156.3, 155.4, 138.7, 130.8, 130.0, 129.3, 129.0, 128.0, 125.9, 124.3, 120.5, 114.0, 111.9, 79.5, 76.2, 72.2, 61.8, 57.3, 55.9, 54.8, 52.3, 39.5, 36.2, 35.4, 26.6, 19.1, 19.1. LRMS (ESI) m/z : $[\text{M} + \text{H}]^+$ 682.2. HRMS (ESI) m/z : $[\text{M} + \text{H}]^+$ calcd $\text{C}_{35}\text{H}_{44}\text{N}_3\text{O}_5\text{SNa}$ 682.2793; found 682.2787.

(3aS,5R,6aR)-3-(2-Methoxyphenyl)-2-oxohexahydro-2H-cyclopenta[d]oxazol-5-yl ((2S,3R)-3-Hydroxy-4-((N-isobutyl-4-methoxyphenyl)sulfonamido)-1-phenylbutan-2-yl)carbamate (4h). Compound 11h (14.5 mg, 0.03 mmol) was treated with isostere amine 12 (15.6 mg, 0.04 mmol) by following the same procedure outlined for inhibitor 4a to give inhibitor 4h (12.2 mg, 51%): ^1H NMR (400 MHz, CDCl_3) δ 7.72 (d, $J = 8.5$ Hz, 2H), 7.37–7.08 (m, 7H), 7.08–6.92 (m, 3H), 6.70 (d, $J = 8.2$ Hz, 1H), 5.18–5.02 (m, 2H), 4.83 (dd, $J = 15.7, 5.4$ Hz, 2H), 3.86 (s, 3H), 3.78 (dt, $J = 13.8, 3.5$ Hz, 5H), 3.68 (s, 1H), 3.14 (dd, $J = 15.1, 8.7$ Hz, 1H), 3.06–2.90 (m, 3H), 2.78 (ddd, $J = 22.2, 13.4, 7.2$ Hz, 2H), 2.43 (d, $J = 15.9$ Hz, 1H), 2.19 (d, $J = 15.5$ Hz, 1H), 2.02–1.79 (m, 3H), 0.88 (d, $J = 6.8$ Hz, 6H). ^{13}C NMR (201 MHz, CD_3OD) δ 163.1, 160.5, 156.1, 155.8, 138.6, 130.8, 129.6, 129.3, 128.9, 127.8, 125.6, 114.0, 112.2, 109.5, 106.6, 78.7, 75.9, 72.1, 61.2, 57.4, 56.1, 54.8, 54.5, 52.4, 39.1, 37.2, 35.7, 26.7, 19.1, 19.0. LRMS (ESI) m/z : $[\text{M} + \text{H}]^+$ 682.2. HRMS (ESI) m/z : $[\text{M} + \text{Na}]^+$ calcd $\text{C}_{35}\text{H}_{43}\text{N}_3\text{O}_5\text{SNa}$ 704.2612; found 704.2602.

(3aS,5R,6aR)-3-Allyl-2-oxohexahydro-2H-cyclopenta[d]oxazol-5-yl ((2S,3R)-3-Hydroxy-4-((N-isobutyl-4-methoxyphenyl)sulfonamido)-1-phenylbutan-2-yl)carbamate (4i). Compound 11i (17 mg, 0.05 mmol) was treated with isostere amine 12 (22 mg, 0.06 mmol) by following the same procedure outlined for inhibitor 4a to give inhibitor 4i (23 mg, 76%): ^1H NMR (400 MHz, CDCl_3) δ 7.75 (d, $J = 8.9$ Hz, 2H), 7.39–7.22 (m, 4H), 7.22–7.11 (m, 1H), 7.04–6.86 (m, 2H), 5.68–5.52 (m, 1H), 5.46 (d, $J = 8.8$ Hz, 1H), 5.20–5.09 (m, 2H), 4.97 (d, $J = 4.1$ Hz, 1H), 4.92 (t, $J = 6.8$ Hz, 1H), 4.16 (t, $J = 7.0$ Hz, 1H), 4.02–3.89 (m, 2H), 3.86 (s, 3H), 3.83–3.70 (m, 2H), 3.29 (dd, $J = 14.8, 5.1$ Hz, 1H), 3.22–2.87 (m, 5H), 2.71 (dd, $J = 14.2, 10.1$ Hz, 1H), 2.32 (d, $J = 15.9$ Hz, 1H), 2.15 (d, $J = 15.3$ Hz, 1H), 2.02–1.93 (m, 1H), 1.85 (dd, $J = 15.0, 9.7$ Hz, 1H), 1.54 (ddd, $J = 15.4, 6.7, 4.1$ Hz, 1H), 0.88 (dd, $J = 16.0, 6.6$ Hz, 6H). ^{13}C NMR (201 MHz, CDCl_3) δ 162.8, 157.4, 155.2, 138.2, 131.9, 130.6, 129.5, 129.4, 128.4, 126.2, 118.6, 114.3, 78.1, 75.6, 71.6, 58.8, 58.2, 55.6, 54.6, 54.5, 52.9, 44.7, 39.4, 35.6, 34.5, 29.7, 27.1, 20.2, 20.0. LRMS (ESI) m/z : $[\text{M} + \text{H}]^+$ 616.2. HRMS (ESI) m/z : $[\text{M} + \text{Na}]^+$ calcd $\text{C}_{31}\text{H}_{41}\text{N}_3\text{O}_5\text{SNa}$ 638.2507; found 638.2498.

(3aS,5R,6aR)-2-Oxo-3-propylhexahydro-2H-cyclopenta[d]oxazol-5-yl ((2S,3R)-3-Hydroxy-4-((N-isobutyl-4-methoxyphenyl)sulfonamido)-1-phenylbutan-2-yl)carbamate (4j). Compound 11j (3.7 mg, 0.01 mmol) was treated with isostere amine 12 (4.7 mg, 0.01 mmol) by following the same procedure outlined for inhibitor 4a to give inhibitor 4j (4 mg, 62%): ^1H NMR (800 MHz, CDCl_3) δ 7.78–7.70 (m, 2H), 7.33–7.22 (m, 4H), 7.20 (s, 1H), 7.02–6.93 (m, 2H), 5.08–5.02 (m, 1H), 4.98 (s, 1H), 4.94 (s, 1H), 4.22 (d, $J = 7.7$ Hz, 1H), 3.87 (d, $J = 2.7$ Hz, 3H), 3.79 (s, 1H), 3.74 (s, 1H), 3.33–3.25 (m, 1H), 3.14 (ddd, $J = 17.8, 8.9, 4.7$ Hz, 2H), 3.07 (d, $J = 14.3$ Hz, 1H), 2.97 (dd, $J = 13.6, 8.2$ Hz, 1H), 2.93–2.86 (m, 1H), 2.75 (t, $J = 12.2$ Hz, 1H), 2.67 (d, $J = 8.7$ Hz, 1H), 2.33 (d, $J = 16.0$ Hz, 1H), 2.13 (d, $J = 15.2$ Hz, 1H), 1.89 (dt, $J = 13.2, 6.2$ Hz, 2H), 1.60–1.50 (m, 3H), 1.48 (d, $J = 7.2$ Hz, 1H), 1.02–0.76 (m, 9H). ^{13}C NMR (201 MHz, CDCl_3) δ 162.9, 157.5, 155.4, 137.8, 130.4, 129.5, 129.4, 128.5, 126.4, 114.3, 77.7, 75.7, 72.1, 59.0, 58.4, 55.6, 54.9, 53.2, 43.7, 39.6, 35.8, 35.4, 29.7, 27.2, 20.3, 20.2, 19.9, 11.2. LRMS (ESI) m/z : $[\text{M} + \text{H}]^+$ 618.2. HRMS (ESI) m/z : $[\text{M} + \text{Na}]^+$ calcd $\text{C}_{31}\text{H}_{43}\text{N}_3\text{O}_5\text{SNa}$ 640.2663; found 640.2669.

(3aS,5R,6aR)-3-(2-Methylallyl)-2-oxohexahydro-2H-cyclopenta[d]oxazol-5-yl ((2S,3R)-3-Hydroxy-4-((N-isobutyl-4-methoxyphenyl)sulfonamido)-1-phenylbutan-2-yl)carbamate (4k). Compound 11k (6.1 mg, 0.02 mmol) was treated with isostere amine 12 (7.5 mg, 0.02 mmol) by following the same procedure outlined for inhibitor 4a to give inhibitor 4k (8 mg, 75%): ^1H NMR

(800 MHz, CDCl_3) δ 7.77 (d, $J = 8.8$ Hz, 2H), 7.36–7.25 (m, 4H), 7.24–7.15 (m, 1H), 7.00 (d, $J = 8.9$ Hz, 2H), 5.19 (s, 1H), 5.03 (s, 1H), 4.96 (t, $J = 6.9$ Hz, 1H), 4.92 (s, 1H), 4.82 (s, 1H), 4.12 (t, $J = 7.1$ Hz, 1H), 4.01–3.95 (m, 1H), 3.93–3.87 (m, 4H), 3.85–3.76 (m, 2H), 3.24 (dd, $J = 15.1, 4.5$ Hz, 1H), 3.14 (dd, $J = 14.8, 8.4$ Hz, 2H), 3.06 (d, $J = 15.4$ Hz, 1H), 3.01 (dd, $J = 13.6, 8.0$ Hz, 1H), 2.96 (dd, $J = 13.6, 7.2$ Hz, 1H), 2.76 (dd, $J = 14.3, 10.1$ Hz, 1H), 2.36 (d, $J = 15.6$ Hz, 1H), 2.16 (d, $J = 15.1$ Hz, 1H), 1.98 (dt, $J = 13.1, 6.5$ Hz, 1H), 1.90 (dt, $J = 15.4, 4.8$ Hz, 1H), 1.68 (s, 3H), 1.59 (ddd, $J = 15.3, 6.7, 4.2$ Hz, 1H), 0.92 (dd, $J = 13.5, 6.6$ Hz, 6H). ^{13}C NMR (201 MHz, CDCl_3) δ 162.9, 157.6, 155.3, 139.4, 138.1, 130.6, 129.5, 129.4, 128.5, 126.3, 114.3, 114.0, 78.0, 75.7, 71.8, 58.6, 58.3, 55.6, 54.7, 53.1, 48.1, 39.5, 35.5, 34.8, 29.7, 27.2, 20.3, 20.0, 19.9. LRMS (ESI) m/z : $[\text{M} + \text{H}]^+$ 630.6. HRMS (ESI) m/z : $[\text{M} + \text{Na}]^+$ calcd $\text{C}_{33}\text{H}_{43}\text{N}_3\text{O}_5\text{SNa}$ 652.2663; found 652.2666.

(3aS,5R,6aR)-3-Isobutyl-2-oxohexahydro-2H-cyclopenta[d]oxazol-5-yl ((2S,3R)-3-Hydroxy-4-((N-isobutyl-4-methoxyphenyl)sulfonamido)-1-phenylbutan-2-yl)carbamate (4l). Compound 11l (9 mg, 0.02 mmol) was treated with isostere amine 12 (11 mg, 0.03 mmol) by following the same procedure outlined for inhibitor 4a to give inhibitor 4l (10 mg, 65%): ^1H NMR (800 MHz, CDCl_3) δ 7.80–7.75 (m, 2H), 7.30 (d, $J = 23.2$ Hz, 4H), 7.21 (t, $J = 7.3$ Hz, 1H), 7.00 (d, $J = 8.8$ Hz, 2H), 5.17–5.11 (m, 1H), 5.04 (t, $J = 4.2$ Hz, 1H), 4.97 (t, $J = 6.8$ Hz, 1H), 4.23 (t, $J = 6.9$ Hz, 1H), 3.98–3.92 (m, 1H), 3.89 (s, 4H), 3.82 (s, 1H), 3.23 (d, $J = 12.5$ Hz, 1H), 3.19–3.04 (m, 3H), 3.04–2.91 (m, 2H), 2.81–2.73 (m, 1H), 2.52 (d, $J = 13.9$ Hz, 1H), 2.37 (d, $J = 15.6$ Hz, 1H), 2.18 (d, $J = 15.0$ Hz, 1H), 2.01–1.94 (m, 1H), 1.94–1.82 (m, 2H), 1.71 (s, 1H), 1.64 (d, $J = 14.7$ Hz, 1H), 0.92 (dq, $J = 19.3, 6.4$ Hz, 12H). ^{13}C NMR (201 MHz, CDCl_3) δ 162.9, 157.8, 155.3, 138.0, 130.6, 129.5, 129.4, 128.5, 126.3, 114.3, 77.8, 75.7, 71.8, 59.3, 58.3, 55.6, 54.8, 53.1, 49.4, 39.5, 35.6, 34.9, 29.7, 27.2, 26.2, 20.3, 20.0, 19.8. LRMS (ESI) m/z : $[\text{M} + \text{H}]^+$ 630.6. HRMS (ESI) m/z : $[\text{M} + \text{Na}]^+$ calcd $\text{C}_{32}\text{H}_{43}\text{N}_3\text{O}_5\text{SNa}$ 654.2820; found 654.2815.

(3aS,5R,6aR)-3-(Methoxymethyl)-2-oxohexahydro-2H-cyclopenta[d]oxazol-5-yl ((2S,3R)-3-Hydroxy-4-((N-isobutyl-4-methoxyphenyl)sulfonamido)-1-phenylbutan-2-yl)carbamate (4m). Compound 11m (3.2 mg, 0.01 mmol) was treated with isostere amine 12 (4.1 mg, 0.01 mmol) by following the same procedure outlined for inhibitor 4a to give inhibitor 4m (3.4 mg, 60%): ^1H NMR (800 MHz, CD_3OD) δ 7.76 (d, $J = 8.8$ Hz, 2H), 7.28–7.19 (m, 4H), 7.19–7.15 (m, 1H), 7.10–7.05 (m, 2H), 5.12 (s, 1H), 5.06 (t, $J = 6.9$ Hz, 1H), 5.02 (t, $J = 4.6$ Hz, 1H), 4.58 (d, $J = 11.0$ Hz, 1H), 4.40–4.33 (m, 2H), 3.88 (s, 3H), 3.75 (ddd, $J = 14.9, 10.4, 5.1$ Hz, 1H), 3.40–3.32 (m, 4H), 3.22 (s, 2H), 3.18 (s, 1H), 3.09 (dd, $J = 14.2, 3.5$ Hz, 1H), 3.05 (dd, $J = 13.6, 7.9$ Hz, 1H), 2.99 (dd, $J = 14.9, 8.1$ Hz, 1H), 2.89 (dd, $J = 13.6, 7.0$ Hz, 1H), 2.57 (dd, $J = 14.2, 10.2$ Hz, 1H), 2.26–2.17 (m, 1H), 2.10 (dd, $J = 15.2, 2.8$ Hz, 1H), 2.08–2.02 (m, 1H), 1.82 (ddd, $J = 15.4, 6.9, 4.7$ Hz, 1H), 0.97–0.82 (m, 6H). ^{13}C NMR (201 MHz, CD_3OD) δ 163.1, 158.6, 156.2, 138.7, 130.8, 129.3, 128.9, 127.9, 125.8, 114.0, 79.5, 76.9, 76.2, 74.7, 72.5, 59.0, 57.3, 55.5, 54.8, 52.4, 38.9, 36.3, 35.2, 31.6, 29.3, 29.0, 26.6, 19.0. LRMS (ESI) m/z : $[\text{M} + \text{H}]^+$ 620.2. HRMS (ESI) m/z : $[\text{M} + \text{Na}]^+$ calcd $\text{C}_{30}\text{H}_{41}\text{N}_3\text{O}_5\text{SNa}$ 642.2456; found 642.2454.

(3aS,5R,6aR)-3-Methyl-2-oxohexahydro-2H-cyclopenta[d]oxazol-5-yl ((2S,3R)-4-((2-Cyclopropylamino)-N-isobutylbenzo[d]thiazole)-6-sulfonamido)-3-hydroxy-1-phenylbutan-2-yl)carbamate (4n). Compound 11b (7.1 mg, 0.02 mmol) was treated with isostere amine 13 (12 mg, 0.02 mmol) by following the same procedure outlined for inhibitor 4a to give inhibitor 4n (10 mg, 69%): ^1H NMR (400 MHz, CDCl_3) δ 8.17–8.07 (m, 1H), 7.72 (dd, $J = 8.5, 1.9$ Hz, 1H), 7.53 (d, $J = 8.6$ Hz, 1H), 7.26 (d, $J = 2.8$ Hz, 5H), 7.19 (dd, $J = 6.7, 2.3$ Hz, 1H), 5.10 (d, $J = 10.3$ Hz, 1H), 5.02 (s, 1H), 4.91 (t, $J = 6.9$ Hz, 1H), 3.89 (dd, $J = 34.2, 5.3$ Hz, 3H), 3.34 (s, 1H), 3.28–3.07 (m, 3H), 3.07–2.88 (m, 2H), 2.74 (td, $J = 9.7, 6.4$ Hz, 3H), 2.57 (s, 3H), 2.30 (d, $J = 15.8$ Hz, 1H), 2.15 (dd, $J = 15.2, 2.9$ Hz, 1H), 2.00–1.80 (m, 2H), 1.60 (ddd, $J = 15.3, 6.5, 4.1$ Hz, 1H), 0.91 (dd, $J = 13.9, 5.7$ Hz, 9H), 0.78 (t, $J = 1.8$ Hz, 2H). ^{13}C NMR (201 MHz, CD_3OD) δ 158.6, 156.3, 155.4, 138.8, 131.4, 130.8, 129.6, 129.0, 127.9, 127.7, 125.7, 125.3, 121.0, 120.7, 117.5, 78.9, 76.0, 72.5, 61.7, 57.4, 55.6, 52.5, 39.2, 35.3, 34.9,

27.9, 26.7, 25.9, 19.1, 19.1, 19.1, 6.5. LRMS (ESI) m/z : $[M + H]^+$ 672.3. HRMS (ESI) m/z : $[M + Na]^+$ calcd $C_{32}H_{42}N_3O_7S_2Na$ 672.2520; found 672.2512.

(1*S*,4*R*)-4-(((4-Methoxyphenyl)carbamoyloxy)cyclopent-2-en-1-yl) Acetate (6a). To a stirring solution of (1*R*,4*S*)-*cis*-4-acetoxy-2-cyclopenten-1-ol **5** (49 mg, 0.34 mmol) in dry dichloromethane were added phenyl isocyanate (45 mg, 0.38 mmol) and 1,8-diazabicyclo[5.4.0]undec-7-ene (5.3 mg, 0.03 mmol) all under an argon atmosphere. Reaction was stirred at 23 °C for 1 h. After this period, the reaction was quenched with in saturated solution of $NaHCO_3$ and the aqueous phase was extracted with EtOAc. The organic extracts were dried with Na_2SO_4 and the solvent was removed under reduced pressure. The crude product was purified by silica gel column chromatography (20% EtOAc in hexane) to afford the known²⁷ carbamate derivative **6a** (73 mg, 81%).

(1*S*,4*R*)-4-(((4-Methoxyphenyl)carbamoyloxy)cyclopent-2-en-1-yl) Acetate (6b). To a stirring solution of (1*R*,4*S*)-*cis*-4-acetoxy-2-cyclopenten-1-ol **5** (0.6 g, 4.2 mmol) in dry dichloromethane were added 4-methoxyphenyl isocyanate (0.7 g, 4.6 mmol) and 1,8-diazabicyclo[5.4.0]undec-7-ene (64 mg, 0.42 mmol) all under an argon atmosphere. Reaction was stirred at 23 °C for 1 h. Upon completion, the residue was taken up in saturated solution of $NaHCO_3$ and the aqueous phase was extracted with EtOAc. The organic extracts were dried with Na_2SO_4 and the solvent was removed under reduced pressure. The crude product was purified by silica gel column chromatography (20% EtOAc in hexane) to afford **6b** (1 g, 81%): 1H NMR (400 MHz, $CDCl_3$) δ 7.33–7.22 (m, 2H), 6.84 (d, J = 9.0 Hz, 2H), 6.57 (s, 1H), 6.12 (dddd, J = 20.7, 5.6, 2.1, 1.1 Hz, 2H), 5.58 (qd, J = 6.1, 3.5, 2.1 Hz, 2H), 3.77 (s, 3H), 2.90 (qt, J = 15.1, 7.5 Hz, 1H), 2.06 (s, 3H), 1.80 (dt, J = 15.0, 3.7 Hz, 1H). ^{13}C NMR (101 MHz, $CDCl_3$) δ 170.6, 156.0, 153.3, 134.9, 134.5, 130.7, 120.6, 114.2, 77.3, 77.0, 76.6, 55.4, 37.2, 21.0. LRMS (ESI) m/z : $[M + Na]^+$ 314.0.

(3*aS*,5*R*,6*aR*)-2-Oxo-3-phenylhexahydro-2*H*-cyclopenta[d]oxazol-5-yl Acetate (7a). In a sealed tube, phenyl carbamate **6a** (60 mg, 0.2 mmol) was dissolved in dry tetrahydrofuran (8.4 mL) followed by the addition of freshly distilled dimethyl sulfoxide (0.84 mL). Freshly made 2-iodoxybenzoic acid (0.13 g, 0.46 mmol) was added all at once. The reaction vessel was heated for 8 h at 90 °C. Another portion of 2-iodoxybenzoic acid (0.13 g, 0.5 mmol) was added, and the reaction was heated for an additional 8 h. Upon completion, the residue was taken up in 5% saturated solution of $NaHCO_3$ and the aqueous phase was extracted with EtOAc. The organic extracts were dried with Na_2SO_4 and the solvent was removed under reduced pressure. The crude product was purified by silica gel column chromatography (60% EtOAc in hexane) to afford **7a** (23 mg, 37%): 1H NMR (800 MHz, $CDCl_3$) δ 7.54 (d, J = 7.7 Hz, 2H), 7.42–7.38 (m, 2H), 7.18 (t, J = 7.4 Hz, 1H), 5.30 (t, J = 4.5 Hz, 1H), 5.18 (t, J = 7.0 Hz, 1H), 4.95 (t, J = 7.2 Hz, 1H), 2.53 (dd, J = 16.0, 3.1 Hz, 1H), 2.30 (dd, J = 15.5, 3.0 Hz, 1H), 2.12 (ddd, J = 16.0, 6.5, 4.5 Hz, 1H), 2.03 (s, 3H), 1.98 (ddd, J = 15.4, 6.8, 4.5 Hz, 1H). ^{13}C NMR (201 MHz, $CDCl_3$) δ 170.6, 154.6, 137.3, 129.3, 124.6, 120.2, 77.4, 77.2, 77.1, 76.9, 75.0, 60.7, 42.7, 39.9, 37.0, 21.2. LRMS (ESI) m/z : $[M + H]^+$ 262.1.

(3*aS*,5*R*,6*aR*)-3-(4-Methoxyphenyl)-2-oxohexahydro-2*H*-cyclopenta[d]oxazol-5-yl Acetate (7b). In a sealed tube, *p*-methoxyphenyl carbamate **6b** (0.8 g, 2.5 mmol) was dissolved in dry tetrahydrofuran (46 mL) followed by the addition of freshly distilled dimethyl sulfoxide (4.6 mL). Freshly made 2-iodoxybenzoic acid (1.4 g, 5 mmol) was added all at once. The reaction vessel was heated for 8 h at 90 °C. Another portion of 2-iodoxybenzoic acid (1.4 g, 5 mmol) was added, and the reaction was heated for an additional 8 h. Upon completion, the residue was taken up in 5% saturated solution of $NaHCO_3$ and the aqueous phase was extracted with EtOAc. The organic extracts were dried with Na_2SO_4 and the solvent was removed under reduced pressure. The crude product was purified by silica gel column chromatography (60% EtOAc in hexane) to afford **7b** (0.48 g, 65%): 1H NMR (400 MHz, $CDCl_3$) δ 7.40–7.34 (m, 2H), 6.94–6.88 (m, 2H), 5.27 (t, J = 4.5 Hz, 1H), 5.14 (t, J = 7.2, 6.7 Hz, 1H), 4.84 (t, J = 7.0 Hz, 1H), 3.80 (s, 3H), 2.49 (dd, J = 15.9, 2.5

Hz, 1H), 2.24 (dd, J = 15.4, 3.0 Hz, 1H), 2.08 (ddd, J = 15.9, 6.4, 4.6 Hz, 1H), 2.03 (s, 3H), 1.88 (ddd, J = 15.4, 6.6, 4.6 Hz, 1H). ^{13}C NMR (101 MHz, $CDCl_3$) δ 170.4, 156.8, 154.8, 130.0, 122.8, 114.5, 77.2, 76.9, 76.6, 74.9, 61.3, 55.4, 39.9, 36.7, 21.1. LRMS (ESI) m/z : $[M + H]^+$ 292.0.

(3*aS*,5*R*,6*aR*)-3-(3-Methoxyphenyl)-2-oxohexahydro-2*H*-cyclopenta[d]oxazol-5-yl Acetate (7c). In a sealed tube, *m*-methoxyphenyl carbamate **6c** (57 mg, 0.2 mmol) was dissolved in dry tetrahydrofuran (7.1 mL) followed by the addition of freshly distilled dimethyl sulfoxide (0.7 mL). Freshly made 2-iodoxybenzoic acid (0.11 g, 0.4 mmol) was added all at once. The reaction vessel was heated for 8 h at 90 °C. Another portion of 2-iodoxybenzoic acid (0.11 g, 0.4 mmol) was added, and the reaction was heated for an additional 8 h. Upon completion, the residue was taken up in 5% saturated solution of $NaHCO_3$ and the aqueous phase was extracted with EtOAc. The organic extracts were dried with Na_2SO_4 and the solvent was removed under reduced pressure. The crude product was purified by silica gel column chromatography (60% EtOAc in hexane) to afford **7c** (24 mg, 42%): 1H NMR (400 MHz, $CDCl_3$) δ 7.30–7.23 (m, 1H), 7.21 (t, J = 2.3 Hz, 1H), 7.03 (ddd, J = 8.2, 2.1, 0.9 Hz, 1H), 6.70 (ddd, J = 8.3, 2.5, 0.8 Hz, 1H), 5.27 (t, J = 4.5 Hz, 1H), 5.14 (t, J = 7.1, 6.6 Hz, 1H), 4.88 (t, J = 7.1 Hz, 1H), 3.81 (s, 3H), 2.50 (dd, J = 15.9, 2.6 Hz, 1H), 2.31 (dd, J = 15.4, 3.0 Hz, 1H), 2.09 (ddd, J = 15.9, 6.2, 4.6 Hz, 1H), 2.00 (s, 3H), 1.99–1.90 (m, 1H). ^{13}C NMR (101 MHz, $CDCl_3$) δ 170.4, 160.2, 154.3, 138.4, 129.8, 112.0, 109.6, 106.3, 77.3, 77.2, 76.9, 76.6, 74.8, 60.6, 55.3, 39.7, 37.0, 21.1. LRMS (ESI) m/z : $[M + H]^+$ 292.0.

(3*aS*,5*R*,6*aR*)-3-(2-Methoxyphenyl)-2-oxohexahydro-2*H*-cyclopenta[d]oxazol-5-yl Acetate (7d). In a sealed tube, *o*-methoxyphenyl carbamate **6d** (17 mg, 0.06 mmol) was dissolved in dry tetrahydrofuran (2.1 mL) followed by the addition of freshly distilled dimethyl sulfoxide (0.2 mL). Freshly made 2-iodoxybenzoic acid (33 mg, 0.1 mmol) was added all at once. The reaction vessel was heated for 8 h at 90 °C. Another portion of 2-iodoxybenzoic acid (33 mg, 0.1 mmol) was added, and the reaction was heated for an additional 8 h. Upon completion, the residue was taken up in 5% saturated solution of $NaHCO_3$ and the aqueous phase was extracted with EtOAc. The organic extracts were dried with Na_2SO_4 and the solvent was removed under reduced pressure. The crude product was purified by silica gel column chromatography (60% EtOAc in hexane) to afford **7d** (11 mg, 65%): 1H NMR (400 MHz, $CDCl_3$) δ 7.34–7.26 (m, 2H), 7.03–6.93 (m, 2H), 5.28 (t, J = 4.5 Hz, 1H), 5.19 (t, J = 7.4, 5.7 Hz, 1H), 4.96 (t, J = 7.2 Hz, 1H), 3.86 (s, 3H), 2.49 (dd, J = 16.0, 2.6 Hz, 1H), 2.13 (s, 3H), 2.11–2.01 (m, 2H), 1.78–1.63 (m, 1H). ^{13}C NMR (101 MHz, $CDCl_3$) δ 170.5, 156.2, 154.8, 129.6, 128.8, 124.7, 120.9, 111.9, 78.2, 77.2, 76.9, 76.6, 75.3, 61.0, 55.5, 42.6, 39.9, 36.6, 21.3. LRMS (ESI) m/z : $[M + H]^+$ 292.0.

(3*aS*,5*R*,6*aR*)-2-Oxohexahydro-2*H*-cyclopenta[d]oxazol-5-yl Acetate (8). To a stirring solution of cyclic *p*-methoxyphenyl carbamate **7b** (0.14 g, 0.5 mmol) in acetonitrile (4.7 mL) and water (0.9 mL) was added cerium ammonium nitrate (1.3 g, 2.4 mmol) at 0 °C. Reaction was stirred for 30 min. Upon completion, the residue was taken up in 5% saturated solution of $NaHCO_3$ and the aqueous phase was extracted with EtOAc. The organic extracts were dried with Na_2SO_4 and the solvent was removed under reduced pressure. The crude product was purified by silica gel column chromatography (80% EtOAc in hexane) to afford **8** (62 mg, 71%): 1H NMR (400 MHz, $CDCl_3$) δ 5.53 (s, 1H), 5.28 (t, J = 4.5 Hz, 1H), 5.17 (t, J = 7.0 Hz, 1H), 4.39 (t, J = 7.0 Hz, 1H), 2.44 (dd, J = 15.9, 2.9 Hz, 1H), 2.12 (dd, J = 15.4, 2.9 Hz, 1H), 2.03 (s, 3H), 1.95 (tdd, J = 15.8, 6.5, 4.6 Hz, 2H). ^{13}C NMR (101 MHz, $CDCl_3$) δ 170.6, 158.7, 81.3, 77.2, 77.12, 76.9, 76.6, 75.3, 55.9, 40.1, 39.3, 21.1. LRMS (ESI) m/z : $[M + H]^+$ 186.1.

(3*aR*,5*S*,6*aS*)-2-Oxohexahydro-2*H*-cyclopenta[d]oxazol-5-yl Acetate (ent-8). To a stirring solution of cyclic *p*-methoxyphenyl carbamate ent-**7b** (20 mg, 0.07 mmol) in acetonitrile (0.7 mL) and water (0.2 mL) was added cerium ammonium nitrate (0.2 g, 0.3 mmol) at 0 °C. Reaction was stirred for 30 min. Upon completion, the residue was taken up in 5% saturated solution of $NaHCO_3$ and the aqueous phase was extracted with EtOAc. The organic extracts were

dried with Na_2SO_4 , and the solvent was removed under reduced pressure. The crude product was purified by silica gel column chromatography (80% EtOAc in hexane) to afford *ent*-8 (7.7 mg, 61%). ^1H NMR (800 MHz, CDCl_3) δ 5.36 (s, 1H), 5.31 (t, J = 4.2 Hz, 1H), 5.20 (t, J = 6.8 Hz, 1H), 4.41 (t, J = 6.9 Hz, 1H), 2.47 (dd, J = 15.9, 2.2 Hz, 1H), 2.15 (dd, J = 15.3, 2.9 Hz, 1H), 2.07 (s, 3H), 1.99 (dddd, J = 30.4, 15.3, 6.6, 4.5 Hz, 2H). ^{13}C NMR (201 MHz, CDCl_3) δ 170.8, 158.7, 81.4, 77.2, 77.0, 76.9, 75.4, 56.0, 40.3, 39.4, 21.2. LRMS (ESI) m/z : $[\text{M} + \text{H}]^+$ 185.9.

(3a*S*,5*R*,6a*R*)-5-Hydroxyhexahydro-2*H*-cyclopenta[d]oxazol-2-one (9). To a stirring solution of protected oxazolidinone 8 (6 mg, 0.03 mmol) in methanol (1 mL) was added potassium carbonate (5.5 mg, 0.04 mmol). Reaction was stirred at 23 °C for 4 h. Upon completion, the residue solvent was removed under reduced pressure. The crude product was purified by silica gel column chromatography (80% EtOAc in hexane) to afford **9** (4.6 mg, 99%). $[\alpha]_D^{20}$ +20.0 (c 1.0, MeOH). ^1H NMR (800 MHz, CD_3OD) δ 5.14 (t, J = 7.0 Hz, 1H), 4.41 (t, J = 4.4 Hz, 1H), 4.33 (t, J = 7.3 Hz, 1H), 2.18 (d, J = 15.2 Hz, 1H), 1.99–1.94 (m, 2H), 1.88 (ddd, J = 14.5, 6.9, 4.4 Hz, 1H). ^{13}C NMR (201 MHz, CD_3OD) δ 160.5, 82.4, 72.1, 56.6, 47.9, 47.8, 47.7, 47.6, 47.5, 47.4, 47.3, 41.6, 41.2. LRMS (ESI) m/z : $[\text{M} + \text{H}]^+$ 144.1. HRMS (ESI) m/z : $[\text{M} + \text{H}]^+$ calcd $\text{C}_6\text{H}_{10}\text{NO}_3$ 144.0655; found 144.0653.

(3a*R*,5*S*,6a*S*)-5-Hydroxyhexahydro-2*H*-cyclopenta[d]oxazol-2-one (*ent*-9). To a stirring solution of protected oxazolidinone *ent*-8 (8 mg, 0.04 mmol) in methanol (1.4 mL) was added potassium carbonate (7.2 mg, 0.05 mmol). Reaction was stirred at 23 °C for 4 h. Upon completion, the residue solvent was removed under reduced pressure. The crude product was purified by silica gel column chromatography (80% EtOAc in hexane) to afford *ent*-9 (5.9 mg, 95%). $[\alpha]_D^{20}$ –7.65 (c 1.35, MeOH). ^1H NMR (800 MHz, CD_3OD) δ 5.14 (t, J = 7.0 Hz, 1H), 4.41 (t, J = 4.3 Hz, 1H), 4.33 (t, J = 7.2 Hz, 1H), 2.18 (d, J = 15.2 Hz, 1H), 1.99–1.94 (m, 2H), 1.88 (ddd, J = 14.5, 6.9, 4.5 Hz, 1H). ^{13}C NMR (201 MHz, CD_3OD) δ 160.5, 82.4, 72.1, 56.6, 47.9, 47.8, 47.7, 47.6, 47.5, 47.4, 47.3, 41.6, 41.2. LRMS (ESI) m/z : $[\text{M} + \text{H}]^+$ 144.1. HRMS (ESI) m/z : $[\text{M} + \text{H}]^+$ calcd $\text{C}_6\text{H}_{10}\text{NO}_3$ 144.0655; found 144.0653.

(3a*S*,5*R*,6a*R*)-5-Hydroxy-3-phenylhexahydro-2*H*-cyclopenta[d]oxazol-2-one (10a). To a stirring solution of cyclic phenyl carbamate **7a** (22 mg, 0.08 mmol) in methanol (2.8 mL) was added potassium carbonate (14 mg, 0.1 mmol). Reaction was stirred at 23 °C for 12 h. Upon completion, the residue solvent was removed under reduced pressure. The crude product was purified by silica gel column chromatography (60% EtOAc in hexane) to afford **10a** (14 mg, 73%). $[\alpha]_D^{20}$ +87.6 (c 1.90, MeOH). ^1H NMR (800 MHz, CDCl_3) δ 7.56 (dt, J = 8.6, 1.2 Hz, 2H), 7.39 (ddt, J = 8.7, 7.3, 1.7 Hz, 2H), 7.16 (td, J = 7.3, 1.3 Hz, 1H), 5.15 (t, J = 7.0 Hz, 1H), 4.88 (t, J = 7.3 Hz, 1H), 4.53 (t, J = 4.4 Hz, 1H), 2.41 (dd, J = 15.6, 3.0 Hz, 1H), 2.20 (ddd, J = 14.9, 3.0, 1.5 Hz, 1H), 2.06 (ddd, J = 15.5, 6.3, 4.3 Hz, 1H), 1.90 (ddd, J = 15.0, 7.0, 4.4 Hz, 1H), 1.84 (s, 1H). ^{13}C NMR (201 MHz, CDCl_3) δ 154.9, 137.6, 129.2, 124.4, 120.4, 78.0, 77.2, 77.0, 76.9, 72.6, 61.1, 42.6, 39.5. LRMS (ESI) m/z : $[\text{M} + \text{H}]^+$ 220.1. HRMS (ESI) m/z : $[\text{M} + \text{Na}]^+$ calcd $\text{C}_{12}\text{H}_{13}\text{NO}_3\text{Na}$ 242.0788; found 242.0786.

(3a*S*,5*R*,6a*R*)-5-Hydroxy-3-(4-methoxyphenyl)hexahydro-2*H*-cyclopenta[d]oxazol-2-one (10b). To a stirring solution of cyclic *p*-methoxyphenyl carbamate **7b** (46 mg, 0.2 mmol) in methanol (6 mL) was added potassium carbonate (26 mg, 0.2 mmol). Reaction was stirred at 23 °C for 12 h. Upon completion, the residue solvent was removed under reduced pressure. The crude product was purified by silica gel column chromatography (60% EtOAc in hexane) to afford **10b** (38 mg, 96%). $[\alpha]_D^{20}$ +75.5 (c 2.00, MeOH). ^1H NMR (400 MHz, CDCl_3) δ 7.45–7.36 (m, 2H), 6.95–6.87 (m, 2H), 5.13 (dd, J = 7.8, 5.2 Hz, 1H), 4.78 (t, J = 7.2 Hz, 1H), 4.54–4.46 (m, 1H), 3.80 (s, 3H), 2.41–2.31 (m, 1H), 2.14 (ddt, J = 14.9, 2.8, 1.2 Hz, 1H), 2.03 (ddd, J = 15.4, 6.4, 4.2 Hz, 1H), 1.78 (ddd, J = 14.9, 6.9, 4.3 Hz, 1H), 1.71 (d, J = 2.4 Hz, 1H). ^{13}C NMR (101 MHz, CDCl_3) δ 156.8, 155.2, 130.3, 123.3, 114.4, 77.9, 77.2, 76.9, 76.6, 72.6, 61.7, 55.4, 42.7, 39.0. LRMS (ESI) m/z : $[\text{M} + \text{H}]^+$ 250.0.

HRMS (ESI) m/z : $[\text{M} + \text{Na}]^+$ calcd $\text{C}_{13}\text{H}_{15}\text{NO}_4\text{Na}$ 272.0893; found 272.0895.

(3a*S*,5*R*,6a*R*)-5-Hydroxy-3-(3-methoxyphenyl)hexahydro-2*H*-cyclopenta[d]oxazol-2-one (10c). To a stirring solution of cyclic *m*-methoxyphenyl carbamate **7c** (24 mg, 0.08 mmol) in methanol (6.7 mL) was added potassium carbonate (17 mg, 0.1 mmol). Reaction was stirred at 23 °C for 12 h. Upon completion, the residue solvent was removed under reduced pressure. The crude product was purified by silica gel column chromatography (60% EtOAc in hexane) to afford **10c** (20 mg, 97%). $[\alpha]_D^{20}$ +98.2 (c 2, MeOH). ^1H NMR (800 MHz, CDCl_3) δ 7.32–7.26 (m, 2H), 7.07 (ddd, J = 8.2, 2.1, 0.9 Hz, 1H), 6.71 (ddd, J = 8.3, 2.5, 0.8 Hz, 1H), 5.14 (t, J = 7.0 Hz, 1H), 4.85 (t, J = 7.3 Hz, 1H), 4.54 (t, J = 4.3 Hz, 1H), 3.84 (s, 3H), 2.40 (dd, J = 15.5, 2.2 Hz, 1H), 2.23 (dd, J = 14.9, 2.9 Hz, 1H), 2.10–2.02 (m, 1H), 1.92 (ddd, J = 15.0, 7.1, 4.4, 0.6 Hz, 1H), 1.71 (s, 1H). ^{13}C NMR (201 MHz, CDCl_3) δ 160.3, 154.7, 138.8, 129.8, 112.2, 109.8, 106.3, 77.9, 77.2, 77.0, 76.9, 72.6, 61.1, 55.4, 42.5, 39.7. LRMS (ESI) m/z : $[\text{M} + \text{H}]^+$ 250.1. HRMS (ESI) m/z : $[\text{M} + \text{Na}]^+$ calcd $\text{C}_{13}\text{H}_{15}\text{NO}_4\text{Na}$ 272.0893; found 272.0895.

(3a*S*,5*R*,6a*R*)-5-Hydroxy-3-(2-methoxyphenyl)hexahydro-2*H*-cyclopenta[d]oxazol-2-one (10d). To a stirring solution of cyclic *o*-methoxyphenyl carbamate **7d** (20 mg, 0.1 mmol) in methanol (5.5 mL) was added potassium carbonate (17 mg, 0.1 mmol). Reaction was stirred at 23 °C for 12 h. Upon completion, the residue solvent was removed under reduced pressure. The crude product was purified by silica gel column chromatography (60% EtOAc in hexane) to afford **10d** (17 mg, 96%). $[\alpha]_D^{20}$ +71.2 (c 2.67, MeOH). ^1H NMR (400 MHz, CDCl_3) δ 7.38 (dd, J = 7.7, 1.7 Hz, 1H), 7.30 (ddd, J = 8.3, 7.5, 1.7 Hz, 1H), 7.05–6.96 (m, 2H), 5.19 (t, J = 7.2 Hz, 1H), 4.82 (t, J = 7.3 Hz, 1H), 4.47 (t, J = 4.4 Hz, 1H), 3.87 (s, 3H), 2.39 (ddd, J = 15.5, 3.1, 0.9 Hz, 2H), 2.10–1.87 (m, 3H), 1.63 (dddd, J = 15.1, 6.7, 4.5, 0.6 Hz, 2H). ^{13}C NMR (101 MHz, CDCl_3) δ 156.1, 155.1, 129.8, 129.0, 125.0, 121.3, 112.1, 79.0, 77.2, 77.1, 76.9, 76.6, 72.7, 62.1, 55.7, 43.0, 38.8, 29.6. LRMS (ESI) m/z : $[\text{M} + \text{H}]^+$ 250.0. HRMS (ESI) m/z : $[\text{M} + \text{H}]^+$ calcd $\text{C}_{13}\text{H}_{15}\text{NO}_4$ 250.1074; found 250.1072.

(3a*S*,5*R*,6a*R*)-5-Hydroxy-3-methylhexahydro-2*H*-cyclopenta[d]oxazol-2-one (10e). Protected oxazolidinone **8** (21 mg, 0.1 mmol) was dissolved with dry acetonitrile (1.4 mL) and was placed under an argon atmosphere. Reaction mixture was cooled to 0 °C, and potassium bis(trimethylsilyl)amide (0.5 M solution) (0.25 mL, 0.1 mmol) was added dropwise. The reaction stirred for 30 min. Iodomethane (18 mg, 0.1 mmol) was then added dropwise, and the reaction mixture was allowed to warm up to 23 °C for 1 h. Upon completion, the residue was taken up in DI water and the aqueous phase was extracted with EtOAc. The organic extracts were dried with Na_2SO_4 , and the solvent was removed under reduced pressure. The crude product was taken up in methanol (3 mL) and followed the addition of potassium carbonate (19 mg, 0.14 mmol). The reaction was stirred at 23 °C for 12 h. Upon completion, the residue solvent was removed under reduced pressure. The crude product was purified by silica gel column chromatography (60% EtOAc in hexane) to afford **10e** (14 mg, 80%). $[\alpha]_D^{20}$ +31.2 (c 2.20, MeOH). ^1H NMR (400 MHz, CDCl_3) δ 4.98 (t, J = 7.0 Hz, 1H), 4.48 (t, J = 4.2 Hz, 1H), 4.17 (t, J = 7.2 Hz, 1H), 2.85 (s, 3H), 2.38 (s, 1H), 2.23 (ddd, J = 34.7, 15.9, 1.9 Hz, 2H), 1.94 (dddd, J = 15.4, 6.6, 4.3, 0.6 Hz, 1H), 1.66 (dddd, J = 14.8, 6.8, 4.3, 0.6 Hz, 1H). ^{13}C NMR (101 MHz, CDCl_3) δ 157.6, 78.4, 77.3, 76.9, 76.6, 72.4, 61.9, 42.4, 37.6, 29.2. LRMS (ESI) m/z : $[\text{M} + \text{H}]^+$ 158.0. HRMS (ESI) m/z : $[\text{M} + \text{Na}]^+$ calcd $\text{C}_7\text{H}_{11}\text{NO}_3\text{Na}$ 180.0631; found 180.0630.

(3a*R*,5*S*,6a*S*)-5-Hydroxy-3-methylhexahydro-2*H*-cyclopenta[d]oxazol-2-one (*ent*-10e). Protected oxazolidinone *ent*-8 (20 mg, 0.1 mmol) was dissolved with freshly distilled dimethylformamide (2.1 mL) and was placed under an argon atmosphere. Reaction mixture was cooled to 0 °C, and sodium hydride (0.1 mmol) was added all at once. Reaction stirred for 20 min, and then iodomethane (21 mg, 0.2 mmol) was added dropwise. Reaction was allowed to warm up to 23 °C for 1 h. Upon completion, the residue was taken up in water and the aqueous phase was extracted with EtOAc. The organic extracts were dried with Na_2SO_4 .

and the solvent was removed under reduced pressure. The crude product was taken up in methanol (2.1 mL) and followed the addition of potassium carbonate (17 mg, 0.1 mmol). Reaction was stirred at 23 °C for 12 h. Upon completion, the residue solvent was removed under reduced pressure. The crude product was purified by silica gel column chromatography (60% EtOAc in hexane) to afford *ent*-**10e** (10 mg, 60%). $[\alpha]_D^{20}$ -16.0 (c 1.00, MeOH). ^1H NMR (800 MHz, CD_3OD) δ 5.04 (t, J = 8.0, 7.0 Hz, 1H), 4.40 (t, J = 4.3 Hz, 1H), 4.27 (t, J = 7.2 Hz, 1H), 2.85 (s, 3H), 2.20–2.13 (m, 2H), 2.03–1.96 (m, 2H), 1.77–1.71 (m, 2H). ^{13}C NMR (201 MHz, CD_3OD) δ 158.6, 79.2, 71.8, 62.1, 47.9, 47.8, 47.7, 47.6, 47.5, 47.4, 47.3, 41.3, 36.9, 27.9. LRMS (ESI) m/z : $[\text{M} + \text{H}]^+$ 158.0. HRMS (ESI) m/z : $[\text{M} + \text{H}]^+$ calcd $\text{C}_9\text{H}_{12}\text{NO}_3$ 158.0812; found 158.0810.

(3aS,5R,6aR)-3-Allyl-5-hydroxyhexahydro-2H-cyclopenta[d]oxazol-2-one (10f). Protected oxazolidinone **8** (17 mg, 0.1 mmol) was dissolved with dry acetonitrile (4 mL) and was placed under an argon atmosphere. Reaction mixture was cooled to 0 °C, and potassium bis(trimethylsilyl)amide (0.5 M solution, 0.2 mL, 0.1 mmol) was added dropwise. The reaction stirred for 30 min. Allyl iodide (17 mg, 0.1 mmol) was then added dropwise, and the reaction mixture was allowed to warm up to 23 °C for 1 h. Upon completion, the residue was taken up in DI water and the aqueous phase was extracted with EtOAc. The organic extracts were dried with Na_2SO_4 , and the solvent was removed under reduced pressure. The crude product was taken up in methanol (2 mL) and followed the addition of potassium carbonate (15 mg, 0.11 mmol). Reaction was stirred at 23 °C for 12 h. Upon completion, the residue solvent was removed under reduced pressure. The crude product was purified by silica gel column chromatography (80% EtOAc in hexane) to afford **10f** (10 mg, 60%). $[\alpha]_D^{20}$ +19 (c 2.0, MeOH). ^1H NMR (800 MHz, CD_3OD) δ 5.76 (ddd, J = 17.2, 10.2, 7.1, 4.9 Hz, 1H), 5.22 (dq, J = 17.1, 1.5 Hz, 1H), 5.16 (dq, J = 10.2, 1.4 Hz, 1H), 4.96 (t, J = 7.1 Hz, 1H), 4.31 (dq, J = 4.3, 2.1, 1.6 Hz, 1H), 4.24 (t, J = 7.3 Hz, 1H), 4.04 (ddt, J = 15.8, 5.0, 1.7 Hz, 1H), 3.58 (ddt, J = 15.8, 7.1, 1.3 Hz, 1H), 2.07 (dd, J = 28.0, 15.3 Hz, 2H), 1.92 (ddd, J = 15.1, 6.5, 4.3 Hz, 1H), 1.63 (ddd, J = 14.7, 6.9, 4.3 Hz, 1H). ^{13}C NMR (201 MHz, CD_3OD) δ 159.7, 133.7, 118.5, 80.9, 73.2, 61.1, 49.1, 49.0, 48.9, 46.1, 42.7, 38.7. LRMS (ESI) m/z : $[\text{M} + \text{H}]^+$ 183.9. HRMS (ESI) m/z : $[\text{M} + \text{H}]^+$ calcd $\text{C}_9\text{H}_{14}\text{NO}_3$ 184.0968; found 184.0967.

(3aS,5R,6aR)-5-Hydroxy-3-propylhexahydro-2H-cyclopenta[d]oxazol-2-one (10g). To a stirred reaction of alcohol **10f** (4.5 mg, 0.02 mmol) in dry methanol (1 mL) under an argon atmosphere were added Pd/C (10 wt %) and a hydrogen balloon. Reaction mixture was stirred at 23 °C for 12 h. Upon completion, the residue was filtered over Celite and rinsed with dichloromethane. The solvent collected was removed under reduced pressure. The crude product was purified by silica gel column chromatography (60% EtOAc in hexane) to afford **10g** (3.9 mg, 86%). $[\alpha]_D^{20}$ +14.3 (c 0.77, MeOH). ^1H NMR (800 MHz, CDCl_3) δ 5.02 (t, J = 7.0 Hz, 1H), 4.51 (t, J = 4.4 Hz, 1H), 4.28 (t, J = 7.2 Hz, 1H), 3.51 (ddd, J = 14.1, 8.7, 7.3 Hz, 1H), 3.04 (ddd, J = 13.9, 8.6, 5.2 Hz, 1H), 2.30–2.26 (m, 1H), 2.20–2.16 (m, 1H), 2.03 (ddd, J = 15.5, 6.5, 4.4 Hz, 1H), 1.75 (ddd, J = 14.9, 6.9, 4.5 Hz, 1H), 1.69–1.64 (m, 1H), 1.61 (ddd, J = 13.5, 8.0, 6.6 Hz, 1H), 0.97 (t, J = 7.4 Hz, 3H). ^{13}C NMR (201 MHz, CDCl_3) δ 157.3, 78.3, 77.2, 77.0, 76.9, 72.8, 59.5, 44.2, 42.7, 38.3, 29.7, 20.5, 11.2. LRMS (ESI) m/z : $[\text{M} + \text{H}]^+$ 186.0. HRMS (ESI) m/z : $[\text{M} + \text{Na}]^+$ calcd $\text{C}_9\text{H}_{15}\text{NO}_3\text{Na}$ 208.0944; found 208.0942.

(3aS,5R,6aR)-5-Hydroxy-3-(2-methylallyl)hexahydro-2H-cyclopenta[d]oxazol-2-one (10h). Protected oxazolidinone **8** (10 mg, 0.06 mmol) was dissolved with dry acetonitrile (1 mL) and was placed under an argon atmosphere. Reaction mixture was cooled to 0 °C, and potassium bis(trimethylsilyl)amide (0.5 M solution, 0.13 mL, 0.07 mmol) was added dropwise. The reaction stirred for 30 min. 3-Bromo-2-methylprop-1-ene (8.8 mg, 0.06 mmol) was then added dropwise, and the reaction mixture was allowed to warm up to 23 °C for 1 h. Upon completion, the residue was taken up in DI water and the aqueous phase was extracted with EtOAc. The organic extracts were dried with Na_2SO_4 and the solvent was removed under reduced pressure. The crude product was taken up in methanol (0.6 mL) and followed the addition of potassium carbonate (4.6 mg, 0.02 mmol).

Reaction was stirred at 23 °C for 12 h. Upon completion, the residue solvent was removed under reduced pressure. The crude product was purified by silica gel column chromatography (80% EtOAc in hexane) to afford **10h** (3.2 mg, 84%). $[\alpha]_D^{20}$ +22.9 (c 0.67, MeOH). ^1H NMR (800 MHz, CDCl_3) δ 5.03 (t, J = 7.0 Hz, 1H), 4.95 (d, J = 20.5 Hz, 2H), 4.51 (s, 1H), 4.19 (t, J = 7.3 Hz, 1H), 4.15 (d, J = 15.2 Hz, 1H), 3.58 (d, J = 15.3 Hz, 1H), 2.30 (dd, J = 15.5, 2.9 Hz, 1H), 2.19 (dt, J = 14.8, 1.8 Hz, 1H), 2.01 (ddd, J = 15.4, 6.4, 4.3 Hz, 1H), 1.77 (s, 2H), 1.69 (ddt, J = 19.2, 7.0, 3.7 Hz, 2H). ^{13}C NMR (201 MHz, CDCl_3) δ 157.5, 140.1, 113.8, 78.5, 77.2, 77.0, 76.9, 72.7, 59.3, 48.9, 42.7, 38.0, 19.9. LRMS (ESI) m/z : $[\text{M} + \text{H}]^+$ 198.0. HRMS (ESI) m/z : $[\text{M} + \text{H}]^+$ calcd $\text{C}_{10}\text{H}_{14}\text{NO}_3$ 198.1125; found 198.1126.

(3aS,5R,6aR)-5-Hydroxy-3-isobutylhexahydro-2H-cyclopenta[d]oxazol-2-one (10i). To a stirred reaction of alcohol **10h** (16 mg, 0.07 mmol) in dry methanol (2.2 mL) under an argon atmosphere were added of Pd/C (10 wt %) and a hydrogen balloon. Reaction mixture was stirred at 23 °C for 12 h. Upon completion, the residue was filtered over Celite and rinsed with dichloromethane. The solvent collected was removed under reduced pressure. The crude product was purified by silica gel column chromatography (60% EtOAc in hexane) to afford **10i** (15 mg, 92%). $[\alpha]_D^{20}$ +65.2 (c 2.00, MeOH). ^1H NMR (800 MHz, CDCl_3) δ 5.02 (t, J = 6.9 Hz, 1H), 4.51 (s, 1H), 4.26 (t, J = 7.4 Hz, 1H), 3.33 (t, J = 12.5, 11.0 Hz, 1H), 2.89 (ddd, J = 14.1, 6.2, 2.3 Hz, 1H), 2.29 (d, J = 15.4 Hz, 1H), 2.19 (d, J = 14.7 Hz, 1H), 2.05–1.91 (m, 2H), 1.78–1.67 (m, 2H), 0.99 (d, J = 6.5 Hz, 3H), 0.94 (d, J = 6.5 Hz, 3H). ^{13}C NMR (201 MHz, CDCl_3) δ 157.7, 78.38, 77.2, 77.0, 76.9, 72.7, 59.9, 50.0, 42.7, 38.0, 26.4, 20.2, 19.8. LRMS (ESI) m/z : $[\text{M} + \text{H}]^+$ 200.1. HRMS (ESI) m/z : $[\text{M} + \text{H}]^+$ calcd $\text{C}_{10}\text{H}_{18}\text{NO}_3$ 200.1281; found 200.1280.

(3aS,5R,6aR)-5-Hydroxy-3-(methoxymethyl)hexahydro-2H-cyclopenta[d]oxazol-2-one (10j). Protected oxazolidinone **8** (8 mg, 0.04 mmol) was dissolved with dry tetrahydrofuran (2.7 mL) and was placed under an argon atmosphere. Reaction mixture was cooled to 0 °C, and potassium bis(trimethylsilyl)amide (0.5 M solution, 0.13 mL, 0.07 mmol) was added dropwise. The reaction stirred for 30 min. Chloromethyl methyl ether (5.7 mg, 0.07 mmol) was then added dropwise, and the reaction mixture was allowed to warm up to 23 °C for 1 h. Upon completion, the residue was taken up in DI water, and the aqueous phase was extracted with EtOAc. The organic extracts were dried with Na_2SO_4 , and the solvent was removed under reduced pressure. The crude product was taken up in methanol (1 mL) and followed the addition of potassium carbonate (8 mg, 0.06 mmol). Reaction was stirred at 23 °C for 12 h. Upon completion, the residue solvent was removed under reduced pressure. The crude product was purified by silica gel column chromatography (60% EtOAc in hexane) to afford **10j** (2.7 mg, 33%). $[\alpha]_D^{20}$ +9.87 (c 2.60, MeOH). ^1H NMR (800 MHz, CD_3OD) δ 5.09 (t, J = 7.1 Hz, 1H), 4.77 (d, J = 11.0 Hz, 1H), 4.68 (d, J = 11.1 Hz, 1H), 4.45–4.40 (m, 2H), 3.35 (s, 3H), 2.20 (dd, J = 14.9, 1.4 Hz, 2H), 2.04–1.98 (m, 1H), 1.83–1.76 (m, 1H). ^{13}C NMR (201 MHz, CD_3OD) δ 158.7, 79.9, 74.8, 71.9, 59.4, 54.8, 47.9, 47.9, 47.8, 47.7, 47.6, 47.5, 47.4, 47.3, 41.1, 38.3. LRMS (ESI) m/z : $[\text{M} + \text{Na}]^+$ 209.9. HRMS (ESI) m/z : $[\text{M} + \text{Na}]^+$ calcd $\text{C}_{18}\text{H}_{13}\text{NO}_3\text{Na}$ 210.0737; found 210.0736.

4-Nitrophenyl ((3aS,5R,6aR)-2-Oxohexahydro-2H-cyclopenta[d]oxazol-5-yl)carbonate (11a). To a stirred solution of alcohol **9** (10 mg, 0.07 mmol) in dry dichloromethane (2 mL) were added 4-methylmorpholine (23 μL , 0.2 mmol) and 4-nitrophenyl chloroformate (42 mg, 0.2 mmol) at 0 °C under an argon atmosphere. The reaction mixture was warmed to 23 °C and stirred for 12 h. Upon completion, solvent was removed under reduced pressure. The crude product was purified by silica gel column chromatography (80% EtOAc in hexane) to afford **11a** (18 mg, 83%). ^1H NMR (800 MHz, CDCl_3) δ 8.29 (d, J = 9.1 Hz, 2H), 7.40 (d, J = 9.1 Hz, 2H), 5.36 (t, J = 4.6 Hz, 1H), 5.29 (s, 1H), 5.26 (t, J = 6.9 Hz, 1H), 4.49 (t, J = 7.2 Hz, 1H), 2.67 (dd, J = 16.3, 3.0 Hz, 1H), 2.34 (dd, J = 15.6, 3.0 Hz, 1H), 2.16 (ddd, J = 16.2, 6.4, 4.6 Hz, 1H), 2.10 (ddd, J = 15.6, 6.8, 4.7 Hz, 1H). ^{13}C NMR (201 MHz, CDCl_3) δ 158.1, 155.4, 151.9, 145.5, 125.3, 121.9, 81.0, 80.7, 77.2, 77.0, 76.9, 55.9, 40.2, 39.5, 29.7. LRMS (ESI) m/z : $[\text{M} + \text{H}]^+$ 309.0.

(3aS,5R,6aR)-3-Methyl-2-oxohexahydro-2H-cyclopenta[d]oxazol-5-yl (4-Nitrophenyl) Carbonate (11b). Alcohol 10e (13 mg, 0.08 mmol) was treated with 4-methylmorpholine (27 μ L, 0.3 mmol) and 4-nitrophenyl chloroformate (50 mg, 0.3 mmol) by following the procedure outline for activated alcohol 11a to afford 11b (15 mg, 56%): ^1H NMR (500 MHz, CDCl_3) δ 8.26 (d, J = 9.2 Hz, 2H), 7.35 (d, J = 9.2 Hz, 2H), 5.32–5.28 (m, 1H), 5.07 (t, J = 7.1 Hz, 1H), 4.28 (t, J = 7.1 Hz, 1H), 2.89 (s, 3H), 2.59 (dd, J = 16.3, 2.7 Hz, 1H), 2.44 (dd, J = 15.7, 3.1 Hz, 1H), 2.21–2.13 (m, 1H), 1.98–1.88 (m, 1H). ^{13}C NMR (126 MHz, CDCl_3) δ 156.9, 155.3, 151.9, 145.5, 125.3, 121.9, 80.5, 77.3, 77.0, 76.8, 61.5, 39.7, 35.6, 29.3. LRMS (ESI) m/z : $[\text{M} + \text{H}]^+$ 323.0.

4-Nitrophenyl ((3aR,5S,6aS)-2-Oxohexahydro-2H-cyclopenta[d]oxazol-5-yl)carbonate (11c). Alcohol *ent*-9 (6.3 mg, 0.04 mmol) was treated with 4-methylmorpholine (15 μ L, 0.1 mmol) and 4-nitrophenyl chloroformate (27 mg, 0.1 mmol) by following the procedure outline for activated alcohol 11a to afford 11c (4.8 mg, 35%): ^1H NMR (800 MHz, CDCl_3) δ 8.29 (d, J = 8.5 Hz, 2H), 7.40 (d, J = 8.7 Hz, 2H), 5.36 (t, J = 4.8 Hz, 1H), 5.26 (t, J = 7.0 Hz, 1H), 5.19 (s, 1H), 4.49 (t, J = 7.2 Hz, 1H), 2.67 (d, J = 15.9 Hz, 1H), 2.34 (d, J = 15.5 Hz, 1H), 2.15 (dt, J = 16.3, 5.5 Hz, 1H), 2.10 (dt, J = 15.6, 5.8 Hz, 1H). ^{13}C NMR (201 MHz, CDCl_3) δ 158.1, 155.4, 151.9, 145.5, 125.3, 121.9, 81.0, 80.7, 77.2, 77.0, 76.9, 55.9, 40.2, 39.5. LRMS (ESI) m/z : $[\text{M} + \text{H}]^+$ 309.0.

4-Nitrophenyl ((3aR,5S,6aS)-2-Oxohexahydro-2H-cyclopenta[d]oxazol-5-yl)carbonate (11d). Alcohol *ent*-10e (5.7 mg, 0.04 mmol) was treated with 4-methylmorpholine (12 μ L, 0.1 mmol) and 4-nitrophenyl chloroformate (22 mg, 0.1 mmol) by following the procedure outline for activated alcohol 11a to afford 11d (11 mg, 94%): ^1H NMR (500 MHz, CDCl_3) δ 8.27 (d, J = 9.2 Hz, 2H), 7.36 (d, J = 9.2 Hz, 2H), 5.30 (t, J = 4.6 Hz, 1H), 5.07 (t, J = 7.0 Hz, 1H), 4.28 (t, J = 7.1 Hz, 1H), 2.89 (s, 3H), 2.45 (dd, J = 15.6, 3.0 Hz, 1H), 2.20–2.13 (m, 1H), 1.96–1.89 (m, 1H). ^{13}C NMR (126 MHz, CDCl_3) δ 156.9, 155.3, 151.9, 145.5, 125.3, 121.9, 80.5, 77.3, 77.2, 77.0, 76.8, 61.5, 39.7, 35.6, 29.3. LRMS (ESI) m/z : $[\text{M} + \text{H}]^+$ 323.0.

4-Nitrophenyl ((3aR,5S,6aS)-2-Oxohexahydro-2H-cyclopenta[d]oxazol-5-yl)carbonate (11e). Alcohol 10a (14 mg, 0.06 mmol) was treated with 4-methylmorpholine (20 μ L, 0.2 mmol) and 4-nitrophenyl chloroformate (37 mg, 0.2 mmol) by following the procedure outline for activated alcohol 11a to afford 11e (19 mg, 78%): ^1H NMR (800 MHz, CDCl_3) δ 8.27 (dd, J = 9.0, 1.8 Hz, 2H), 7.54 (d, J = 7.9 Hz, 2H), 7.44–7.38 (m, 2H), 7.33–7.26 (m, 3H), 7.21 (t, J = 7.4 Hz, 1H), 5.33 (t, J = 4.6 Hz, 1H), 5.25 (t, J = 7.0 Hz, 1H), 5.02 (t, J = 7.1 Hz, 1H), 2.72 (dd, J = 16.3, 3.2 Hz, 1H), 2.49 (dd, J = 15.7, 3.2 Hz, 1H), 2.27 (dddd, J = 16.2, 6.4, 4.5, 1.6 Hz, 1H), 2.09 (dddd, J = 15.8, 6.5, 4.4, 1.5 Hz, 1H). ^{13}C NMR (201 MHz, CDCl_3) δ 155.3, 154.3, 151.8, 145.5, 137.0, 129.3, 125.3, 124.9, 121.9, 120.7, 80.4, 77.2, 77.0, 76.9, 60.6, 39.9, 36.9. LRMS (ESI) m/z : $[\text{M} + \text{H}]^+$ 385.0.

(3aS,5R,6aR)-3-(4-Methoxyphenyl)-2-oxohexahydro-2H-cyclopenta[d]oxazol-5-yl (4-Nitrophenyl) Carbonate (11f). Alcohol 10b (6.8 mg, 0.03 mmol) was treated with 4-methylmorpholine (9.0 μ L, 0.08 mmol) and 4-nitrophenyl chloroformate (17 mg, 0.08 mmol) by following the procedure outline for activated alcohol 11a to afford 11f (11 mg, 97%): ^1H NMR (500 MHz, CDCl_3) δ 8.27 (d, J = 9.2 Hz, 2H), 7.38 (d, J = 9.1 Hz, 2H), 7.32 (d, J = 9.2 Hz, 2H), 6.92 (d, J = 9.1 Hz, 2H), 5.31 (t, J = 4.5 Hz, 1H), 5.22 (t, J = 7.1 Hz, 1H), 4.92 (t, J = 7.0 Hz, 1H), 3.81 (s, 3H), 2.69 (dd, J = 16.3, 2.8 Hz, 1H), 2.43 (dd, J = 15.7, 3.1 Hz, 1H), 2.27–2.19 (m, 1H), 2.03–1.95 (m, 1H). ^{13}C NMR (126 MHz, CDCl_3) δ 157.2, 155.3, 154.7, 151.9, 145.5, 129.8, 125.3, 123.5, 121.9, 114.6, 80.5, 77.3, 77.0, 76.8, 61.3, 55.6, 40.0, 36.7. LRMS (ESI) m/z : $[\text{M} + \text{H}]^+$ 415.0.

(3aS,5R,6aR)-3-(3-Methoxyphenyl)-2-oxohexahydro-2H-cyclopenta[d]oxazol-5-yl (4-Nitrophenyl) Carbonate (11g). Alcohol 10c (20 mg, 0.08 mmol) was treated with 4-methylmorpholine (26 μ L, 0.2 mmol) and 4-nitrophenyl chloroformate (48 mg, 0.2 mmol) by following the procedure outline for activated alcohol 11a to afford 11g (13 mg, 60%): ^1H NMR (800 MHz, CDCl_3) δ 8.27 (d, J = 9.2 Hz, 2H), 7.32–7.29 (m, 3H), 7.22 (t, J = 2.3 Hz, 1H), 7.05 (dd, J

= 8.0, 1.7 Hz, 1H), 6.75 (dd, J = 8.3, 2.3 Hz, 1H), 5.32 (t, J = 4.5 Hz, 1H), 5.24 (t, J = 7.0 Hz, 1H), 4.98 (t, J = 7.1 Hz, 1H), 3.81 (s, 3H), 2.71 (dd, J = 16.2, 3.1 Hz, 1H), 2.52 (dd, J = 15.8, 3.1 Hz, 1H), 2.26 (ddd, J = 16.2, 6.6, 4.6 Hz, 1H), 2.09 (ddd, J = 15.8, 6.8, 4.5 Hz, 1H). ^{13}C NMR (201 MHz, CDCl_3) δ 160.4, 155.3, 154.1, 151.8, 145.5, 138.2, 130.0, 125.3, 121.9, 112.6, 109.9, 107.3, 80.4, 77.2, 77.0, 76.9, 60.6, 55.4, 39.9, 37.0. LRMS (ESI) m/z : $[\text{M} + \text{H}]^+$ 415.0.

(3aS,5R,6aR)-3-(2-Methoxyphenyl)-2-oxohexahydro-2H-cyclopenta[d]oxazol-5-yl (4-Nitrophenyl) Carbonate (11h). Alcohol 10d (21 mg, 0.08 mmol) was treated with 4-methylmorpholine (28 μ L, 0.3 mmol) and 4-nitrophenyl chloroformate (51 mg, 0.3 mmol) by following the procedure outline for activated alcohol 11a to afford 11h (15 mg, 42%): ^1H NMR (800 MHz, CDCl_3) δ 8.32 (d, J = 9.0 Hz, 2H), 7.42 (t, J = 8.0 Hz, 3H), 7.33 (t, J = 7.8 Hz, 2H), 7.00 (d, J = 8.0 Hz, 2H), 5.33 (t, J = 4.3 Hz, 1H), 5.28 (t, J = 7.2 Hz, 1H), 5.09 (t, J = 7.2 Hz, 1H), 3.90 (s, 3H), 2.71 (dd, J = 16.2, 3.1 Hz, 2H), 2.28–2.21 (m, 3H), 1.85 (ddd, J = 15.8, 6.8, 4.6 Hz, 2H). ^{13}C NMR (201 MHz, CDCl_3) δ 156.0, 155.4, 154.9, 152.0, 145.5, 129.8, 129.0, 125.4, 124.6, 121.9, 121.1, 112.0, 80.8, 77.9, 77.2, 77.0, 76.9, 60.8, 55.7, 40.1, 36.7. LRMS (ESI) m/z : $[\text{M} + \text{H}]^+$ 415.1.

(3aS,5R,6aR)-3-Allyl-2-oxohexahydro-2H-cyclopenta[d]oxazol-5-yl (4-Nitrophenyl) Carbonate (11i). Alcohol 10f (14 mg, 0.08 mmol) was treated with 4-methylmorpholine (25 μ L, 0.2 mmol) and 4-nitrophenyl chloroformate (46 mg, 0.2 mmol) by following the procedure outline for activated alcohol 11a to afford 11i (17 mg, 66%): ^1H NMR (800 MHz, CDCl_3) δ 8.30 (d, J = 9.2 Hz, 2H), 7.39 (d, J = 9.2 Hz, 2H), 5.83 (dddd, J = 17.2, 10.1, 7.1, 5.4 Hz, 1H), 5.34–5.27 (m, 3H), 5.10 (t, J = 7.1 Hz, 1H), 4.37 (t, J = 7.2 Hz, 1H), 4.20 (ddt, J = 15.5, 5.4, 1.6 Hz, 1H), 3.69 (ddt, J = 15.5, 7.1, 1.2 Hz, 1H), 2.63 (dd, J = 16.2, 2.5 Hz, 1H), 2.48 (dd, J = 15.7, 3.0 Hz, 1H), 2.18 (dddd, J = 16.2, 6.6, 4.6, 0.7 Hz, 1H), 1.92 (dddd, J = 15.6, 6.8, 4.7, 0.7 Hz, 1H). ^{13}C NMR (201 MHz, CDCl_3) δ 156.6, 155.3, 151.9, 145.5, 132.3, 125.3, 121.9, 118.9, 80.5, 77.6, 77.2, 77.0, 76.9, 59.3, 45.6, 39.7, 36.0. LRMS (ESI) m/z : $[\text{M} + \text{H}]^+$ 349.0.

4-Nitrophenyl ((3aS,5R,6aR)-2-oxo-3-propylhexahydro-2H-cyclopenta[d]oxazol-5-yl)carbonate (11j). Alcohol 10g (7 mg, 0.04 mmol) was treated with 4-methylmorpholine (12 μ L, 0.1 mmol) and 4-nitrophenyl chloroformate (23 mg, 0.1 mmol) by following the procedure outline for activated alcohol 11a to afford 11j (4 mg, 30%): ^1H NMR (500 MHz, CDCl_3) δ 8.27 (d, J = 9.2 Hz, 2H), 7.36 (d, J = 9.2 Hz, 2H), 5.29 (t, J = 4.6 Hz, 1H), 5.07 (t, J = 7.0 Hz, 1H), 4.35 (t, J = 7.2 Hz, 1H), 3.47 (ddd, J = 14.0, 8.8, 7.1 Hz, 1H), 3.02 (ddd, J = 14.0, 8.6, 5.2 Hz, 1H), 2.60 (ddd, J = 16.3, 3.0, 1.0 Hz, 1H), 2.43 (dd, J = 15.7, 3.0 Hz, 1H), 2.16 (dddd, J = 16.1, 6.5, 4.7, 0.7 Hz, 1H), 1.94 (dddd, J = 15.6, 6.8, 4.7, 0.7 Hz, 1H), 1.73–1.57 (m, 2H), 0.95 (t, J = 7.4 Hz, 3H). ^{13}C NMR (126 MHz, CDCl_3) δ 156.9, 155.3, 151.9, 145.5, 125.3, 121.9, 80.5, 77.3, 77.0, 76.8, 59.4, 44.3, 39.7, 36.2, 29.7, 20.7, 11.2. LRMS (ESI) m/z : $[\text{M} + \text{H}]^+$ 351.0.

(3aS,5R,6aR)-3-(2-Methylallyl)-2-oxohexahydro-2H-cyclopenta[d]oxazol-5-yl (4-Nitrophenyl) Carbonate (11k). Alcohol 10h (6 mg, 0.03 mmol) was treated with 4-methylmorpholine (10 μ L, 0.09 mmol) and 4-nitrophenyl chloroformate (19 mg, 0.09 mmol) by following the procedure outline for activated alcohol 11a to afford 11k (7.2 mg, 66%): ^1H NMR (500 MHz, CDCl_3) δ 8.27 (d, J = 9.3 Hz, 2H), 7.36 (d, J = 9.2 Hz, 2H), 5.30 (t, J = 4.6 Hz, 1H), 5.08 (t, J = 7.0 Hz, 1H), 4.95 (d, J = 17.9 Hz, 2H), 4.26 (t, J = 7.2 Hz, 1H), 4.09 (d, J = 15.2 Hz, 1H), 3.59 (d, J = 15.2 Hz, 1H), 2.61 (dd, J = 16.4, 2.7 Hz, 1H), 2.43 (dd, J = 15.7, 3.0 Hz, 1H), 2.15 (dddd, J = 16.2, 6.5, 4.6, 0.7 Hz, 1H), 1.89 (dddd, J = 15.8, 7.0, 4.8, 0.7 Hz, 1H), 1.76 (t, J = 0.8 Hz, 3H). ^{13}C NMR (126 MHz, CDCl_3) δ 157.0, 155.3, 151.9, 145.5, 139.9, 125.3, 121.9, 114.2, 80.5, 77.6, 77.3, 77.0, 76.8, 59.3, 49.2, 39.7, 35.9, 19.9. LRMS (ESI) m/z : $[\text{M} + \text{H}]^+$ 363.0.

(3aS,5R,6aR)-3-Isobutyl-2-oxohexahydro-2H-cyclopenta[d]oxazol-5-yl (4-Nitrophenyl) Carbonate (11l). Alcohol 10i (11 mg, 0.05 mmol) was treated with 4-methylmorpholine (18 μ L, 0.2 mmol) and 4-nitrophenyl chloroformate (33 mg, 0.2 mmol) by following the procedure outline for activated alcohol 11a to afford 11l (15 mg, 77%): ^1H NMR (800 MHz, CDCl_3) δ 8.29 (d, J = 9.2 Hz, 2H), 7.38 (d, J = 9.2 Hz, 2H), 5.32 (t, J = 4.7 Hz, 1H), 5.10 (t, J = 7.0 Hz, 1H), 4.36 (t, J = 7.2 Hz, 1H), 3.33 (dd, J = 14.0, 8.9 Hz, 1H),

2.88 (dd, $J = 14.0$, 6.3 Hz, 1H), 2.63 (dd, $J = 16.2$, 2.6 Hz, 1H), 2.45 (dd, $J = 15.7$, 3.0 Hz, 1H), 2.20–2.15 (m, 1H), 2.01–1.93 (m, 2H), 1.00 (d, $J = 6.7$ Hz, 3H), 0.96 (d, $J = 6.7$ Hz, 3H). ^{13}C NMR (201 MHz, CDCl_3) δ 157.2, 155.3, 151.9, 145.5, 125.3, 121.9, 80.5, 77.4, 77.2, 77.0, 76.9, 59.7, 50.2, 39.7, 36.0, 26.5, 20.2, 19.8. LRMS (ESI) m/z : $[\text{M} + \text{H}]^+$ 365.0.

(3a5,5R,6aR)-3-(Methoxymethyl)-2-oxohexahydro-2H-cyclopenta[d]oxazol-5-yl (4-Nitrophenyl) Carbonate (11m). Alcohol 10j (5 mg, 0.03 mmol) was treated with 4-methylmorpholine (9.0 μL , 0.08 mmol) and 4-nitrophenyl chloroformate (16 mg, 0.08 mmol) by following the procedure outline for activated alcohol 11a to afford 11m (7 mg, 74%). ^1H NMR (800 MHz, CDCl_3) δ 8.29 (d, $J = 9.2$ Hz, 2H), 7.38 (d, $J = 9.2$ Hz, 2H), 5.35 (t, $J = 4.6$ Hz, 1H), 5.14 (t, $J = 7.1$ Hz, 1H), 4.79 (d, $J = 0.6$ Hz, 2H), 4.48 (t, $J = 7.1$ Hz, 1H), 3.41 (s, 3H), 2.70–2.59 (m, 2H), 2.18 (dddd, $J = 16.2$, 6.6, 4.6, 0.7 Hz, 1H), 2.02 (dddd, $J = 15.7$, 6.9, 4.7, 0.7 Hz, 1H). ^{13}C NMR (201 MHz, CDCl_3) δ 157.1, 155.3, 151.9, 145.5, 125.3, 121.8, 80.6, 78.0, 77.2, 77.0, 76.9, 75.8, 59.4, 56.2, 39.5, 37.4. LRMS (ESI) m/z : $[\text{M} + \text{Na}]^+$ 375.0.

Determination of X-ray Structures of HIV-1 Protease–Inhibitor Complexes. HIV-1 protease was expressed and purified as described.³⁷ The protease complexes with inhibitors 4a and 4e were crystallized using the hanging drop vapor diffusion method with well solutions of 1.0 M NaCl, 0.1 M sodium acetate, pH 4.8 for 4a, and 1.4 M NaCl, 0.1 M sodium acetate, pH 5.5 for 4e. X-ray diffraction data were collected on a single crystal cooled to 90 K at SER-CAT (22-ID beamline), Advanced Photon Source, Argonne National Lab (Chicago, IL, USA) with X-ray wavelength of 1.0 Å. X-ray data were processed by HKL-2000³⁸ to give R_{merge} values of 9.9% for 4a-bound protease and 8.2% for 4e-bound protease. The crystal structures were solved by PHASER³⁹ in CCP4i Suite^{40–42} using one of the previously reported isomorphous structures⁴³ as the initial model, and refined using both SHELX-2014^{44,45} and Refmac5⁴⁶ with X-ray data at 1.22 and 1.30 Å resolution for 4a and 4e complexes, respectively. PRODRG-2⁴⁸ was used to construct the inhibitors and geometric restraints for refinement. COOT^{47,49} was used for modification of the models. Alternative conformations were modeled, and isotropic atomic displacement parameters (B factors) were applied for all atoms including solvent molecules. The final refined solvent structure comprised two Na^+ ions, two Cl^- ions, one formic acid, and 190 waters for 4a-bound protease and two Na^+ ions, four Cl^- ions, and 155 water molecules for the 4e-bound protease structure. The crystallographic data collection and refinement statistics are listed in Table 1 of Supporting Information. The coordinates and structure factors of the HIV-1 protease structures have been deposited in the Protein Data Bank⁴⁹ with accession code of 6E9A for 4a-bound protease and 6E7J for 4e-bound protease.

■ ASSOCIATED CONTENT

Supporting Information

The Supporting Information is available free of charge on the ACS Publications website at DOI: 10.1021/acs.jmedchem.8b01227.

Full NMR spectroscopic data for all final compounds and X-ray structural data for inhibitors 4a and 4e-bound HIV-1 protease (PDF)

Molecular formula strings and some data (CSV)

Accession Codes

The PDB accession codes for inhibitor 4a-bound HIV-1 protease and inhibitor 4e-bound HIV-1 protease X-ray structures are 6E9A and 6E7J. Authors will release the atomic coordinates and experimental data upon article publication.

■ AUTHOR INFORMATION

Corresponding Author

*Phone: (765) 494-5323. Fax: (765) 496-1612. E-mail: akghosh@purdue.edu.

ORCID

Arun K. Ghosh: 0000-0003-2472-1841

Irene T. Weber: 0000-0003-4876-7393

Notes

The authors declare no competing financial interest.

■ ACKNOWLEDGMENTS

This research was supported by the National Institutes of Health (Grant GM53386, A.K.G., and Grant GM62920, I.T.W.). X-ray data were collected at the Southeast Regional Collaborative Access Team (SER-CAT) beamline 22ID at the Advanced Photon Source, Argonne National Laboratory. Use of the Advanced Photon Source was supported by the U.S. Department of Energy, Basic Energy Sciences, Office of Science, under Contract W-31-109-Eng-38. This work was also supported by the Intramural Research Program of the Center for Cancer Research, National Cancer Institute, National Institutes of Health, and in part by a Grant-in-Aid for Scientific Research (Priority Areas) from the Ministry of Education, Culture, Sports, Science, and Technology of Japan (Monbu Kagakusho), a Grant for Promotion of AIDS Research from the Ministry of Health, Welfare, and Labor of Japan, and the Grant to the Cooperative Research Project on Clinical and Epidemiological Studies of Emerging and Reemerging Infectious Diseases (Renkei Jigyō) of Monbu-Kagakusho. The authors thank the Purdue University Center for Cancer Research, which supports the shared NMR and mass spectrometry facilities.

■ ABBREVIATIONS USED

APV, amprenavir; ART, antiretroviral therapy; ATV, atazanavir; bis-THF, bis-tetrahydrofuran; DIPEA, *N,N*-diisopropylethylamine; DRV, darunavir; LPV, lopinavir; PI, protease inhibitor; TFA, trifluoroacetic acid; Cp-THF, cyclopentanyltetrahydrofuran; IBX, *O*-iodoxybenzoic acid

■ REFERENCES

- (1) Naggie, S.; Hicks, C. Protease Inhibitor-Based Antiretroviral Therapy in Treatment-Naive HIV-1-Infected Patients: The Evidence Behind the Options. *J. Antimicrob. Chemother.* **2010**, *65*, 1094–1099.
- (2) Broder, S. The Development of Antiretroviral Therapy and Its Impact on the HIV-1/AIDS Pandemic. *Antiviral Res.* **2010**, *85*, 1–18.
- (3) Montaner, J. S. G.; Lima, V. D.; Barrios, R.; Yip, B.; Wood, E.; Kerr, T.; Shannon, K.; Harrigan, P. R.; Hogg, R. S.; Daly, P.; Kendall, P. Association of Highly Active Antiretroviral Therapy Coverage, Population Viral Load, and Yearly New HIV Diagnoses in British Columbia, Canada: a Population-based Study. *Lancet* **2010**, *376*, 532–539.
- (4) Lohse, N.; Hansen, A. B.; Gerstoft, J.; Obel, N. Improved Survival in HIV-Infected Persons: Consequences and Perspectives. *J. Antimicrob. Chemother.* **2007**, *60*, 461–463.
- (5) Brik, A.; Wong, C.-H. HIV-1 Protease: Mechanism and Drug Discovery. *Org. Biomol. Chem.* **2003**, *1*, 5–14.
- (6) Pettit, S. C.; Everitt, L. E.; Choudhury, S.; Dunn, B. M.; Kaplan, A. H. Initial Cleavage of the Human Immunodeficiency Virus Type 1 GagPol Precursor by Its Activated Protease Occurs by an Intramolecular Mechanism. *J. Virol.* **2004**, *78*, 8477–8485.
- (7) Kohl, N. E.; Emini, E. A.; Schleif, W. A.; Davis, L. J.; Heimbach, J. C.; Dixon, R. A.; Scolnick, E. M.; Sigal, I. S. Active Human Immunodeficiency Virus Protease is Required for Viral Infectivity. *Proc. Natl. Acad. Sci. U. S. A.* **1988**, *85*, 4686–4690.
- (8) Smith, R.; Brereton, I. M.; Chai, R. Y.; Kent, S. B. H. Ionization States of the Catalytic Residues in HIV-1 Protease. *Nat. Struct. Biol.* **1996**, *3*, 946–950.

- (9) Wlodawer, A.; Vondrasek, J. Inhibitors of HIV-1 Protease: A Major Success of Structure-Assisted Drug Design. *Annu. Rev. Biophys. Biomol. Struct.* **1998**, *27*, 249–284.
- (10) Ghosh, A. K.; Osswald, H. L.; Prato, G. Recent Progress in the Development of HIV-1 Protease Inhibitors for the Treatment of HIV/AIDS. *J. Med. Chem.* **2016**, *59*, 5172–5208.
- (11) Edmonds, A.; Yotebieng, M.; Lusiana, J.; Matumona, Y.; Kitetele, F.; Napravnik, S.; Cole, S. R.; Van Rie, A.; Behets, F. The Effect of Highly Active Antiretroviral Therapy on the Survival of HIV-Infected Children in a Resource-Deprived Setting: A Cohort Study. *PLoS Med.* **2011**, *8*, e1001044.
- (12) Hue, S.; Gifford, R. J.; Dunn, D.; Fernhill, E.; Pillay, D. Demonstration of Sustained Drug-Resistant Human Immunodeficiency Virus Type 1 Lineages Circulating among Treatment-Naïve Individuals. *J. Virol.* **2009**, *83*, 2645–2654.
- (13) Ghosh, A. K.; Chapsal, B. D. Design of the Anti-HIV-1 Protease Inhibitor Darunavir. In *Introduction to Biological and Small Molecule Drug Research and Development: Theory and Case Studies*; Ganellin, C. R., Jefferis, R., Roberts, S., Eds.; Elsevier: London, 2013; pp 355–384.
- (14) Ghosh, A. K.; Dawson, Z. L.; Mitsuya, H. Darunavir, a Conceptually New HIV-1 Protease Inhibitor for the Treatment of Drug-Resistant HIV. *Bioorg. Med. Chem.* **2007**, *15*, 7576–7580.
- (15) Koh, Y.; Nakata, H.; Maeda, K.; Ogata, H.; Bilcer, G.; Devasamudram, T.; Kincaid, J. F.; Boross, P.; Wang, Y. F.; Tie, Y.; Volarath, P.; Gaddis, L.; Harrison, R. W.; Weber, I. T.; Ghosh, A. K.; Mitsuya, H. Novel bis-Tetrahydrofuranylethane-Containing Non-peptidic Protease Inhibitor (PI) UIC-94017 (TMC114) with Potent Activity Against Multi-PI-Resistant Human Immunodeficiency Virus In Vitro. *Antimicrob. Agents Chemother.* **2003**, *47*, 3123–3129.
- (16) De Meyer, S.; Azijn, H.; Surleraux, D.; Jochmans, D.; Tahi, A.; Pauwels, R.; Wigerinck, P.; de Béthune, M. P. TMC114, a Novel Human Immunodeficiency Virus Type 1 Protease Inhibitor Active Against Protease Inhibitor-Resistant Viruses, Including a Broad Range of Clinical Isolates. *Antimicrob. Agents Chemother.* **2005**, *49*, 2314–2321.
- (17) Koh, Y.; Matsumi, S.; Das, D.; Amano, M.; Davis, D. A.; Li, J.; Leshchenko, S.; Baldrige, A.; Shioda, T.; Yarchoan, R.; Ghosh, A. K.; Mitsuya, H. Potent Inhibition of HIV-1 Replication by Novel Non-peptidyl Small Molecule Inhibitors of Protease Dimerization. *J. Biol. Chem.* **2007**, *282*, 28709–28720.
- (18) Hayashi, H.; Takamune, N.; Nirasawa, T.; Aoki, M.; Morishita, Y.; Das, D.; Koh, Y.; Ghosh, A. K.; Misumi, S.; Mitsuya, H. Dimerization of HIV-1 Protease Occurs Through Two Steps Relating to the Mechanism of Protease Dimerization Inhibition by Darunavir. *Proc. Natl. Acad. Sci. U. S. A.* **2014**, *111*, 12234–12239.
- (19) Ghosh, A. K.; Sridhar, P. R.; Kumaragurubaran, N.; Koh, Y.; Weber, I. T.; Mitsuya, H. Bis-Tetrahydrofuran: a Privileged Ligand for Darunavir and a New Generation of HIV Protease Inhibitors That Combat Drug Resistance. *ChemMedChem* **2006**, *1*, 939–950.
- (20) de Béthune, M. P.; Sekar, V.; Spinoza-Guzman, S.; Vanstockem, M.; De Meyer, S.; Wigerinck, P.; Lefebvre, E. Darunavir (Prezista, TMC114): From bench to clinic, improving treatment options for HIV-infected patients. In *Antiviral Drugs: From Basic Discovery through Clinical Trials*; Kazmierski, W. M., Ed.; John Wiley & Sons, Inc.: Hoboken, NJ, 2011; pp 31–45. DOI: 10.1002/9780470929353.ch3.
- (21) Tie, Y.; Boross, P. L.; Wang, Y.-F.; Gaddis, L.; Hussain, A. K.; Leshchenko, S.; Ghosh, A. K.; Louis, J. M.; Harrison, R. W.; Weber, I. T. High Resolution Crystal Structures of HIV-1 Protease with a Potent Non-peptide Inhibitor (UIC-94017) Active Against Multi-Drug-Resistant Clinical Strains. *J. Mol. Biol.* **2004**, *338*, 341–352.
- (22) Kovalevsky, A. Y.; Liu, F.; Leshchenko, S.; Ghosh, A. K.; Louis, J. M.; Harrison, R. W.; Weber, I. T. Ultra-High Resolution Crystal Structure of HIV-1 Protease Mutant Reveals Two Binding Sites for Clinical Inhibitor TMC114. *J. Mol. Biol.* **2006**, *363*, 161–173.
- (23) Ghosh, A. K.; Chapsal, B. D.; Weber, I. T.; Mitsuya, H. Design of HIV Protease Inhibitors Targeting Protein Backbone: An Effective Strategy for Combating Drug Resistance. *Acc. Chem. Res.* **2008**, *41*, 78–86.
- (24) Ghosh, A. K.; Anderson, D. D.; Weber, I. T.; Mitsuya, H. Enhancing Protein Backbone Binding—A Fruitful Concept for Combating Drug-Resistant HIV. *Angew. Chem., Int. Ed.* **2012**, *51*, 1778–1802.
- (25) Deardorff, D. R.; Windham, C. Q.; Carnney, C. L. Enantioselective Hydrolysis of *cis*-3,5-Diacetoxycyclopentene: (1R,4S)-(+)-4-Hydroxy-2-Cyclopentenyl Acetate. *Org. Synth., Collect. Vol.* **1998**, *9*, 487.
- (26) Ghosh, A. K.; Chapsal, B. D.; Baldrige, A.; Ide, K.; Koh, Y.; Mitsuya, H. Design and Synthesis of Stereochemically Defined Novel Spirocyclic P2-Ligands for HIV-1 Protease Inhibitors. *Org. Lett.* **2008**, *10*, 5135–5138.
- (27) Nicolaou, K. C.; Baran, P. S.; Zhong, Y.-L.; Barluenga, S.; Hunt, K. W.; Kranich, R.; Vega, J. A. Iodine(V) Reagents in Organic Synthesis. Part 3. New Routes to Heterocyclic Compounds via *o*-Iodoxybenzoic Acid-Mediated Cyclizations: Generality, Scope, and Mechanism. *J. Am. Chem. Soc.* **2002**, *124*, 2233–2244.
- (28) Ghosh, A. K.; Chapsal, B. D.; Baldrige, A.; Steffey, M. P.; Walters, D. E.; Koh, Y.; Amano, M.; Mitsuya, H. Design and Synthesis of Potent HIV-1 Protease Inhibitors Incorporating Hexahydrofuro-pyranol-Derived High Affinity P₂ Ligands: Structure – Activity Studies and Biological Evaluation. *J. Med. Chem.* **2011**, *54*, 622–634.
- (29) Ghosh, A. K.; Rao, K. V.; Nyalapatla, P. R.; Osswald, H. L.; Martyr, C. D.; Aoki, M.; Hayashi, H.; Agniswamy, J.; Wang, Y.-F.; Bulut, H.; Das, D.; Weber, I. T.; Mitsuya, H. Design and Development of Highly Potent HIV-1 Protease Inhibitors with a Crown-like Oxotricyclic Core as the P2-Ligand to Combat Multidrug-Resistant HIV Variants. *J. Med. Chem.* **2017**, *60*, 4267–4278.
- (30) Toth, M. V.; Marshall, G. R. A Simple, Continuous Fluorometric Assay for HIV Protease. *Int. J. Pept. Protein Res.* **1990**, *36*, 544–550.
- (31) Koh, Y.; Amano, M.; Towata, T.; Danish, M.; Leshchenko-Yashchuk, S.; Das, D.; Nakayama, M.; Tojo, Y.; Ghosh, A. K.; Mitsuya, H. In Vitro Selection of Highly Darunavir-Resistant and Replication-Competent HIV-1 Variants by Using a Mixture of Clinical HIV-1 Isolates Resistant to Multiple Conventional Protease Inhibitors. *J. Virol.* **2010**, *84*, 11961–11969.
- (32) Hughes, P. J.; Cretton-Scott, E.; Teague, A.; Wensel, T. M. Protease Inhibitors for Patients with HIV-1 Infection: A Comparative Overview. *Pharm. Ther.* **2011**, *36*, 332–345.
- (33) Aoki, M.; Danish, M. L.; Aoki-Ogata, H.; Amano, M.; Ide, K.; Das, D.; Koh, Y.; Mitsuya, H. Loss of the Protease Dimerization Inhibition Activity of Tipranavir (TPV) and Its Association with the Acquisition of Resistance to TPV by HIV-1. *J. Virol.* **2012**, *86*, 13384–13396.
- (34) Amano, M.; Tojo, Y.; Salcedo-Gómez, P. M.; Campbell, J. R.; Das, D.; Aoki, M.; Xu, C.-X.; Rao, K. V.; Ghosh, A. K.; Mitsuya, H. GRL-0519, a Novel Oxatricyclic Ligand-Containing Nonpeptidic HIV-1 Protease Inhibitor (PI), Potently Suppresses Replication of a Wide Spectrum of Multi-PI-Resistant HIV-1 Variants In Vitro. *Antimicrob. Agents Chemother.* **2013**, *57*, 2036–2046.
- (35) For details of X-ray studies, see [Supporting Information](#).
- (36) Mahalingam, B.; Louis, J. M.; Hung, J.; Harrison, R. W.; Weber, I. T. Structural Implications of Drug-Resistant Mutants of HIV-1 Protease: High-Resolution Crystal Structures of the Mutant Protease/Substrate Analogue Complexes. *Proteins: Struct., Funct., Genet.* **2001**, *43*, 455–464.
- (37) Otwinowski, Z.; Minor, W. Processing of X-ray Diffraction Data Collected in Oscillation Mode. *Methods in Enzymology*, 276: *Macromolecular Crystallography, Part A*; Carter, C. W., Jr., Sweet, R. M., Eds.; Academic Press: New York, 1997; pp 307–326.
- (38) McCoy, A. J.; Grosse-Kunstleve, R. W.; Adams, P. D.; Winn, M. D.; Storoni, L. C.; Read, R. J. Phaser Crystallographic Software. *J. Appl. Crystallogr.* **2007**, *40*, 658–674.
- (39) Winn, M. D.; Ballard, C. C.; Cowtan, K. D.; Dodson, E. J.; Emsley, P.; Evans, P. R.; Keegan, R. M.; Krissinel, E. B.; Leslie, A. G. W.; McCoy, A.; McNicholas, S. J.; Murshudov, G. N.; Pannu, N. S.; Potterton, E. A.; Powell, H. R.; Read, R. J.; Vagin, A.; Wilson, K. S.

Overview of the CCP4 Suite and Current Developments. *Acta Crystallogr., Sect. D: Biol. Crystallogr.* **2011**, *67*, 235–242.

(40) Collaborative Computational Project, Number 4. The CCP4 Suite: Programs for Protein Crystallography. *Acta Crystallogr., Sect. D: Biol. Crystallogr.* **1994**, *50*, 760–763.

(41) Potterton, E.; Briggs, P.; Turkenburg, M.; Dodson, E. A Graphical User Interface to the CCP4 Program Suite. *Acta Crystallogr., Sect. D: Biol. Crystallogr.* **2003**, *59*, 1131–1137.

(42) Shen, C.-H.; Wang, Y.-F.; Kovalevsky, A. Y.; Harrison, R. W.; Weber, I. T. Amprenavir Complexes with HIV-1 Protease and its Drug-Resistant Mutants Altering Hydrophobic Clusters. *FEBS J.* **2010**, *277*, 3699–3714.

(43) Sheldrick, G. M. A Short History of SHELX. *Acta Crystallogr., Sect. A: Found. Crystallogr.* **2008**, *64*, 112–122.

(44) Sheldrick, G. M.; Schneider, T. R. SHELXL: High-Resolution Refinement. *Methods Enzymol.* **1997**, *277*, 319–343.

(45) Murshudov, G. N.; Vagin, A. A.; Dodson, E. J. Refinement of Macromolecular Structures by the Maximum-Likelihood Method. *Acta Crystallogr., Sect. D: Biol. Crystallogr.* **1997**, *53*, 240–255.

(46) Schuettelkopf, A. W.; van Aalten, D. M. F. PRODRG: a Tool for High-Throughput Crystallography of Protein–Ligand Complexes. *Acta Crystallogr., Sect. D: Biol. Crystallogr.* **2004**, *60*, 1355–1363.

(47) Emsley, P.; Lohkamp, B.; Scott, W. G.; Cowtan, K. Features and Development of Coot. *Acta Crystallogr., Sect. D: Biol. Crystallogr.* **2010**, *66*, 486–501.

(48) Emsley, P.; Cowtan, K. Coot: Model-Building Tools for Molecular Graphics. *Acta Crystallogr., Sect. D: Biol. Crystallogr.* **2004**, *60*, 2126–2132.

(49) Berman, H. M.; Westbrook, J.; Feng, Z.; Gilliland, G.; Bhat, T. N.; Weissig, H.; Shindyalov, I. N.; Bourne, P. E. The Protein Data Bank. *Nucleic Acids Res.* **2000**, *28*, 235–242.